NASA CONTRACTOR REPORT

NASA CR-2701

EFFECTS OF MOTION ON JET EXHAUST NOISE FROM AIRCRAFT

K. S. Chun, C. H. Berman, and S. J. Cowan

Prepared by
BOEING COMMERCIAL AIRPLANE COMPANY
Seattle, Wash. 98124
for Lewis Research Center

NATIONAL AERONAUTICS AND SPACE ADMINISTRATION • WASHINGTON, D. C. • JUNE 1976

1. Report No.	2. Government Accession No.	3. Recipient's Catalog No.
NASA CR-2701		

4. Title and Subtitle	5. Report Date
EFFECTS OF MOTION ON JET EXHAUST NOISE FROM AIRCRAFT	June 1976
	6. Performing Organization Code

7. Author(s)	8. Performing Organization Report No.
K. S. Chun, C. H. Berman, and S. J. Cowan	D6-41995
	10. Work Unit No.

9. Performing Organization Name and Address	11. Contract or Grant No.
Boeing Commercial Airplane Company P. O. Box 3707 Seattle, Washington 98124	NAS3-18539
	13. Type of Report and Period Covered
12. Sponsoring Agency Name and Address	Contractor Report
National Aeronautics and Space Administration Washington, D.C. 20546	14. Sponsoring Agency Code

15. Supplementary Notes

Final Report. Project Manager, Allen M. Karchmer, V/STOL and Noise Division, NASA Lewis Research Center, Cleveland, Ohio

16. Abstract

A fundamental study is presented of the various problems involved in the evaluation of the jet noise field prevailing between an observer on the ground and an aircraft in flight in a typical take-off or landing approach pattern. The study was performed by dividing the work into four tasks: (1) literature survey and preliminary investigation, (2) propagation effects, (3) source alteration effects, and (4) investigation of verification techniques. Sixteen problem areas were identified and studied. Six follow-on programs were recommended for further work. The results of this study and the proposed follow-on programs will provide a practical general technique for predicting flyover jet noise for conventional jet nozzles.

17. Key Words (Suggested by Author(s))	18. Distribution Statement
Jet noise Motion effects Propagation Source alteration	Unclassified - unlimited STAR Category 71

19. Security Classif. (of this report)	20. Security Classif. (of this page)	21. No. of Pages	22. Price*
Unclassified	Unclassified	220	$7.75

* For sale by the National Technical Information Service, Springfield, Virginia 22161

CONTENTS

CONTENTS (Concluded)

FIGURES

FIGURES (Continued)

FIGURES (Continued)

FIGURES (Concluded)

TABLES

EFFECTS OF MOTION ON JET EXHAUST NOISE FROM AIRCRAFT

K. S. Chun, C. H. Berman, and S. J. Cowan

1.0 SUMMARY

A fundamental study is presented of the various problems involved in evaluating the jet noise from an aircraft in flight as received by an observer on the ground. The aircraft was assumed to be flying overhead in a typical takeoff or landing approach pattern. The study was performed by dividing the work into the following four tasks:

Task 1 Literature Survey and Preliminary Investigation
Task 2 Propagation Effects
Task 3 Source Alteration Effects
Task 4 Investigation of Verification Techniques

Task 1 was a survey of the literature and computer programs relevant to the subject and a preparation of the detailed work plans for Tasks 2, 3, and 4. The results were documented and submitted to NASA during the second month of the contract period. The results of the survey of the literature, updated to the time of this writing, are included in this report as section 6.0.

Task 2 was a study to determine and recommend what theoretical and experimental approaches and techniques would be required to characterize the propagation of the jet noise from the flying aircraft to the ground. For this task, seven problem areas were selected and studied as described in section 3.1. Based on the study, recommendations (see sec. 4.0) for further work in the subject area have been made.

Task 3 was a study to determine and recommend what theoretical and experimental approaches would be required to accurately define the phenomenon of jet noise source alteration and its consequences; i.e., the fluid dynamic changes occurring in and around the jet and the alteration in the acoustic generation mechanisms caused by aircraft motion. This problem was studied using a theoretical model, the Boeing Flow/Noise Computer Program. The model is an excellent tool for investigating the flow field and noise generation of a single- or dual-flow jet as affected by the changes in the nozzle performance parameters, as well as by the ambient airflow.

The problem of understanding the different effects the jet noise field is subjected to in various test arrangements (the wind tunnel, free jet tunnel, flyby testing, etc.) is closely associated with the source alteration problem. A theoretical study performed to evaluate the different effects and to derive relationships for correlating the different effects has been presented. The Task 3 study described in section 3.2 resulted in the recommended follow-on programs presented in section 4.0.

Task 4 was a study to determine and recommend experimental techniques to measure the jet noise from the airplane as observed on the ground. Six areas of study that play important roles in relation to the task theme were selected; detail studies were performed as presented in section 3.3. A number of recommendations presented in section 4.0 were derived from this study.

A brief summary of the current status and recommendations for further effort for each subtask studied in the contract is presented in table form at the end of this section. The contract effort resulted in a thorough and detailed review of all problem areas involved in the effects of motion on the jet noise field being generated by an airplane in flight and perceived by an observer on the ground. The study identified the areas where further work is required and led to a number of new techniques that would provide additional insight into the motion effects. A continuing effort in the recommended follow-on work is essential for a complete understanding and prediction of motion effects.

	Work item	Status	Recommendation
Task 2			
3.1.1	Atmospheric Absorption Coefficient in Homogeneous Still Air	ARP 866 information is satisfactory in audiofrequency range.	Extrapolation equations require experimental substantiation in the ultrasonic frequency range; discrepancies exceeding 30% of test values were found.
3.1.2	Atmospheric Variation Effects	For frequencies below 1000 Hz, effects of upper air profiles are not important; ground conditions can can be used with less than a fraction of a dB error.	If required, use layered atmosphere equation or ray acoustics formulas.
	Effect of Time Dependent Fluctuation From Mean	Adequate analytical formulas for "excess" attenuation due to turbulence are available.	Requires more precise and extensive measurement of turbulence. Needs additional experiments for the turbulence effects on sound propagation.
3.1.3	Microphone Placement Effect	For research purposes, ground microphone technique is an excellent method.	Recommend use of the monitoring system for assuring the quality of data.
		This technique requires a hard surface from source to receiver for full advantages.	Further pursue the use of high and ground microphone combination method.
	Engine Installation Effect	Sufficient experimental data are available for static installation effects.	Needs more experimental work for inflight installation effects.
3.1.4	Doppler Effects	Simple identification of the effects is possible for static jet and jet with ambient airflow operating with same V_R.	Further analysis is required for the case where static jet operates with V_j and jet with ambient airflow with V_R.
3.1.5	Noise Prediction Computer Program (Empirical)	The Full Standard Prediction Procedure implemented with JEN2, the flight effect, and ground reflection computation procedures gives good results. Prediction errors in aft arc SPL for the low and high BPR engine jet noise studied were within 3dB in most cases.	Continued improvement of the program is recommended.

	Work item	Status	Recommendation
3.1.6	Weather Change Effects and Tolerance Boundaries	Undetected weather changes may cause substantial test data scatter (as large as 6 dB in some cases). The test window, within which measuring error bands of temperature and relative humidity (HR) are not very critical (e.g., $\pm 1.1^0$ C and $\pm 2\%$ RH), is reasonably wide.	Frequent weather condition measurements should be made.
3.1.7	Trailing Vortex Effects	Vortex cores trailing the wing tips of current aircraft do not interfere with jet noise propagation.	
Task 3			
3.2.1	Flow/Noise Program Analysis	The flow/noise program has proven to be a valuable tool for the source alteration effect study; it predicts aft arc OASPL of shock-free jet within about 4 dB for the cases studied.	Further improvement of the mathematical model is recommended; e.g., inclusion of shear noise term in the noise generation model and the propagation effects within the jet flow itself.
3.2.2	Comparison of Experimental Techniques	The analyses presented can be used to estimate the noise levels and the forward velocity effects resulting from various experimental techniques.	The analyses are based on several idealized conditions. Extend the study to more realistic cases.
3.2.3	Lilley Equation Solution	Special analytical solutions and general numerical solutions have been found.	A better understanding of noise generation and propagation in critical layers must be obtained. The Lilley equation should be coupled to actual turbulent jet data inputs.

Task 4	Work item	Status	Recommendation
3.3.1	Measurement of Aircraft Position and Altitude	No airplane position measuring system available today can provide a significant improvement in data accuracy over that by photo position measuring system. Either an inertial navigation system or a flight test gyro system is satisfactory for attitude measurement.	Laser system is recommended if online position data are required.
3.3.2	Atmospheric Property Instrumentation	Accuracy and response are inadequate. Data acquisition frequency is too low.	Improve accuracy and response of instruments; desired values are $\pm 0.25^0$ C and 3 Hz for temperature in still air, $\pm 3\%$ RH and 0.2 Hz in 3 m/s aspiration for relative humidity, ± 0.09 m/s and 0.3 Hz for wind speed, and $\pm 4^0$ and 0.3 Hz for wind direction. Use tethered balloon/winch system. Turbulence data acquisition is required.
3.3.3	Averaging Technique of Flight Test Data	Sampling time required for analysis of noise data degrades the airplane position and noise emission angle resolution when a single microphone is used.	Use of multimicrophone averaging improves the airplane position resolution without degrading the quality of noise data; use of four microphones will improve airplane position resolution to one-fourth of that with one microphone at overhead.
3.3.4	Duplication of Static Jet Condition In flight	The proper criterion is to realize the same flow conditions at the jet exit for the static and in-flight jet.	The criterion is difficult to meet with an engine. Examine whether the difference between the static and in-flight engine performance causes a noise level difference at the noise source. This difference with a high-bypass engine was found to be about 0.4 dB OASPL at all angles.

	Work item	Status	Recommendation
3.3.5	Extraction of Jet Noise Component From Total Noise		Identify the jet noise by comparing the total noise spectra and the predicted jet noise spectra by the use of a prediction program.
3.3.6	Verification Aircraft		Use an airplane with a single jet noise source: a single engine airplane or an airplane with one engine at high thrust.

2.0 INTRODUCTION

Accurate prediction of the characteristics of the jet noise field prevailing between an observer on the ground and an aircraft flying overhead has been a consistent problem in the acoustic engineering of commercial jet airplanes. The problem has become more important since the effect of the jet noise level on the overall airplane noise became more pronounced because of the reduction of fan noise of high bypass ratio (BPR) engines by the use of noise suppression material.

There are a considerable number of factors that affect the jet noise levels received by a microphone on the ground from a flying aircraft in contrast to the noise levels received from a stationary engine. For example, the airplane structure close to the jet flow may cause noise reflection; the aerodynamic flow surrounding the airplane and the relative velocity of the ambient air would distort the jet flow from that of the static condition; variations of the atmospheric conditions between the source and microphone will cause changes in the sound path as well as atmospheric sound energy absorption; the impedance of the ground surface surrounding the receiver microphone will change from one place to the next; and different techniques of processing the nonstationary random noise signal may result in scatter in the processed noise data.

These factors and others, however, can be grouped in three broad categories:

1. The propagation effects

2. The source alteration effects

3. The effects of the means and techniques used in measuring these phenomena

A systematic review and careful study of each of these and other factors must be conducted to understand clearly the jet noise field and to determine what further work is required in enhancing the understanding. Through the work of this contract, such a review and study have been conducted.

The work results identified various areas where the knowledge available is sufficient. Since it also revealed a number of areas where a better understanding or definition is vitally needed, suggestions and recommendations for further analytical and experimental studies have been made.

3.0 ANALYSES

The characteristics of jet noise received from a stationary engine are well understood based on the results of numerous theoretical and experimental studies done to date. Thus, accurate predictions of the jet noise from a stationary engine can be made. Predictions of the jet noise from an aircraft as perceived by an observer on the ground, however, cannot be made with equal accuracy. The reason for this is that the changes in the jet noise characteristics caused by the airplane forward motion (the motion effects) are not yet well understood.

The various problems involved in the evaluation of the jet noise from an aircraft can be grouped in three basic categories: (1) the propagation effects, (2) the source alteration effects, and (3) the verification techniques. A clear understanding in each of these categories is essential for an accurate evaluation of the jet noise. The technical problems included in each of these categories have been reviewed and studied in detail. The results of this effort are presented in the following sections.

3.1 PROPAGATION EFFECTS

The jet noise generated by an aircraft in flight must propagate to an observer on the ground. The noise propagation is affected by a number of factors, for example, the steady and transient variations of the atmosphere, the proximity of airplane and ground surfaces, the Doppler frequency shift and amplitude change. These and other phenomena that have an important bearing on the propagation of jet noise have been studied in detail. The results of this study together with recommendations for further work in this problem area are presented in the following paragraphs.

3.1.1 ATMOSPHERIC ABSORPTION COEFFICIENTS IN HOMOGENEOUS STILL AIR

In performing the analysis of jet noise propagation, various occasions arise when evaluation of the atmospheric absorption of sound energy is required. For example, when several flight test noise data are recorded at different atmospheric conditions and distances, the atmospheric absorption must be assessed to compare the data on an equal basis; in the case where the noise data of a model nozzle are taken at a high frequency range (e.g., above 10 kHz), the data must be scaled down to the audiofrequency range for simulation of a full-scale nozzle.

Use of inaccurate atmospheric absorption coefficients in these cases would introduce errors in the data analyzed. It is thus concluded that a review of the current method of determining the atmospheric absorption coefficient is important. In this section, the background and method of determining the coefficient in homogeneous still air is reviewed, and areas that require further work are discussed.

3.1.1.1 Absorption Coefficients in the Audiofrequency Range

Currently in the acoustic analysis work related to aircraft, the atmospheric absorption coefficients are computed by the use of information presented in Aerospace Recommended Practice (ARP) 866 (ref. 1). Four principal relationships shown as the solid portions of the curves in figure 1 are required for the computation. The curves were established based on theoretical curves for the energy dissipation of sound waves in air, which was modified to fit experimental data available in the audiofrequency range. Detailed discussions on the theory and the test data that led to the modifications can be found in references 2 through 6.

Values of the atmospheric absorption coefficients in the audiofrequency range obtained from the use of these curves were found to be in good agreement with many field measurements (ref. 7). Thus, no inadequacy is considered to exist in the ARP 866 information in the audiofrequency range. A discussion is included in the following section on a set of equations representing the portion of four ARP 866 curves in the audiofrequency range.

3.1.1.2 Equations for Absorption Coefficient Including the Ultrasonic Frequency Range

An assessment of atmospheric absorption is necessary in scale model nozzle tests where the noise measurement involves the ultrasonic frequency range (10 to 100 kHz). As the demand for the evaluation of atmospheric absorption in the ultrasonic frequency range increased, attempts were made to extrapolate the ARP 866 curves into the high frequency range. A natural approach for the extrapolation was to extend the existing curves guided by the trends of curves established in the audiofrequency range.

Results of one attempt are shown by the broken lines in figure 1a, 1b, and 1c. The curve of figure 1d, not having temperature or frequency as independent variables, is assumed to be applicable for the ultrasonic frequencies. Since modification of this curve from that of theory (refs. 2 and 6) was based on test data mainly in the audiofrequency range, proof of whether this assumption is justified or not requires additional test data in the ultrasonic frequency range. Similarly, verification of the extrapolated curves in figure 1a, 1b, and 1c also require additional test data in the high frequency range.

Table 1 lists a set of equations used at Boeing to represent the curves shown in figure 1. Because the equations are derived to fit the audiofrequency range as well as the extrapolated ultrasonic range, they are applicable for both frequency ranges.

Committee A-21 of SAE issued a revision (ref. 8) to the ARP 866. Reference 8 presents a set of equations similar to those of table 1 to replace the curve representations of the original ARP 866. The equations may be considered applicable for both the audio and ultrasonic frequency ranges, although no definite discussions are made in the publication regarding the applicable frequency range.

From a different theoretical approach, Evans, Sutherland, and Bass (ref. 9) and Working Group S1-57 of ANSI (ref. 10) derived another set of equations for a frequency range from 100 Hz to 100 kHz. Work to finalize this set of equations is not completed at the time of this writing.

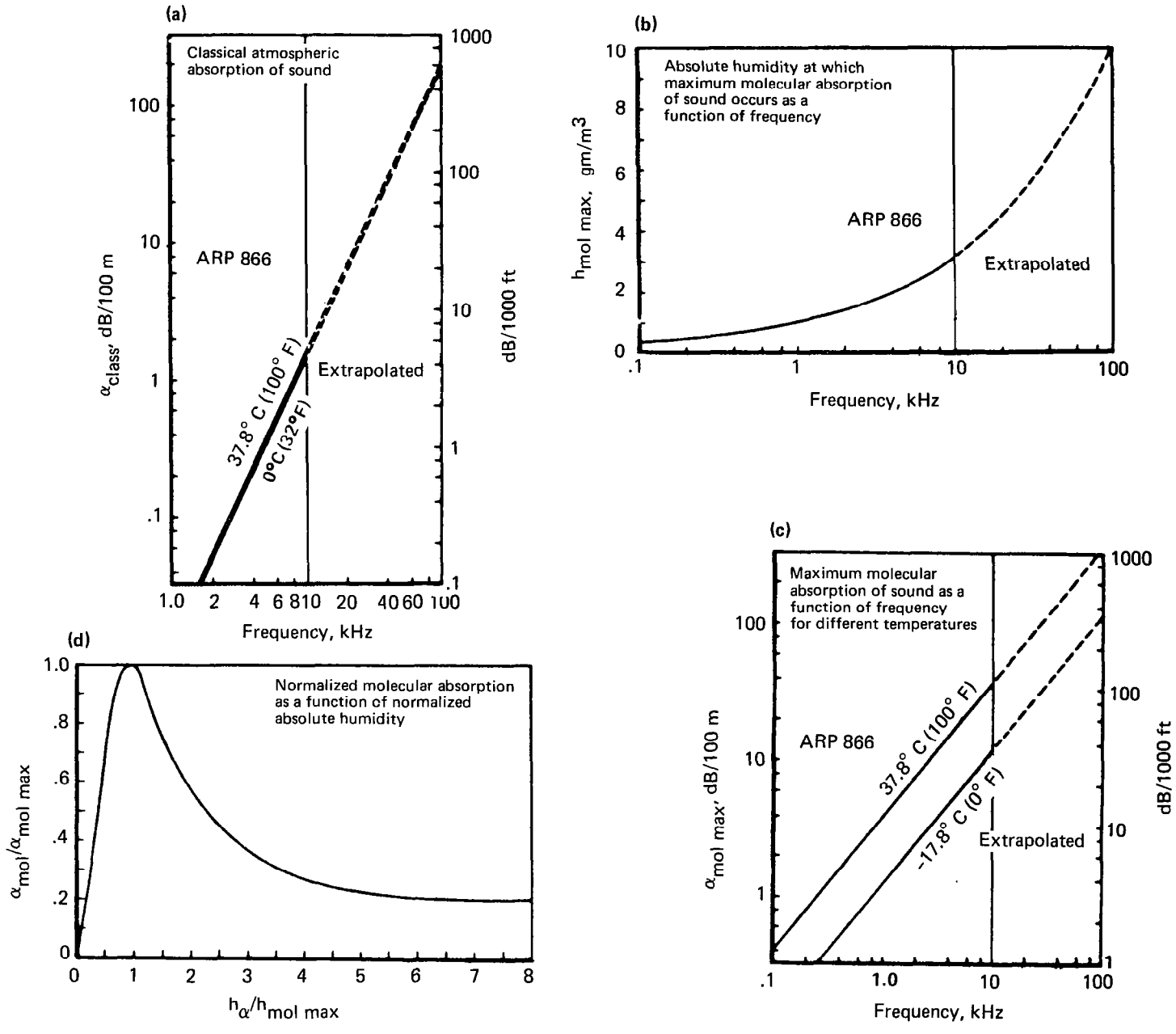

Figure 1.–Curves Used for Computation of Atmospheric Absorption Coefficient

Table 1.–Equations to Represent Curves Shown in Figure 1

Figure number	Range	Equation
1a	–	$\alpha_{class} = \frac{1}{26.8697} (f/1000)^{2.045} e^{0.09 (1.8\ T)/68}$
1b	–	$h_{mol\ max} = (f/1000)^{0.5}$
1c	$T \leq 1°\ C$	$\alpha_{mol\ max} = (f/1000)\ e^{[0.0141(1.8T + 32) + 1.24]}$
	$T > 1°\ C$	$= (f/1000)\ e^{[0.0104(1.8T + 32) + 1.37]}$
1d	$0 \leq h_a/h_{mol\ max} \leq 0.25$	$\alpha_{mol}/\alpha_{mol\ max} = 1.2\ (h_a/h_{mol\ max})$
	$0.25 < \quad \leq 0.6$	$= 1.543\ (h_a/h_{mol\ max}) - 0.86$
	$0.6 < \quad \leq 0.95$	$= 0.84 + 0.27\ (h_a/h_{mol\ max} - 0.6)$
	$0.95 < \quad \leq 1.25$	$= 0.87 + 0.13 \cos [\pi\ (h_a/h_{mol\ max} - .95)/.6]$
	$1.25 < \quad \leq 6.5$	$= 0.2\ (5.75 - [22.75 - (h_a/h_{mol\ max} - 5.8)^2]^{0.5})$
	$6.5 < h_a/h_{mol\ max}$	$= 0.2$

Note: T in ° C and f in Hz . Refer to figure 1 for units for other parameters.

Since the equations of table 1 have been used at Boeing for a considerable length of time and since the equations from reference 8 are a proposed revision to the current ARP 866, a preliminary comparison was made of the coefficients computed from the two sources in the audiofrequency range (no computer results are available for the ultrasonic range in ref. 8). A sample of the comparison is presented in table 2. The comparison results indicated that the differences are small, particularly for the lower frequency range in which the jet noise normally predominates other component noise.

A similar comparison between the absorption coefficients read off from the ARP 866 curves and that computed from the equations of table 1 indicated that the agreement is within about 0.5 dB/100 m (1.5 dB/1000 ft) in the audiofrequency range.

To gain some credibility of the Boeing equations in the ultrasonic frequency range, a comparison of the absorption coefficients calculated by the Boeing equations with the test data of Sivian (ref. 11) was made. Figure 2 shows this result which reveals a substantial separation in the high frequency range. Included in this figure is the classical absorption coefficient which shows that it is a small portion of the total absorption at these high frequencies.

In conjunction with the development of the Boeing 20 x 23 x 9 m (65 x 75 x 30 ft) anechoic room, a considerable amount of atmospheric absorption test data at ultrasonic frequencies has been accumulated. Figure 3 presents a preliminary evaluation result at 80 kHz, which shows a substantial difference between the computed and the measured values.

The above two preliminary comparisons sugggest that the extrapolation of the four curves (fig. 1) and the equations (table 1) derived from it may not be accurate for the ultrasonic frequency range. It also may be possible that additional variables are required for accurately computing the absorption coefficients in the high frequency range. Thus, tests to establish credibility of the equations for the ultrasonic frequency range should be conducted. A laboratory-type test similar to that conducted by Harris (ref. 5) is believed to be required for firm establishment of the basic information. A contract has been recently let by NASA-Lewis to provide ultrasonic absorption data.

3.1.2 ATMOSPHERIC VARIATION EFFECTS

The homogeneous air assumed in the previous section exists only in very controlled conditions; the properties and conditions of the air (temperature, humidity, velocity, etc.) in the atmosphere constantly vary in space and time. These facts generated numerous questions and problems regarding the certainties of acoustic test data measured in an actual atmospheric environment. Two important areas related to noise propagation through a nonhomogeneous atmosphere will be discussed in the following paragraphs.

3.1.2.1 Time Independent Atmospheric Variation

The discussion in this section is limited to the atmospheric conditions for which the variations of mean temperature, relative humidity, and wind velocity can be

Table 2.–A Sample Comparison Between Atmospheric Absorption Coefficients Due to Reference 8 and Boeing Equations

RH, %	Temp °C	Frequency kHz	α, dB/100 m									
			1.25	1.6	2.0	2.5	3.15	4.0	5.0	6.3	8.0	10
70	10	Reference 8	0.6	0.8	1.1	1.5	2.1	3.1	3.7	5.2	7.6	11.1
		Boeing	0.6	0.8	1.1	1.5	2.2	3.2	3.8	5.5	8.1	11.4
	15.5	Reference 8	0.6	0.8	1.0	1.3	1.8	2.5	2.9	4.1	5.9	8.8
		Boeing	0.6	0.8	1.0	1.3	1.7	2.5	2.9	4.3	6.3	9.1
	21.2	Reference 8	0.7	0.9	1.1	1.4	1.8	2.3	2.7	3.6	5.0	7.2
		Boeing	0.7	0.9	1.1	1.4	1.8	2.4	2.6	3.4	4.9	7.1
80	10	Reference 8	0.6	0.7	1.0	1.3	1.8	2.7	3.2	4.6	6.7	9.8
		Boeing	0.6	0.7	1.0	1.3	1.9	2.9	3.3	4.9	7.1	10.1
	15.5	Reference 8	0.6	0.8	1.0	1.3	1.7	2.3	2.7	3.7	5.2	7.7
		Boeing	0.6	0.8	1.0	1.3	1.6	2.2	2.6	3.7	5.5	8.0
	21.2	Reference 8	0.7	0.9	1.1	1.4	1.8	2.3	2.7	3.4	4.7	6.6
		Boeing	0.7	0.9	1.1	1.4	1.8	2.4	2.7	3.4	4.5	6.3

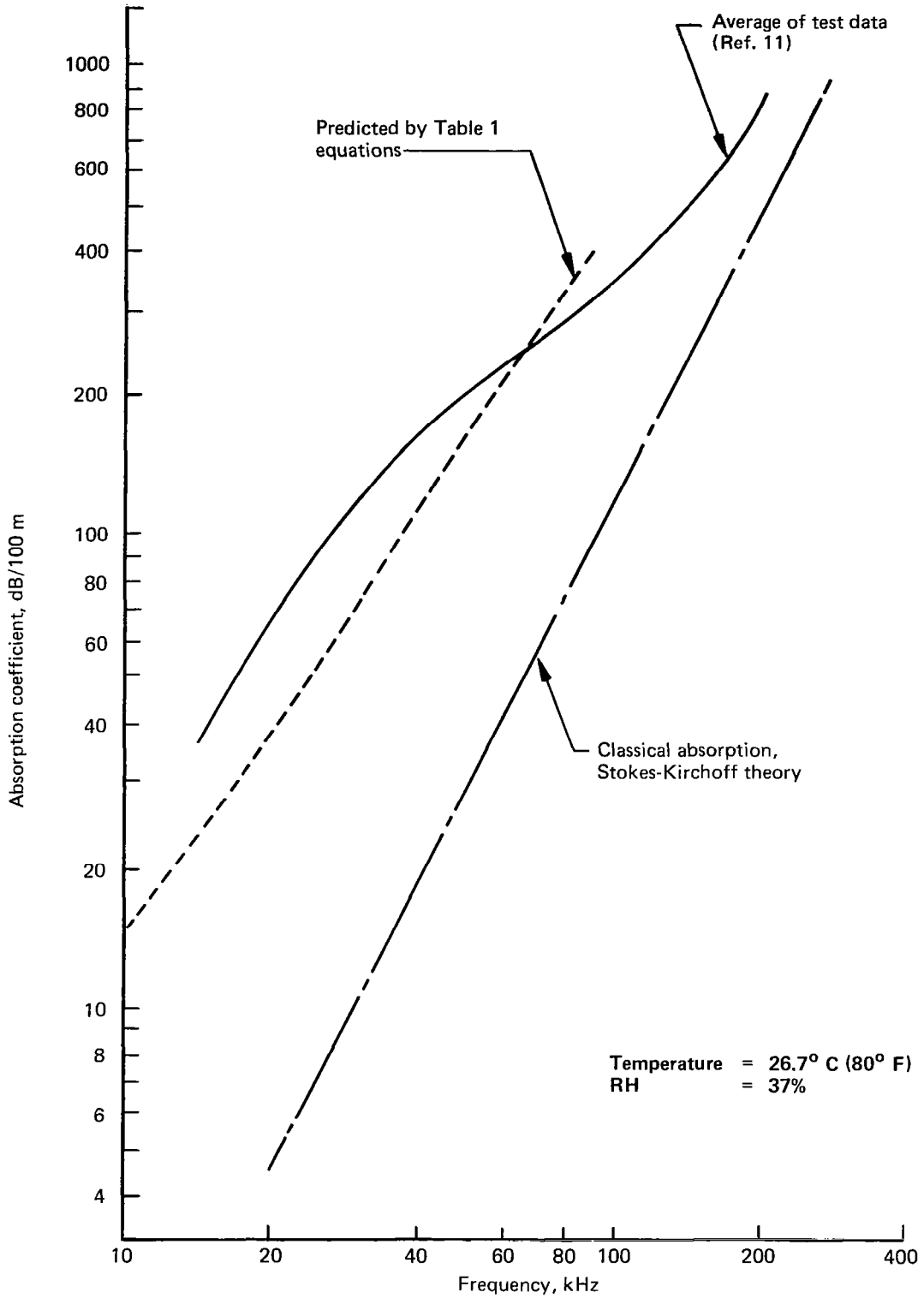

Figure 2.–Comparison of Absorption Coefficients

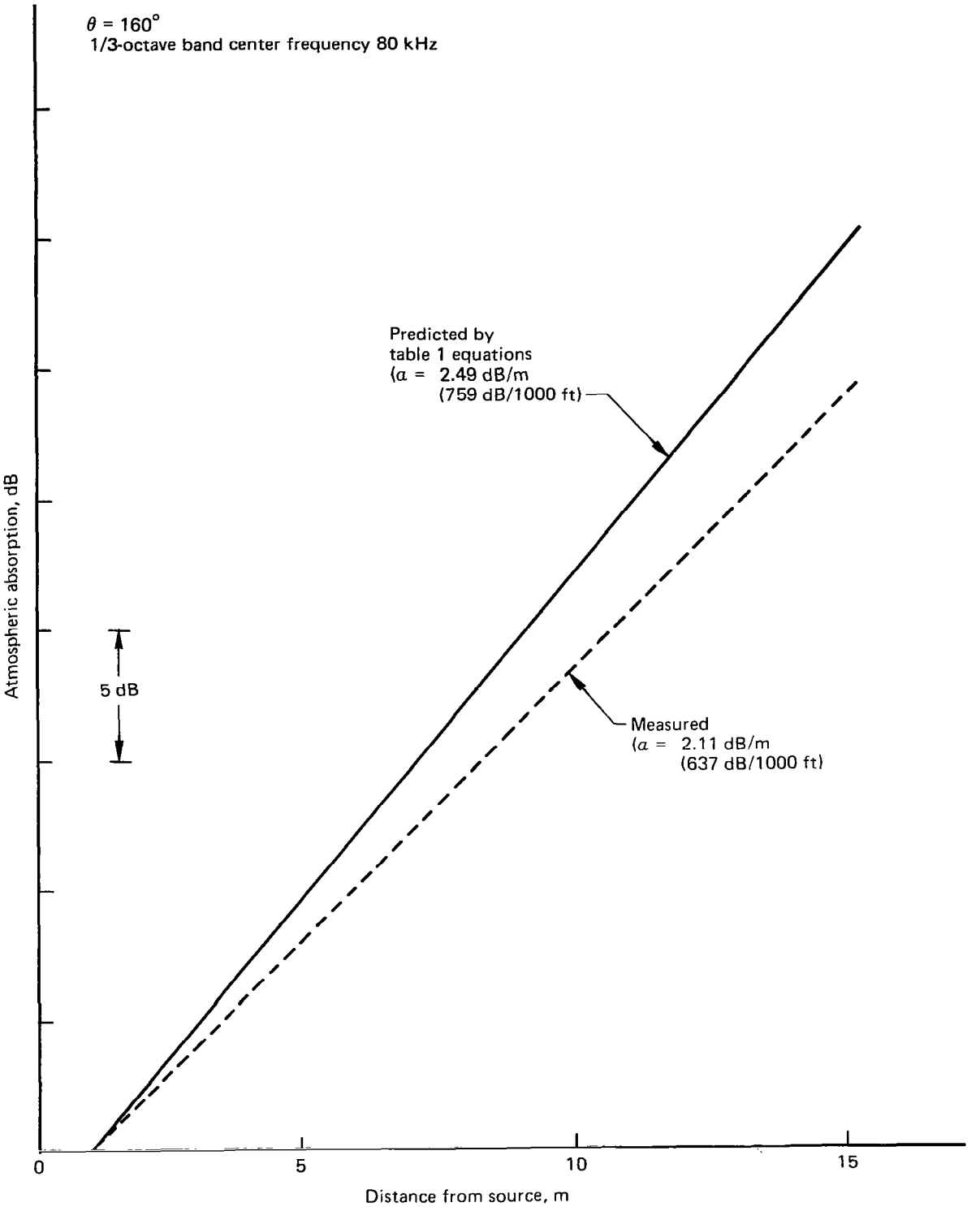

Figure 3.–Comparison of Measured With Predicted Atmospheric Absorption

represented by a set of smoothly varying profile curves as functions of altitude. The assumed condition is considered reasonable for representing the atmospheric conditions of an acoustic flight test, because acoustic flight tests are normally conducted within a weather window where the magnitudes and gradients of the three variables are expected to be small. The mean profiles actually measured in the field have been examined, some of which are included in this report. Selected from these profiles, a set of typical profiles was used to study noise propagation; results are presented in this section. The problems of shadow zone and effects of two-dimensional wind variation on sound propagation are also discussed. The effects of atmospheric turbulence are discussed in a later section.

Measured Mean Atmospheric Profiles.—The collection of atmospheric profile data obtained during the Moses Lake, Washington, flight test (ref. 12) is an excellent example of the shapes of the profiles and their variations. In the test, the upper air temperature and humidity were measured by free-rising weather balloons; the horizontal wind data were obtained by measuring the elevations and azimuth angles of the free-rising balloons at regular time intervals.

Samples of the profile data from the test are presented in figures 4 through 6. Each of the figures shows two or three sets of profile data measured at 1- to 2-hr intervals. The variations of the atmospheric absorption coefficient determined by the measured temperature and relative humidity based on ARP 866 are also included in the figures. Some insight to the rate of change of the atmospheric variables is shown. In most cases, if linear variations are assumed between the two consecutive measurements, the computed rates of change are small compared to the normal time duration (2 to 3 min) for noise measurement during a flight test. These slow rate changes also support the time independence assumed previously.

Sound Propagation Through the Atmosphere With Temperature, Relative Humidity, and Wind Velocity Gradients.—Sound passing through the atmosphere with temperature, relative humidity, and wind velocity gradients will be affected in two ways: the bending of the sound path due to refraction caused by the temperature and wind velocity changes, and the sound attenuation caused by the atmospheric absorption and spreading of the sound field. Bending of the sound ray will normally result in an additional attenuation compared to that for the straight path because of the increased path length. The attenuation caused by spreading is a function of the sound energy distribution at a point away from the source, which in turn is a function of the distribution of ray paths emanating from the noise source. Rigorous treatment of the spreading attenuation based on ray distribution will require a fair amount of time and effort, and it is not treated here.

Normally, however, the elevation angle toward the airplane in flight from a microphone is larger than 10° during a flight test. For this elevation angle range and with a moderate wind profile, the ray bending is calculated to be small. Hence, it may be assumed that the atmospheric absorption and the spreading attenuation can be estimated by assuming straight paths.

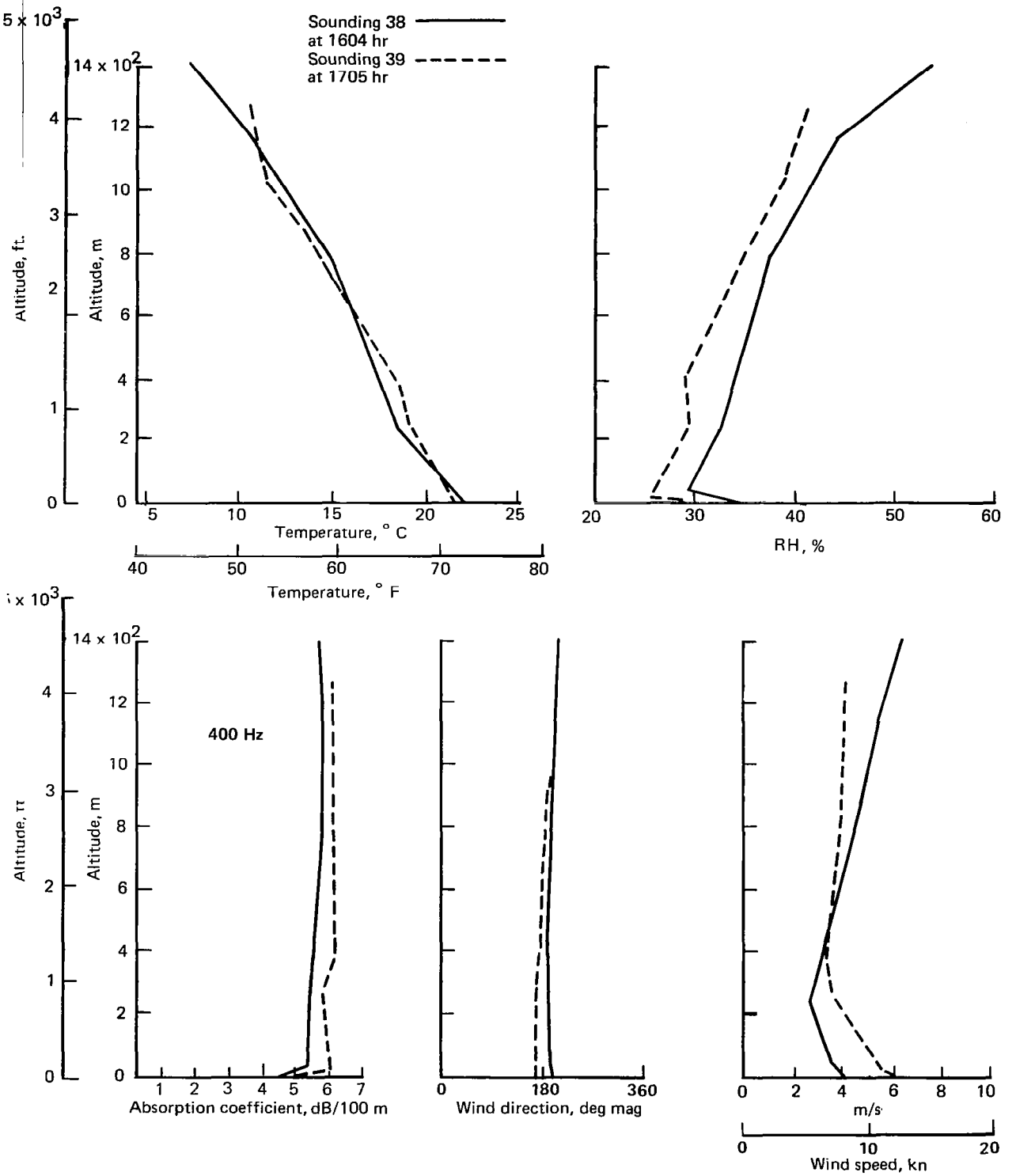

Figure 4.–Weather Profiles,Ascension Nos. 38 and 39, September 7, 1972 (ref. 12)

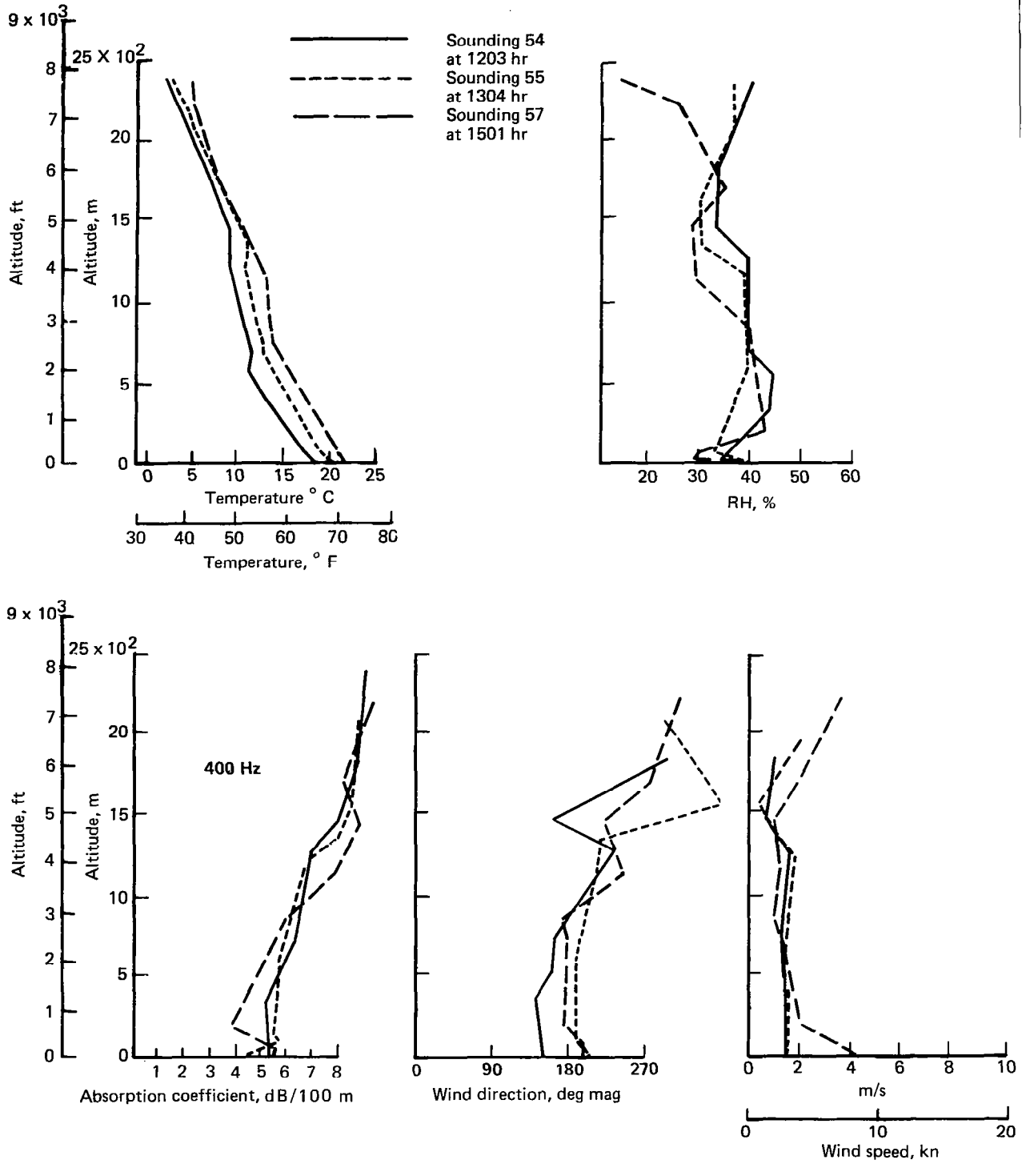

Figure 5.–Weather Profiles, Ascension Nos. 54, 55, and 57, September 13, 1972 (ref. 12)

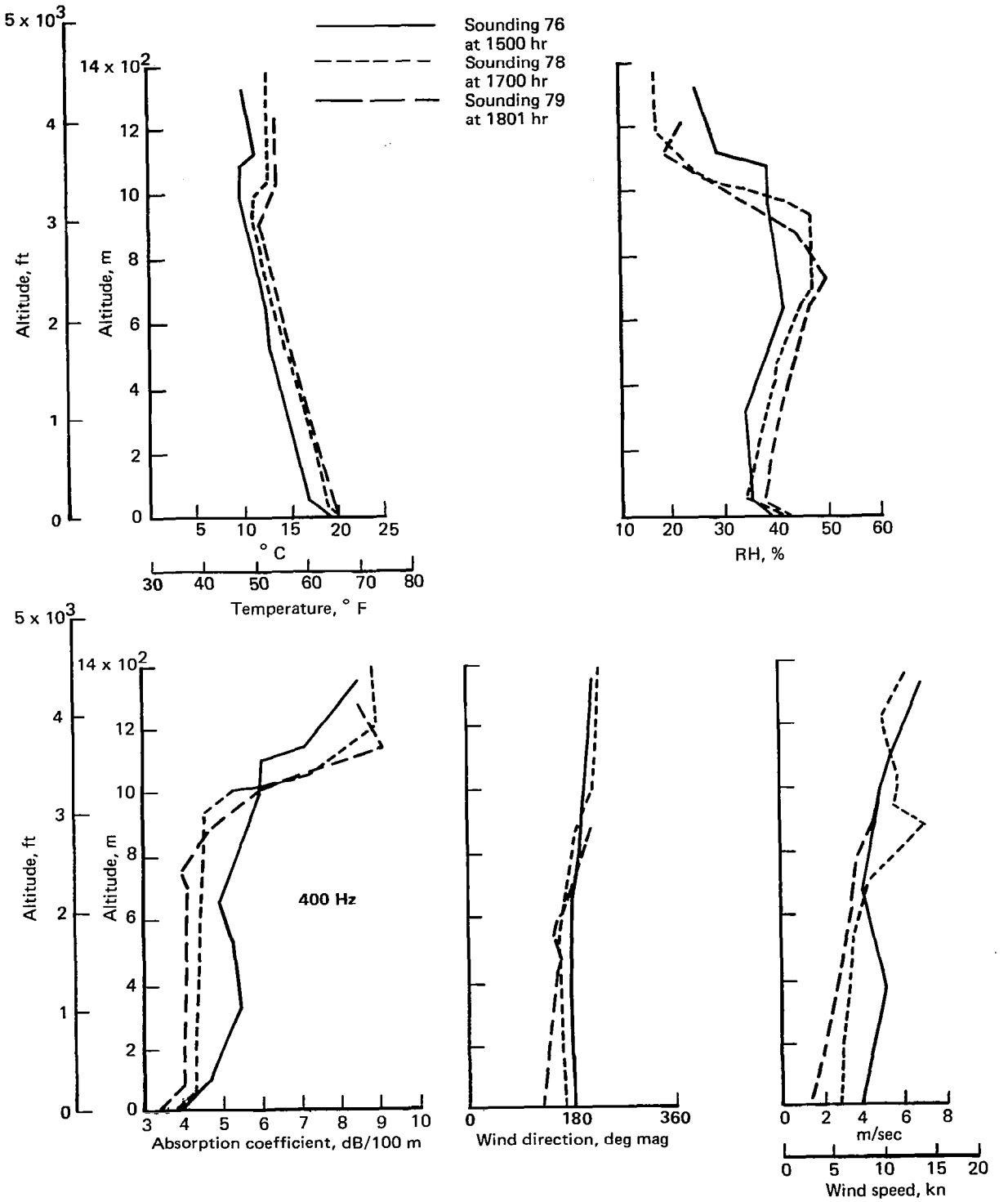

Figure 6.–Weather Profiles, Ascension Nos. 76, 78, and 79, September 29, 1972

A sound ray computation program was used to compute the sound propagation. The sample calculation was made to demonstrate the use of such a procedure and to examine the differences in sound propagation between the ray path method and the conventional straight line method. For this sample calculation, one set of weather conditions (fig. 7) was selected from the group obtained during the Moses Lake, Washington, flight test. The assumed profiles of the variables from the ground to the altitude of 15.25 m (50 ft) are also shown. These are based on a combination of the actual measurements and the analyses described in refs. 3 and 13. The wind direction is assumed to be constant for the sample calculation. The effect of wind direction variation is discussed in a later section.

Results of the computer calculation are summarized in figure 8. The upper portion of the figure shows the ray paths for three selected initial ray angles. The lower portion presents a comparison of the atmospheric attenuation and path length along the bent and the straight paths. The atmospheric absorption attenuations along straight lines were computed in two ways: (1) the "simplified method" which uses an effective absorption coefficient of the stratified atmosphere (described in the following section), and (2) the current conventional method which uses the absorption coefficient of air near the ground.

The result of the sample calculation shows that the path length difference between the bent and straight paths with an initial ray angle of 10^0 is about 10%, then decreases rapidly to an insignificant amount as the ray angle increases above 20^0. It also shows that, in the frequency range below 1000 Hz, the magnitude of the total atmospheric absorption from source to receiver by any of the three methods as well as the differences among them are rather small. At higher frequencies, however, as indicated by the case for 4000 Hz in figure 8, the magnitude and difference may become substantial.

Based on the above, it is concluded that the use of a straight line and ground atmospheric conditions would normally be satisfactory for the evaluation of full-scale airplane jet noise data taken within a reasonable weather window (defined in FAR Part 36). However, when the jet noise includes higher frequency components or a requirement exists for more accurate assessment of weather conditions, examination of the atmospheric effects by the given methods is recommended.

Simplified Method for Computing Absorption Coefficient.—In view of the minor increase in path length attributed to the bent ray path for the elevation angle range of interest, the following simplified method is proposed. It is assumed that sound rays from the source are all straight radial lines, and the sound waves suffer the atmospheric absorption in proportion to the absorption coefficient, which varies as a function of altitude as determined by the given set of temperature and RH profiles.

An existing computer subroutine is programmed along the proposed method using an equivalent absorption coefficient instead of that as a function of altitude. The equivalent absorption coefficient is computed by weighting six coefficients that represent the successive 5%, 5%, 10%, 20%, 30%, and 30% layers of the total atmospheric layer between the source and the receiver:

$$\alpha_{EFF} = 0.05\alpha_{2.5} + 0.05\alpha_{7.5} + 0.1\alpha_{15} + 0.2\alpha_{30} + 0.3\alpha_{55} + 0.3\alpha_{85} \quad (1)$$

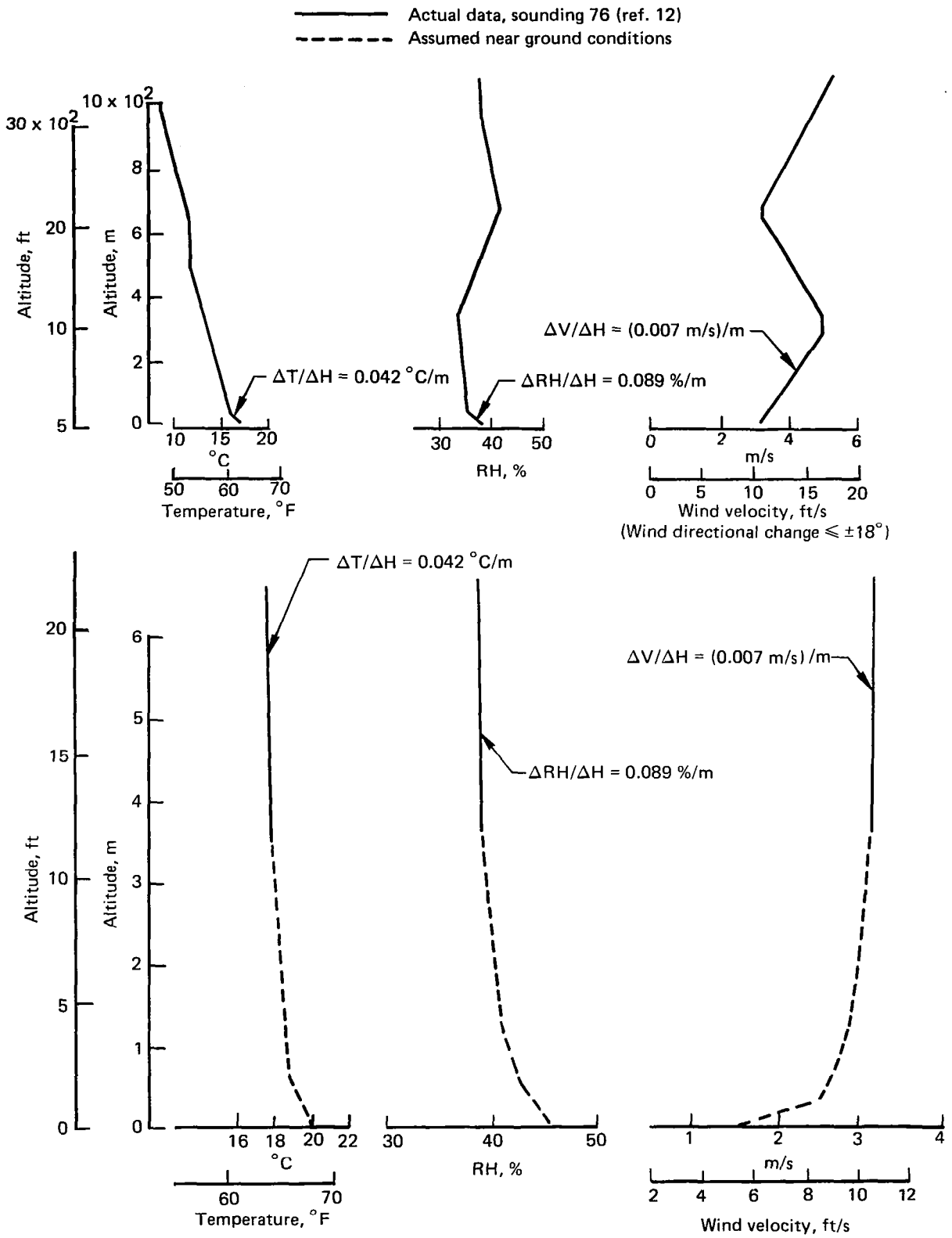

Figure 7.–Model Atmospheric Gradients

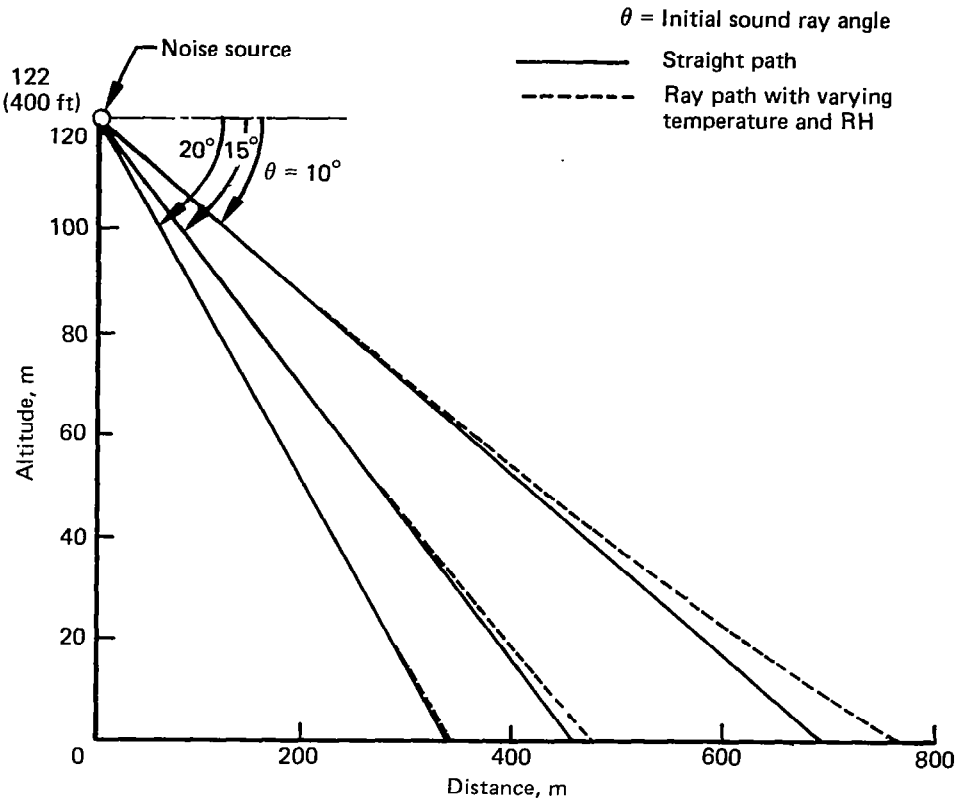

	Along ray path					Straight path								
	Varying temperature and RH*					Equation (1)				Ground temperature and RH*				
	Absorption, dB				Path length, m	Absorption, dB				Absorption, dB				Path length, m
θ deg	125 Hz	500	1000	4000		125 Hz	500	1000	4000	125 Hz	500	1000	4000	
10	0.47	1.92	4.54	37.3	772	0.3	1.5	4.5	37.1	0.45	1.84	3.74	22.2	702
15	0.29	1.21	2.87	23.6	488	0.2	1.0	3.0	24.9	0.30	1.23	2.51	14.9	471
20	0.22	0.89	2.12	17.5	361	0.2	0.8	2.3	18.8	0.23	0.93	1.89	11.3	356
40	0.12	0.47	1.12	9.2	189									189
70	0.08	0.32	0.76	6.3	129									129

*Refer to figure 7.

Figure 8.–Path Length and Atmospheric Absorption Attenuation Comparisons

where α_{EFF} is the effective absorption coefficient; and $\alpha_{2.5}$, $\alpha_{7.5}$, . . . , and α_{85} are the local absorption coefficients evaluated at 2.5%, 7.5%, . . . , and 85% of the total altitude from ground to the source, respectively.

The atmospheric absorption along the three straight paths computed by the weighting method for the same sample case is shown in figure 8. The results show that this method computes the attenuation so close to that of the ray method that the method should be acceptable for most applications.

Figure 9 shows the variation of absorption coefficient for four 1/3-octave-band (OB) center frequencies for the temperature and humidity profiles shown in figure 7. In the low frequency range where the jet noise is significant, the variation is not very critical.

Shadow Zones.—Boundaries of shadow zones could range from a circle to an open curve around the noise source (fig. 10), depending on the net effects of the temperature and wind velocity variations to the sound wave propagation velocity. Formation of shadow zone is important when the noise measuring points are located in the zone. During the normal flyby noise test, however, this situation is seldom expected to happen, because of the long distance from the nearest shadow boundary to the point of airplane projection on the ground.

An approximate estimate of the shadow boundary distance for a 122 m altitude flyby test with the weather profile (fig. 7) is 1036 m, making the elevation angle to the airplane from the boundary point of about 7° (refer fig. 8), which is outside the elevation angle range of interest. For this reason, it is concluded that shadow zone formation would not interfere with the jet noise propagation from an aircraft to an observer on the ground (ref. 14).

Effects of Wind Direction Variation.—It is possible that the wind variation is large enough that the analysis with a constant wind direction becomes questionable. A brief study on this subject indicates that this may not be the case with the procedure in which the test is conducted within selected weather conditions. During the Moses Lake test, the variation of wind direction was measured in addition to other weather variables (see figs. 4 through 6). An estimate of the frequently encountered rate of change of the mean horizontal wind direction at lower altitudes is about 60°/hr. If a test duration of 5 min is assumed, this rate would result in a total wind direction change of 5° during a test period.

The wind component in a vertical plane (perpendicular to the ground) is not generally measured, and data on it are rather scarce. Available information, including that presented in reference 15, indicates that the vertical component is less than 5 cm/sec in regions of good weather at lower altitudes.

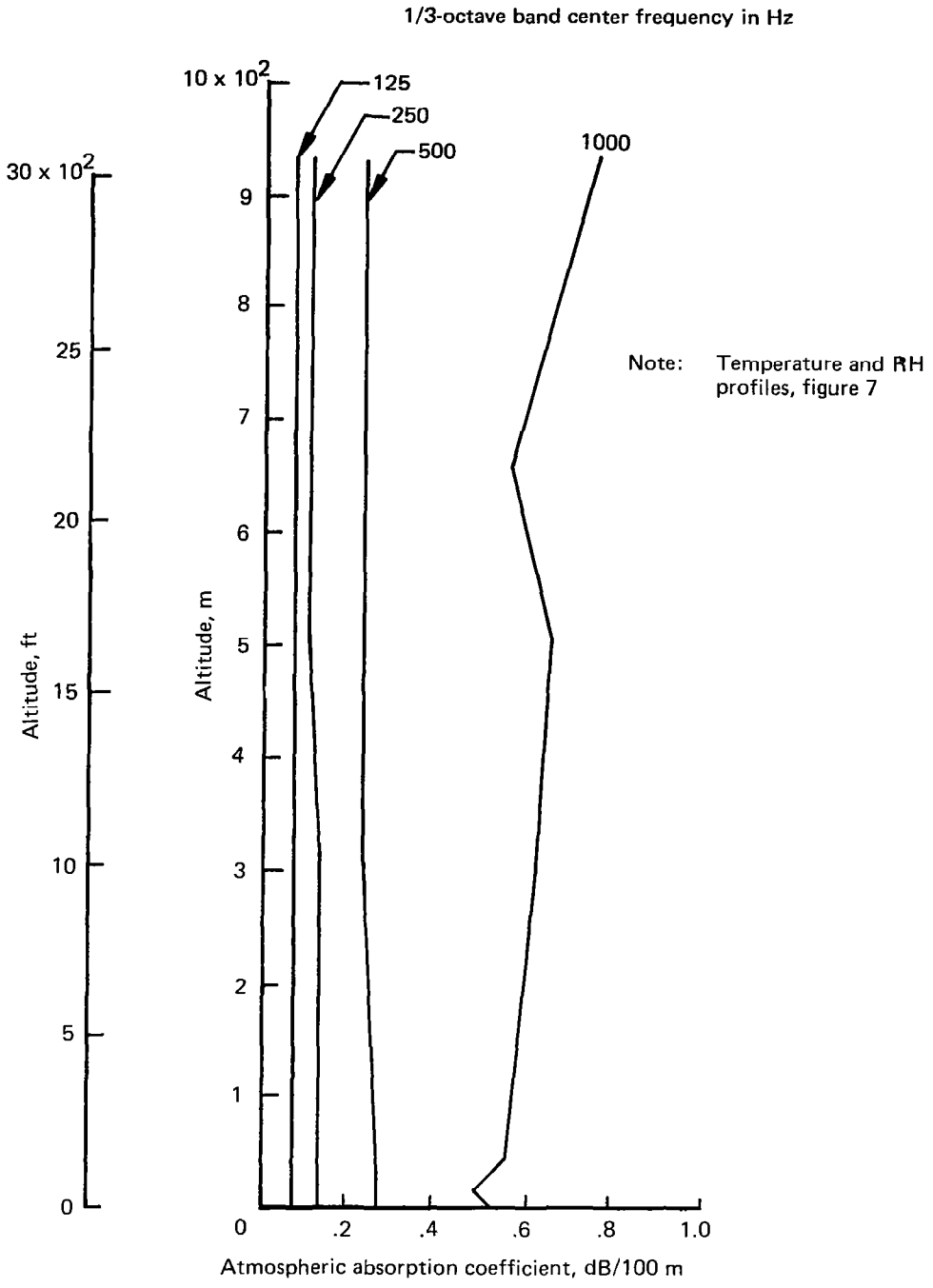

Figure 9.—Variation of Atmospheric Absorption Coefficient for the Atmospheric Gradients Shown in Figure 7

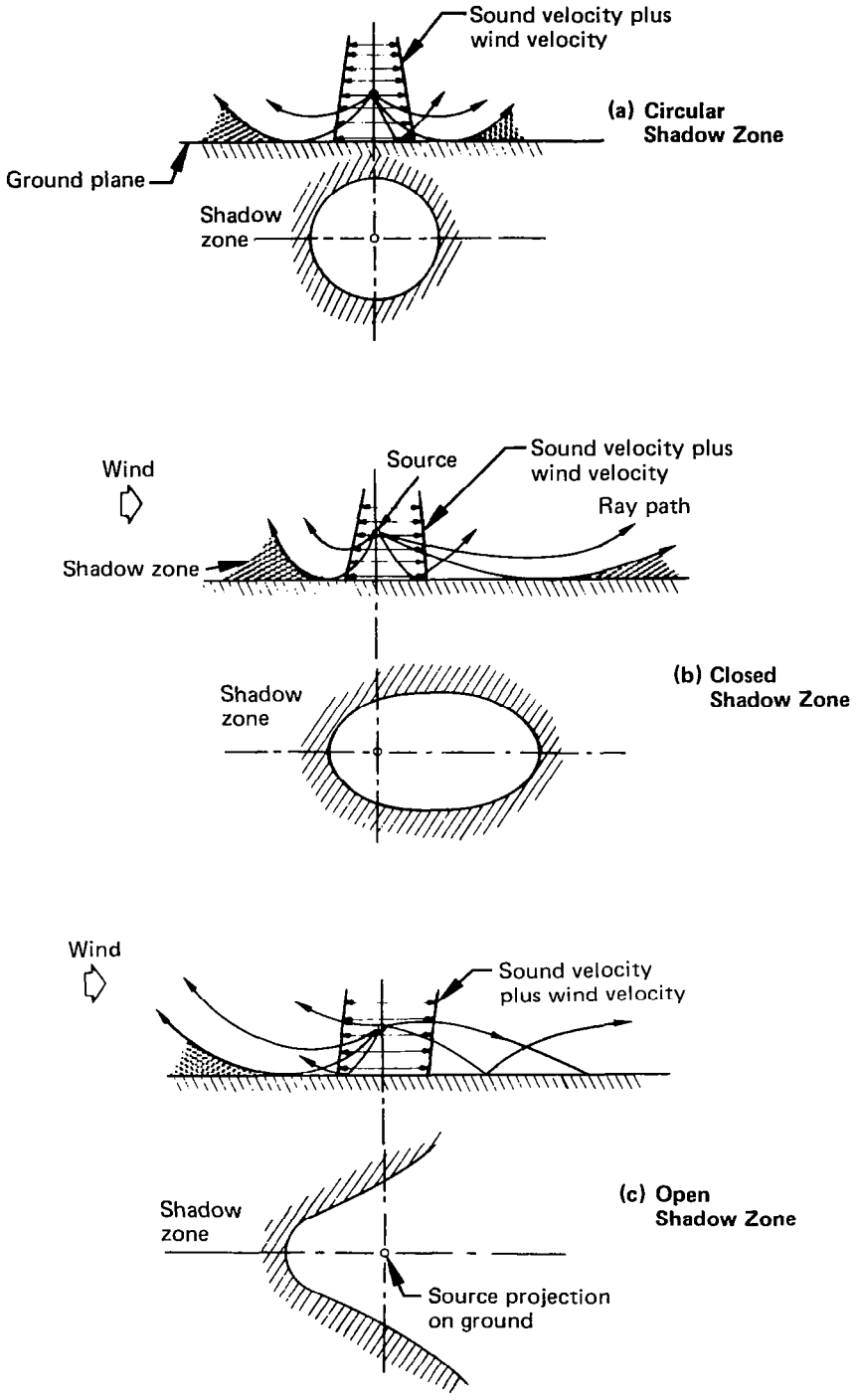

Figure 10.–Illustration of Mechanisms of Shadow Zone Formation

These findings on the side wind components indicate that the components would not cause a large deviation in the sound ray path so as to invalidate the result with the assumption of a constant horizontal direction. If, however, the horizontal side component is substantially large while the vertical component is negligibly small, the effect can be handled by the analysis presented in reference 16. In this case, the ray paths can be computed by:

$$\frac{dx}{dz} = \pm [u\,(1 - k_1\,u - k_2\,v) + k_1\,c^2]/D$$

$$\frac{dy}{dz} = \pm [v\,(1 - k_1\,u - k_2\,v) + k_2\,c^2]/D$$

$$D = c\,[(1 - k_1\,u - k_2\,v)^2 - c^2(k_1^2 + k_2^2)]^{1/2} \qquad (2)$$

where, in reference to a rectangular coordinate system with the origin at the projection of the noise source on the ground plane (fig. 11), u is the x-component of the wind vector, v is the y-component, c is the sonic velocity (all of which are functions only of z), and

$$k_1 = \frac{\sin\Phi\cos\Theta}{d} - \frac{u_s}{d^2 + u_s\,d\sin\Phi\cos\Theta}$$

$$k_2 = \frac{\sin\Phi\sin\Theta}{d}$$

$$d = [(u_s \sin\Phi\cos\Theta)^2 + c_s^2 - u_s^2]^{1/2} \qquad (3)$$

are constants defined by the conditions at the noise source on the z-axis; i.e., Φ and Θ, the initial directions of a ray path of interest; u_S, the x-component wind velocity with x-axis selected so that $v_S = 0$; and c_S, the sonic velocity at the noise source.

For the case when u, v, and c are represented by piecewise linear functions of z, it is possible to solve for the x and y coordinates of a ray path in piecewise integrations. Examinations of the above equations reveal that variation of y-coordinates compared to x-coordinates of a given ray path would be as small as the v-component compared to the u-component.

In the case of noise emission from an airplane flying in a constant direction (in negative x-axis direction) at a constant altitude and a constant airplane velocity v_{AP}, equation (2) is still applicable with k_1, k_2, and d computed replacing u_S with $(v_{AP} + u_S)$.

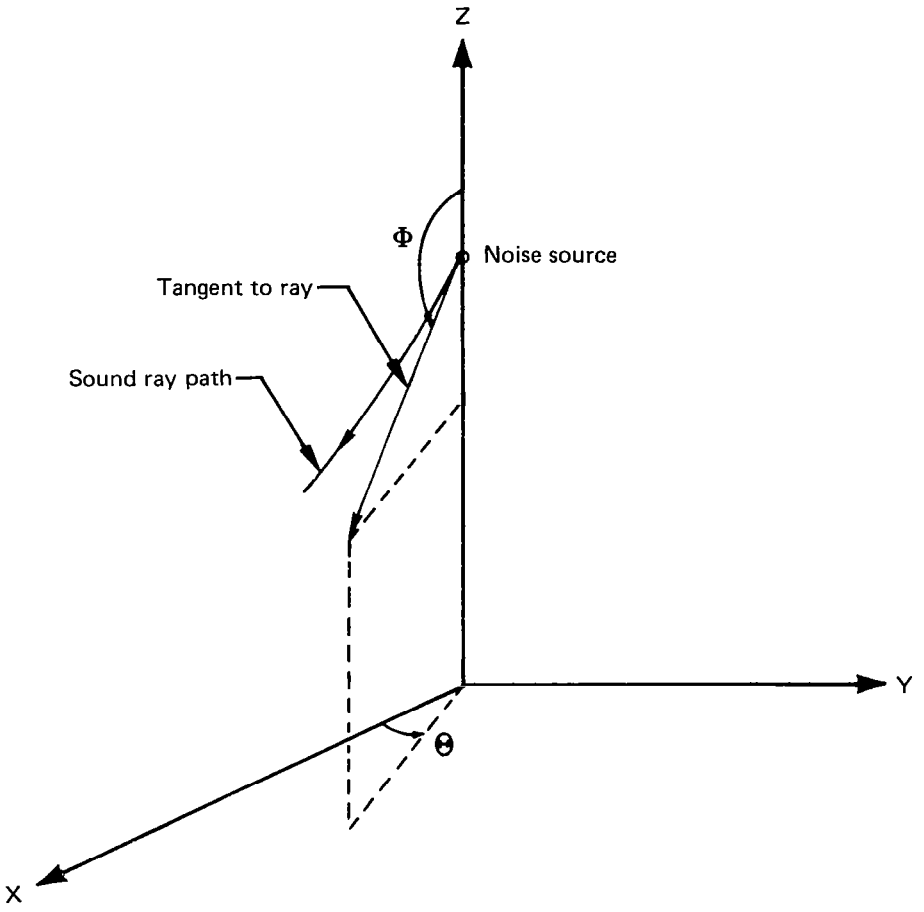

Figure 11.–Coordinate System and Symbols Used for Three-Dimensional Ray Path Computation

3.1.2.2 Effects of Time Dependent Fluctuation From the Mean

The standard values of atmospheric absorption coefficient published in ARP 866 are for evaluating the atmospheric absorption of sound energy and have been widely used in the acoustic tests conducted by the aircraft industry. These standard values are based on the theoretical and laboratory experimental work of Kneser (ref. 2), Harris (ref. 5), Evans and Bazley (ref. 4), etc. Since the absorption coefficients established in the laboratory environment were found to require modification for applying to the outdoor sound propagation problems, adjustments were made to the laboratory values utilizing the then available field test data (ref. 17, for example) to arrive at the standard values.

The adjusted coefficients have been found to be satisfactory in accounting for the atmospheric absorption in many acoustic tests. However, a substantial number of cases have also been experienced in which the computation of atmospheric absorption was suspected to be the reason for discrepancies in the noise levels measured during the tests (see ref. 12, for example). The discrepancies were more frequent when there was atmospheric turbulence in the field where noise measurements were conducted. This caused renewed interest for research and investigation of the effects of atmospheric conditions; i.e., mean value gradients and turbulence. In section 3.1.2.1, a discussion was presented on the effects of the mean value profiles. Discussions on the effects of time dependent fluctuations from mean values are presented in the following paragraphs.

Review of Theoretical Studies.—One of the important facts about the atmosphere is that it is usually in a state of constant motion; i.e., an irregular condition of flow in which the various quantities (wind velocity and direction, temperature, humidity, etc.) show random variations with time and space coordinates. The continuous variations can be divided into slow and fast variations compared to some time element relevant to the problem on hand. The slow variations (time independent variations) and the effects on sound wave propagation were discussed in section 3.1.2.1. The effects of fast variations or fluctuations on sound propagation are discussed in the following paragraph.

When a sound wave passes through an atmosphere that contains fluctuations of atmospheric quantities (atmospheric turbulence), two effects will be present: (1) sound velocity fluctuations caused by the temperature fluctuations and (2) random distortions of the wave front due to the convective actions of the velocity fluctuations. These effects in turn lead to two effects: scattering of sound energy and fluctuations in sound wave amplitude and phase. The effect of these phenomena is to direct some of the incident sound energy away from the original propagation direction, resulting in a diminished noise intensity for a receiver located in the original propagation direction.

The phenomenon of excess attenuation associated with the atmospheric turbulence scattering has attracted interest from industry because of its importance in acoustic radar techniques, airplane acoustics, etc. The theory of sound wave scattering, utilized in the following discussions, is based on the approach where turbulence is represented by energy density functions. Among the authors who have used this approach are Tatarski (ref. 18), Kallistratova and Tatarski (ref. 19), Pekeris (ref. 20), Lighthill (ref. 21), Monin (ref. 22), and Batchelor (ref. 23). The work of these authors and others ultimately led to the following scattering cross-section formula

$$\frac{d\sigma(\theta)}{d\Omega} = 2\pi k^4 W \cos^2\theta \left[\frac{E(2k \sin\theta/2)}{c^2} \cos^2\frac{\theta}{2} + \frac{\Phi(2k \sin\theta/2)}{4T^2} \right] \quad (4)$$

where $d\sigma(\theta)/d\Omega$ is the differential scattering cross section (the fraction of the incident acoustic energy scattered into a solid angle $d\Omega$ in the direction of angle θ with respect to the incident direction); k is the acoustic wave number, W is the volume of turbulence which causes the scattering, E and Φ are the energy (power) spectral density functions describing the velocity and temperature fluctuations, respectively, T is the mean absolute temperature, and c is the speed of sound corresponding to T.

Equation (4) indicates that scattering does not occur normal to the incident direction, and back scattering occurs only as a result of turbulent temperature irregularities but not velocity irregularities. The experimental results obtained by Baerg and Schwarz (ref. 24) have shown that equation (4) agrees with test data.

Equation (4) had to be further reduced to a form directly applicable to evaluation of the excess attenuation. This work was performed by DeLoach (ref. 25. Starting with equation (4), DeLoach derives two equations for excess attenuation coefficients: the first for an idealized atmosphere for which the sound wave scattering by turbulence may be treated similar to the X-ray diffraction by crystals (Bragg diffraction) and the second for the real atmosphere for which the Bragg diffraction condition may be considered as only a first approximation. The results are:

$$\alpha_{S,I} = 1910\, k^2 K_L^{-5/3} [C_V^2/c^2 + (0.136\, C_T^2/T^2)] \quad (5)$$

$$\alpha_{S,R} = 602\, [C_V^2/c^2 + 0.136\, (C_T^2/T^2)]\, k^{1/3} [\pi/kL + \sin(\theta_c/2)]^{-5/3} \quad (6)$$

where $\alpha_{S,I}$ and $\alpha_{S,R}$ are the excess attenuation coefficients for ideal and real atmosphere, respectively; $K_L = 2\pi/L$ represents a threshold turbulence wave number, where L is a scale of the turbulence; C_V and C_T are the structure constants for wind shear and thermally induced turbulence, respectively; and θ_c represents the difference between the actual scattering direction and the scattering direction under the Bragg diffraction condition. In equations (5) and (6), the constants are so determined that the unit of α will result in dB/304.8 m (dB/1000 ft) when the parameters are in the International System (SI) of Units.

Equation (5) represents a first-order formula for the coefficient of attenuation caused by scattering in a homogeneous isotropic medium with a low mean flow speed for the case of audio-wavelengths, which are small compared with the eddy size defined by K_L. It is derived utilizing the energy density functions (ref. 25) for the range of K considered; i.e.,

$$E(K) = \frac{11\, \Gamma(8/3) \sin(\pi/3)}{24\pi^2} C_V^2 K^{-11/3} \quad (7)$$

$$\Phi(K) = \frac{\Gamma(8/3)\sin(\pi/3)}{4\pi^2} C_T^2 K^{-11/3} \quad (8)$$

where Γ denotes the Gamma function. However, DeLoach shows that the forms of energy density functions outside this range do not alter the result of equation (5) for a physically realizable turbulence spectrum.

DeLoach finds that the frequency squared dependence of equation (5) cannot explain a good part of available experimental data and concludes that the simple scattering model in the idealized atmosphere is responsible for the discrepancies. Thus, the author derived a modified Bragg equation and used it to derive equation (6). Direct verification of this equation was not made because no test was available in which all of the parameters for evaluation of $\alpha_{S,R}$ were measured. Therefore, by an indirect method, the author showed the validity of the equation.

Depending on the relative magnitude of π/kL compared to sin $(\theta_c/2)$, equation (6) shows that the frequency dependence of $\alpha_{S,R}$ varies between $f^2$and $f^{1/3}$. First, equation (6) reduces to equation (5) when θ_c is equal to zero (the Bragg condition) and then the frequency dependence follows f^2. If π/kL dominates sin $(\theta_c/2)$, $\alpha_{S,R}$ becomes proportional to f^2. If π/kL is much smaller than sin $(\theta_c/2)$, then the frequency dependence becomes milder and tends to follow $f^{1/3}$. DeLoach points out that, except for very low frequencies, a small θ_c would make sin $(\theta_c/2)$ exceed π/kL. Therefore, it is suggested that, if a sound wave is actually scattered in a direction which differs by a small θ_c from the direction it would have been scattered in an idealized medium, the frequency dependence of the excess attenuation coefficient would then be much milder than the f^2 law. DeLoach lists the inhomogeneity and anisotrophy of the real atmosphere as possible reasons for θ_c not being equal to zero.

The results of two example cases of the use of equation (6) are presented in table 3. Both the π/kL and sin $(\theta_c/2)$ terms were included in the calculation. Values of the parameters required for calculation were obtained from reference 25.

Reference 25 also shows that sum of the excess attenuation calculated using equation (6), and that calculated for the molecular, classical, and divergence agree well with the test data. For the two example cases where turbulence levels were relatively high, the order of magnitude of the excess attenuation coefficient is the same as that for the ARP 866 coefficient. Reference 25 further shows that the calculated molecular and classical absorption coefficients are smaller than the ARP coefficients. This shows that the ARP values include sound energy absorption attributable to other causes than the molecular and classical absorption; e.g., the excess attenuation.

Review of Experimental Studies.—Richardson's study (ref. 26) was one of the early studies where measurements of atmospheric turbulence in relation to the propagation of sound were conducted. Turbulence intensities, turbulence eddy diameter, velocity correlation functions, and sound intensity fluctuations caused by atmospheric fluctuation were measured at two locations of extreme weather difference—England and Egypt. Electronic instruments, specially devised for the test, enabled Richardson to record turbulence velocity as a function of mean velocity, turbulence intensity versus temperature lapse rate, sound intensity decrements versus turbulence intensity, etc.

Table 3.—Example Calculation of Excess Attenuation Coefficient

	Case 1		Case 2	
C_V, $m^{2/3}/s$	0.34		0.15	
C_T, ° $C/m^{1/3}$	0.17		0.17	
c, m/s	344.9		336	
T, ° C	21.5		5.5	
L, m	150		72	
θ_c, deg	1.2		0.65	
Frequency, Hz	Attenuation coefficient, dB/100 m			
	Equation (6)	ARP 866	Equation (6)	ARP 866
1000	0.89	0.55	0.41	0.50
800	0.79	0.44	0.34	0.39
500	0.60	0.27	0.21	0.24
250	0.36	0.13	0.09	0.12
125	0.18	0.07	0.03	0.06

Another investigation that dealt with noise measurement in conjunction with micrometeorological measurements was that of Schilling, et al. (ref. 27). In the Schilling, et al.'s test, whistles operated by compressed air or nitrogen were used as noise sources. The authors found as one of their most significant conclusions that the lower layer of the atmosphere was a scattering medium. Thin nickel wire resistance thermometers, hot wire anemometers, and wind-velocity-difference meters of rapid response were used for the measurement of micrometeorological quantities. In addition to the shadow zone effect, the absorption effect, the effects of scattering, etc., were obtained.

A review published by Ingard (ref. 28) clearly explains various aspects of the influence of meteorological conditions on sound wave propagation. It should be noted that Ingard presents a plot of noise attenuation caused by turbulence as a function of frequency for different gustiness. The trend of the attenuation computed from this plot is found to be proportional to the cube root of sound wave frequency.

A considerable improvement in experimental technique and instruments used in the search for turbulence effects can be found in reference 29. Part I of this reference reports on a field measurement of noise attenuation; Part II is a laboratory experiment on scattering of sound by turbulence. An electrically driven exponential horn was used in Part I to represent a noncollimated sound located on the ground and directed toward a height of 19 m where the last microphone was located. The distance between the source and the last microphone was approximately 1220 m between which 10 additional microphones were positioned. Pure tone trains were issued, and noise levels were measured, properly gating each microphone. Mean wind velocities were also simultaneously recorded. In general, the scatter attenuation extracted from the test data showed increasing attenuation at increasing frequency and wind velocity.

Part II used an electrostatic speaker that generated a collimated beam of sound, a turbulence generator which utilized a cluster of centrifugal blowers, and specially designed electronic instruments. The test results showed that the time-averaged scattered noise intensity became weaker as it departed from the sound beam direction (tested up to 25^{0}), but for all cases tested it was observed that there was a finite probability that the scattered noise intensity would actually exceed the nonturbulence scattered sound beam intensity in a given direction.

Baerg and Schwarz (ref. 24) and Hunter (ref. 30) conducted similar tests to measure the scattering sound from turbulence. Both used a small nozzle or wind tunnel, upstream of which was a grid work for generation of turbulence. Baerg and Schwarz heated the grid to induce thermal fluctuations. In Baerg and Schwarz's test, the noise source and receiver were positioned outside the nozzle flow, whereas they were within the wind tunnel in Hunter's test. Baerg and Schwarz found an excellent agreement in the differential-scattering cross section between the test data and theory.

An outdoor measurement of the acoustic attenuation in the turbulent atmosphere was recently conducted by Aubry and Baudin (ref. 31). In the experiment, a tethered balloon was used to carry microphones, meteorological probes, and telemetry transmitters to various altitudes from about 100 m to 900 m. A horn noise source mounted on a turret

was located on the ground. During the tests, the horn was continuously aimed nearly vertically toward the microphones. The meteorological measurements were made by the use of fast response thermistance, hygristor, and a cup anemometer. The authors compared the total measured attenuations with the computed total attenuations (molecular, classical, and divergence) in an attempt to isolate the excess attenuation. It was concluded that the excess attenuation was generally smaller than the uncertainty in the molecular attenuation calculation. A similar outdoor test has been reported in reference 32. However, the final report of this work is not available at this time.

3.1.3 EFFECTS OF THE PROXIMITY OF SOLID SURFACES

Solid surfaces that invariably exist in the jet noise propagation field generate various and, in many cases, difficult problems. Reflection and diffraction of sound waves, absorption and transmission of sound energy, and generation of extraneous noise caused by jet-flow induced aerodynamics are some of the problems. These can cause changes in the jet noise levels measured from an airplane inflight from that measured statically.

Theories that explain the fundamentals of most of the effects are available. But in general, application of these theories to the actual cases is not easy because of the variety of surface conditions and the complex geometrical relationship between the jet and the surfaces. Two topics, which are believed to be the most important effects on the jet noise field between a ground observer and a flying airplane, were selected for detailed study.

3.1.3.1 Microphone Placement Effect

Considerable experience and empirical data have been accumulated by Boeing on the use of the microphones installed very close to the ground (ground microphones). The ground microphones have many advantages over the conventionally mounted high microphones. The ground microphone technique not only eliminates most of the ground reflection effect on the measured noise levels in the low frequency ranges but has demonstrated better data repeatability.

Additional Ground Microphone Test Data.—Examples of ground microphone data are presented in figures 12 through 14. Figure 12 (from ref. 33) shows data from a JT8D-1 engine tested at the Boeing Boardman, Oregon, test site. This site has a concrete surface from the engine stand to the microphone positions. The high microphones used had a height equal to the engine centerline height, approximately 3.5 m. The ground microphones were installed 1.3 cm above the concrete surface with the diaphragms pointing downward.

The plots in figure 12 show that the augmentation and cancellation of sound waves in the low frequency range are eliminated for the ground microphone data, and the difference between the high and ground microphone noise levels at the high frequency range is approximately 3 dB, which is explained by theory. Theory shows that, for an incoherent distributed noise source, the high microphone will have a 3-dB noise increase over freefield by energy doubling, whereas the ground microphone will have a 6-dB increase due to pressure doubling.

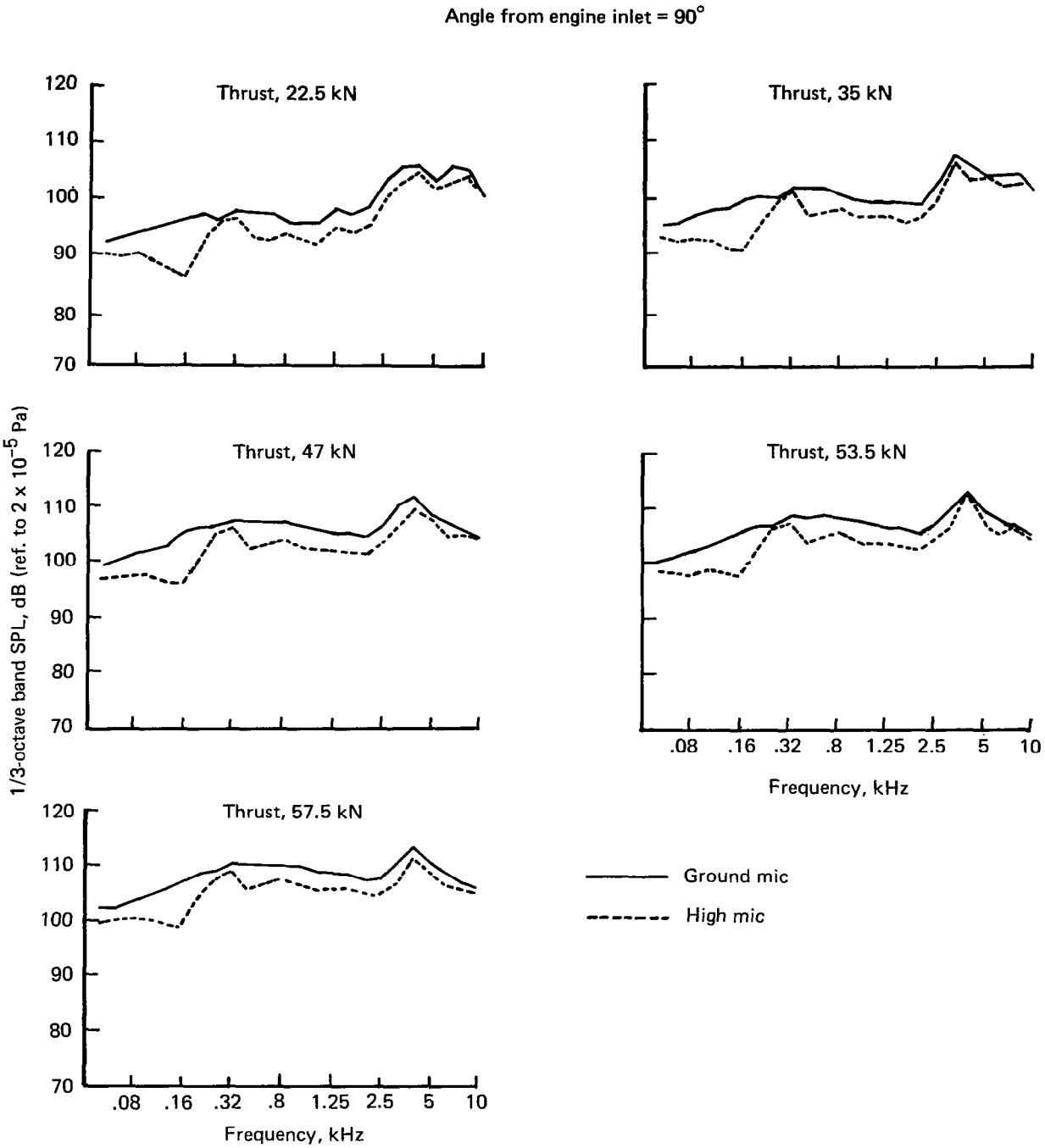

Figure 12.—Spectrum Comparison, High Microphone Versus Ground Microphone

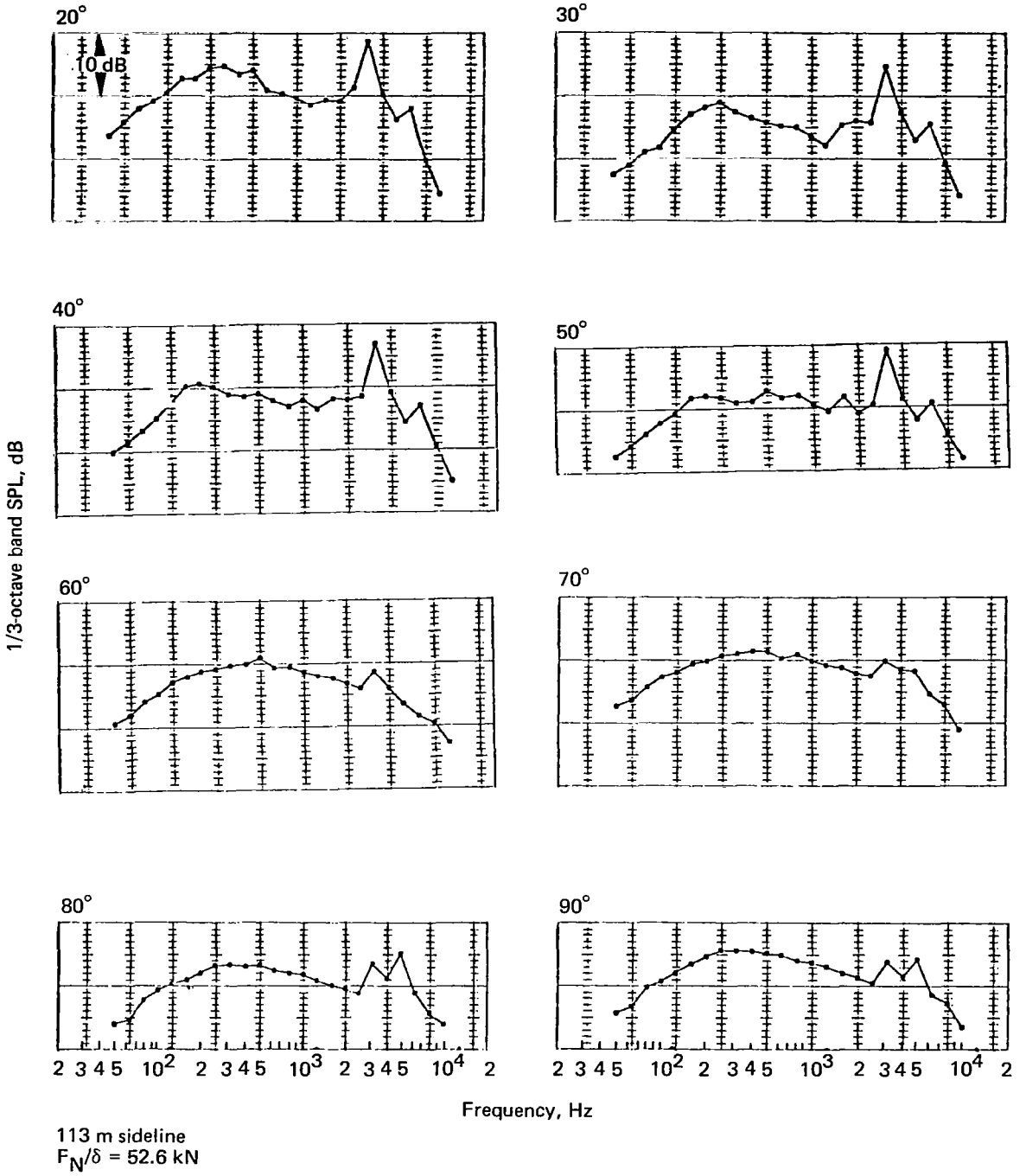

Figure 13.—Noise Data Obtained by Ground Microphones, JT8D-9 Baseline, (θ = 20° - 90°)

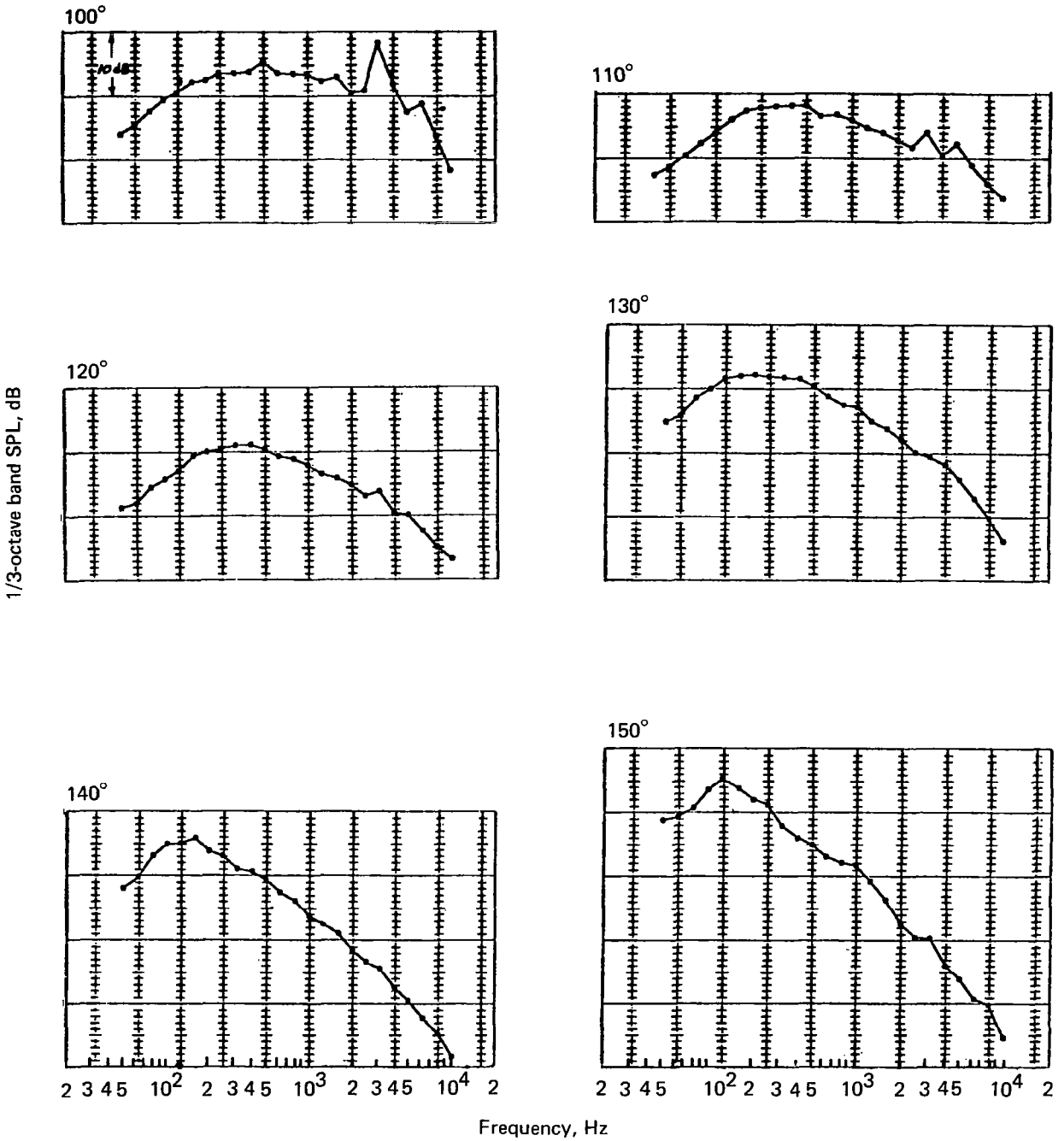

Figure 14.— Noise Data Obtained by Ground Microphones, JT8D-9 Baseline, ($\theta = 100^0 - 150^0$)

Figures 13 and 14 show other Boardman ground microphone data with a JT8D-9 engine. They also show reflection-free noise spectra at all radiation angles from 10° to 150°, measured with reference to the engine inlet centerline.

The reflection phenomena (ref. 34) are depicted in figure 15, for the Boardman facility. The results of the theoretical prediction show that the high microphone has the first destructive reflection effect at a lower frequency than that for the ground microphone, because the length difference between the direct and reflected paths is larger with the high microphone. Since the actual jet noise source is an incoherent distributed source, both curves ultimately oscillate around the 3-dB level as seen from the curve for the high microphone.

Figure 16 shows examples of Boardman high and ground microphone data simultaneously recorded during a recent test. For this test, the centerline height microphones were at 3.05 m (10 ft) sideline, and the ground microphones were at 30.5 m (100 ft) sideline. Because of the large difference in the direct and reflected noise paths and consequent reduction in noise level of the reflected paths, the noise level measured by the 3.05 m (10 ft) high microphones can be considered to be freefield. Since the path difference was small, the 30.5 m (100 ft) sideline ground microphone had the 6-dB pressure doubling for most of the frequency range. Therefore, this difference was applied in converting the 30.5 m (100 ft) sideline noise level to that for the 3.05 m (10 ft) sideline freefield condition.

For the 3.05 m (10 ft) sideline microphones, the jet noise source cannot be approximated as a point source because the noise source spread is larger in comparison to the microphone distance. Thus, in plotting the curves in figure 16, the equivalent radiation angles of the near-field microphones (compared to that for the far field) were estimated. In general, the extension downstream of the jet noise source makes the equivalent radiation angles of the near-field microphones smaller than the angles for the far field.

The plots in figure 16 are additional examples proving that the ground microphones can be used for measuring the freefield noise data, moving the ground reflection effects far into the high frequency range.

Limitations of the Technique and Recommended Solutions.—Studies have been conducted to investigate the limitations of the ground microphone technique (ref. 13). Knowledge gained and recommendations reached through this study and others are discussed in the following paragraphs.

A test setup was arranged in a Boeing anechoic room to investigate the effects of microphone height and the extent of the hard reflecting surface (fig. 17). The noise was from a broadband source that had a frequency bandwidth from 400 Hz to 20 kHz.

Variations of 1/3-octave-band noise spectra as the microphone height was varied are presented in figure 18. As the height was reduced, the first cancellation frequency moved from low to high frequency; the cancellation frequencies recorded closely agreed with the computed values (1340, 2680, 5370, 10 720 Hz). The difference in noise levels between the source height and ground microphone data at higher frequencies is close to 3 dB, as previously discussed.

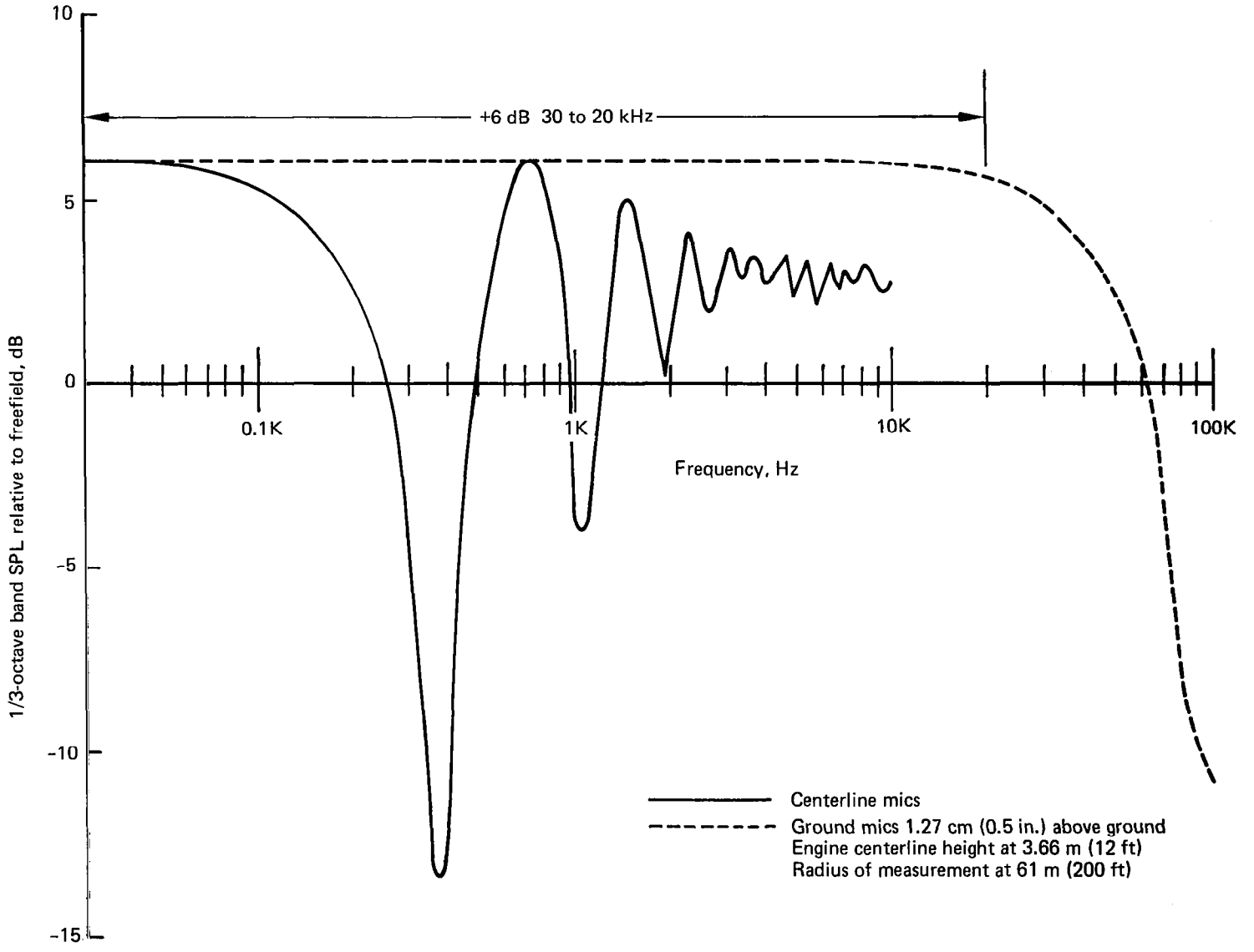

Figure 15.— Calculated Reflection Interference Effects, Incoherent Sources Distributed Within a Circle, Hard Reflecting Surface (ref. 35)

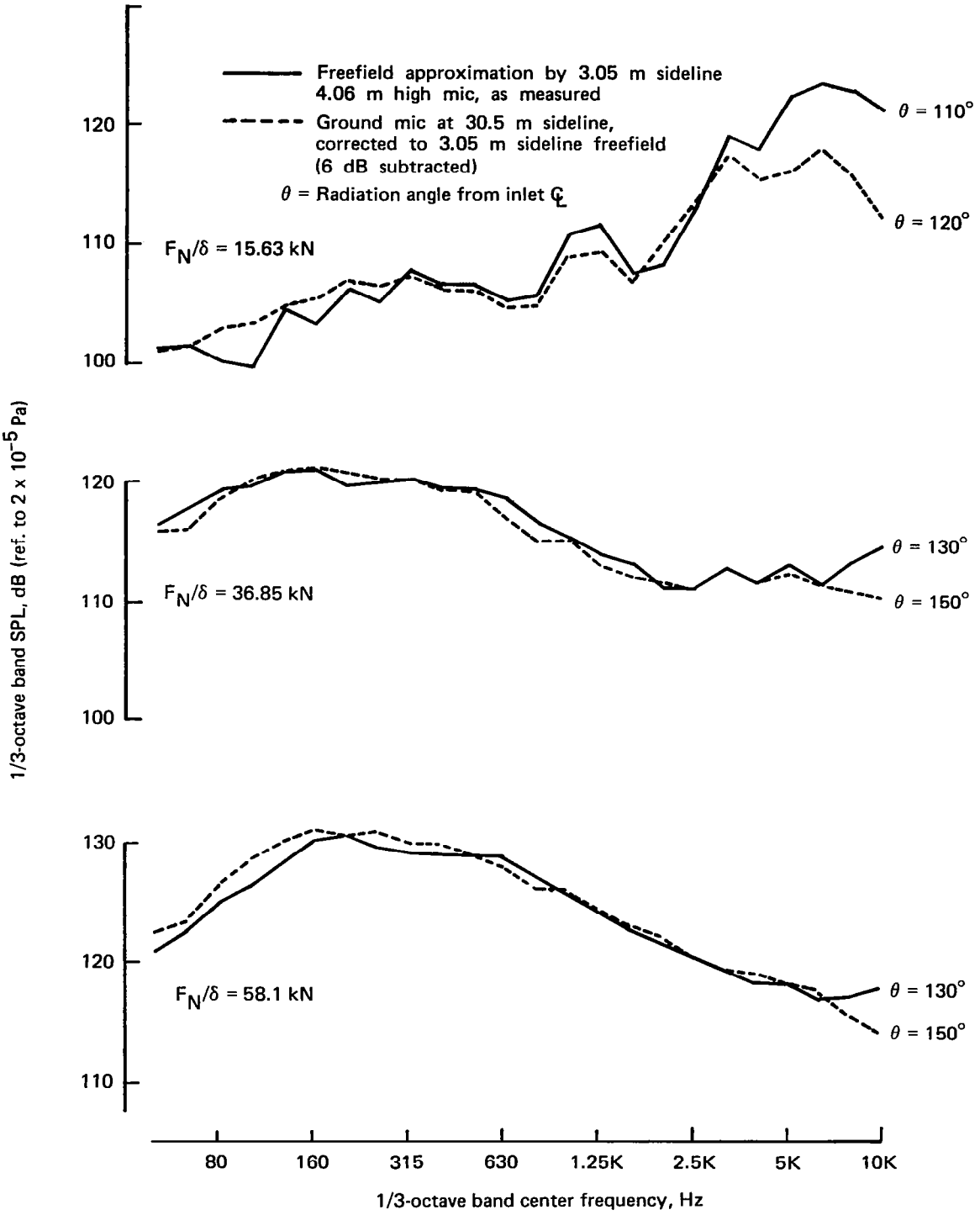

Figure 16.—Comparison Between Approximated Freefield and Ground Microphone Spectra, JT8D-1 Baseline

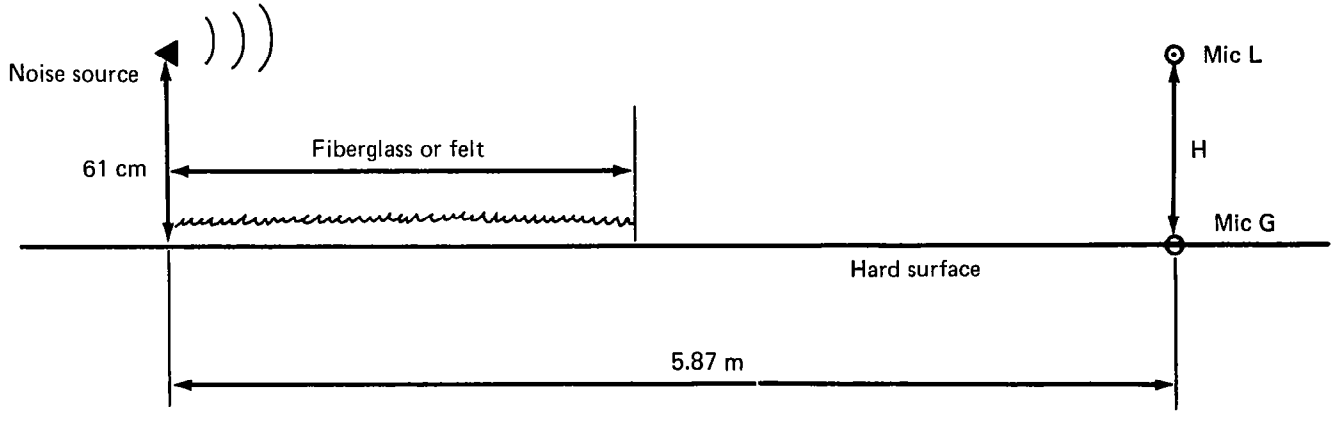

Figure 17.—Anechoic Room Test Installation to Measure Ground Surface Effects

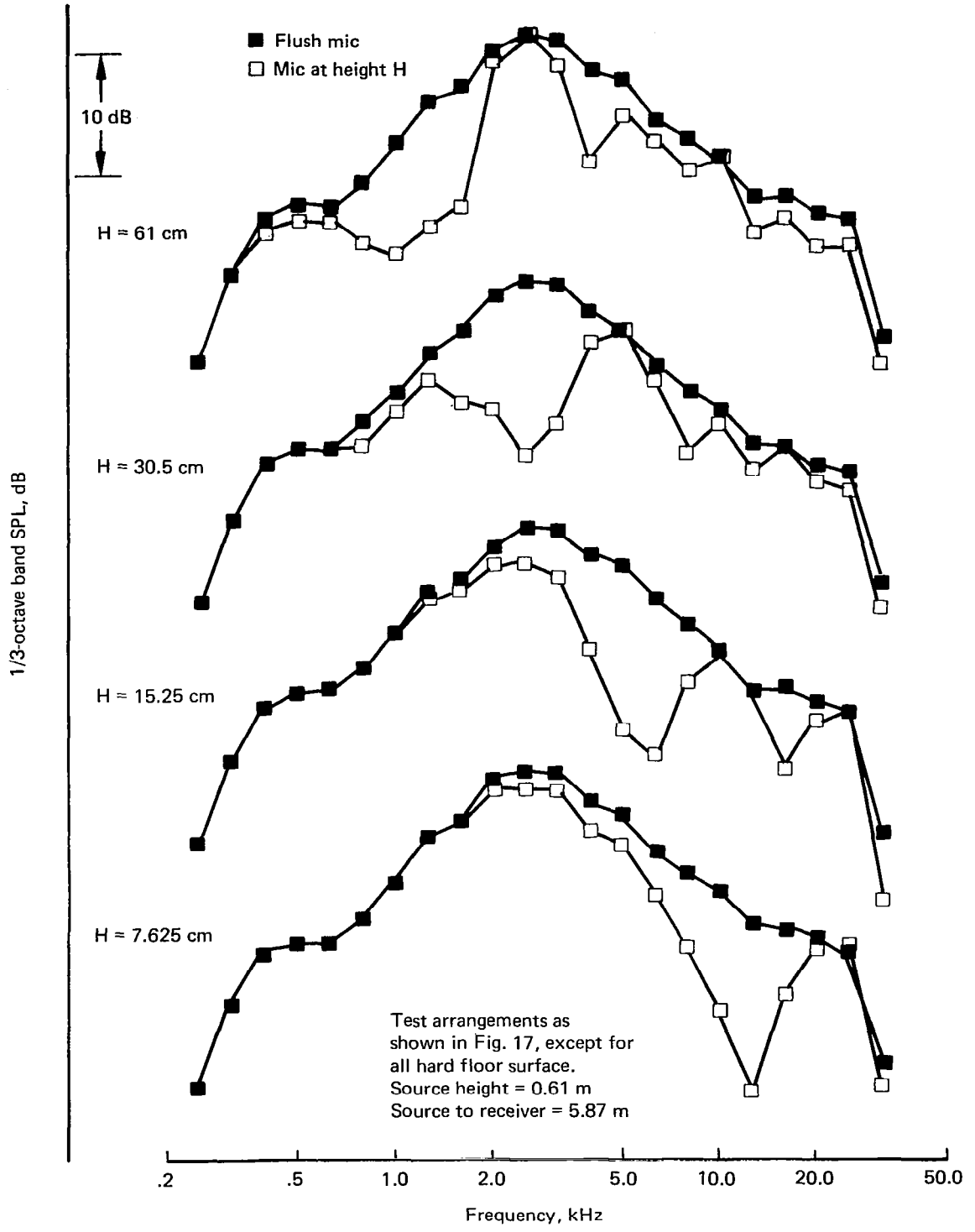

Figure 18.—Effects of Microphone Height

Figure 19 shows the effect of expanse of hard surface between a ground microphone and the noise source. It shows that the measured noise data are strongly affected by the amount of soft surface existing between the source and receiver, suggesting that sound wave cancellation and augmentation may not follow a simple theory in such cases. The test result indicates that for the complete advantage of 6-dB pressure doubling a hard surface covering the entire distance between the source and receiver is required. The Boardman test site has a concrete surface which meets this requirement for normal acoustic testing.

Another interesting point to note from the test data is that, for very low frequencies (below about 300 Hz for this case), the 6-dB rise is realized for all configurations.

The ground microphone is easily influenced by the atmospheric variations near the ground, which can result in unacceptable test data. The major cause for the adverse effect is the formation of a shadow zone due to acoustic ray bending as discussed in section 3.1.2.1. Two theoretical sample cases of acoustic ray bending, extracted from reference 13, are presented in figure 20. It may be seen in figure 20b that a ground microphone located 48.8 m (160 ft) away from a noise source for the example case may not receive any noise signal.

Figure 21 is a summary plot showing the extent of the shadow zone obtained from a number of plots similar to figure 20 with a negative wind vector (wind speed component along sound path against direction of sound travel). It indicates that shadow zone formation must be closely monitored during the use of a ground microphone system when there is a negative wind. More favorable situations are predictable with a positive wind, but wind conditions frequently encountered at the open test sites preclude reliance on the desirable wind direction.

A monitoring system that assures acquisition of the proper quality data by the use of a ground microphone system is presented in reference 13. This system can be used on-line and does not require measurements of meteorological properties for its use. The system utilizes the characteristics of the high and ground microphones shown in figure 15. Actual noise measurements by a high microphone and a ground microphone located at positions with the same radiation angle and horizontal distance are shown in figure 22. The difference sound pressure level (SPL) spectra obtained from the absolute SPL spectra (fig. 22a) reveal similar features to the theoretical features shown in figure 15, indicating that the measured data are of an acceptable quality. In contrast to this, figure 22b shows a case with unacceptable or questionable quality.

Based on these findings, an on-line acoustic data system that could display absolute and difference SPL spectra from high and ground microphones at one location (ref. 13) was developed. This system comprised a general radio real-time analyzer, a PDP8 computer, and a teletype for displaying the computed data. A sample of the difference SPL spectra obtained by use of such a system is presented in figure 23.

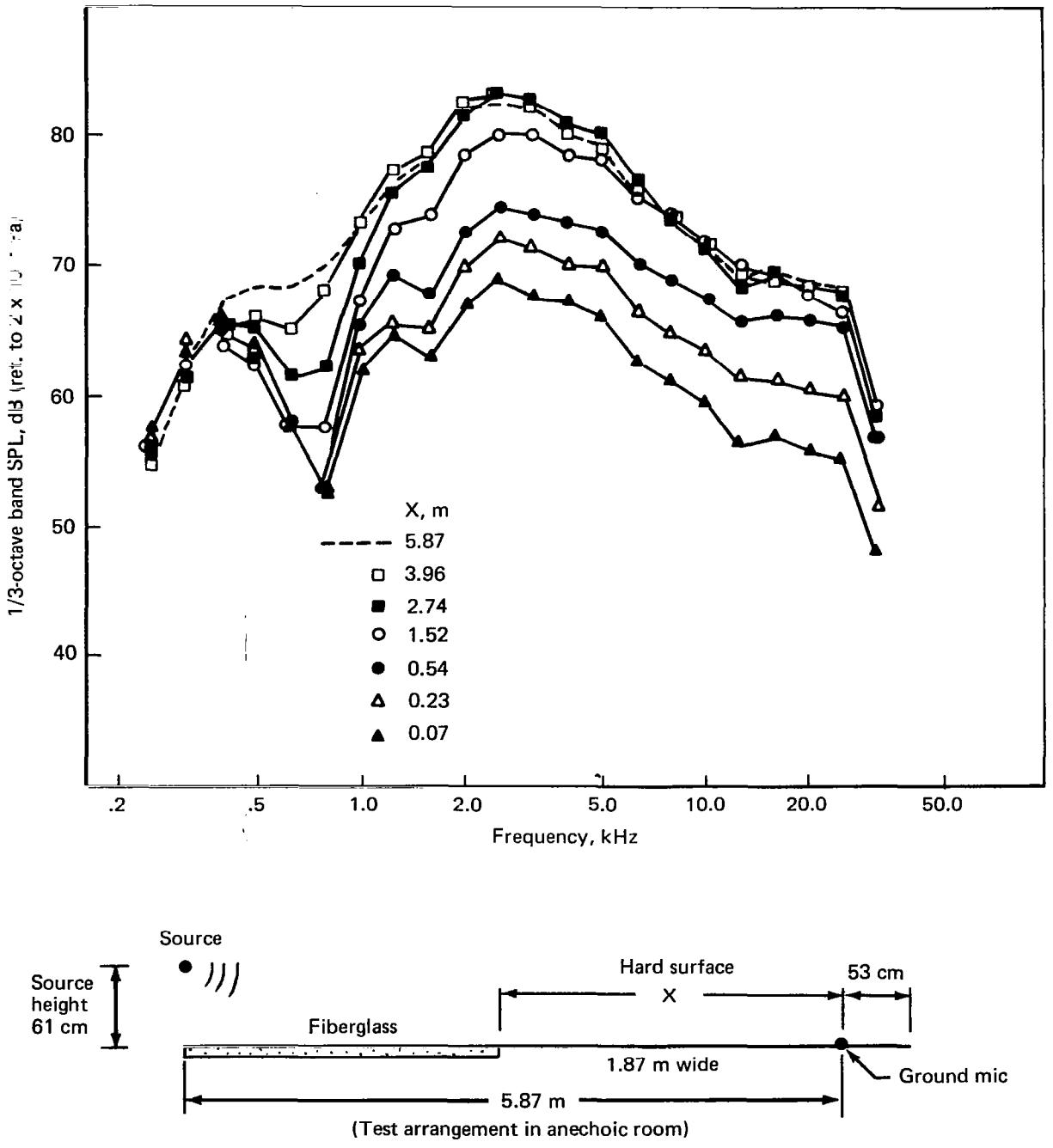

Figure 19.—Effect of Decreasing Hard Surface Length on Microphone Response

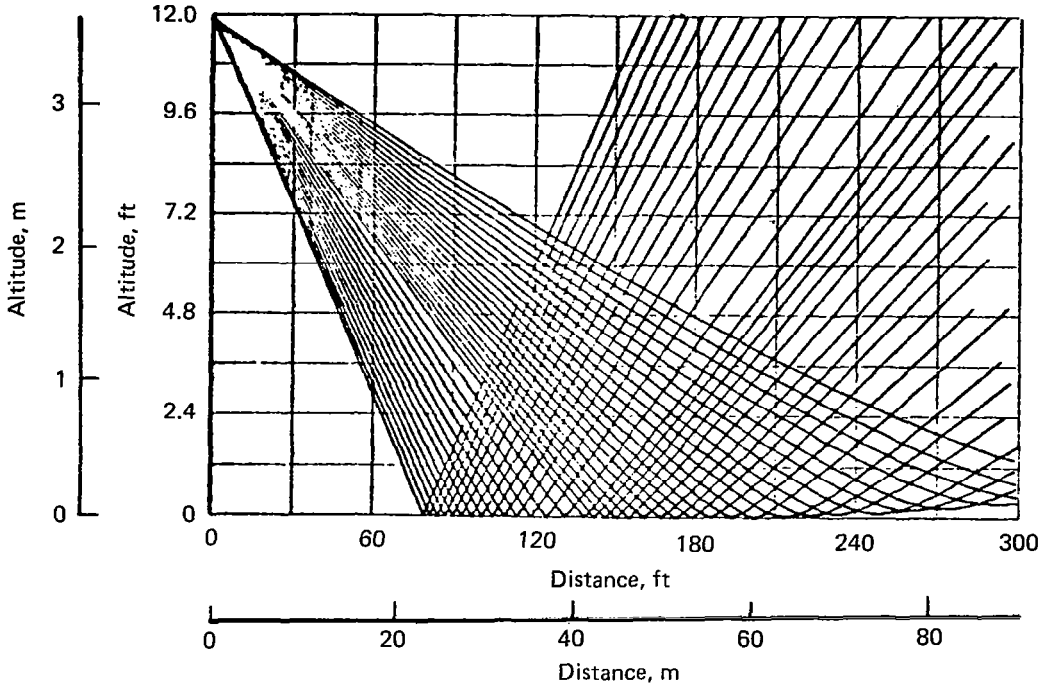

(a) Negative Wind Vector 1.5 m/s, Temperature Neutral*

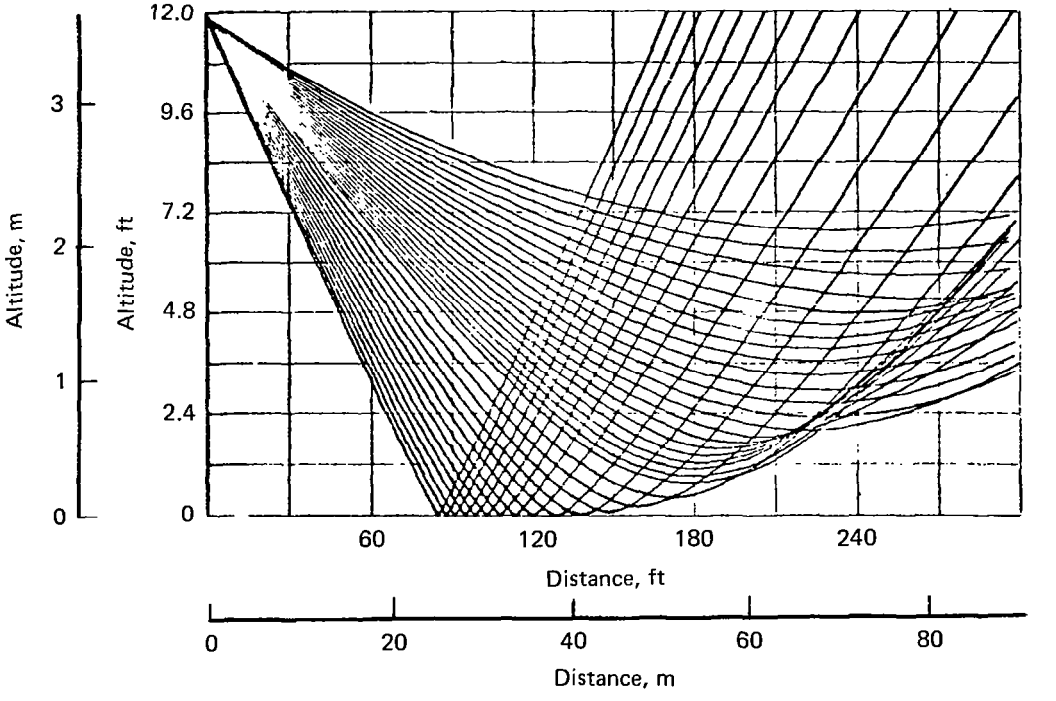

(b) Negative Wind Vector 1.5 m/s, Temperature Lapse*

*For assumed profiles, see reference 13

Figure 20.—Acoustic Ray Tracing

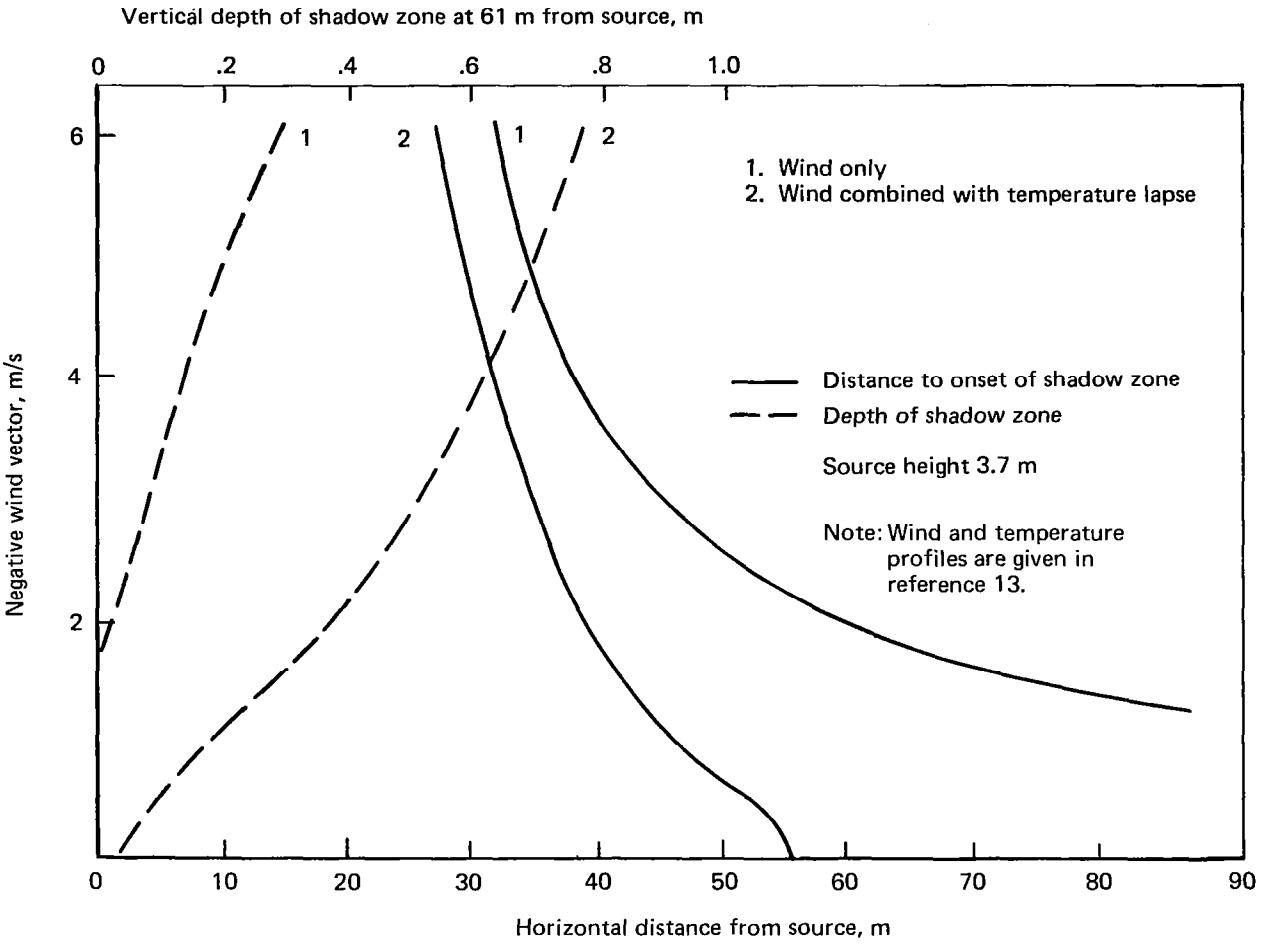

Figure 21.—Extent and Depth of Shadow Zone as a Function of Negative Vector Wind With and Without Temperature Lapse

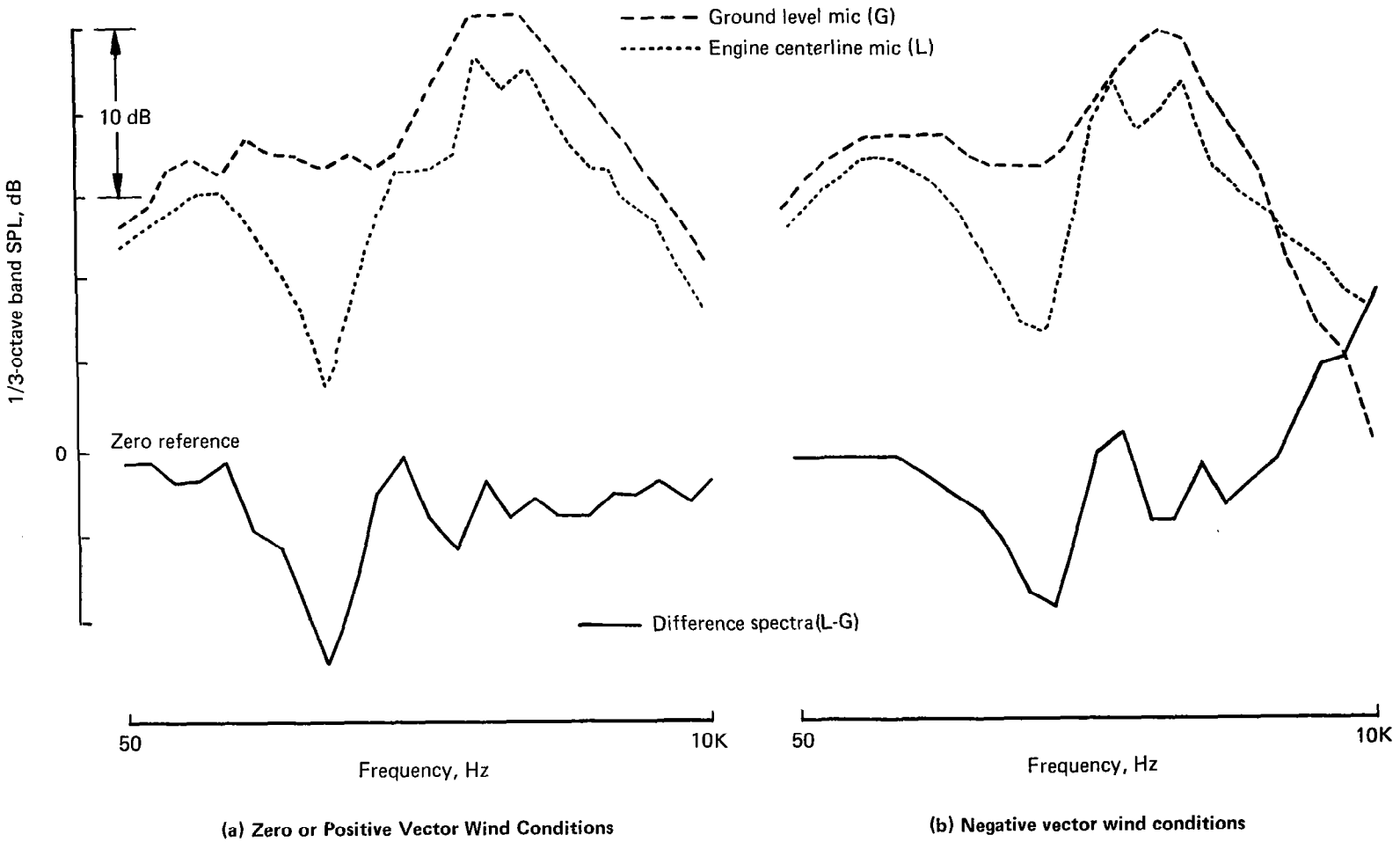

Figure 22.—Absolute and Difference SPL Spectra for Positive and Negative Wind Vectors

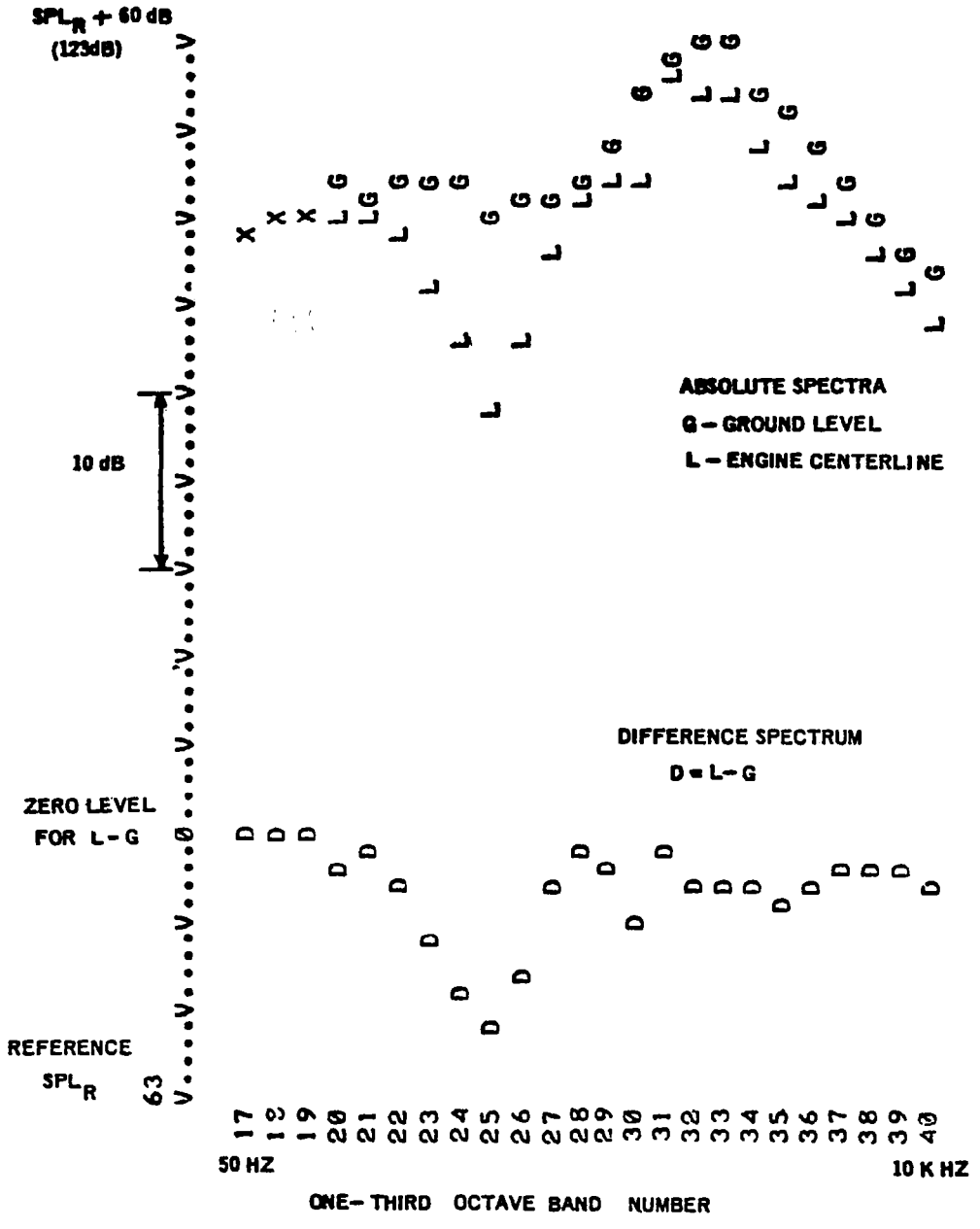

Figure 23.—On-Line Data Sample: Absolute and Difference SPL Spectra

Experience with the monitoring system has shown that it is valuable not only for assuring the quality of the ground microphone data but also for establishing acceptable atmospheric conditions for testing.

Combination of High and Ground Microphone Data.—The required expanse of hard surface and the associated cost for constructing such surfaces and the susceptibility to atmospheric conditions of the ground microphones, discussed previously, have motivated searches for another solution for acquiring reflection free noise data. One result of this search is to combine data taken by both the engine centerline height microphones and the ground microphones.

It was found that a limited area of hard reflecting surface around a ground microphone would provide the 6-dB pressure doubling in the very low frequency range (fig. 19). Theory reveals that the reflection interference effects, similar to those shown in figure 15, are also present for a soft surface, although the frequencies of noise cancellation and augmentation and the degree of noise interference vary as functions of surface characteristics. These findings suggested that the data from the ground microphone with a small reflecting surface and the data from the engine centerline height microphone may be combined to obtain a composite spectra.

Validity of this idea was studied at the Tulalip test site with data from a JT9D engine. The ground microphone reflection surface for this test had dimensions of 2.4 x 3.7 m (8 ft x 12 ft), and the rest of the ground between source and microphones was covered with egg-size gravel. The points shown in figure 24 for various power settings and figure 25 for different radiation angles are the test data points obtained by the high and ground microphones. The SPL spectrum curves shown were generated by combining the data and inserting segments of smooth curves in between the high and low frequency regions.

The process for selecting portions from each of the ground and high microphone noise data and combining the two to obtain a composite curve is based on the reasoning that the ground microphone will provide the 6-dB pressure doubling at low frequencies while the high microphones will provide the energy doubling (2 to 4 dB) at high frequencies. Theory and experimental data presented in reference 35 show that the pressure doubling is achieved at frequencies below a frequency satisfying the equation $\Delta r/\lambda \approx 0.1$ and the energy doubling, at frequencies above a frequency satisfying $\Delta r/\lambda \approx 1.7$, where Δr is the difference between the reflected sound path and the direct sound path from the noise source to microphone, and λ is the sound wave length.

Application of these equations to the Tulalip test arrangement resulted in 200 Hz for $\Delta r/\lambda \approx 0.1$ and 630 Hz for $\Delta r/\lambda \approx 1.7$, which are used as the general boundary in constructing the composite curves. Theory and test data also show that the noise levels of ground microphones at frequencies above 200 Hz and that of high microphones at frequencies below 630 Hz are oscillatory, being subjected to the augmentation and cancellation effects of ground reflection (see fig. 15).

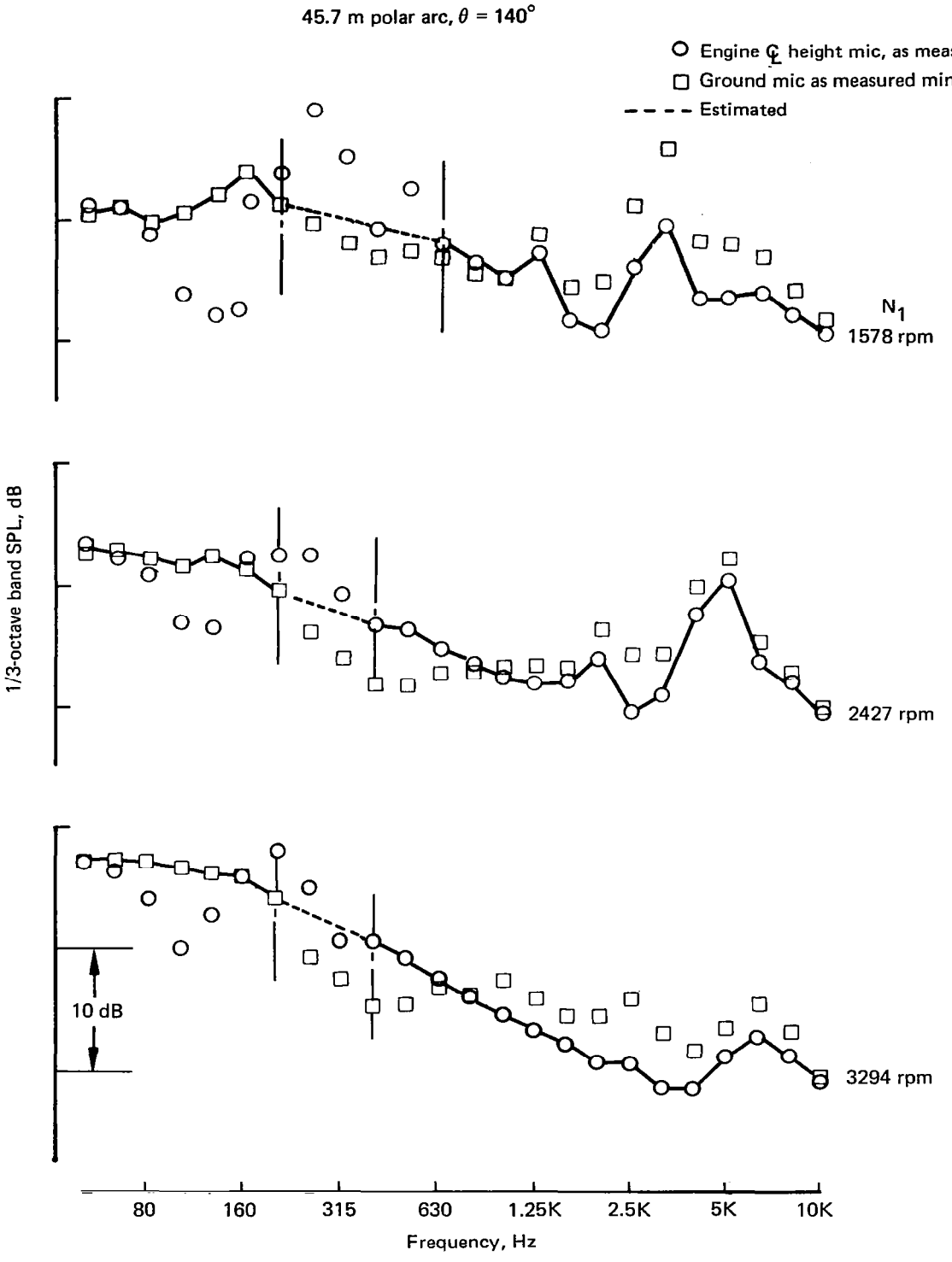

Figure 24.—Combination of High and Ground Microphone Noise Data, JT9D Engine, θ = 140°

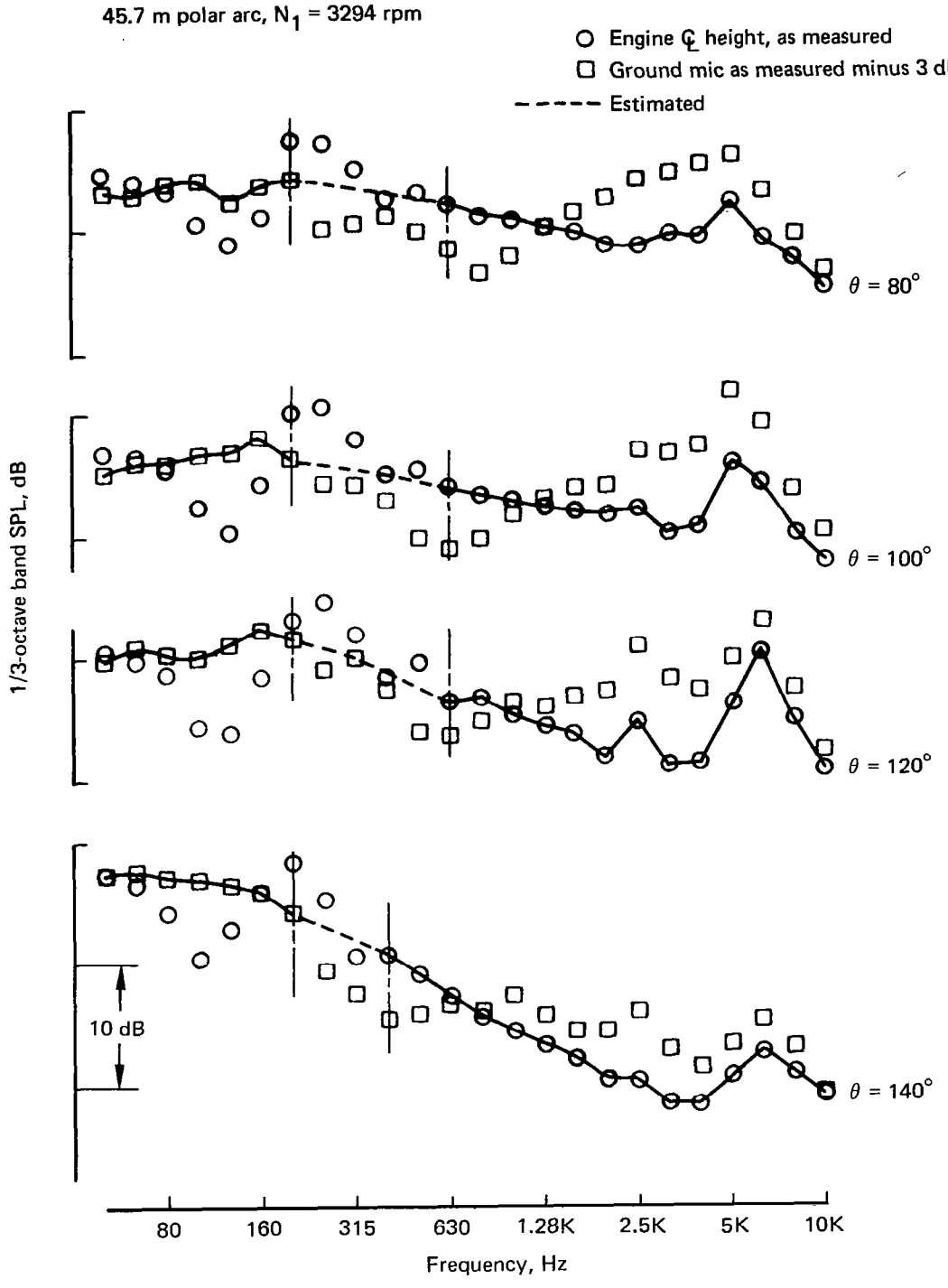

Figure 25.—Combination of High and Ground Microphone Noise Data, JT9D Engine, N_1 = 3294 rpm

The composite curves, shown in figures 24 and 25, compare reasonably well with those ground microphone data presented in figures 12, 13, 14, and 16, which are the data taken with hard surface from noise source to microphone. One clear advantage of the combined curves is the elimination of sound level fluctuations at the lower frequency range. The example has thus substantiated a definite possibility of the practical use of combining the ground and high microphone data. Therefore, it is recommended that this technique be considered for use when a hard surfaced acoustic arena is not available.

3.1.3.2 Engine Installation Effects

Evaluation of engine installation effects is one of the more difficult problems included in the study of the effects of motion on jet noise from aircraft. It involves a variety of installation configurations and types of jets and aerodynamic and acoustic phenomena in static and in-flight conditions. In this study, some fundamentals of the problem are discussed. The installation effects at static condition are discussed first. Test methods for installation effects in flight are then discussed. Recommended future work is presented at the end of the section.

Comparisons of Jet Noise From Installed and Uninstalled Engines on the Ground.–The knowledge of engine installation effects on the jet noise from a static airplane is a valuable first step in the analysis and understanding of the flight effects on jet noise. A model test is a good substitute for a full-scale airplane test, but lack of a complete similarity in the installation configuration often is a cause for uncertainty about the test data.

Two tests are described in the following paragraphs which provide information regarding the installation effects on the noise level of static airplane. The first test is of a 727-100 airplane with JT8D-9 engines, and the second is of a 747-100 airplane with JT9D-3 engines.

For the 727 test the airplane was parked on a ground runup apron and one of the side engines and the center engine were separately operated, and the jet noise was recorded. A plan view of the airplane and the microphone arrays is shown in figure 26. Also indicated in the figure are the radiation angles of the microphones with respect to the side- and center-engine nozzles. Some of the microphones were not at the exact angles designated, but the discrepancies were within ± 2 degrees.

The uninstalled noise data used in the comparison were from a ground static test condition at the Boeing Boardman full-scale engine test facility. The microphones used for this test were 30.48-m (100-ft) sideline ground microphones, as were those for the 727-100 airplane ground runup test. The centerline height of the uninstalled engine nozzle for the Boardman static test as well as for the installed engine nozzles was approximately 4 m (13 ft). This geometrical similarity with regard to the jet noise source and microphone positions to the hard ground surface provided an equal basis for noise comparison, eliminating the possible differences in the ground reflection effects.

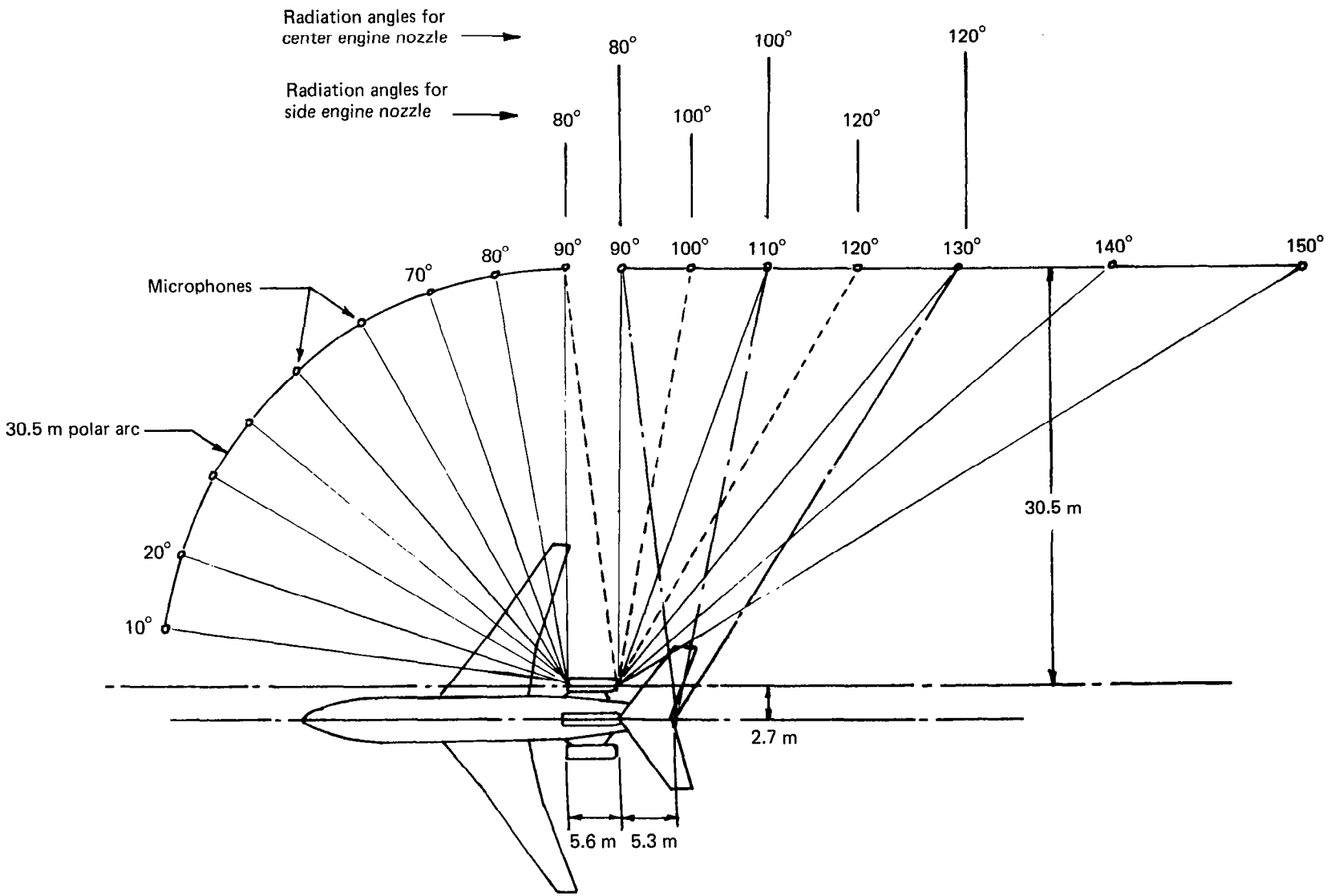

Figure 26.—Microphone Arrays for 727-100 Ground Runup Test

Comparisons of the installed and uninstalled JT8D-9 engine jet noise are presented in figures 27 and 28. Figure 27 shows data for the side engine (baseline), and figure 28 shows data for the center engine (baseline).

As seen in these figures, the disagreement between the jet noise (50 to 1000 Hz) of the installed and uninstalled engines is comparatively small, indicating that there are no differences consistent enough to suggest that the installed engine jet noise should not be the same as that for the uninstalled engine.

The second test comparison is not as conclusive as the first. The installed JT9D-3 engine noise (only full-octave-band data was readily available) was measured from the no. 1 engine of a 747-100 airplane on a runway apron with a hard surface. The uninstalled JT9D-3 engine noise was measured at the Boeing Tulalip test site. This site has the ground surface covered with egg-size gravel. Neither the nozzle centerline nor the microphone heights from the ground were the same for the two tests. Thus, the measured data had to be converted to a comparable basis: 61-m (200-ft) polar arc freefield noise. Evaluation of the ground reflection effects was made by referring to reference 34.

The corrected results for two radiation angles are presented in figure 29. The data suggests some similarity in spectral shapes between the installed and uninstalled noise. Definite conclusions, however, cannot be drawn without more extensive data.

Wing Shielding Effect Test in a Free-Jet Wind Tunnel.—The tests described in the previous sections were performed without the surrounding airflow; therefore, the test data do not include the effects of the forward motion of the aircraft on jet noise. One method of investigating the shielding effects with the surrounding airflow is to test a model in a free-jet wind tunnel.

Results on the wing-shielding effect as a function of forward velocity are available in reference 36. A schematic drawing of the test arrangement of this study is shown in figure 30. The test was conducted by Boeing and Pratt and Whitney. The engine model (powered nacelle) consisted of a model fan and a compressed air powered turbine.

Several parameters were varied in this study; e.g., the tunnel wind velocity, the nacelle location, the model fan rpm, and wing-on and wing-off configurations. Two sample noise spectra showing the effects of wing shielding with and without wind tunnel flow are presented in figure 31. A substantial reduction in noise due to wing shielding is evident from this figure both with and without wind tunnel flow. However, it indicates that tunnel flow causes no significant change in the spectral level.

Wing-Shielding Effect Tests in Flight.—A light airplane test has been conducted by Boeing to provide preliminary information on flight effects on wing-shielding (ref. 36). The test was designed to simulate an overwing engine installation. The noise source was an electrically operated horn that could generate 1/3-octave-band broadband noise by means of a 1/3-octave-band filter network. This horn was mounted at representative positions on the light airplane wing to simulate the noise source to wing relationship. Two such arrangements are shown in figure 32.

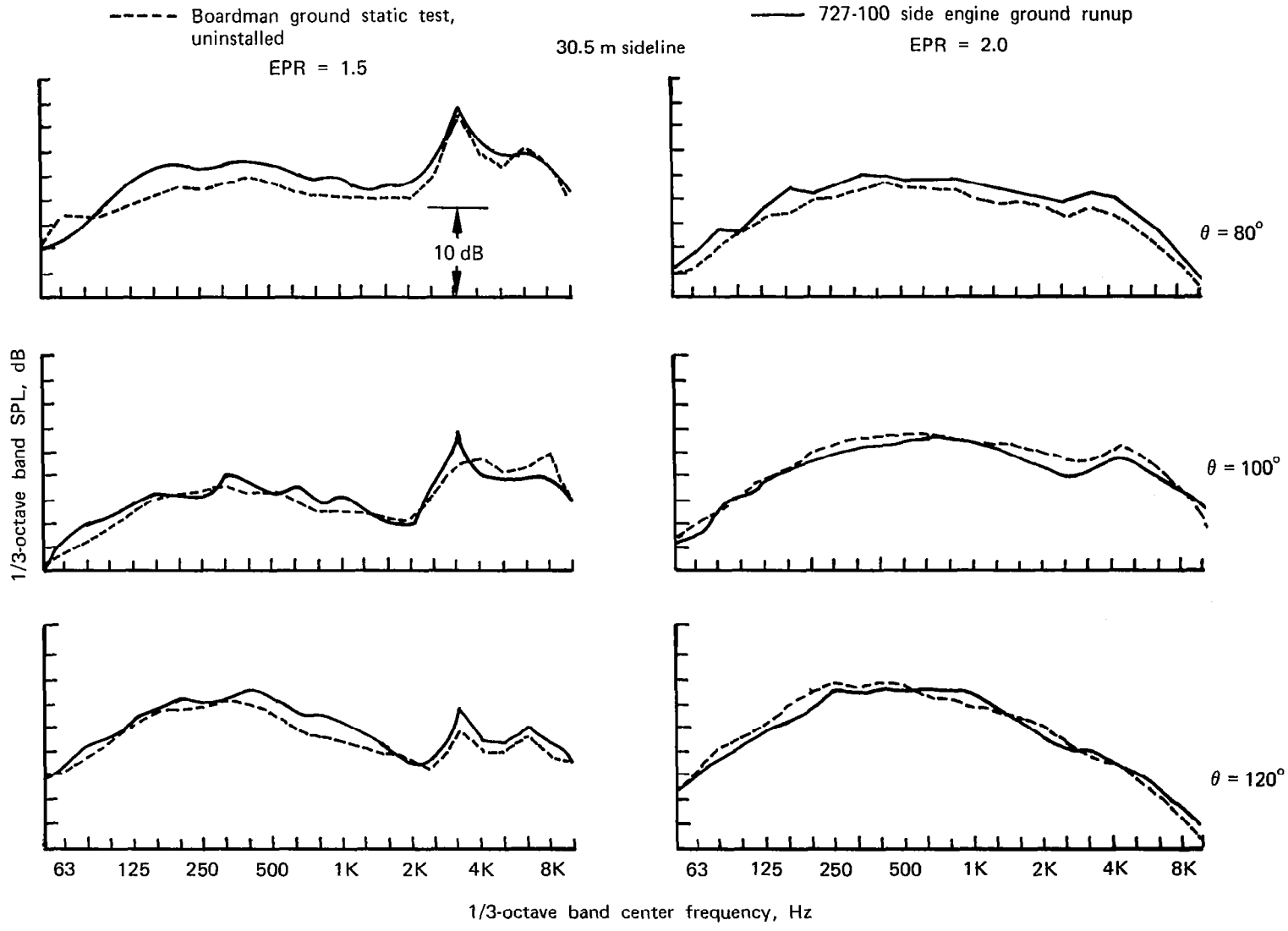

Figure 27.—Comparison Between Installed and Uninstalled Engine Noise Levels (Approximately Same Nozzle ℄ Height and Ground Mic), JT8D-9 Baseline

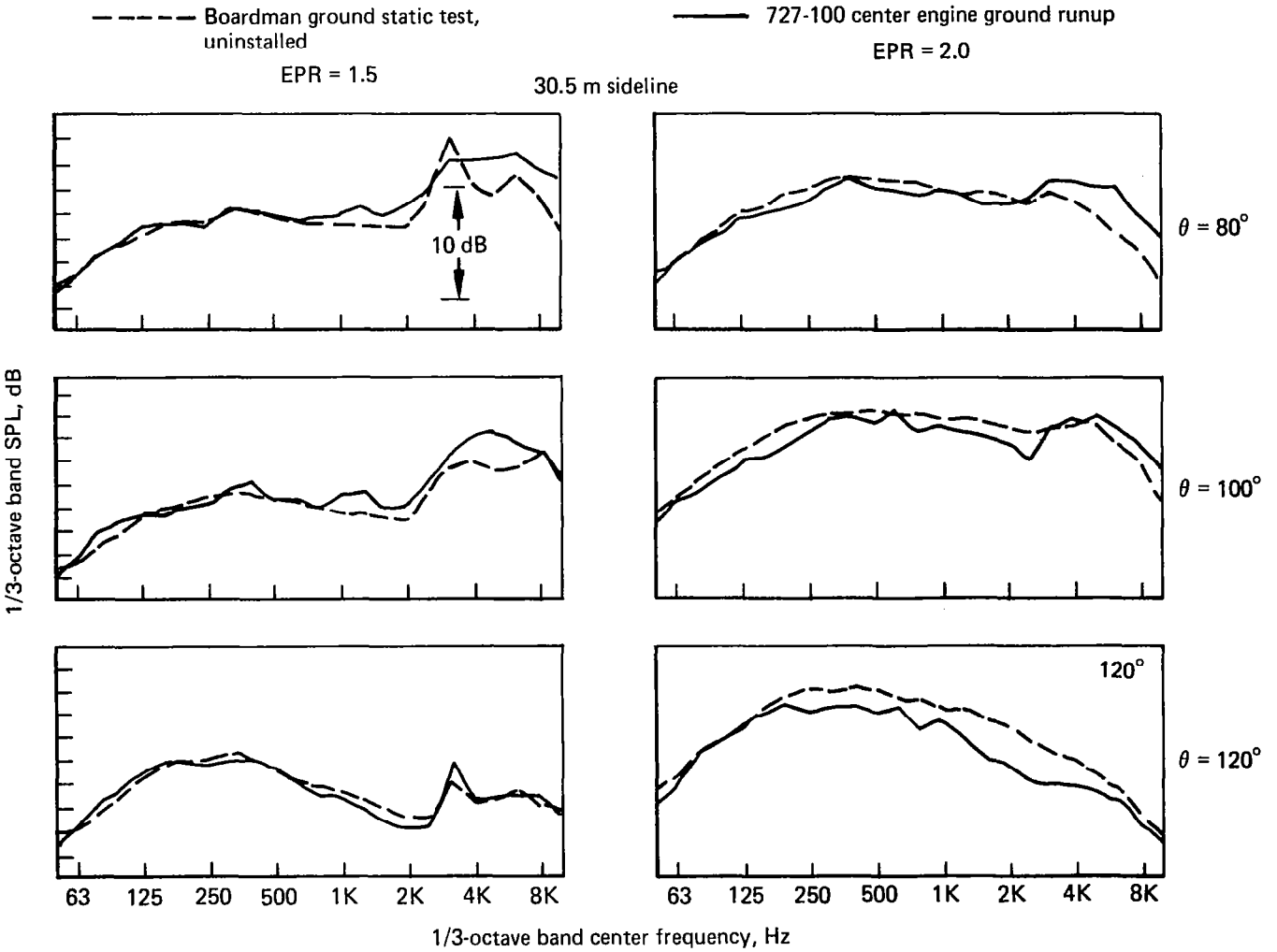

Figure 28.—Comparison Between Installed and Uninstalled Engine Noise Levels (Approximately Same Nozzle ℄ Height and Ground Mic), JT8D-9 Baseline

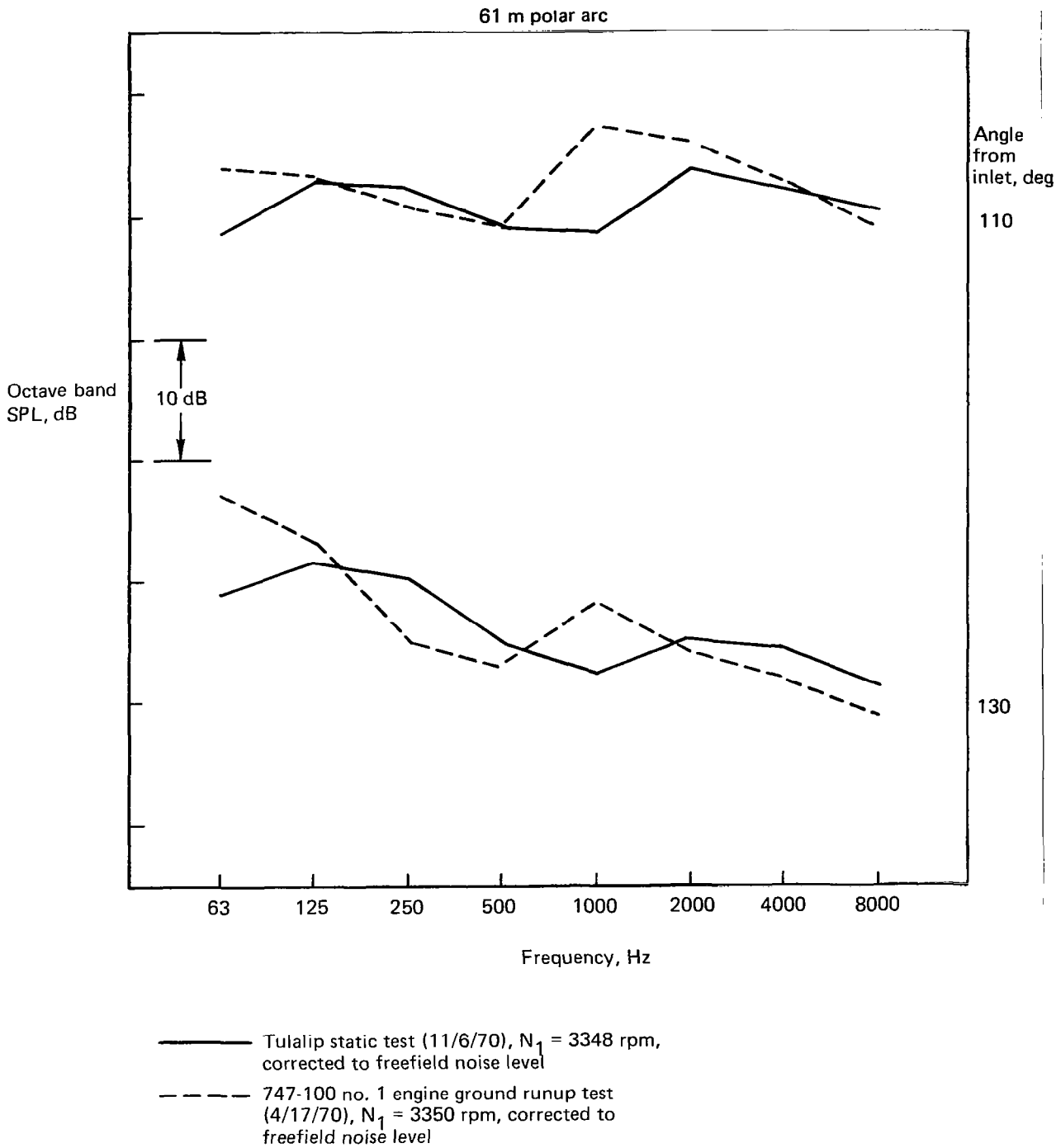

Figure 29.—Comparisons Between Installed and Uninstalled Engine Noise Levels, JT9D-3

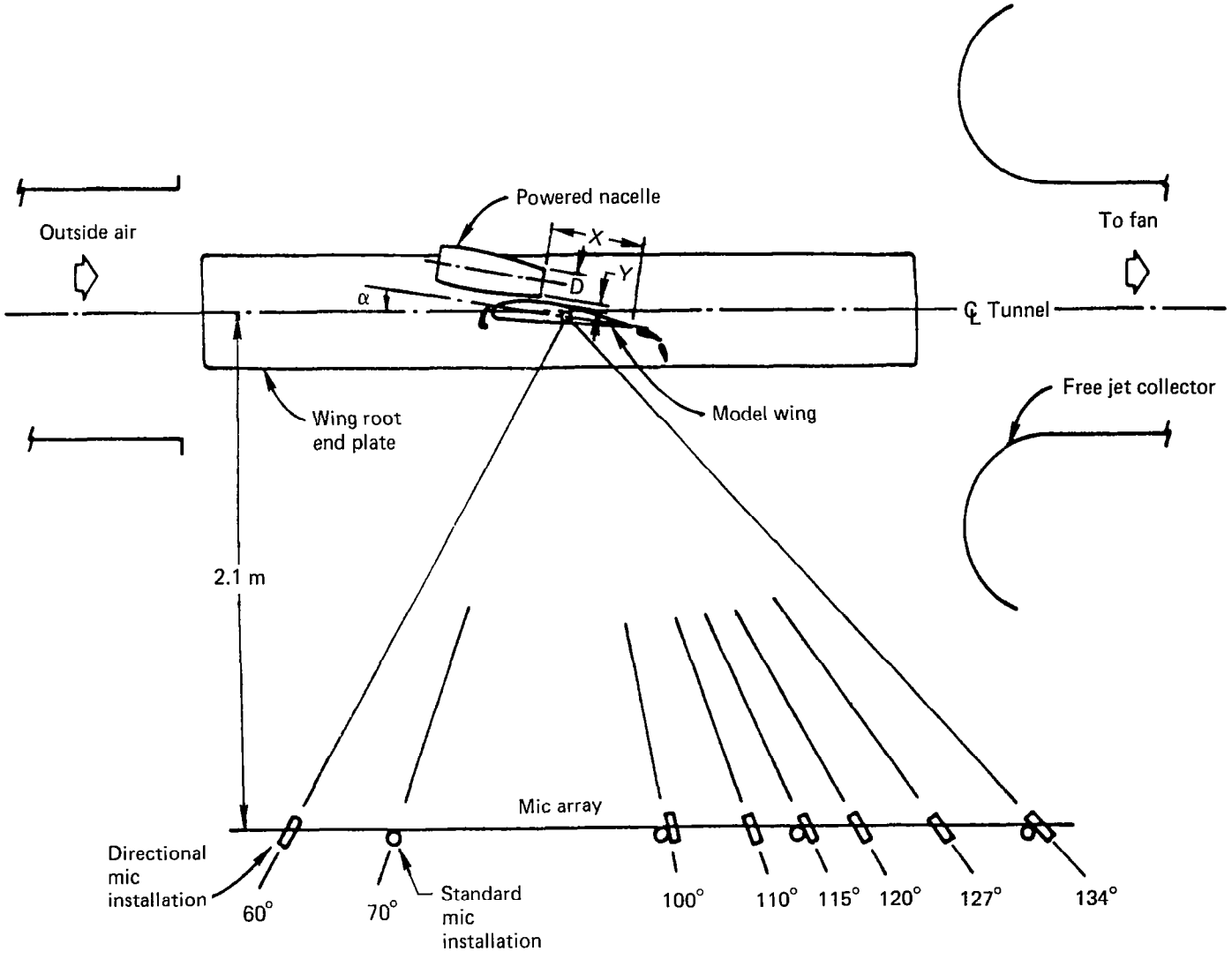

Figure 30.—Test Arrange for Wing Shielding Effect in Free Jet Wind Tunnel

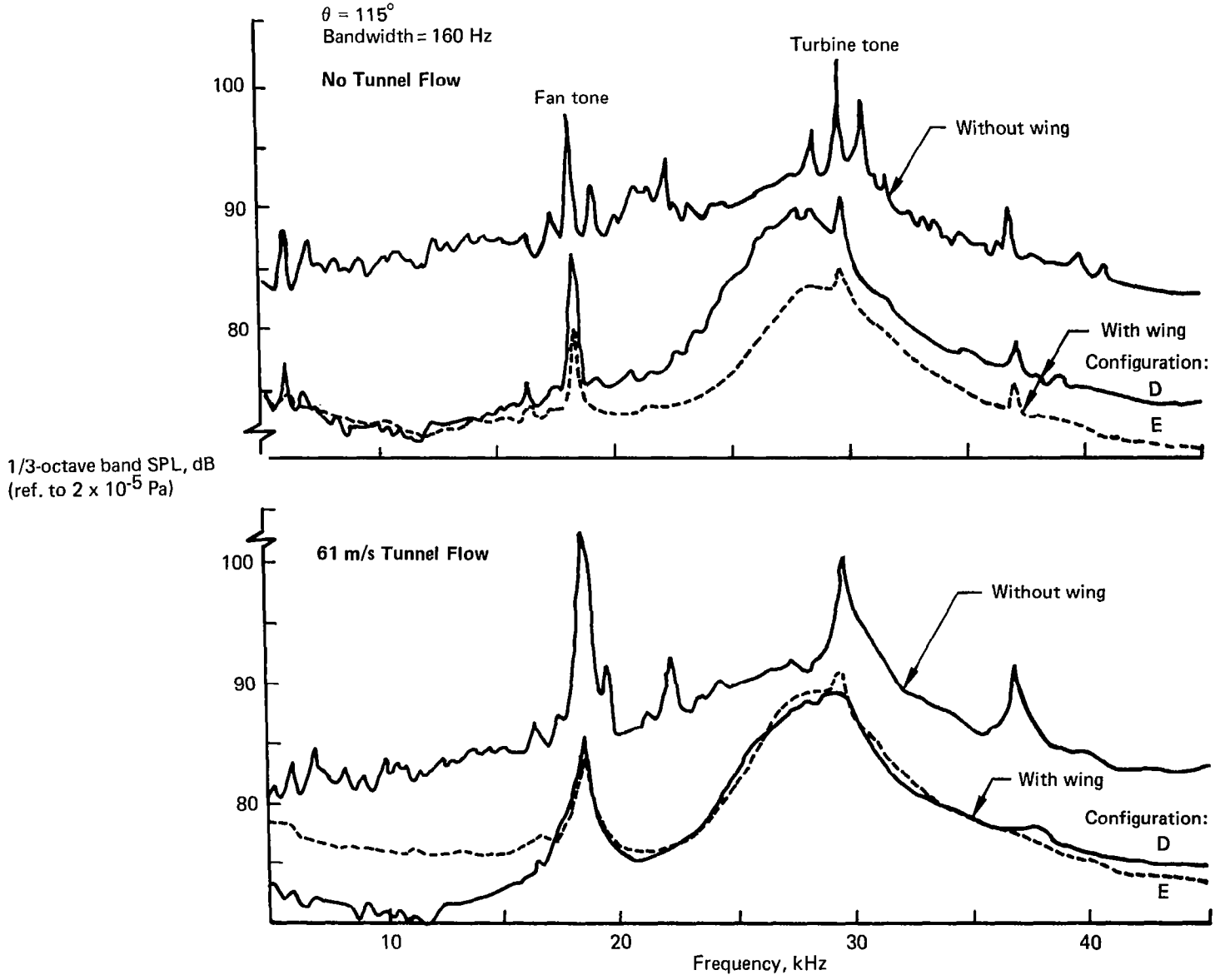

Figure 31.—Powered Nacelle Noise Spectra, Free Jet Wind Tunnel With and Without Wing Shielding

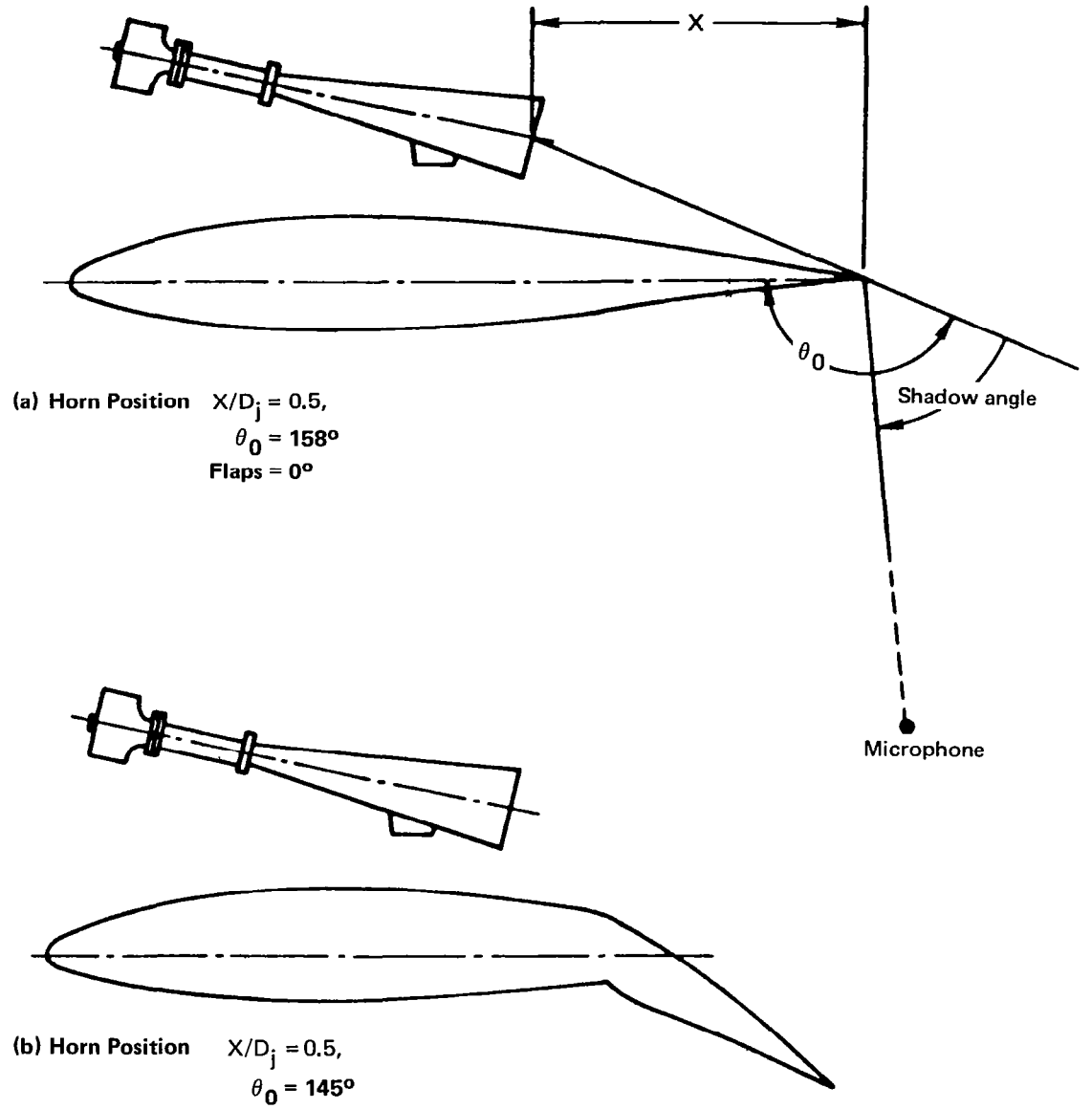

(a) Horn Position $X/D_j = 0.5$,
$\theta_0 = 158°$
Flaps = 0°

(b) Horn Position $X/D_j = 0.5$,
$\theta_0 = 145°$
Flaps = 30°

Figure 32.—Light Airplane Wing-Shielding Horn-Mounting Configurations

Prior to the flight test, the horn and light airplane wing configuration were statically tested to establish a baseline to which the flight test data could be compared. The light airplane with the horn installed was flight-tested, and the inflight noise was recorded. A number of different horn locations and wing configurations were tested at several different airplane speeds.

As fig. 18 of ref. 36 shows, trends were found from these test data that some of the noise reduction benefit due to shielding was lost by the forward velocity, but the directivity patterns remained about the same independent of the flight velocity. The relatively simple test was valuable for learning about the techniques of flight testing for shielding effects, as well as for obtaining some preliminary information on shielding effects in flight.

Additional Work Recommended for the Investigation of Engine Installation Effects.—It is believed that an empirical or semiempirical approach is best suited for the engine installation effect study, as it is expected to yield an easily applicable noise prediction procedure in a short time period. The prediction procedures required here are those which would compute the increments (or decrements) in jet noise from a single- or dual-flow round nozzle of the conventional underwing or overwing engine installation. Those nozzles and installation configurations categorized as nonconventional should be treated separately. For the empirical or semiempirical approach, a systematic parametric test work would be required with model configurations in a facility that utilizes an appropriate flight effect simulation technique (refer sec. 3.2.2).

3.1.4 DOPPLER EFFECTS

In the study of the effects of motion on jet noise from aircraft, there are two cases in which evaluation of the Doppler effects is of practical importance: (1) extrapolation of ground static noise data (or static prediction values) to the noise for a given airplane flight condition and vice versa and (2) extrapolation of wind tunnel noise data to the noise for a given flight condition. The evaluation is needed in developing airplane jet noise prediction procedures based on static or wind tunnel data and for comparing flight test data with static or wind tunnel noise data. Doppler effects for dual-flow or complex nozzles are not well understood at this time. The analysis for a single-flow nozzle is given below.

The Doppler frequency shift is governed by the relative motion between the noise source and the receiver by the equation

$$f_G = f_S (1 - M \cos \theta)^{-1} \tag{9}$$

where f_G is the received (measured) frequency away from source; f_S is the source frequency; M is the Mach number of the source in the direction of motion; and θ is the included angle between the source motion vector and the receiver position vector with respect to the source.

The Doppler amplitude change is the result of the relative motion between the noise source and the ambient air (ref. 37); motion of the receiver does not have anything to do with this change. Ffowcs-Williams (ref. 38) has derived the following equation.

$$\text{Noise Intensity} \propto c_o^{-5} (\rho_j^2/\rho_o)\, V_j^8 \left(\frac{V_j - V_{AP}}{V_j}^7\right) (1 + M_c \cos\theta)^{-5} (1 - M_{AP} \cos\theta)^{-1} \qquad (10)$$

where c_0 is the speed of sound in ambient air; ρ_j is the density of the jet; ρ_0 is the density of ambient air; V_j is the jet velocity; V_{AP} is the airplane velocity; M_c is the eddy convection Mach number; M_{AP} is the airplane Mach number; and θ is the angle included between the airplane velocity and the receiver position vectors. This equation expresses the Doppler amplitude change as being proportional to $(1 + M_c \cos\theta)^{-5}$ $(1 - M_{AP} \cos\theta)^{-1}$, the former representing jet noise level dependence on eddy convection velocity and the latter the jet noise level dependence due to relative motion between the source and the ambient air. In equation (10), the third term and the fourth term on the right-hand side represent the jet noise dependence on V_j and the reduction in jet noise at the source due to forward velocity, respectively. Based on these equations, two cases are discussed in the following paragraphs for which evaluation of the Doppler effect is normally required.

3.1.4.1 Doppler Effects With Equal Relative Velocity

This case assumes that the jet relative velocity with respect to the ambient air, $V_R = (V_j - V_0)$, is the same for all the ground static, wind tunnel, and airplane flyby arrangements. Therefore, it is noted that the static jet is operating with a jet velocity of V_R, while the jets of the wind tunnel and airplane are operating with a jet velocity of V_j surrounded by ambient air which has a velocity of V_0 with respect to the nozzle.

Table 4 summarizes the results of the Doppler effect evaluation. In making this table, the noise emission angles are matched properly, considering the sound wave drift in moving ambient air.

The table shows that there is no need to apply the frequency shift in extrapolating the ground static test data to the flight condition because, at the instant the jet of a flying aircraft has a noise emission angle of θ to the ground microphone (table 4c), the jet exhaust discharged out of the aircraft exhaust nozzle has the same relationship to the ground microphone as the static jet has to the microphone located at a radiation angle θ in the ground static test arrangement (table 4, sketch a). On the other hand, the motion similarity between the cases of table 4, sketches b and c, is only obtained when the microphones in the wind tunnel are moved along with the tunnel air with the same velocity. Since this is not the case, the application of the Doppler frequency shift is required as noted in the table.

In comparing the jet fluid mechanics of a static jet and a jet with the surrounding airflow, it is generally accepted that the jet fluid mechanics are similar when the relative velocities of the two jets are equal. Validity of this similarity, as one might expect in view of the jet noise generation mechanism, is corroborated by many test data.

Table 4.—Doppler Effects

With equal $V_R = (V_j - V_0)$	Frequency shift	Level change
Extrapolation of ground static test data to flight Extrapolation of ground static prediction to flight	No shift	$(SPL)_G = (SPL)_{ST} - 10 \log(1 - M_{AP} \cos \theta)$
Extrapolation of wind tunnel test data to flight	$f_G = \frac{f_w}{(1-M_0 \cos \theta)}$	No change

Note: Proper matching of noise emission angles is assumed.

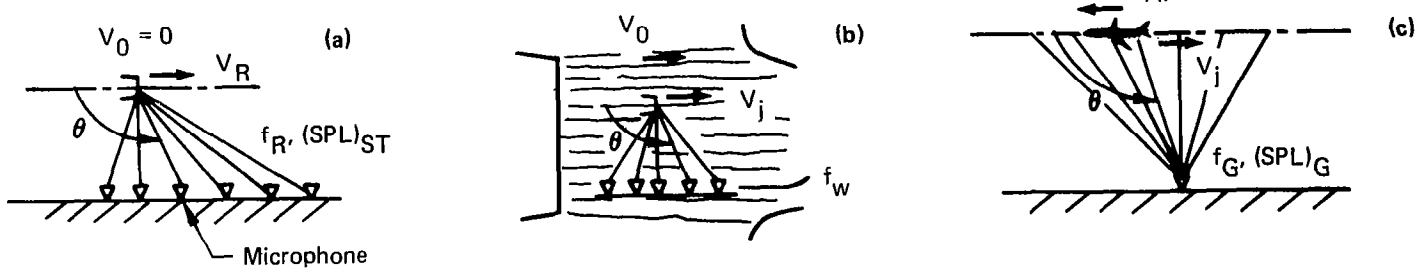

When this is accepted, the convection Doppler term (second from the last in eq. (10)) may be assumed equal and the Doppler amplitude change effects can be accounted for by the application of the last term, $(1 - M_{AP} \cos \theta)^{-1}$. The results are shown in table 4. This table also shows that the Doppler amplitude change between the ground static and the flyby cases is $10 \log (1 - M_{AP} \cos\theta)$ dB. This difference comprises a portion of the gross flight effects being sought.

3.1.4.2 Recommended Method With Ground Static Jet Operating With V_j

This case assumes that the ground static jet operates with V_j instead of V_R, while the wind tunnel and airplane jet remain operating with $V_R = V_j - V_0$ as in the previous case.

The relationship is more complex in this case, because the eddy convection speed of the static jet operating at V_j is different from the speed of a jet operating at V_R. The relationship in this case may be established by defining first the differences between the two static jets operating with V_j and V_R and then by using the equations in table 4.

The frequency relationship between the two static jets may be estabished by the equation:

$$f_R = f_V (1 - M_c \cos \theta)^{-1} \tag{11}$$

where f_R and f_V are the frequencies measured with the static jets operating at V_R and V_j, respectively; and M_c is a Mach number representing the difference in eddy convection velocities.

For the Doppler amplitude change, the second from last term in equation (10), $(1 + M_c \cos \theta)^{-5}$ should be used.

3.1.5 NOISE PREDICTION COMPUTER PROGRAM (EMPIRICAL)

One of the important objectives of this contract effort is to contribute to the perfecting of an empirical computer program that would predict the jet noise of a flying airplane with acceptable accuracy. Development of jet noise prediction procedures has been an important subject in aircraft acoustics technology. As a result, there are several different procedures currently available for prediction of the jet noise (refs. 39 through 42). A review of these procedures led to the selection of the Boeing JEN2 prediction procedure for further study of the jet noise prediction part of this contract work. Discussions of this procedure and the additional features which supplement the procedure are presented in the following paragraphs.

To predict the total noise from an airplane, a prediction program is required that includes procedures for calculating remaining noise components (fan, turbine, core, airframe noise, etc.) in addition to the jet noise procedure. The Boeing Full Standards Prediction Program, which is used for prediction of total airplane noise, was used in this work when needed, as described in later sections.

3.1.5.1 Static Jet Noise Prediction Program (JEN2)

The JEN2 program is a prediction program applicable for predicting static jet noise of single-flow nozzles, coaxial/coplanar nozzles, or fully mixed dual-flow nozzles. For predicting the jet noise as received by a ground microphone from a flying airplane, an additional procedure must be implemented in the program to account for the effects of motion on jet noise. The JEN2 prediction program is recommended for use with the following restrictions:

- Source-to-microphone distance greater than 50 jet diameters
- Jets with circular cross sections
- Noise generated by shocks in the jet flows not included (Work to include this noise is in progress.)
- Primary jet flow calculations (total temperature and jet velocity) are limited to:

$$300 \text{ K} \leqslant T_{TjP} \leqslant 900 \text{ K}$$

$$122 \text{ m/s} \leqslant V_{jP} \leqslant 878 \text{ m/s}$$

- Secondary flow jet calculations (total temperature, fully expanded jet area ratio, and jet velocity ratio) are limited to:

$$237 \text{ K} \leqslant T_{TjS} \leqslant 400 \text{ K}$$

$$1 \leqslant A_{jS}/A_{jP} \leqslant 6$$

$$0.25 \leqslant V_{jS}/V_{jP} \leqslant 1.0$$

The procedures of the JEN2 program for prediction of noise from single-flow nozzles are essentially the same as those for one version of the proposed SAE method (ref. 40). A block diagram of the procedure is presented in figure 33. The procedure consists of three components: a density exponent "m" as a function of jet velocity V_j/c_0 (where c_0 is the ambient speed of sound); a normalized OASPL as a function of radiation angle θ and V_j/c_0; and a normalized spectra as a function θ and a temperature corrected Strouhal number, $(fD_j/V_j)/T_{Tj}/T_0)^{0.26}$; where f is the frequency; D_j is the fully expanded jet diameter; T_{Tj} is the jet total temperature; and T_0 is the ambient air temperature. Inputs required for the procedure are the fully expanded jet area A_j, the jet flow rate W_j, and V_j, T_{Tj}, T_0 and the radial distance from source to receiver R. The calculated outputs are the 1/3-octave-band jet noise SPL polar spectra for the radiation angles from 10^0 to 170^0.

The part of the JEN2 program for predicting the jet noise of dual-flow nozzles is presented in figure 34. As seen in figure 34, the procedure consists of three branches of computations to take into account the three noise producing regions: (1) the innermost

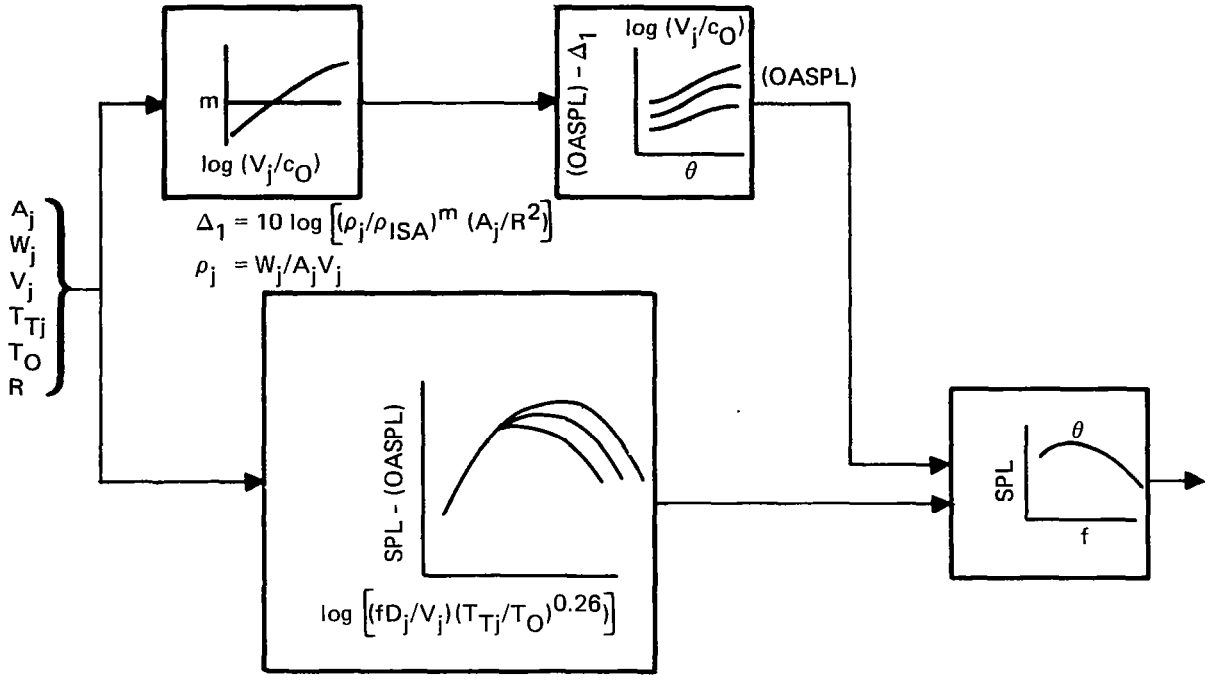

Figure 33.—Static Jet Noise Prediction Procedure (JEN2 Program), Single Flow

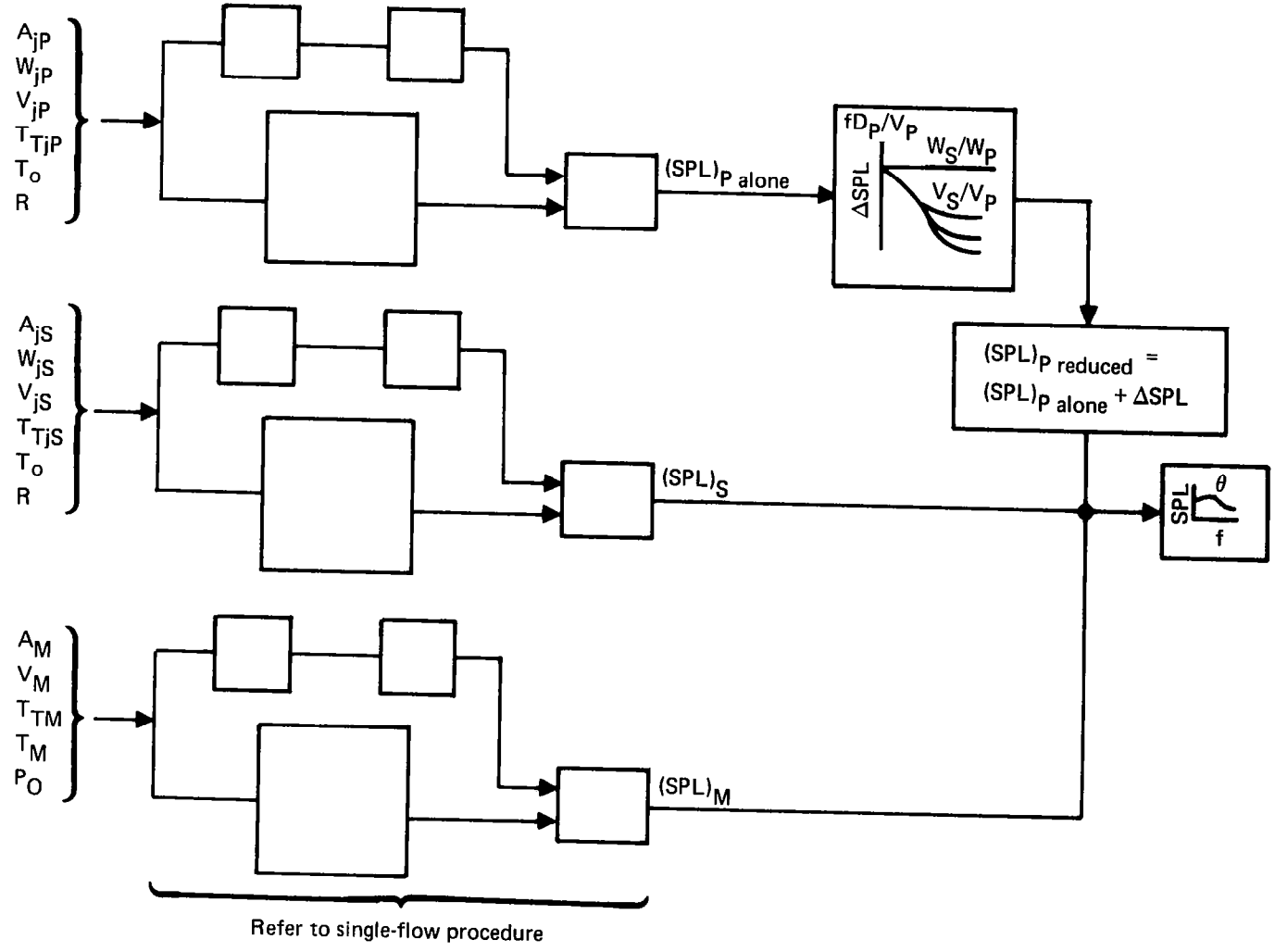

Figure 34.—Static Jet Noise Prediction Procedure (JEN2 Program), Coaxial/Coplanar Flow

primary jet region, (2) the secondary jet surrounding the primary jet, and (3) the primary-secondary merged or mixed region. Since the primary and the surrounding secondary jet undergoes fluid dynamic interactions with consequent effects on noise generation, a jet interaction correction was derived and applied in the computation of the primary jet noise.

Except for the jet interaction correction in the primary procedure, each of the three branches shown in figure 34 has the same steps of computations as that for a single-flow jet of figure 33. The inputs required for the primary are the same parameters as for the single-flow jet. The jet interaction correction ΔSPL included in this branch is calculated as a function of the primary Strouhal number fD_{jP}/V_{jP}, mass flow ratio W_{jS}/W_{jP}, and velocity ratio V_{jS}/V_{jP}.

The inputs for the secondary jet noise are the same parameters as for the primary. However, the diameter used to calculate the secondary jet noise is the equivalent total diameter, which is calculated with the following equation:

$$D_{jS}/D_{jP} = [1 + (A_{jS}/A_{jP})]^{0.5} \tag{12}$$

where A_{jS} and A_{jP} are the fully expanded secondary and primary areas, respectively.

The inputs for the mixed region noise are derived from the conservation equations for energy, momentum and mass, and the equation of state.

$$\frac{V_M}{V_{jP}} = \frac{1 + (W_{jS}\, V_{jS}/W_{jP}\, V_{jP})}{1 + (W_{jS}/W_{jP})} \tag{13}$$

$$\frac{T_{TM}}{T_{TjP}} = \frac{1 + (W_{jS}\, T_{TjS}/W_{jP}\, T_{TjP})}{1 + (W_{jS}/W_{jP})} \tag{14}$$

$$T_M = T_{TM} - V_M^2/(2gJC_p) \tag{15}$$

$$\frac{A_M}{A_{jP}} = \frac{1 + (W_{jS}/W_{jP})}{\rho_M V_M/\rho_{jP}\, V_{jP}} \tag{16}$$

$$\rho_M = P_o/R\, T_M \tag{17}$$

where ρ is the density; P_o is the ambient air static pressure; and subscript M stands for the properties of the mixed flow region. The jet noise level of a dual flow/coplanar nozzle is then obtained by the sum of the three noise components calculated by the three branches shown in figure 34.

The validity of the JEN2 prediction program has been checked against noise test data obtained with various types of nozzles. Comparisons between the test data and the

predicted noise of hot and cold single-flow model jets, J75 turbojet, JT8D low-bypass jet, and JT9D and RB211 high-bypass jets showed good agreement (refs. 41 and 42). Some examples of these comparison studies are presented in figures 35 through 38. Figures 35 and 36 show comparisons of SPL and OASPL of a 2.5-cm hot model jet at jet velocities from 244 m/s to 549 m/s. Figures 37 and 38 present similar comparisons for the JT8D-1 engine dual-flow nozzle (bypass ratio about one). The bottom of figure 38 includes the breakdown into three subcomponents of the dual-flow jet noise. These and other comparisons have substantiated that the JEN2 program predicts jet noise of various types of jets with good accuracy.

3.1.5.2 Flight Jet Noise Computation Procedures

Two methods were considered for computing the jet noise from an airplane in flight. The first method was to compute the static jet noise operating with a given jet velocity V_j, then convert the static jet noise to the flight condition (the jet now operating with the relative velocity V_R) by applying corrections for the noise levels and the Doppler frequency shift. The second method was to directly compute the static jet noise levels operating with V_R and then to apply the Doppler effects.

The second method has the advantages of cancelling out the Doppler frequency effects and identifying the Doppler level changes, as discussed in section 3.1.4. But, the first method has the advantage of providing two levels of jet noise, one for the static condition and the other for flight. The first method also is simpler for applying the JEN2 static jet noise prediction procedures. In this contract work, the first method was chosen. In the following discussions, the procedures used with the first method for level corrections, the Doppler frequency corrections, and ground reflection effects are presented.

3.1.5.3 Noise Level Change for In-Flight Jet Noise

The static jet noise computed by the JEN2 program was corrected for the forward velocity effects of an airplane in flight. It is generally known that the forward velocity effects of a circular nozzle are in the direction of reducing the static noise level (at least in the aft quadrant). The method selected for this work is represented in figure 39. In this method, the reduction in 1/3-octave-band noise level is computed by $10\ n \log \left[(V_{jP} - V_0)/V_{jP}\right]$, which is a function of n, primary jet velocity V_{jP}, and airplane velocity V_0. The exponent n of the ratio of relative velocity (V_{jP} minus V_0) to primary jet velocity is to be calculated as a function of the radiation angle θ, frequency f, V_{jP}, and a constant C. In figure 39, $(SPL)_{ST}$ and $(SPL)_{FT}$ indicate the 1/3-octave-band static jet and flight jet noise spectra, respectively.

3.1.5.4 Doppler Frequency Shift

The Doppler frequency shift effect was dealt with based on the analysis presented in reference 43. The static jet noise spectra, SPL_i, were first reduced to spectrum levels S_i for each 1/3-octave band, assuming that acoustic power level in each 1/3-octave band was uniform; then the spectrum levels at 1/3-octave band center frequencies were shifted in frequency to get frequency-shifted spectrum levels S_i'. The acoustic energy

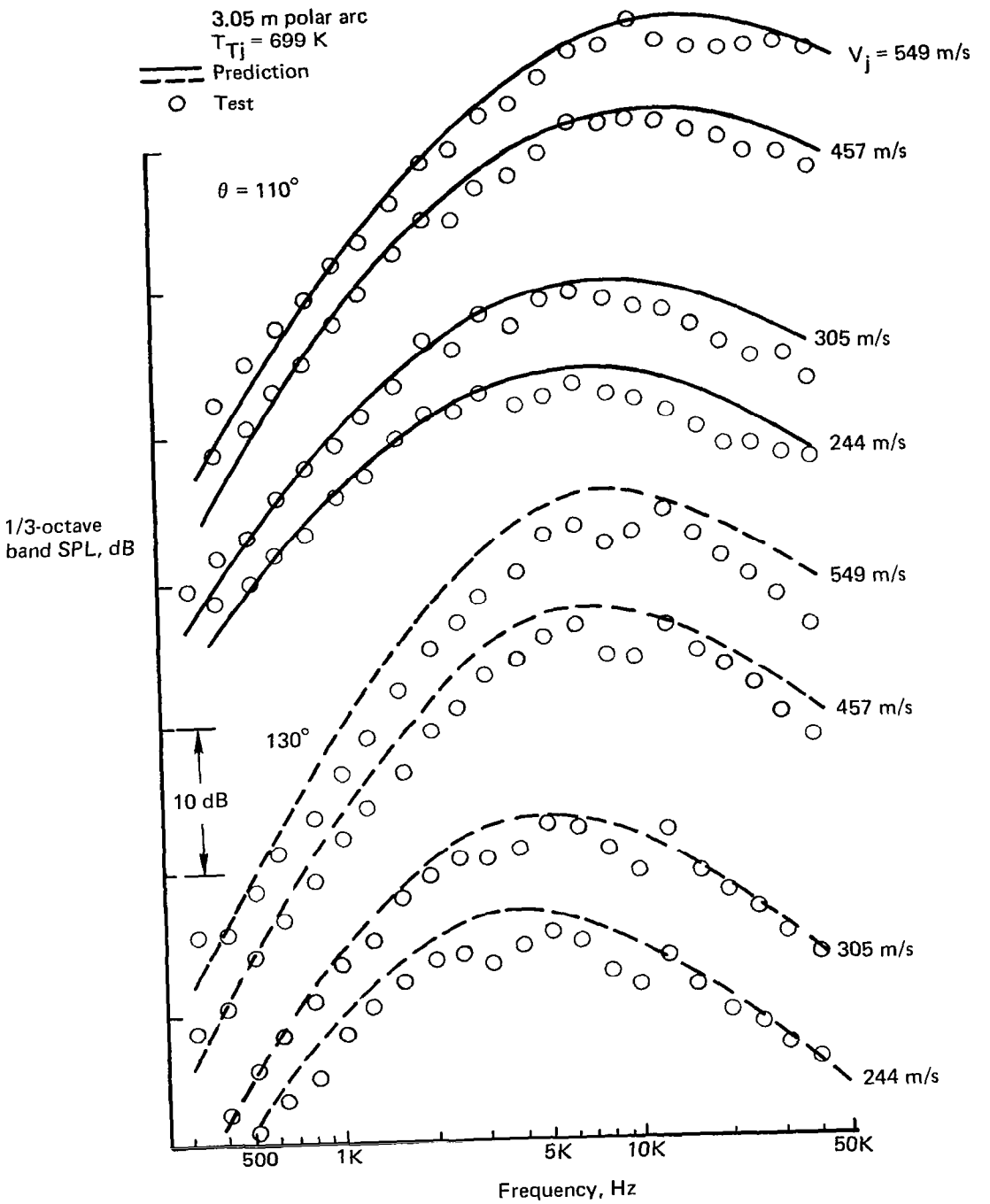

Figure 35.—Spectrum Comparison Between Prediction and Test, Single-Flow Nozzle, Clean 2.54-cm Jet

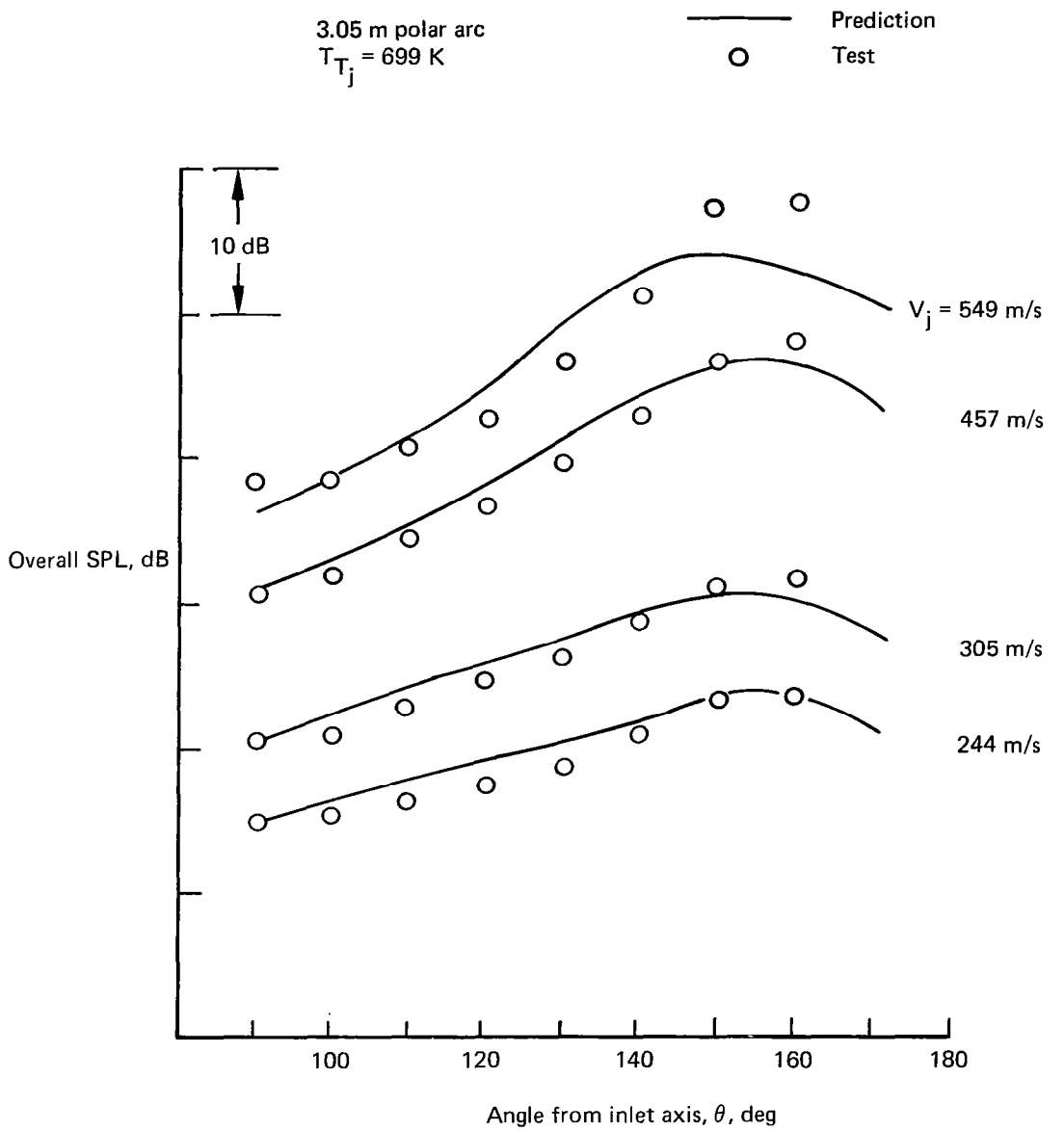

Figure 36.—Comparisons of Overall Sound Pressure Level Between Prediction and Test of Single-Flow Nozzle, Clean 2.54-cm Jet

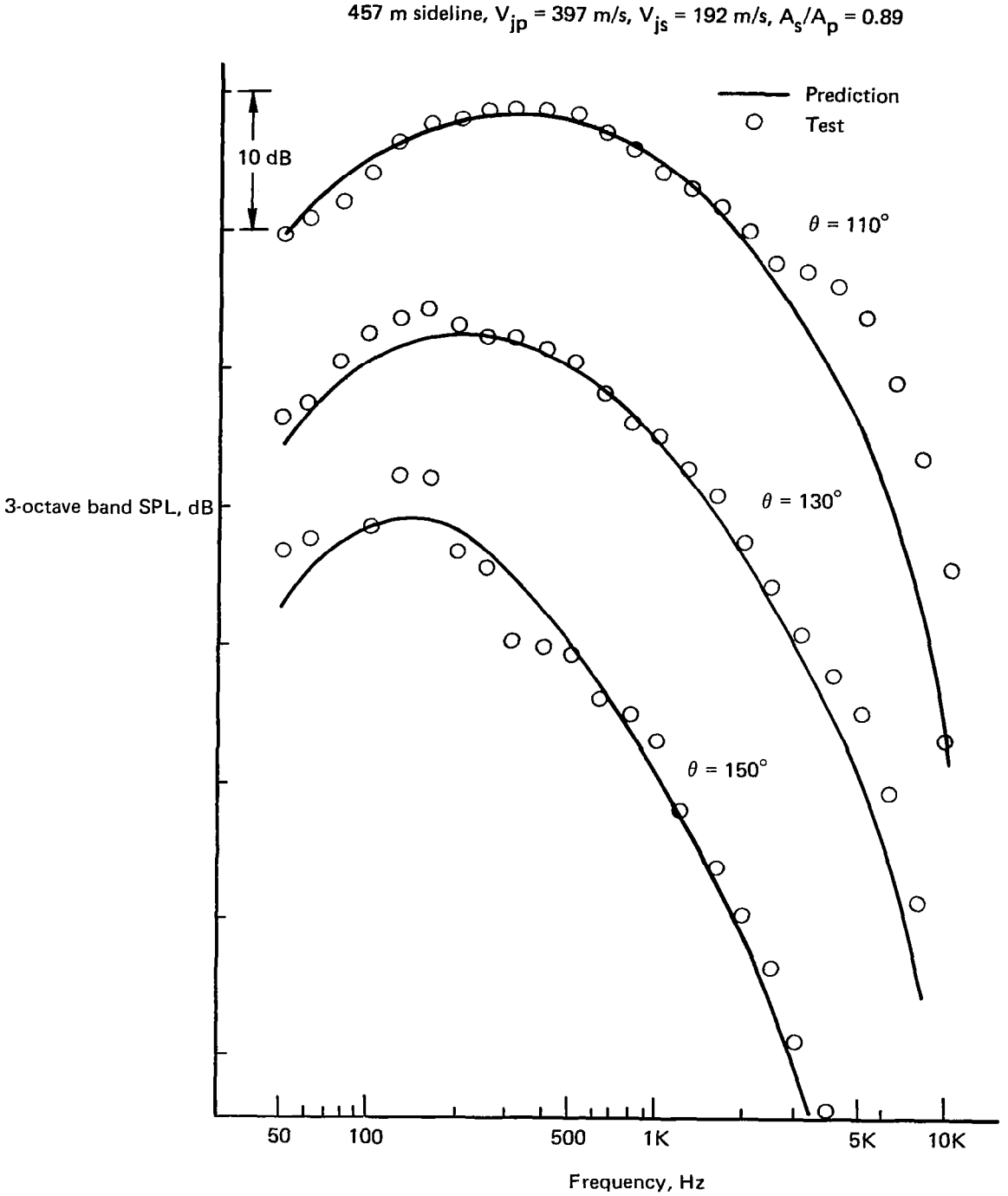

Figure 37.—Spectrum Comparison Between Prediction and Test, Dual-Flow Nozzle (JT8D-1 Static Test)

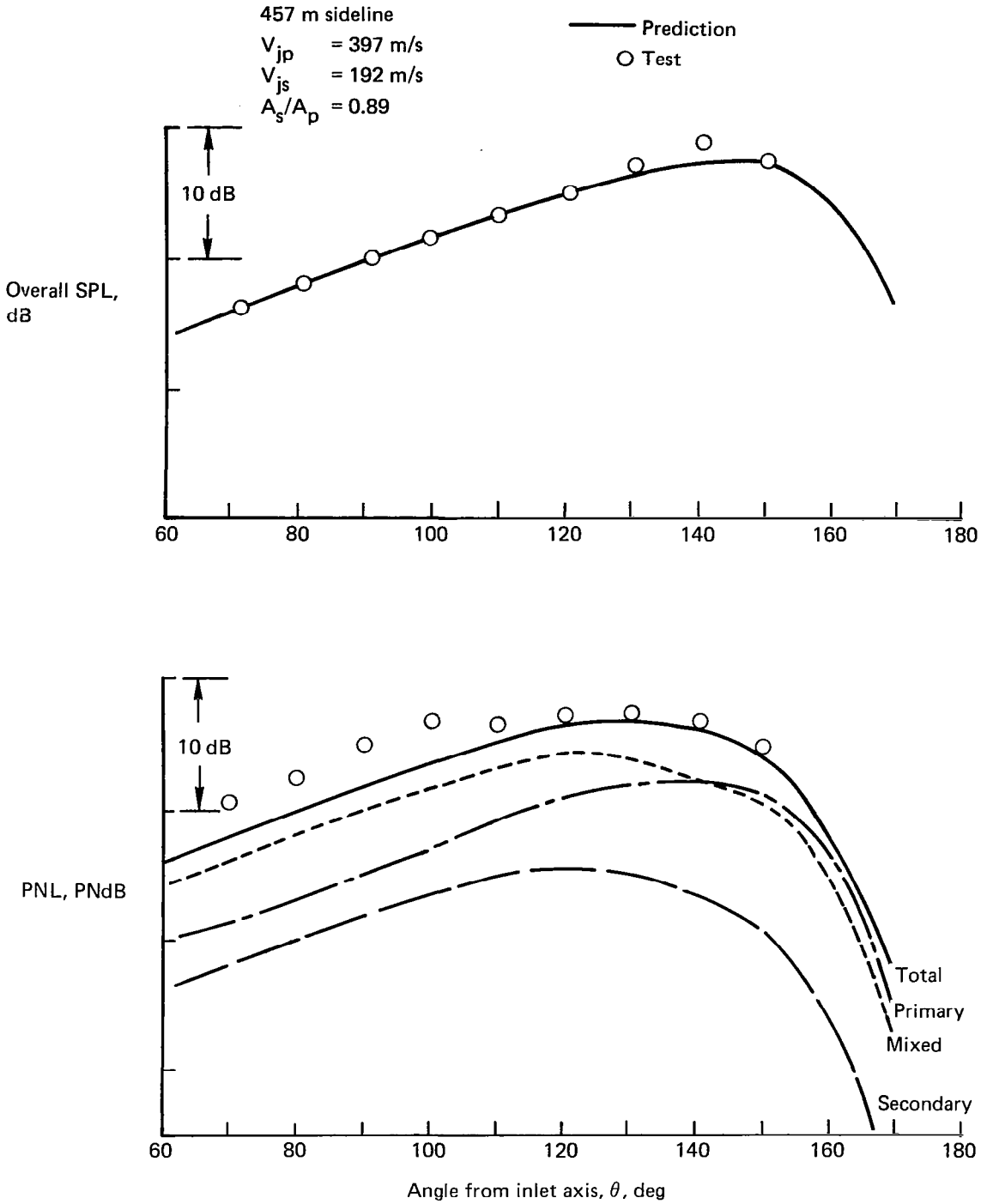

Figure 38.—Comparisons of Overall Sound Pressure and Perceived Noise Levels Between Prediction and Test, Dual-Flow Nozzle (JT8D-1 Static Test)

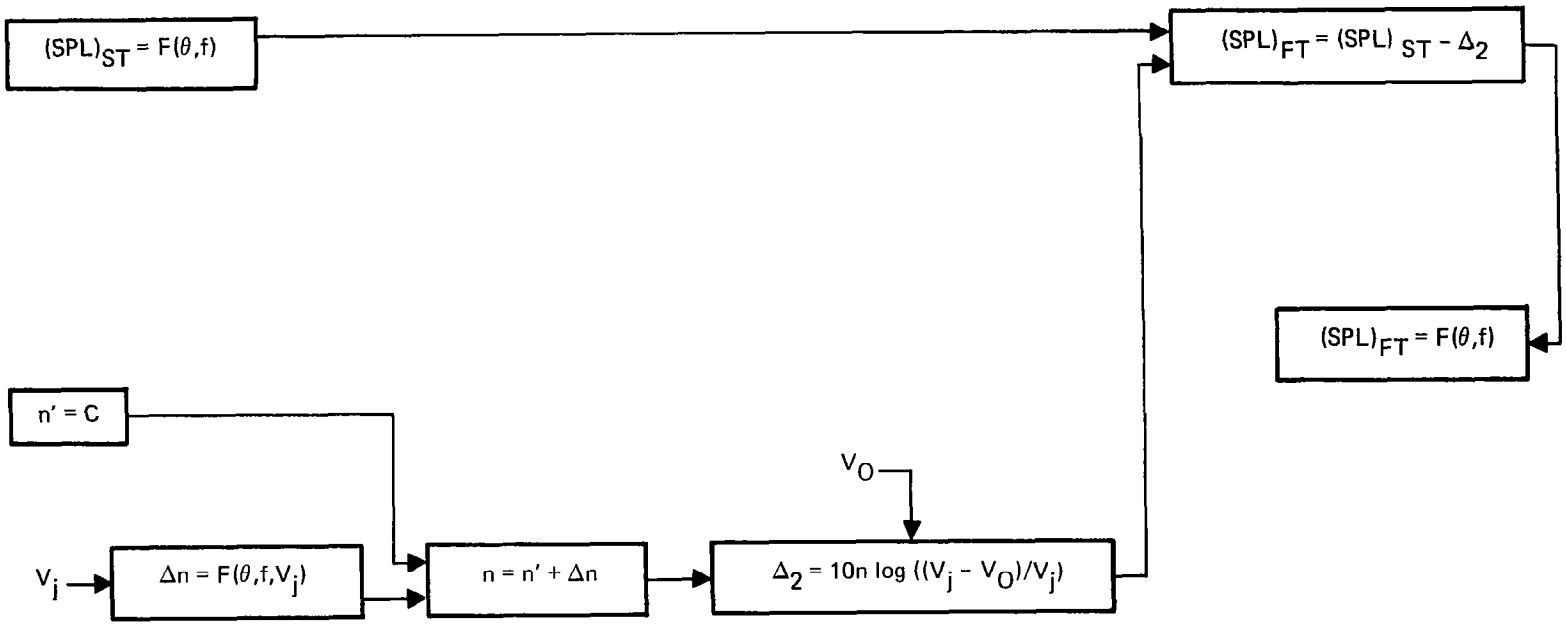

Figure 39.—Flight Effect (Noise Level Change) Computation Procedure, to be Used With JEN2 Program

contained in the frequency-shifted and unshifted bands was conserved. These frequency-shifted spectrum levels may not now be at the standard 1/3-octave-band center frequencies. Therefore, to get the frequency-shifted spectrum levels S_i'' at the standard 1/3-octave-band frequencies, the frequency-shifted spectrum levels are interpolated at the standard center frequencies. The frequency-shifted jet noise spectra SPL_i'' were then computed using S_i''.

The equations involved are

$$S_i = SPL_i - 10 \log (\Delta f_i) \tag{18}$$

$$i = 1, 2, \ldots . 24 \tag{19}$$

$$f'_{c,i} = D \cdot f_{c,i}$$

where Δf_i is the band width of the i-th 1/3-octave band; f_c is the center frequency, and

$$D = (1 - M_A \cos \theta)^{-1} \tag{20}$$

where M_A is the Mach number corresponding to the relative velocity between the source and the receiver; θ is the angle included between the flightpath and the line connecting airplane and microphone. For the conservation of energy, S_i must be corrected for the frequency band extension (or contraction); i.e.,

$$S_i' = S_i - 10 \log D \tag{21}$$

The S_i' and $f'_{c,i}$ form a curve of frequency-shifted spectrum level. Using this curve, the spectrum levels S_i'' at the standard 1/3-octave bands are determined by interpolation. The frequency-shifted spectra SPL_i'' are then computed by

$$SPL_i'' = S_i'' + 10 \log (\Delta f_i) \tag{22}$$

3.1.5.5 Ground Reflection Effect Computation Procedure

The ground reflection effects evidenced from most of the flight airplane noise data clearly indicated the requirement of implementing a ground reflection computation procedure. Thus, the computer program formulated in reference 39 was added to the Boeing Full Standards Prediction Program.

This procedure was derived for 1/3-octave-band noise under the following simplifying assumptions: a point source, homogeneous air and ground media, and a smooth infinite reflecting interface. Referring to figure 40, if the noise measured by the microphone with and without the ground reflection effects are designated by SPL_M and SPL_F, respectively, reference 39 shows that

$$SPL_M - SPL_F = 10 \log [1 + A^2 + 2A \cos (S_2 - \theta)(\sin S_1)/S_1] \tag{23}$$

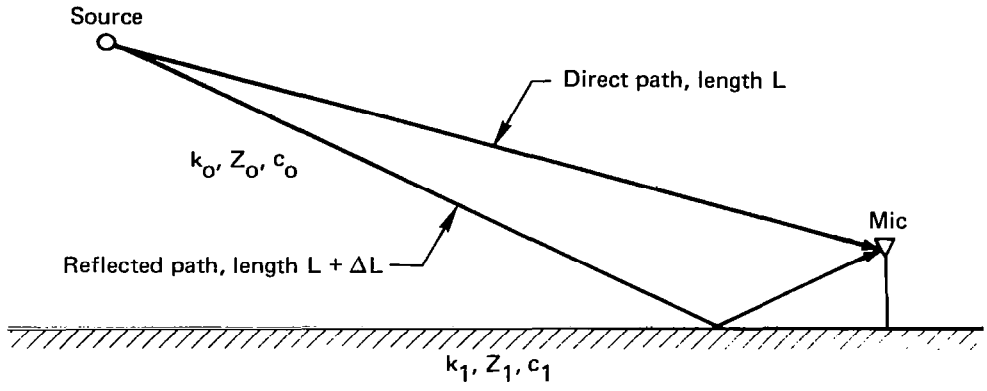

k_o = Wave number for air = $2\pi f/c_o$

Z_o = Acoustic wave impedance for air

c_o = Speed of sound in air

k_1 = Wave number for ground = $2\pi f/c_1$

Z_1 = Acoustic wave impedance for reflecting ground plane

c_1 = Speed of sound in the ground

Figure 40.—Geometry and Nomenclature for Ground Reflection Computation Procedure

where

$$S_1 = \pi \Delta L \, (f_u - f_L)/c_o \tag{24}$$

$$S_2 = \pi \Delta L \, (f_u + f_L)/c_o \tag{25}$$

A = length of vector G

θ = argument of vector G

and

$$G = [R + (1 - R) \, F(W)] / (1 + \Delta L/L) \tag{26}$$

In equations (24), (25), and (26), ΔL is the difference between the direct and reflected sound paths; f_u and f_L are the upper and lower limit frequencies of the 1/3-octave band in question; R is the reflection coefficient; and F(W)is the boundary loss factor (ref. 39). In the calculation of R and F(W), the impedance ratio Z_0/Z_1 and the wave number ratio k_0/k_1 (see fig. 40) must be determined. For the impedance ratio, information given in reference 44 was used; for k_0/k_1, unity was used. This resulted in reasonable reflection patterns.

3.1.5.6 Effects of Atmospheric Property Variations (Mean Value Profiles)

The computer programs for calculating these effects are available, and implementation of one of the programs in the Boeing Full Standard Prediction Program can be readily made, if required, but it was not carried out for this study.

3.1.5.7 Examples of In-Flight Jet Noise Prediction

Work for the flight jet noise computation method is being continued to develop more accurate and broadly applicable methods. However, use of the method described in this section for prediction of two current turbofan engines (one low bypass and the other high bypass) showed a reasonable accuracy. Figures 41 and 42 present some examples of these comparisons. The figures show measured and predicted noise spectra at key radiation angles for airplanes in level flight at takeoff power. The airplane noise predictions were performed with the Boeing Full Standards Prediction Program which included the JEN2 jet noise procedure and the flight effect procedure of figure 39, in addition to other subprograms required for computing an airplane noise in flight. It also included the programs for computing the ground reflection and Doppler effects, which are described in the preceding paragraphs.

Both figures 41 and 42 indicate reasonable agreement between the measured and predicted total noise at aft radiation angles. Compatibility of predicted jet noise spectra (frequency range below 1000 Hz) with the measured total noise spectra in this angle range also is reasonable. The differences between the test and predicted PNL's are included in the figures. It is noted that some of the total noise disagreement seen at the forward angles and at the high frequency ranges may indicate a need for improvement in the prediction program.

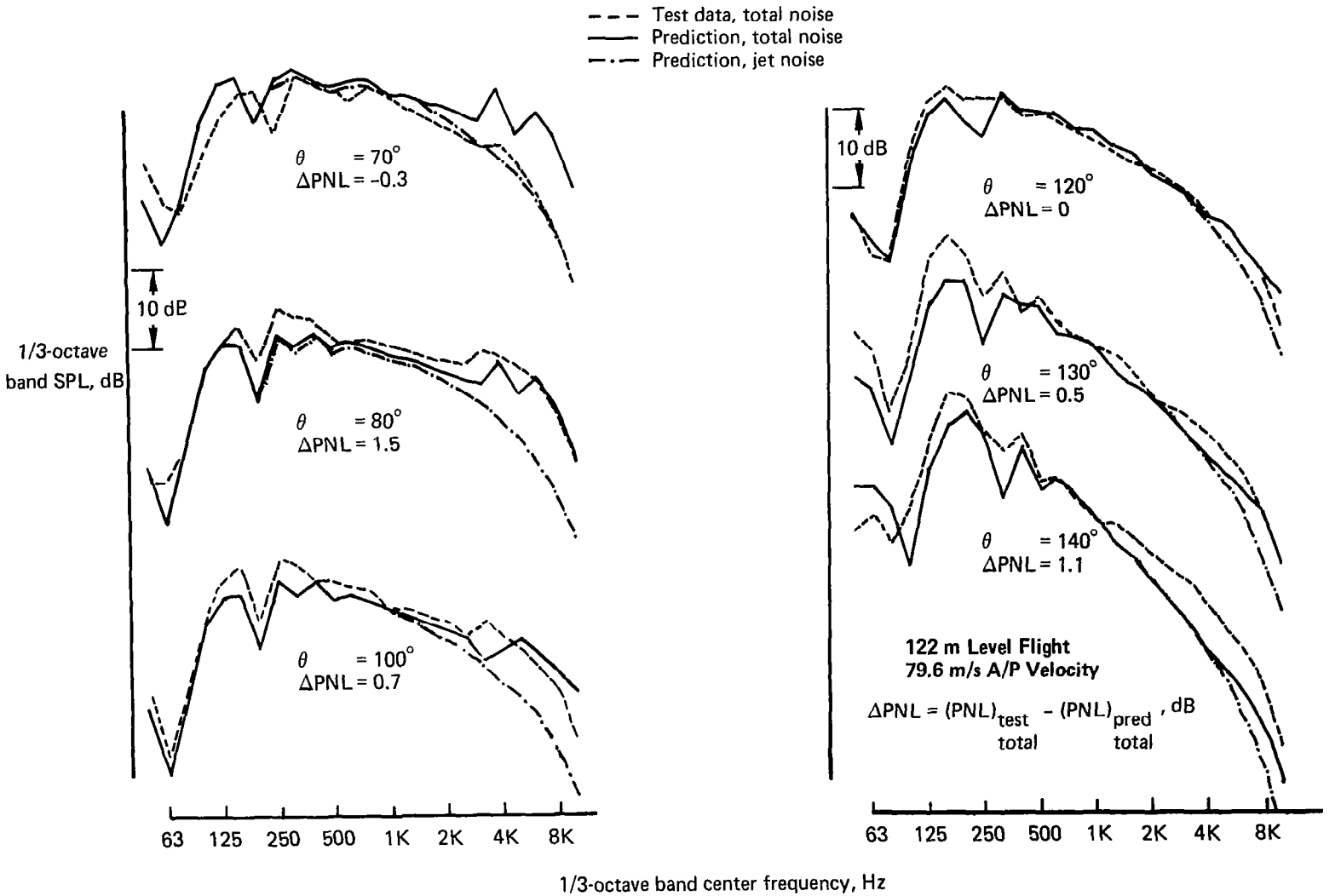

Figure 41.—Predicted and Measured Spectrum Comparison–Low-Bypass Engine, Takeoff Power

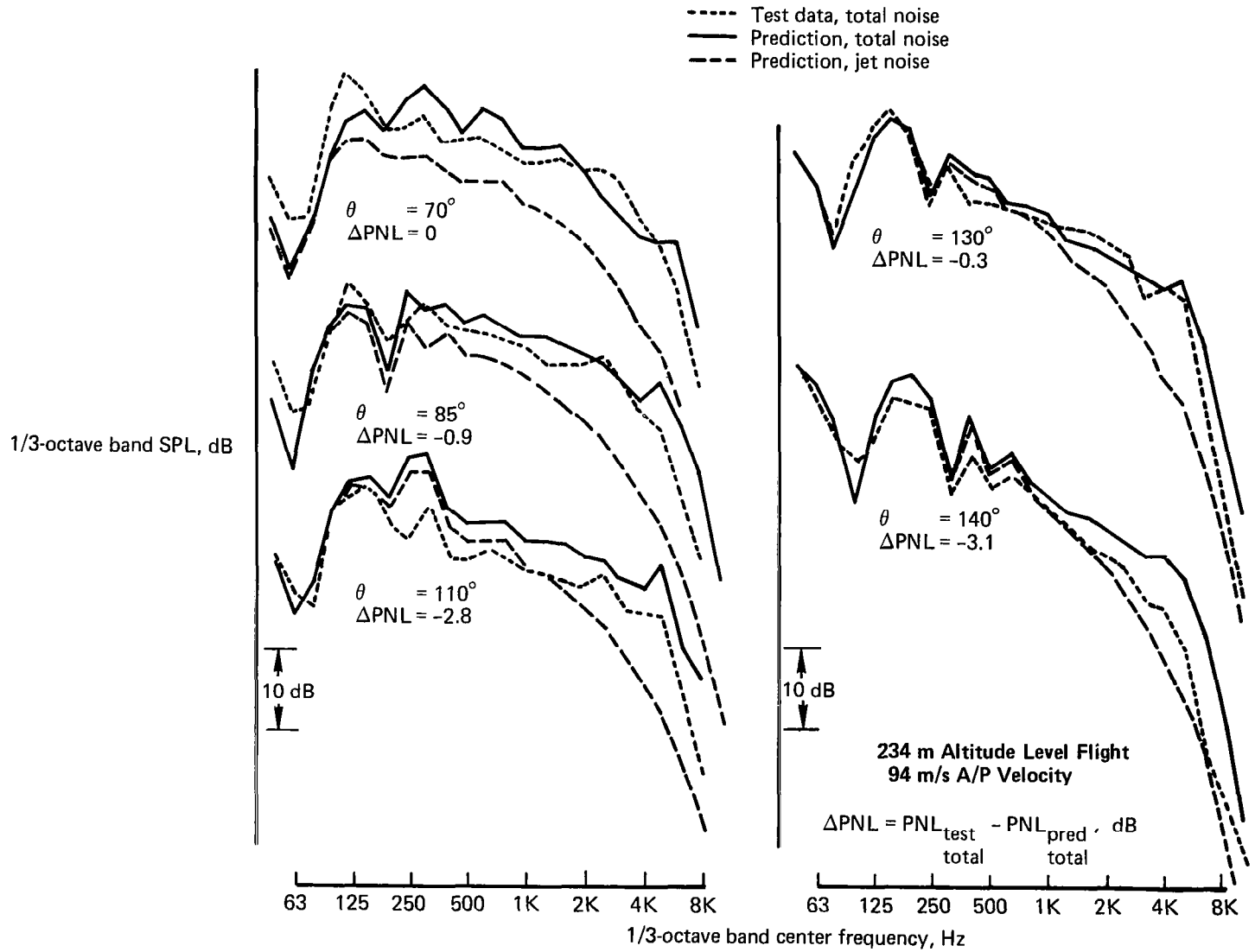

Figure 42.—Predicted and Measured Spectrum Comparison–High-Bypass Engine, Takeoff Power

3.1.6 WEATHER CHANGE EFFECTS AND TOLERANCE BOUNDARIES

The weather changes that may occur during a series of tests are believed to be one cause for the flight test jet noise data scatter. The probable data scatter resulting from assumed weather changes is discussed in the following section. The test window boundaries within which error tolerances for atmospheric temperature and relative humidity measurements are not very critical are also discussed.

3.1.6.1 Weather Change Effects

A study was conducted to calculate the maximum intensity changes and the maximum deviation of acoustic rays of jet noise caused by a change in atmospheric temperature, relative humidity, and wind. The noise is considered to be propagating from an airplane flying overhead to a microphone on the ground. The effects of atmospheric turbulence were not included. The purpose of this study was to investigate the possible causes of test data scatter in the jet noise levels obtained from a set of repeat runs during an acoustic flight test.

It was assumed that two repeat test flights were conducted, between which a weather change had taken place. This weather change, however, was not measured nor detected because of insufficient instrumentation. What would be the noise level change in the second flight test compared to the first, for an assumed probable weather change? All other variables (engine operating condition, airplane altitude, altitude, flight velocity, etc.) were assumed to be the same for both flights. Sets of temperatures, RH, and wind changes were assumed in order to compute the magnitude of the jet noise changes. Extreme, but realistic, values were used.

In accordance with the work definition of the contract, a typical takeoff pattern (overhead flight) was considered,and the jet noise source was assumed to be at 457 m (1500 ft) altitude. The radiation angle was assumed to be 15° from the jet axis. This would give the longest propagation distance affecting the jet noise for an angle of practical interest.

The temperature and RH affect the absorption. The extent of the effect of temperature and RH were examined by plotting the absorption contours at a number of 1/3-octave bands, which are important for jet noise. Three examples of these plots are presented in figures 43 through 45. The absorption computation is the result of a computer program based on ARP 866.

Using figures 43 through 45 and other similar plots, the portion of jet noise data scatter contributed by a change in temperature and RH can be theoretically estimated. For example, assume for the takeoff case that the weather changes between the two repeat flights from 14° C/48% RH to 11° C/32% RH. The difference in the level of the 1000-Hz 1/3-octave-band component noise of the two repeat flights may be computed from figure 43 to be about 6 dB on a 15° radiation path (1766 m). The similar change for the 500-Hz 1/3-octave band was found to be much smaller. These results are determined under the assumption of constant temperature and relative humidity between the source and receiver, since figures 43 through 45 assume the same state. These noise

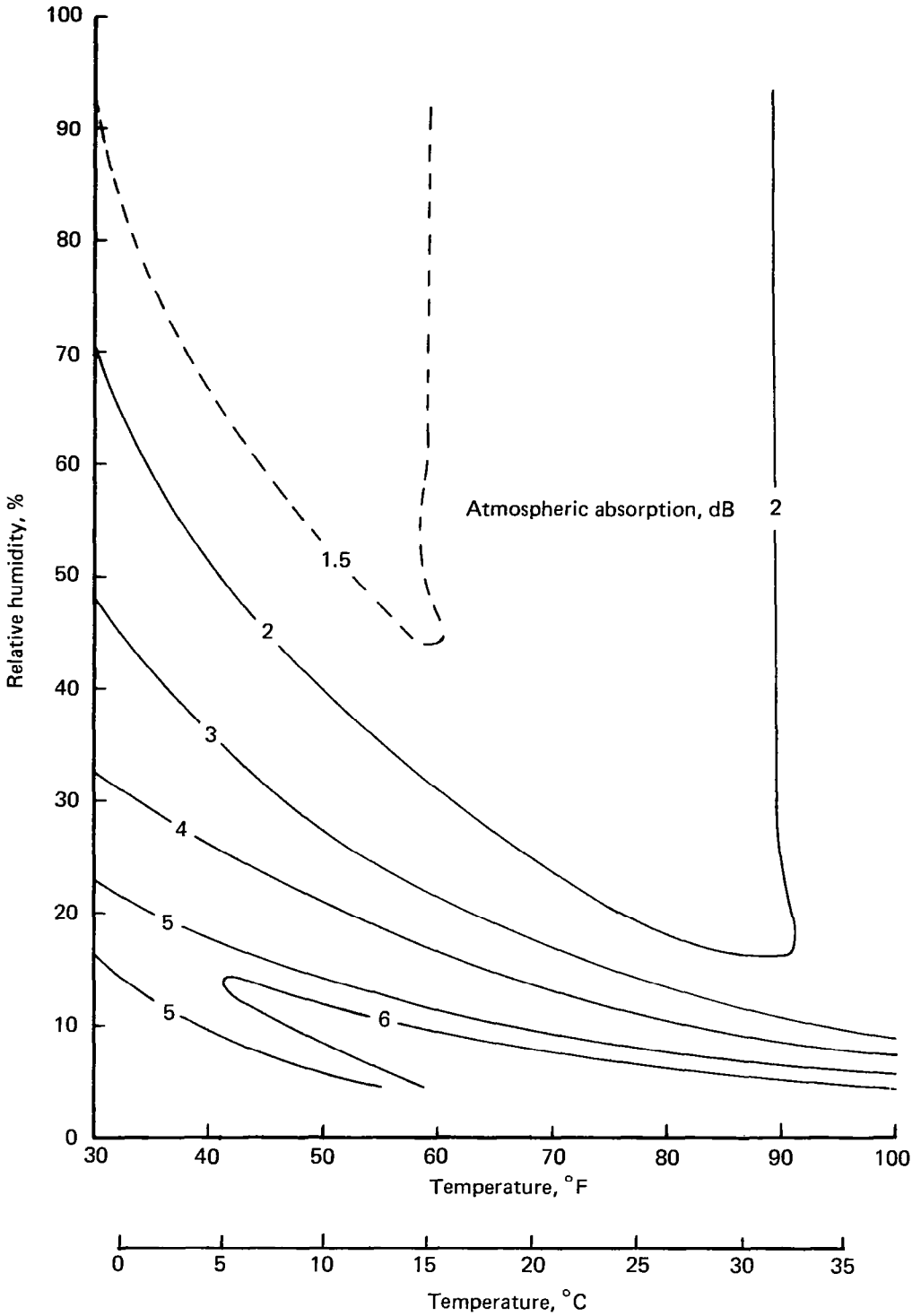

Figure 43.—Atmospheric Absorption, 1000 Hz 1/3-Octave Band, 305 m (1000 ft) Distance

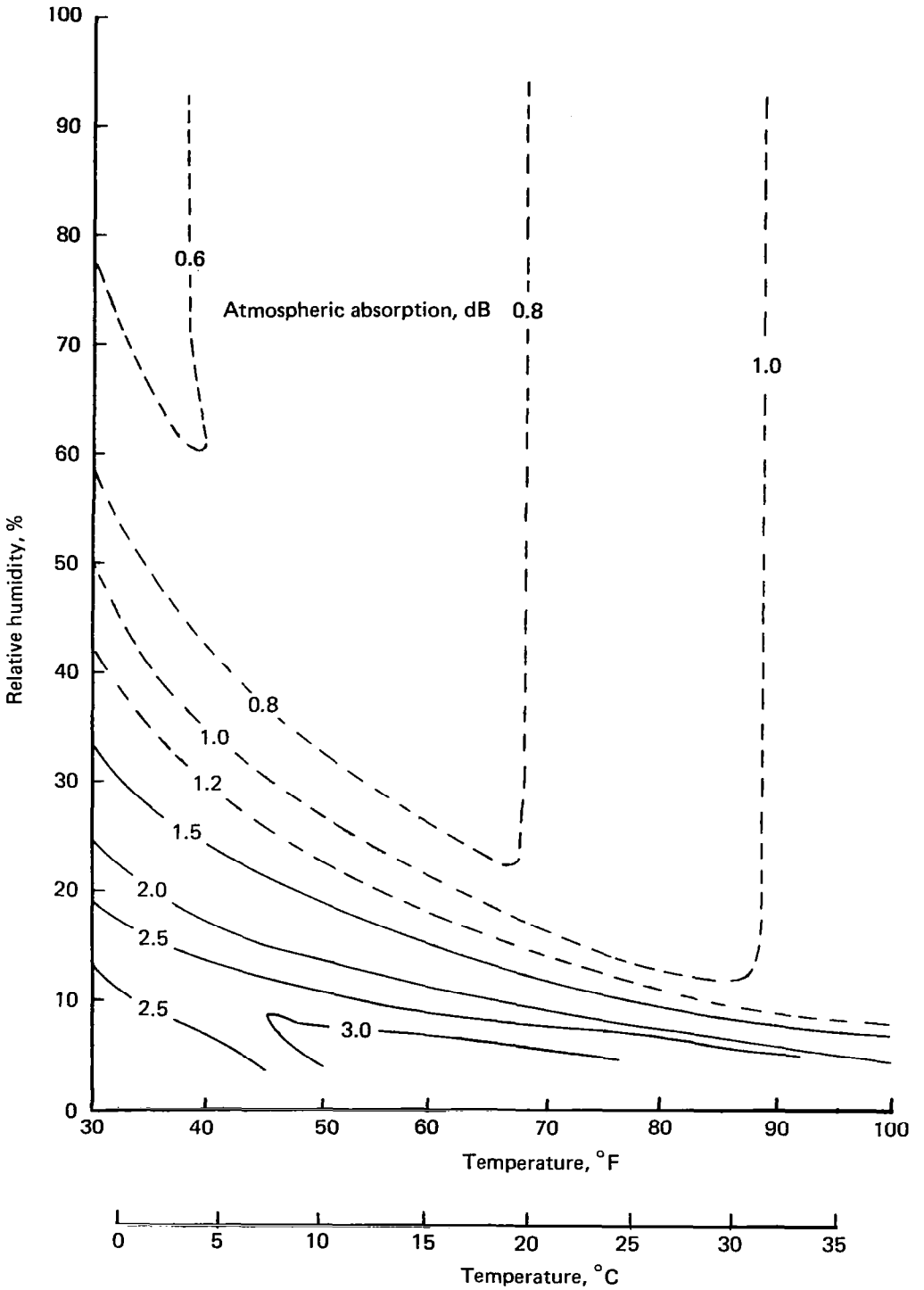

Figure 44.—Atmospheric Absorption, 500 Hz 1/3-Octave Band, 305 m (1000 ft) Distance

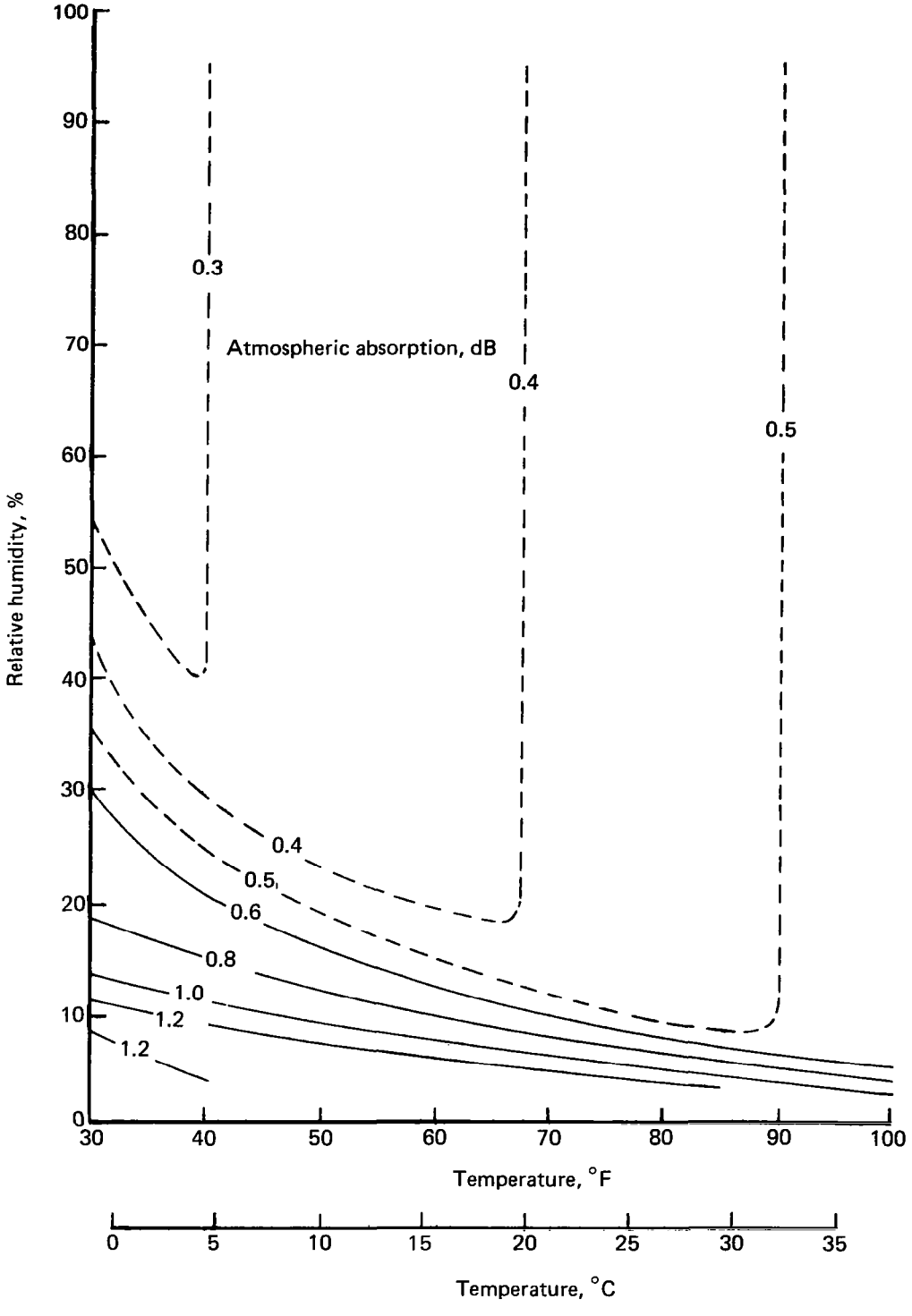

Figure 45.—Atmospheric Absorption, 250 Hz 1/3-Octave Band, 305 m (1000 ft) Distance

level changes, of course, can be corrected if the temperature and RH data are measured for the second flight.

The effects of acoustic ray bending caused by the temperature and wind gradients were examined for a similar set of repeat tests with the same premise as for the mean temperature and RH; i.e., with an undetected weather change between the two repeat tests. The assumed temperature and wind gradients are shown in figure 46. First, it was assumed that the wind direction was the only change taking place while the temperature gradient remained the same. The wind was assumed to completely reverse its flow direction; i.e., negative to positive or 180°. The maximum nominal wind velocity considered was 6.1 m/s (20 fps).

The two consequences of sound ray bending are: (1) the sound impact point on the ground deviates from that under the assumption of a straight ray path, and (2) the sound path length differs depending upon the initial sound departure angle. The first phenomenon will cause the microphone to receive noise with a different emission angle from that determined by assuming a straight ray path; i.e., noise emitted at 16° to the jet axis instead of 15°, and consequent noise level change. The second phenomenon causes the changes in atmospheric absorption losses and the spherical attenuation. Figure 47 shows the computation results of sound ray impact point considered in this study. Figure 48 shows the ray path length as a function of the initial ray angle.

The ray path computation results with the temperature profiles and negative and positive 6.1 m/s wind profiles of figure 47 show that the total noise emission angle change for the 15° nominal emissions angle is approximately 0.8° for the takeoff case. Now, the 1000-Hz 1/3-octave-band jet noise component variation as a function of emission angle near the jet axis is less than 1 dB/deg. It is concluded that the 1000-Hz 1/3-octave-band noise measured during the second flight would differ from the first flight by less than 1 dB. A similar calculation for the 500-Hz band shows the change is less than 0.5 dB.

The differences in the length of the bent ray paths that impact on the microphone for the two cases were found to be small. Thus, the noise level changes due to the sound path length changes are negligible.

3.1.6.2 Error Tolerance Boundaries

The error bands in the measurements of temperature and RH will result in uncertainties in the absorption coefficients. Figures 49 and 50 show such uncertainty boundaries for the assumed temperature and RH error bands listed in the figures. The figures indicate that, if the measuring error bands are $\pm 1.1\ ^{0}C(\pm 2^{0}\ F)$ and $\pm 2\%$ RH (which are normally attainable), the boundary where the uncertainty is less than 0.2 dB/100 m (± 0.6/1000 ft) is very large. This indicates that the test window within which measurement of atmospheric absorption is not so critical is fairly wide.

3.1.7 TRAILING VORTEX EFFECTS

A brief study was conducted to examine whether the vortices trailing the wing tips of an airplane in flight overhead would affect the jet noise propagation toward an observer

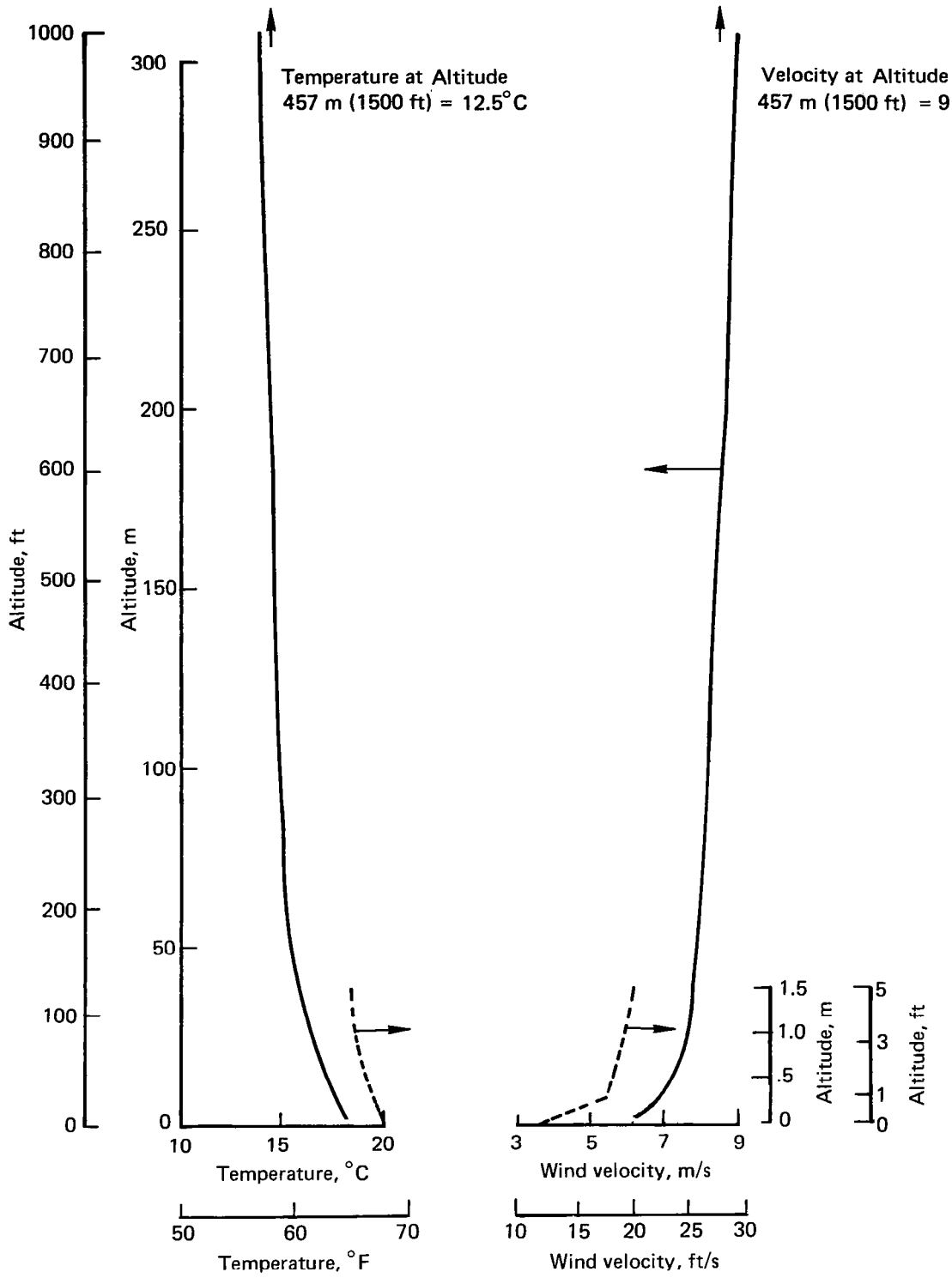

Figure 46.—Temperature and Wind Velocity Assumed

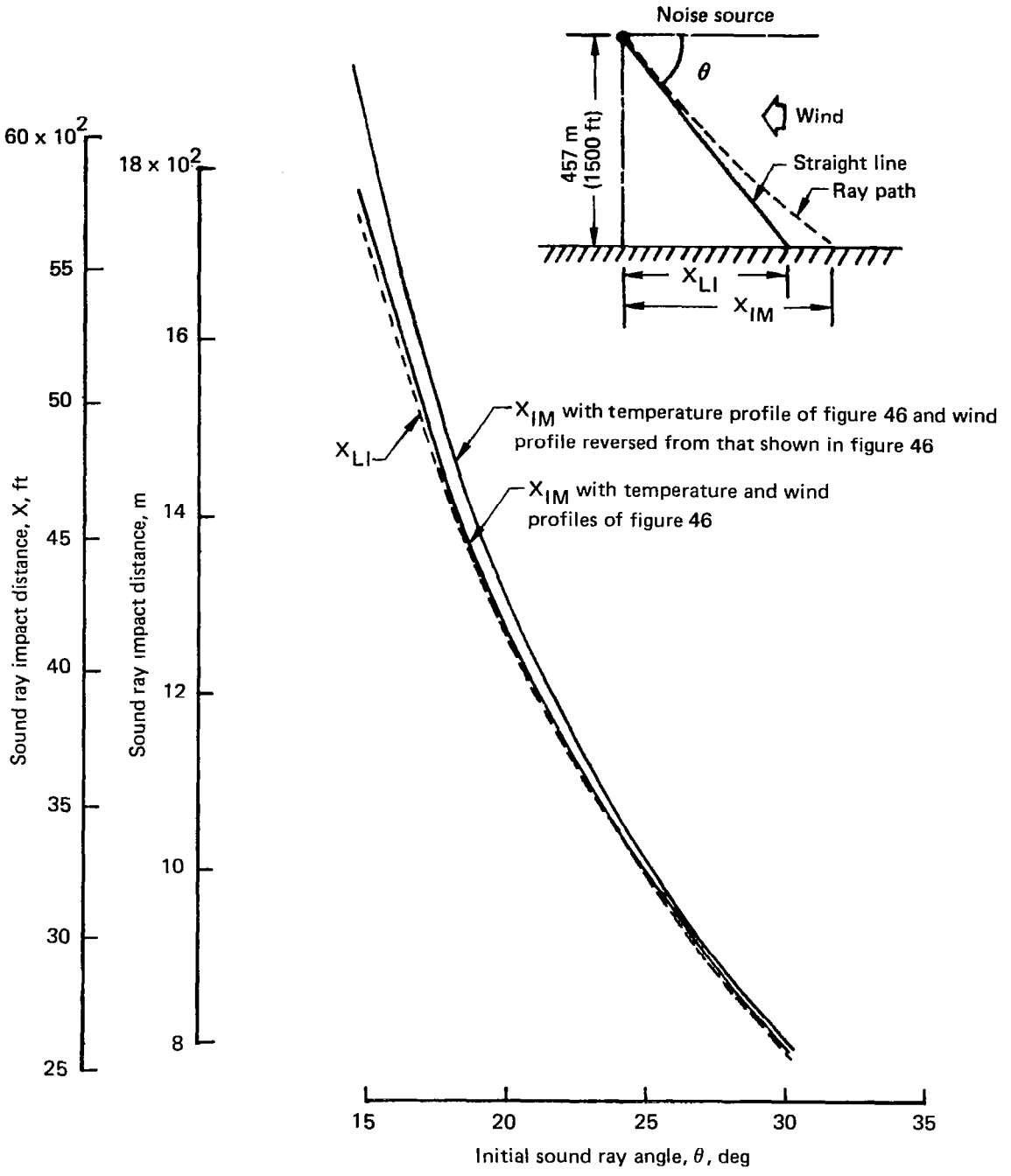

Figure 47.—Sound Ray Impact point Versus Wind Velocity, 457 m Altitude

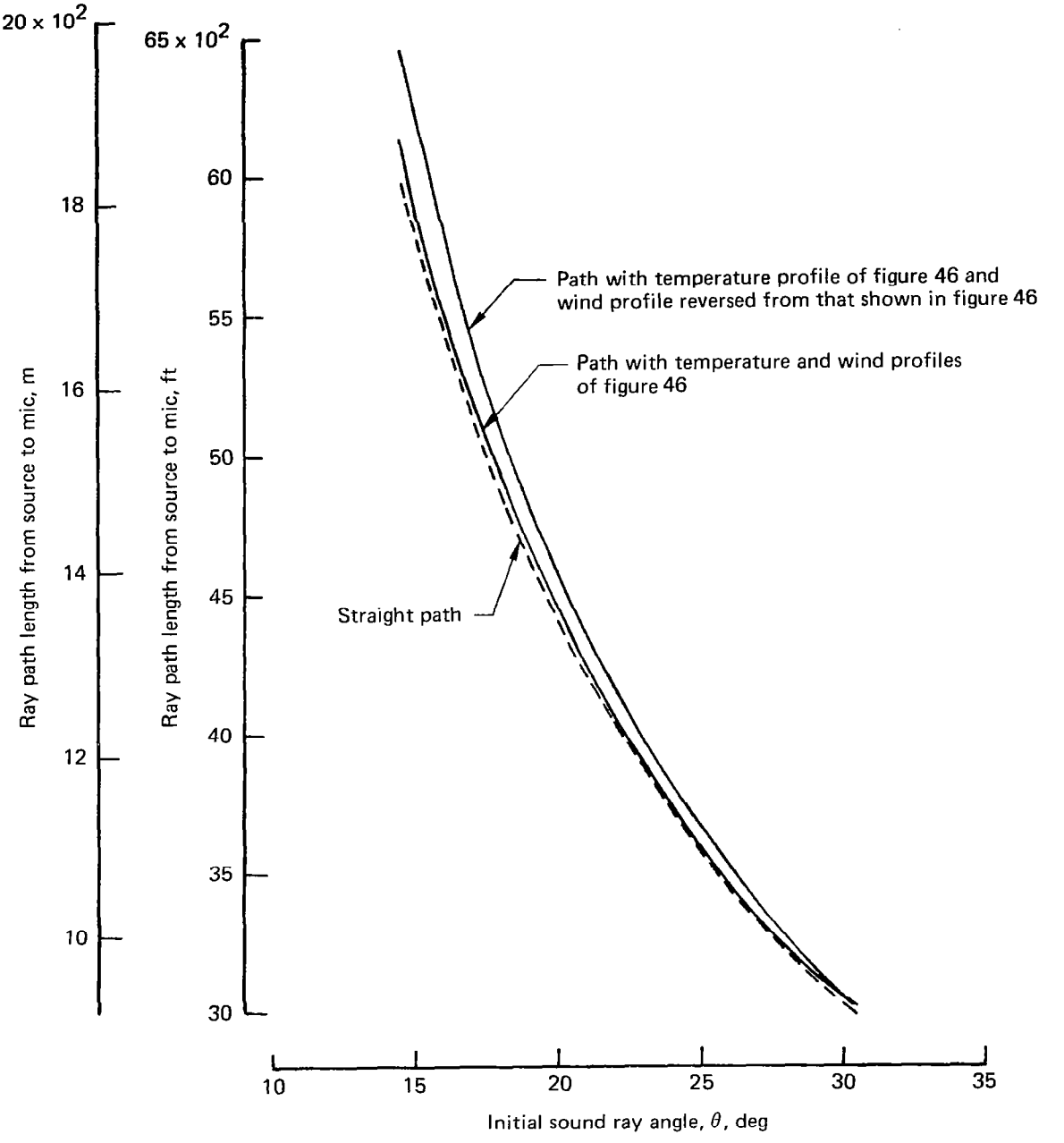

Figure 48.—Ray Path Length at 457 m Altitude

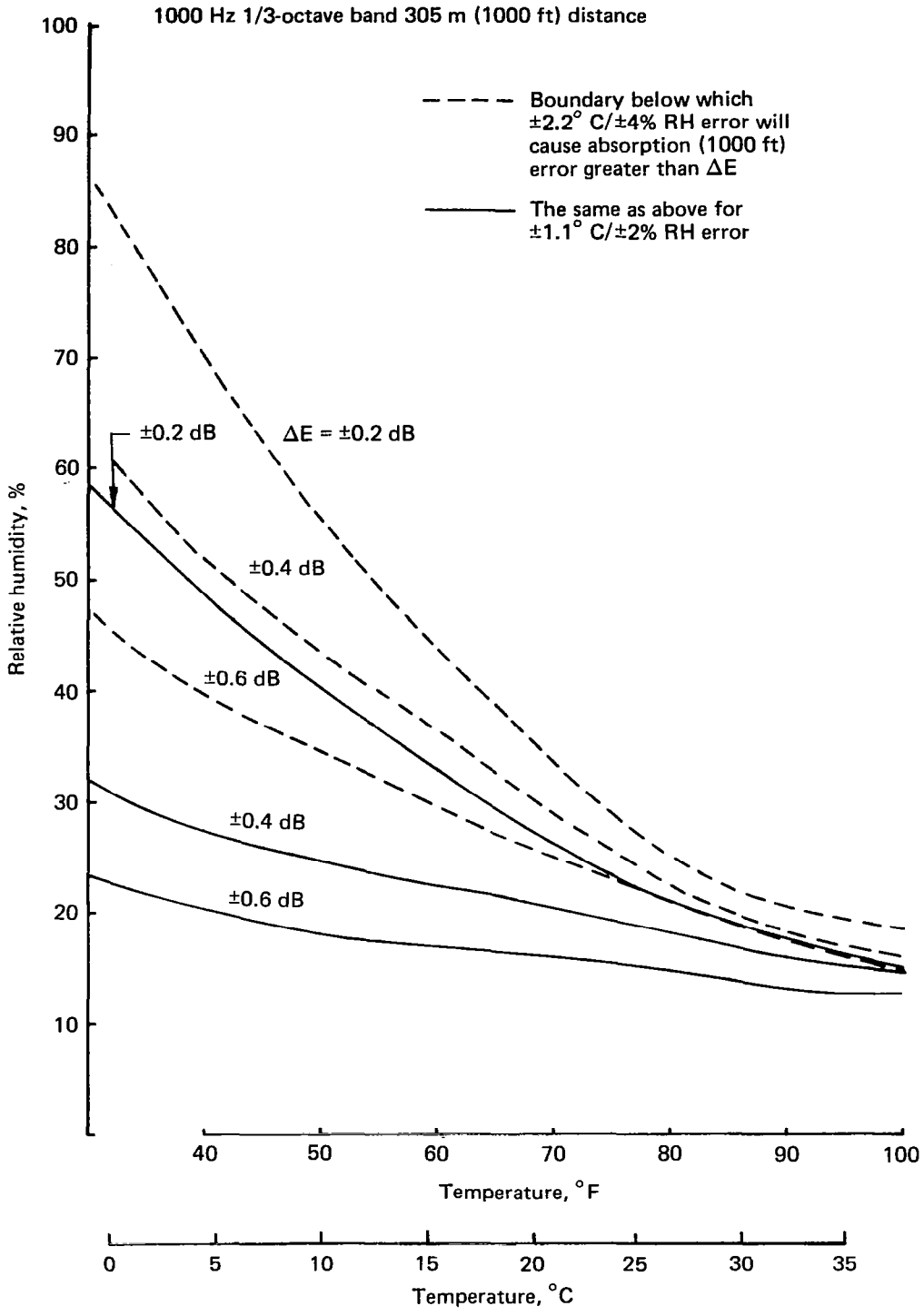

Figure 49.—Error Tolerance Boundaries for Atmospheric Absorption

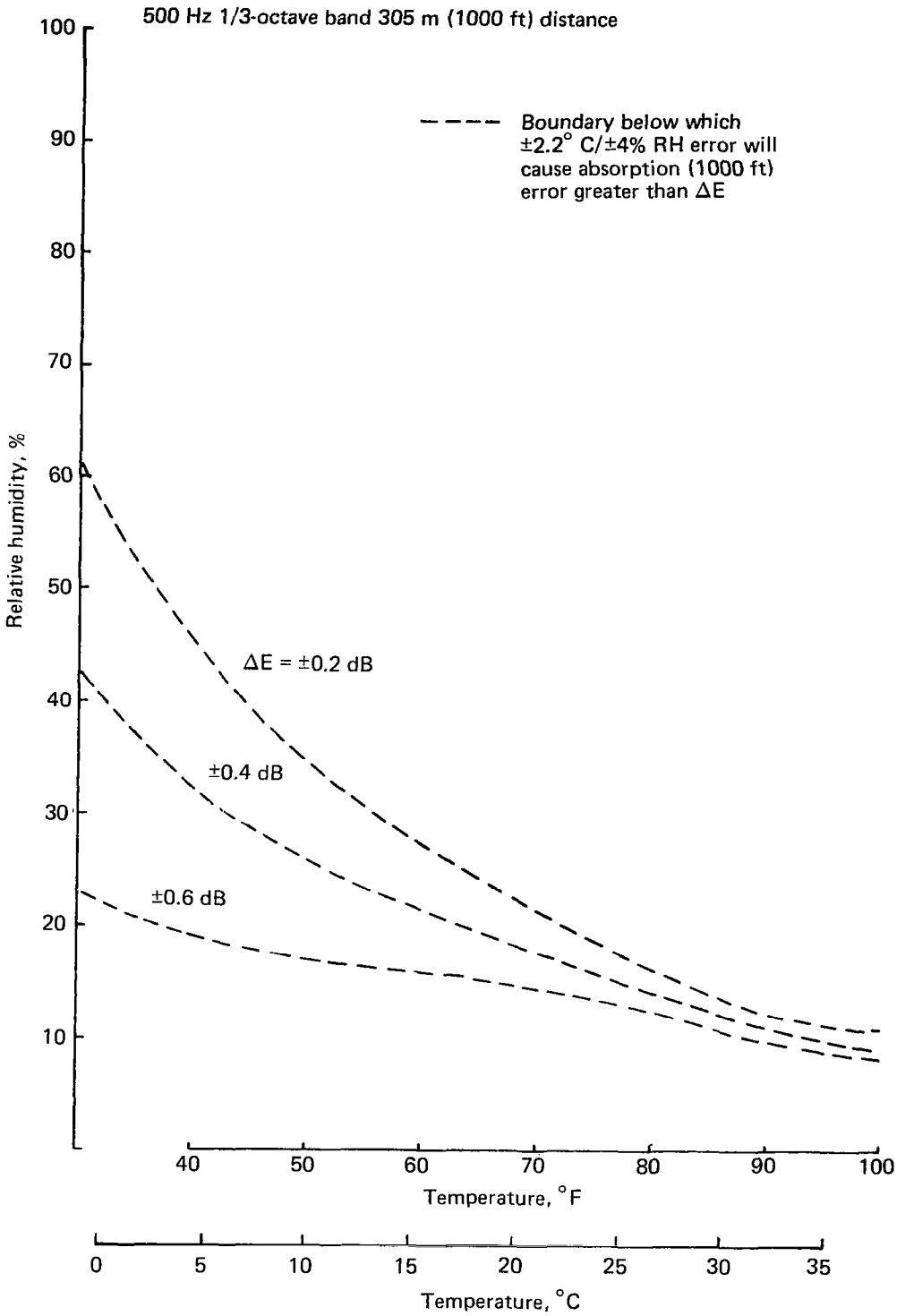

Figure 50.—Error Tolerance Boundaries for Atmospheric Absorption

on the ground. Various analytical and experimental study results reveal that the vortices from a current commercial transport persist with a considerable rotational velocity long enough so that a light airplane straying into them may experience a hazardous flight condition. This study was conducted to determine if the cores of the vortices would interfere with the propagation of jet noise from an aircraft flying overhead to an observer on the ground.

The study results of references 45 through 47 indicate that the centerline of the trailing vortex of current heavyweight airplanes (707, C-5A, and 747) sinks 244 m (800 ft) at an approximate separation distance of 7400 m (4 nmi). A plot extracted from reference 45, showing some of the test results, is presented in figure 51. When it is assumed that the sinking is linear and the vortex centerline distance remains equal to the wing span, the sinking angle with respect to the flightpath is 2^0. Theories (ref. 48) and experiments (refs. 49 and 50) show that the distance between the centerline of vortices may be assumed to be equal to the wing span near the airplane, and the diameter of the vortex core within one second of vortex age is estimated to be less than 3 m for the heavy aircraft.

Consideration of the relative location of the vortex cores to the noise propagation path leads to the conclusion that the cores themselves will not be in the path of jet noise propagation from the aircraft (in flight overhead) to the observer on the ground.

3.2 SOURCE ALTERATION EFFECTS

When a jet is in motion relative to the ambient air, the noise production mechanisms are altered. This causes a change in the effective strength of the noise source. An accurate determination of jet noise motion effects requires a fundamental understanding of the source alteration mechanisms. For this reason, analytical study of this phenomenon is underway at Boeing and has resulted in the flow/noise computer program (ref. 51), which is discussed in section 3.2.1.

The jet noise is computed in a reference frame at rest with respect to the nozzle. This method represents the wind tunnel jet noise test condition and allows a simpler treatment in the analysis of source alteration effects by an ambient airflow. In an acoustic flight test, the noise measured is in reference to the ground or to the ambient air. To correlate this noise level with that in reference to the nozzle, a transformation of coordinates is required. Section 3.2.2 discusses comparisons of various experimental techniques for the forward motion effects; e.g., wind tunnel method, flyby method, etc., including the aspect of transformation of coordinates required between the wind tunnel test and flyby test conditions.

3.2.1 FLOW/NOISE PROGRAM ANALYSIS

The accurate prediction of jet noise as affected by ambient airflow requires extensive knowledge of two aspects of the problem: description of the mean and turbulent fluid mechanic properties of jet flows and an understanding of the noise production mechanism. The flow/noise mathematical models and the computer program which utilizes them have proven to be valuable tools. In the following paragraph, a brief

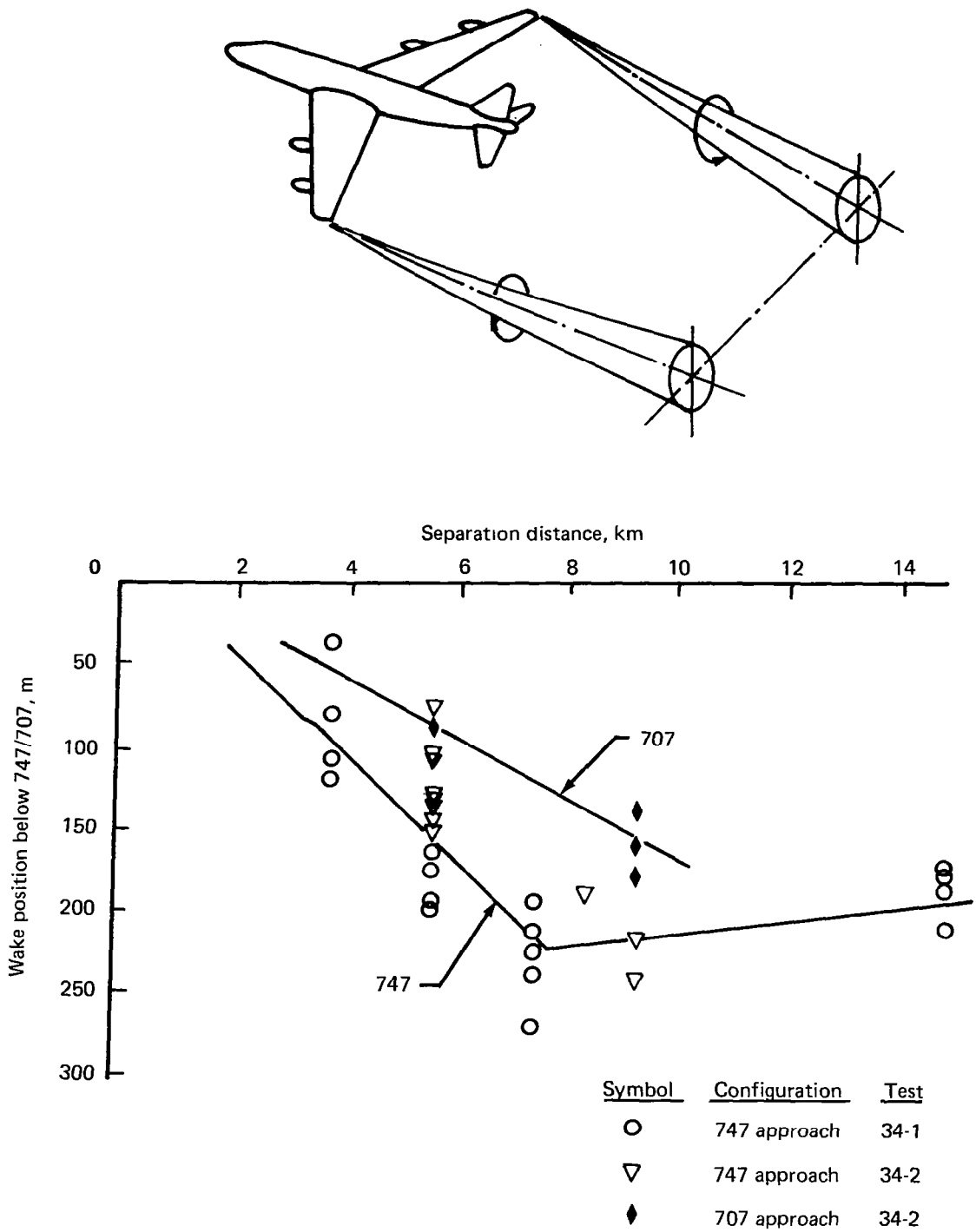

Figure 51.—Vertical Wake Position Versus Separation Distance From Aircraft Rev. (Ref. 45)

discussion on the derivation of the mathematical models and some examples of application of this program are presented.

3.2.1.1 Calculation of Axisymmetric Compressible Turbulent Jet Flows

The mathematical model (ref. 52) computes the mean flow properties and turbulence intensities within axisymmetric jets. The approach taken in the derivation of the model is similar to that used by Heck and Ferguson (ref. 53). The continuity, momentum, energy, and turbulent kinetic energy equations, are transformed into the following set of parabolic differential equations by the applications of Von Mise's transformation and are numerically solved with the known boundary conditions:

$$\frac{\partial v}{\partial \xi} = \left[\frac{\nu_j}{V_j D_j}\right] \frac{\partial}{\partial \psi}\left(\nu_e \rho^2 v\, y^2 \frac{\partial v}{\partial \psi}\right) \tag{27}$$

$$\frac{\partial e}{\partial \xi} = \left[\frac{\nu_j}{V_j D_j}\right] \frac{\partial}{\partial \psi}\left(a\, \nu\, \rho^2 v\, y^2 \frac{\partial e}{\partial \psi}\right) + \left[\frac{V_j}{\sqrt{E_j}}\right] \alpha \sqrt{e} \rho^2 \ell_t v y^2 \left(\frac{\partial v}{\partial \psi}\right)^2 - \left[\frac{\nu_j}{V_j D_j}\right] \frac{ab\nu e}{v \ell_t^2} \tag{28}$$

$$\frac{\partial \theta}{\partial \xi} = \left[\frac{\nu_j}{V_j D_j}\right] \frac{\partial}{\partial \psi}\left(\nu_e \rho^2 v y^2 \frac{\partial \theta}{\partial \psi}\right) + \left[\frac{\nu_j V_j}{C_p T_j D_j}\right] \nu_e \rho^2 v y^2 \left(\frac{\partial v}{\partial \psi}\right)^2 \tag{29}$$

The boundary conditions are:

$\xi = \xi_o$; v, e, and θ are known functions of ψ

ψ = o ; v, e, and θ are finite

$\psi = \psi_b$ (outside jet boundary); v, e, and θ approach external values.

In the previous equations, the axial and radial coordinates of jet, x and y (with the origin at the center of jet exit plane) are related to ξ and ψ by

$$x = \xi$$

$$1/4\, y^2 = \int_o^{\psi} (1/\rho v)\, d\psi \text{ along } \xi = \text{constant};$$

$v = V/V_j$, $e = E/E_j$, and $\theta = T/T_j$ designate the normalized local axial velocity, energy, and temperature, respectively; V, E, and T are local velocity, energy, and temperature, respectively; V_j, E_j, t_j, ν_j, and D_j are the reference velocity, energy, temperature, kinematic viscosity, and jet diameter, respectively; ν_e, ρ, and ν are the nondimensional effective kinematic viscosity, density, and kinematic viscosity, respectively, being

normalized by the respective reference values; $\ell_t = L_t/D_j$, where L_t is the characteristic length of turbulent mixing; C_p is the constant pressure specific heat; a is the coefficient of turbulent kinetic energy diffusion, b and α are constants.

The analysis uses the standard assumptions of steady turbulence, small fluctuations in comparison with time-averaged quantities, a constant static pressure inside and outside the jet flow, small radial velocity in comparison with axial velocity, and the perfect gas law. The analysis also uses a turbulent shear stress model in which the turbulent viscosity is proportional to the product of the local turbulent momentum and the characteristic length of the turbulence.

The inputs normally required for this program are D_j, V_j, T_j, and E_j, at the jet exit, in addition to the ambient air pressure and temperature. The program computes all jet flow parameters starting from the jet exit and progressively proceeding downstream in this case. The program can also be used to compute the jet flow conditions downstream of a certain axial station, if V, T, and E are given as functions of jet radius at that station.

The computer program constructed from the mathematical model can be applied to predict jet flows of single- and dual-flow nozzles with and without ambient flows. Comparisons of the predicted values with test data showed excellent agreement. Examples of these comparisons are presented in section 3.2.1.3.

The jet flow information computed by this program serves as an input to the noise prediction program, which is discussed in the following paragraph. The flow computer program makes possible the study of the effects of jet pressure and temperature ratios, upstream turbulence level, nozzle exit plane mean flow profiles, relative velocity, etc.

3.2.1.2 Noise Generation and Propagation

By extending the general theory of sound generated aerodynamically given by Lighthill (ref. 54), Ffowcs-Williams (ref. 38) derived equations for the noise from the turbulent noise sources convecting at high speed with respect to the ambient air. The method used in the flow/noise program is essentially the same as that of Ffowcs-Williams except for the expression used for the turbulence. Whereas the Ffowcs-Williams turbulence model was based on a Gaussian turbulence correlation function, the correlation function used in the flow/noise program came from the experimental measurements of Jones (refs. 55 and 56). The basic equation involved is Lighthill's wave equation for a turbulence source

$$\frac{\partial^2 \rho}{\partial t^2} - c_o^2 \frac{\partial^2 \rho}{\partial x_i^2} = \frac{\partial^2 T_{ij}}{\partial x_i x_j} \tag{30}$$

where

$$T_{ij} = \rho v_i v_j + P_{ij} - c_o^2 \rho \delta_{ij} \tag{31}$$

Here ρ is the density; t is the time; c_0 is the speed of sound; x is the space coordinate; v is the fluid element velocity; P is the pressure; i and j are coordinate directions; and δ_{ij} is the Kronecker delta. In the analysis, the sum of the pressure perturbation term (second) and the density fluctuation term (third) of the right side of equation (31) was neglected. The "shear noise" is also neglected in the first term. From the general solution of equation (30) the density perturbation is given by

$$\rho - \rho_O = \frac{1}{4\pi c_0{}^2} \frac{\partial^2}{\partial x_i x_j} \int T_{ij} (\vec{y}, t - r/c_0) \frac{d\vec{y}}{r} \tag{32}$$

The pressure perturbation can be written simply in terms of the above density perturbation since the disturbances are isentropic in the acoustic field. The square of the pressure perturbation divided by the acoustic impedance of air yields the acoustic intensity. Since only the velocity fluctuations in T_{ij} are being considered, the resultant expression for intensity will involve correlations of T_{ij}. The procedures used are similar to those described in reference 38. The jet noise power spectral density (PSD) can be found by taking the space-time Fourier transform of the intensity, i.e.,

$$PSD = \frac{\rho_j{}^2 (V_j - V_O)^8}{\rho_O c_O{}^5} \frac{D_j}{V_j} \left(\frac{q_j}{V_j - V_O} \right)^4 S_t{}^4 I \tag{33}$$

where the integrated source strength is expressed as

$$I = \int_W G(P,V,q,\ell_{cr},\phi)\, F\,(S_t,\theta,V_c,V_j,V_O,\ell_{cr}) \frac{dW}{r^2} \tag{34}$$

This expression contains the Fourier transform of the T_{ij} correlations, which is also known as the turbulence wave number frequency spectrum. The correlations were obtained from the experimental data of references 55 and 56. The data were nondimensionalized using relative velocity as the characteristic velocity. The data were then curve-fitted so that they could be easily programmed into the expression for I.

In equation (32), ρ_0 is the ambient density of air; y denotes the source position vector with respect to the ambient air (or to the observer on the ground); and r is the distance between the airplane and the observer at the time of noise emission. In equation (33), V_0 is the ambient air velocity with respect to the nozzle; q_j is the reference rms turbulence velocity within the jet; and $S_t = [fD_j/(V_j - V_0)]/[1 + (V_0 \cos \phi)/c_0]$ where f is the sound wave frequency and ϕ is the sound emission angle from the jet toward the observer. In equation (34), G denotes the source strength function and F denotes the wave number frequency spectrum. These in turn are functions of the local jet density ρ, local velocity V, local turbulence velocity q, turbulence correlation length ℓ_{cr}, emission angle ϕ, the Strouhal number S_t, and the turbulence convection velocity V_c, V_j, and V_0. The integration is performed over the entire jet volume W.

Evaluation of G is done with the jet flow characteristics computed by the "flow program" discussed previously, and F is evaluated by the known conditions. Finally, the PSD is integrated for each 1/3-octave band, obtaining the entire 1/3-octave-band jet noise spectra for a specific noise emission angle ϕ.

3.2.1.3 Examples of the Flow/Noise Program Application

Six examples of the jet flow computations are shown in figures 52 through 57. The velocity profiles at various stations downstream of the single- and dual-flow nozzle exits are presented in figures 52 and 53. The test data points shown in figure 52 indicate that the computed values are in excellent agreement with them. Figure 53 shows what may be expected to happen in the velocity profiles in a dual-flow nozzle, although no test data were available to substantiate the prediction.

Figures 54 and 55 show the core length variation as functions of the ambient airflow velocity. The end of core is defined as the point at which the centerline jet velocity has dropped by 0.01 $(V_j-V_0)/V_j$, where V_j is the jet velocity and V_0 is the ambient airflow velocity. Figure 55 shows the core length of cold and hot jets within which the flow Mach number is supersonic. It shows that the length rapidly increases as V_0/V_j increases for the hot jet.

The predicted centerline velocity decay of a single subsonic round jet is represented in figure 56. Agreement with the test data of Laurence (ref. 57) appears to be excellent. The calculated turbulent intensity profiles at a downstream station of the same nozzle are shown in figure 57 in comparison with test data. The agreement between the calculated and the test data is reasonable.

The examples to follow are for the application of the combination of the flow and noise computation programs. The flow/noise program is constructed in such a way that the program can compute the contribution of each segment of the jet, in addition to calculating the noise of the whole jet. This was to evaluate source strength as a function of axial location.

Figure 58 presents an example of application of the flow/noise program to the source strength problem. The figure shows the relative noise levels of three 1/3-octave bands (500, 1000, 2000 Hz) contributed by each 1-dia length of jet. The noise level is for the radiation angle of 90° from inlet centerline and for a 7.6 m (25 ft) distance from the nozzle exit center. The contribution of 500-Hz noise by each 1-dia length slice of jet is seen to be small near the nozzle exit but larger toward the downstream nozzle station. The 2000-Hz noise is higher than the 500 Hz noise near the exit but lower downstream. The 1000-Hz noise is in between the two. The trends are well corroborated by experiments (refs. 58 and 59). Also included in the figure is the variation of the contribution to the OASPL by each 1-dia length slice of jet showing a monotonic decrease from the jet exit to the downstream.

The next two examples (figs. 59 through 62) present the prediction of jet noise of single- and dual-flow nozzles. The 1-in. dia single-flow nozzle had a cold flow. Figure 59 shows the comparison of spectra at three jet velocities. Whereas the agreement between the

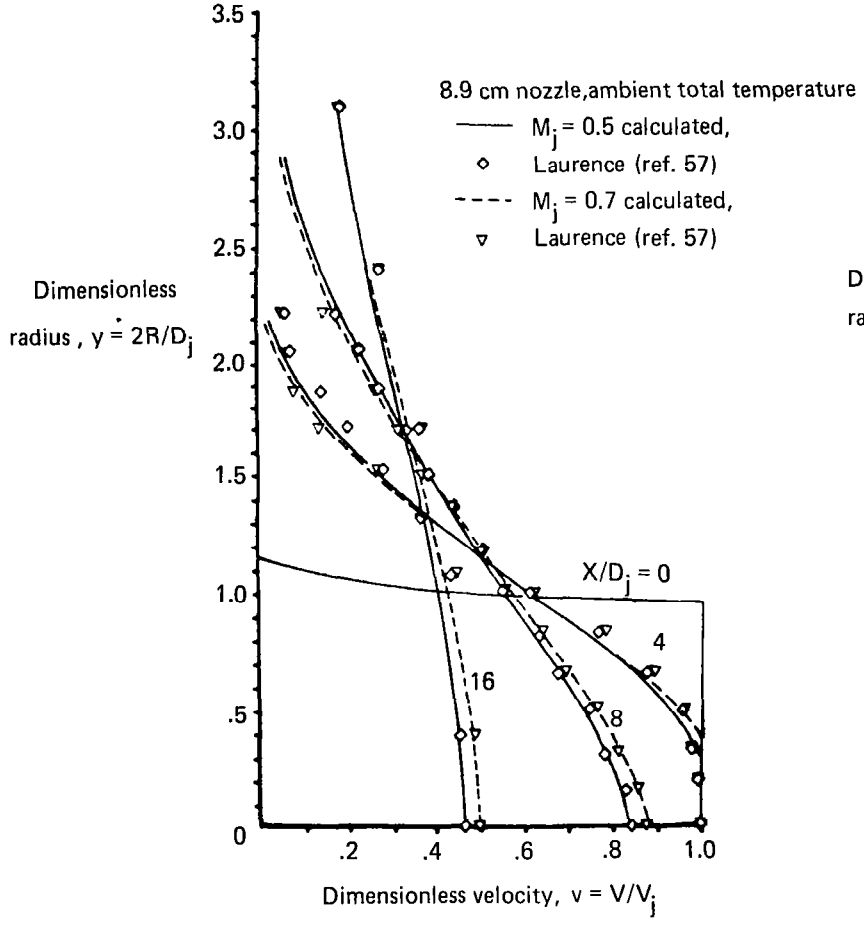

Figure 52.—Velocity Profiles of a Single Subsonic Round Jet, No Ambient Flow

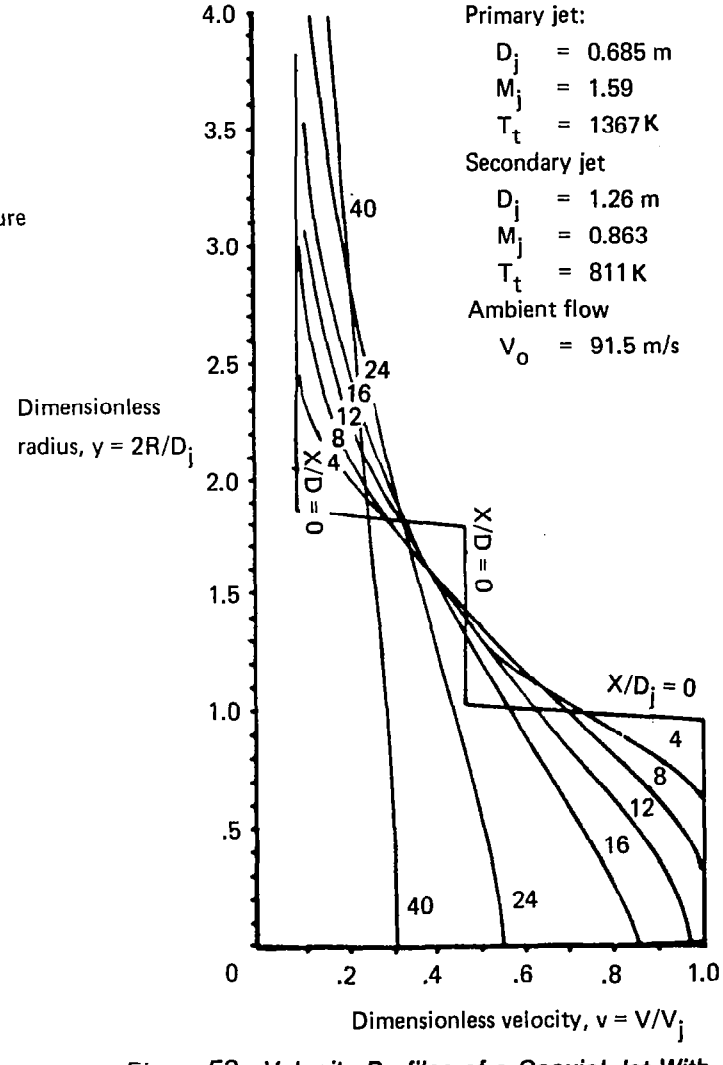

Figure 53.—Velocity Profiles of a Coaxial Jet With Parallel Ambient Flow

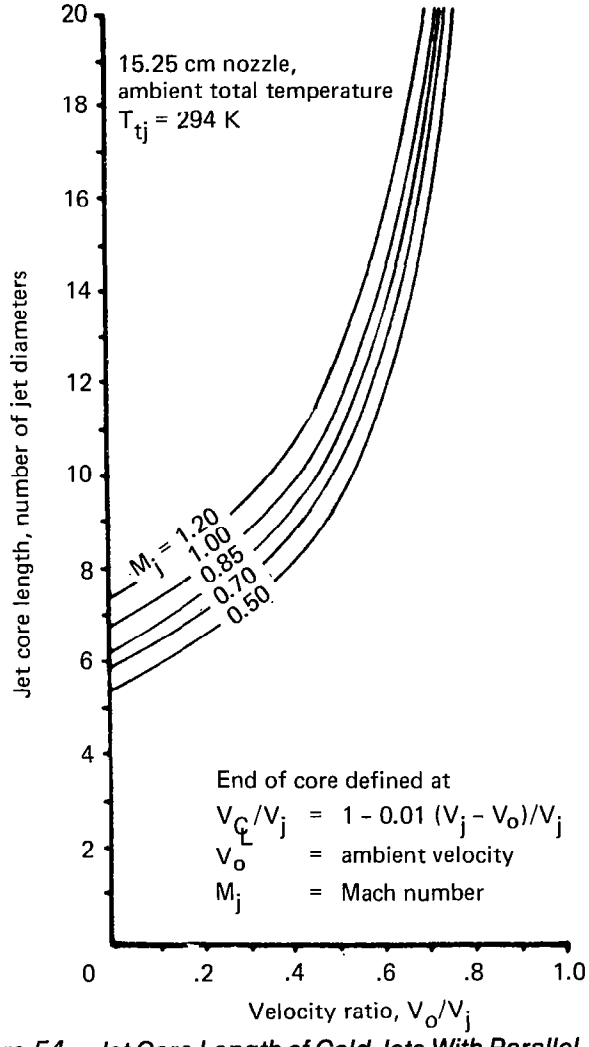

Figure 54.—Jet Core Length of Cold Jets With Parallel Ambient Flow

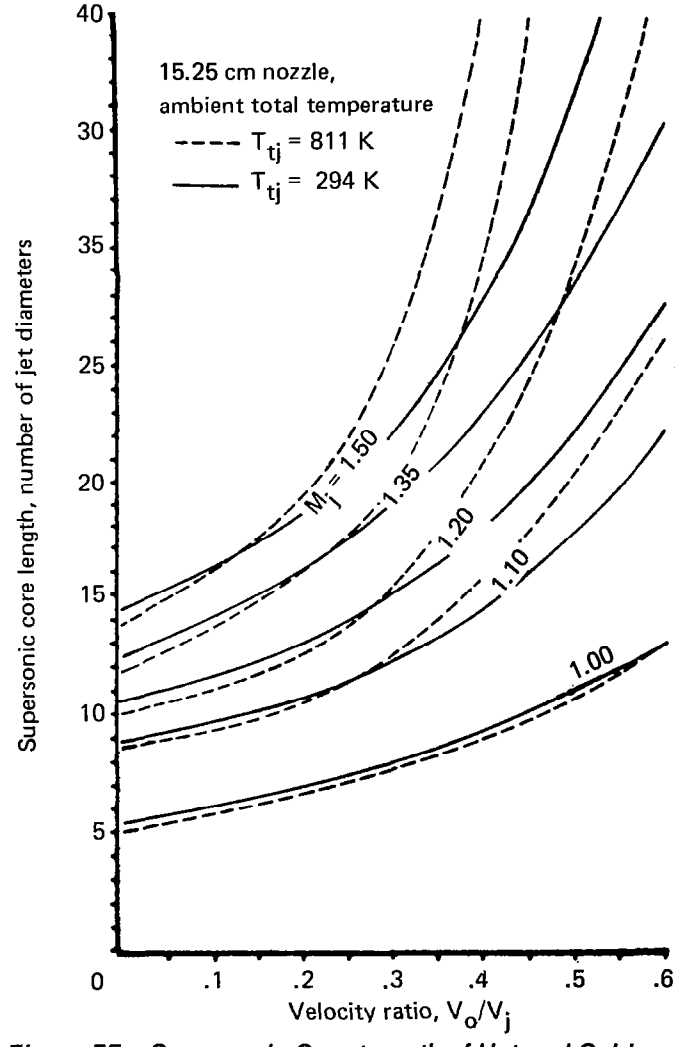

Figure 55.—Supersonic Core Length of Hot and Cold Jets With Parallel Ambient Flow

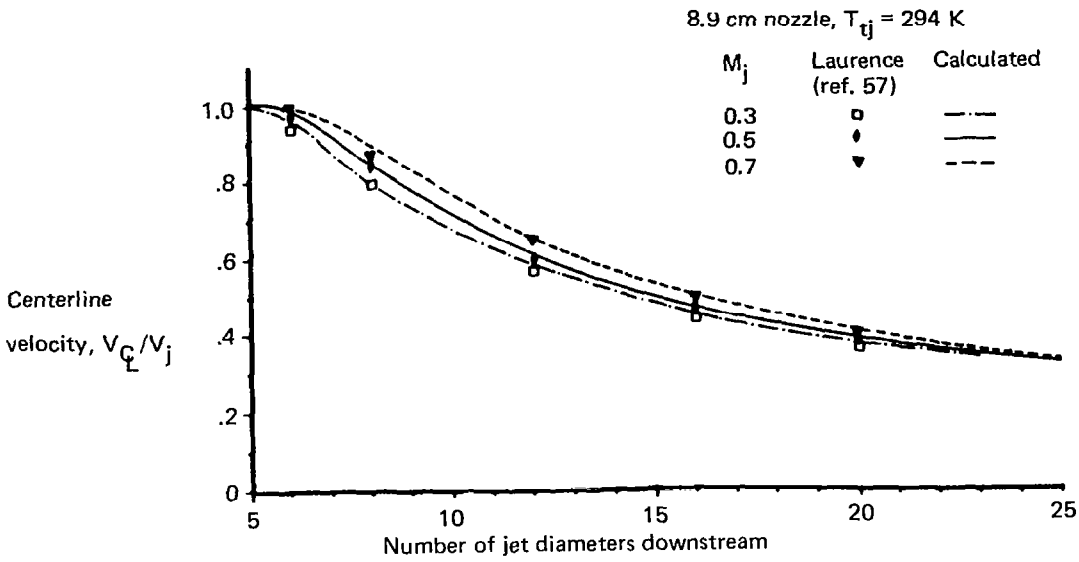

Figure 56.—Centerline Velocity Decay of a Single Subsonic Round Jet, No Ambient Flow

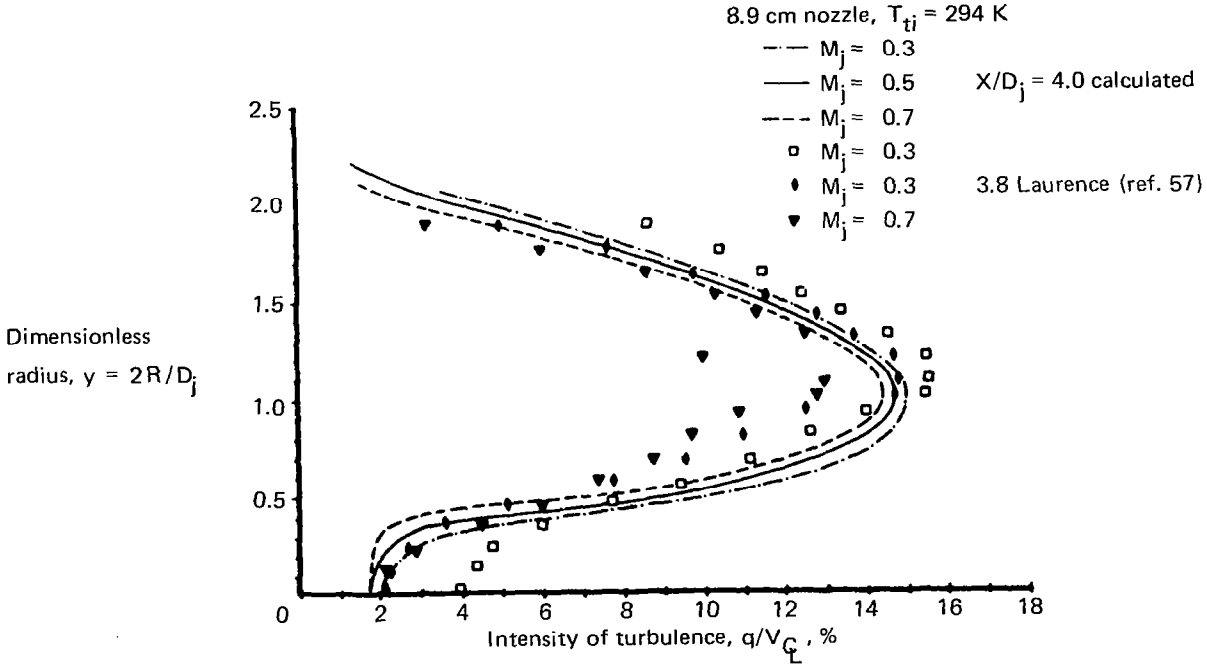

Figure 57.—Turbulence Intensity of a Single Subsonic Round Jet Near the End of the Jet Core, No Ambient Flow

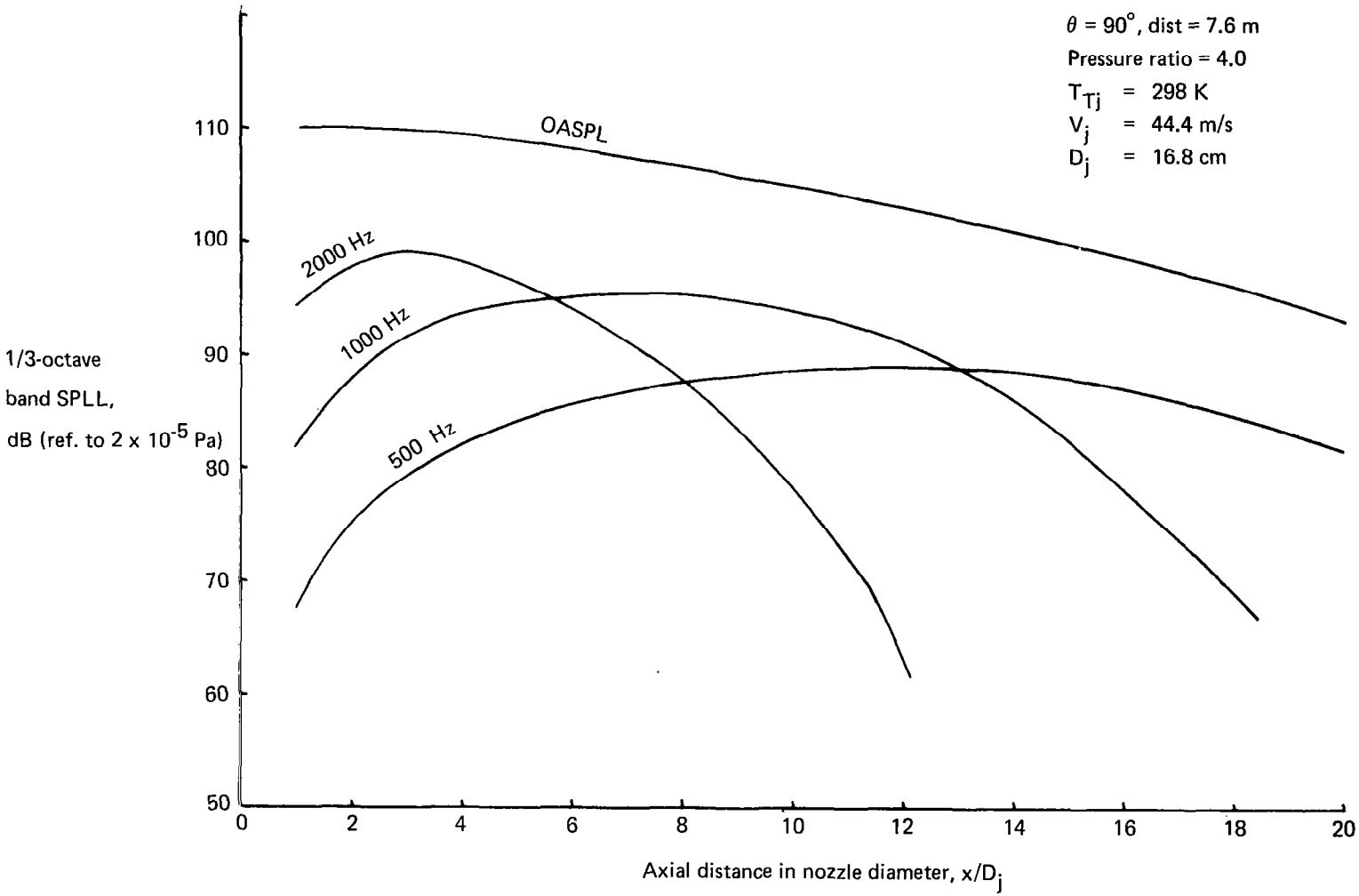

Figure 58.—Overall and 1/3-Octave Band Sound Pressure Levels Per 1-Die Length of Jet Versus Axial Distance From Nozzle Exit

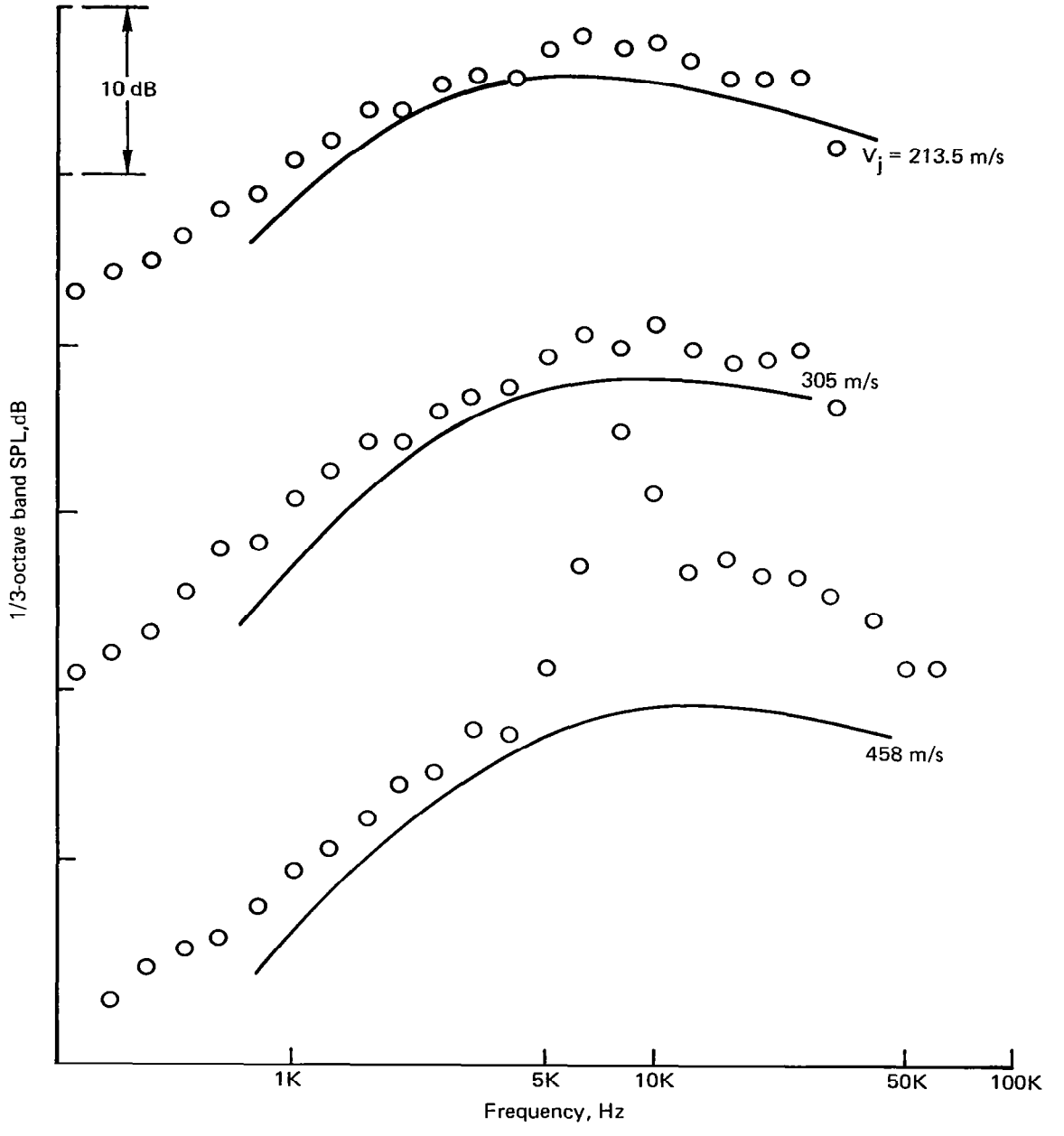

Figure 59.—Spectral Comparison (Single Jet), Flow/Noise Program

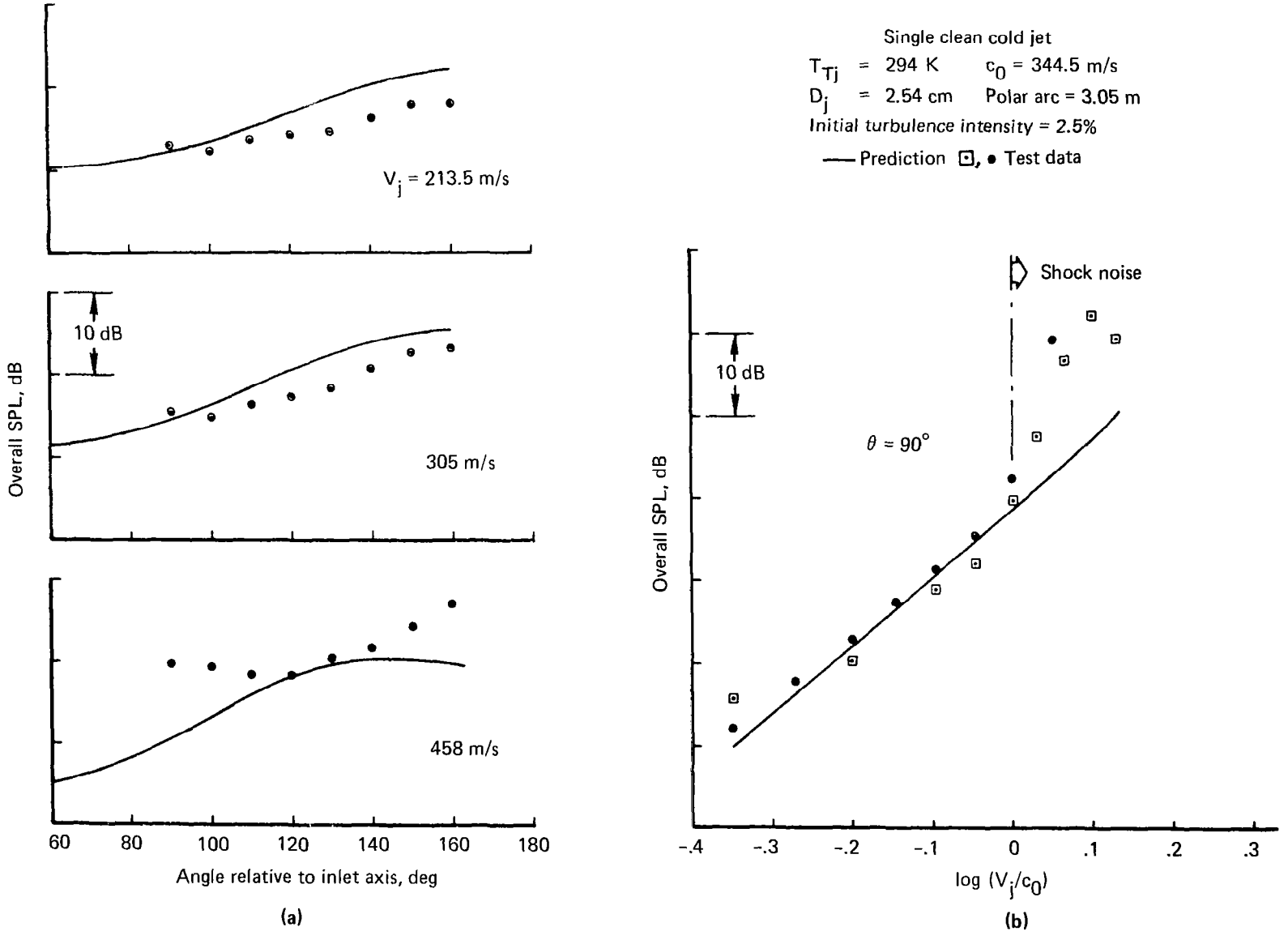

Figure 60.—Overall Sound Pressure Level Comparisons (Single Jet), Flow/Noise Program

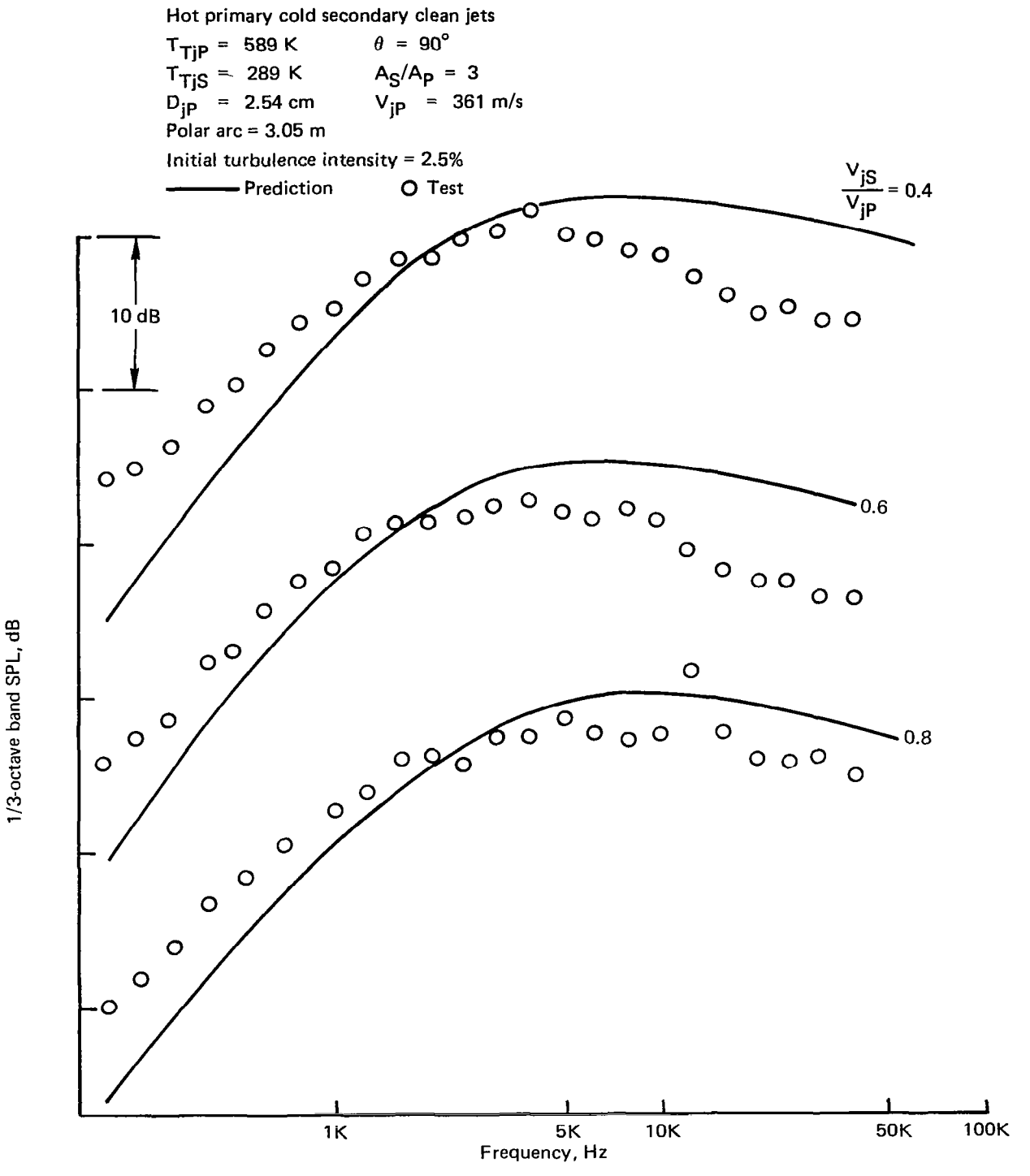

Figure 61.—Spectral Comparison (Dual Jet), Flow/Noise Program

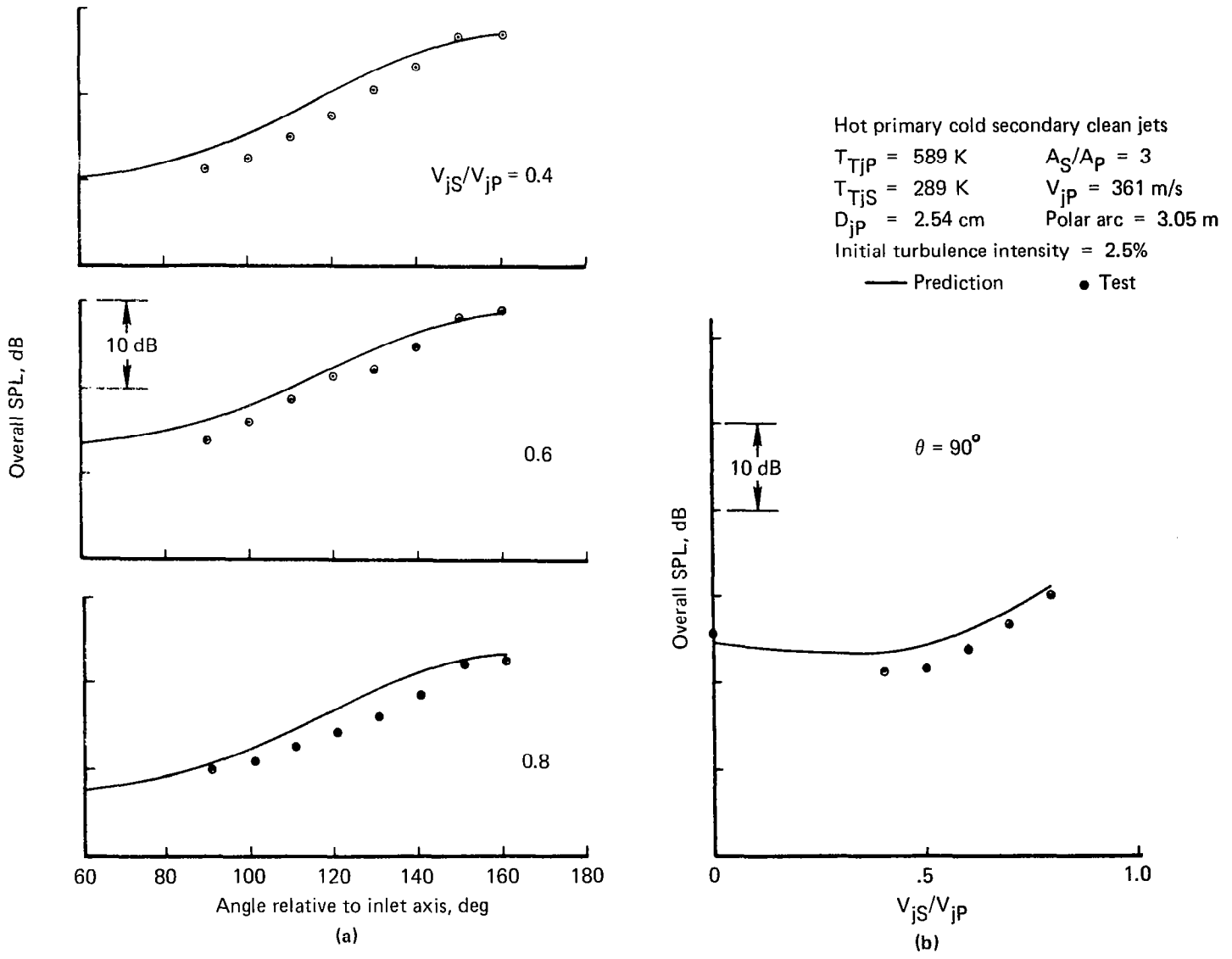

Figure 62.—Overall Comparisons (Dual Jet), Flow/Noise Program

prediction and test data is good at the two subsonic jet velocities, the prediction is off for the supersonic jet. This is attributable to the shock noise.

Figure 60 shows the comparisons of OASPL's. Again, the OASPL variations as functions of radiation angle show (left portion of fig. 60) a reasonable agreement between the predicted and the test data for subsonic jet velocities. Disagreement is seen in the supersonic case due to shock noise. The comparison of OASPL at 90^0 radiation angle for various jet velocities is presented on the right of figure 60. Two sets of test data are compared with the predicted data. The predicted levels are in excellent agreement with test data for the subsonic range.

Comparisons of the computed and experimental noise spectra and OASPL's of a dual-flow nozzle, having a hot primary flow, are presented in figures 61 and 62. The spectral comparison of figure 61 indicates a trend that the computed result underpredicts the lower frequency noise and overpredicts the high frequency noise. However, the comparisons of OASPL are seen to be reasonable in figure 62. Reasons why this may be the case are discussed in section 3.2.1.4.

An example of the application of the program to a comparison study is illustrated in figure 63. It compares two nozzles, one that has a coplanar-coaxial dual flow and the other that has a single fully mixed flow in which the energy flow rate at the nozzle exit is the same as the dual-flow nozzle. Velocity profiles, turbulent intensity profiles, and finally, the expected noise levels are computed as shown in the figure.

Figure 64 is a result of a parametric study of the effect of velocity ratio (V_{jS}/V_{jP}) on sound power level (PWL) with and without the ambient airflow. The primary jet condition of the dual-flow nozzle was kept constant, while the secondary jet condition was varied to realize the specified velocity ratio. The curves indicate that the minimum noise is not attained at V_{jS}/V_{jP} of zero, but at a nonzero point (0.35), which is a function of the ambient air velocity. In figure 64, the PWL curve for the case with the ambient airflow was shifted upward so that the PWL at V_{jS}/V_{jP} of zero coincided with that for the case without ambient airflow. Thus, the PWL differences seen between the two curves are additional noise reductions resulting from the ambient airflow for those cases in which V_{jS}/V_{jP} is neither zero nor unity.

Figure 65 shows the results of the same parametric study as that for figure 64, performed with test data obtained at Boeing. The prediction results computed by the flow/noise program are included. The computed curves show a fair agreement with the test data in level as well as trend.

Figures 66 and 67 show further examples of the parametric studies conducted. Figure 66 shows the effect of increasing jet core turbulence on the change in jet core length and total acoustic power. The figure also indicates that jet noise could be reduced by lower initial turbulence intensity.

Figure 67 shows the OASPL variations as functions of the jet velocity or the relative velocity (jet velocity minus ambient air velocity) for cold and hot single-flow jets. It indicates that the slope of the curves (the velocity exponent) is not a constant; instead,

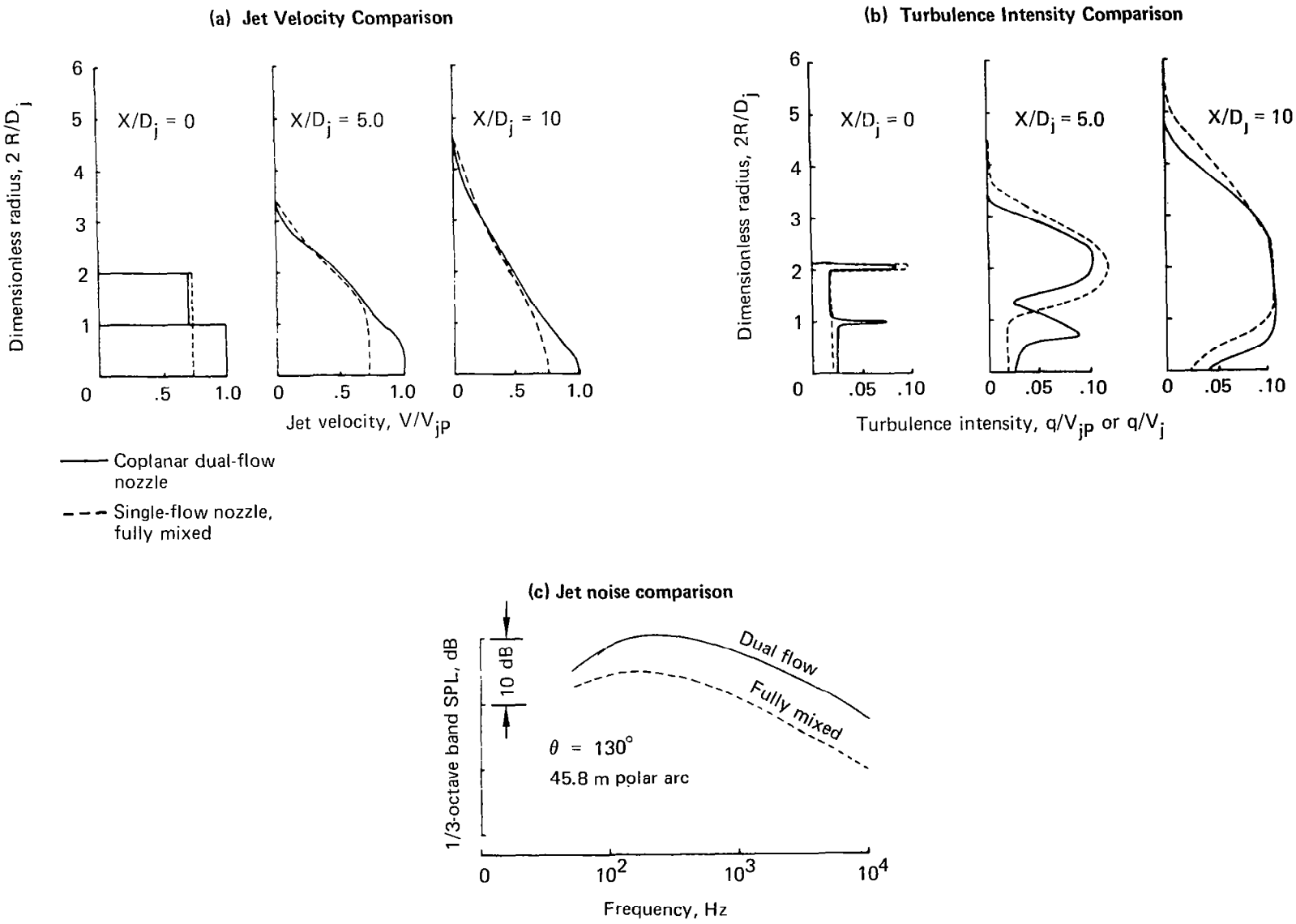

Figure 63.—Jet Flow and Noise Calculated by Flow/Noise Program

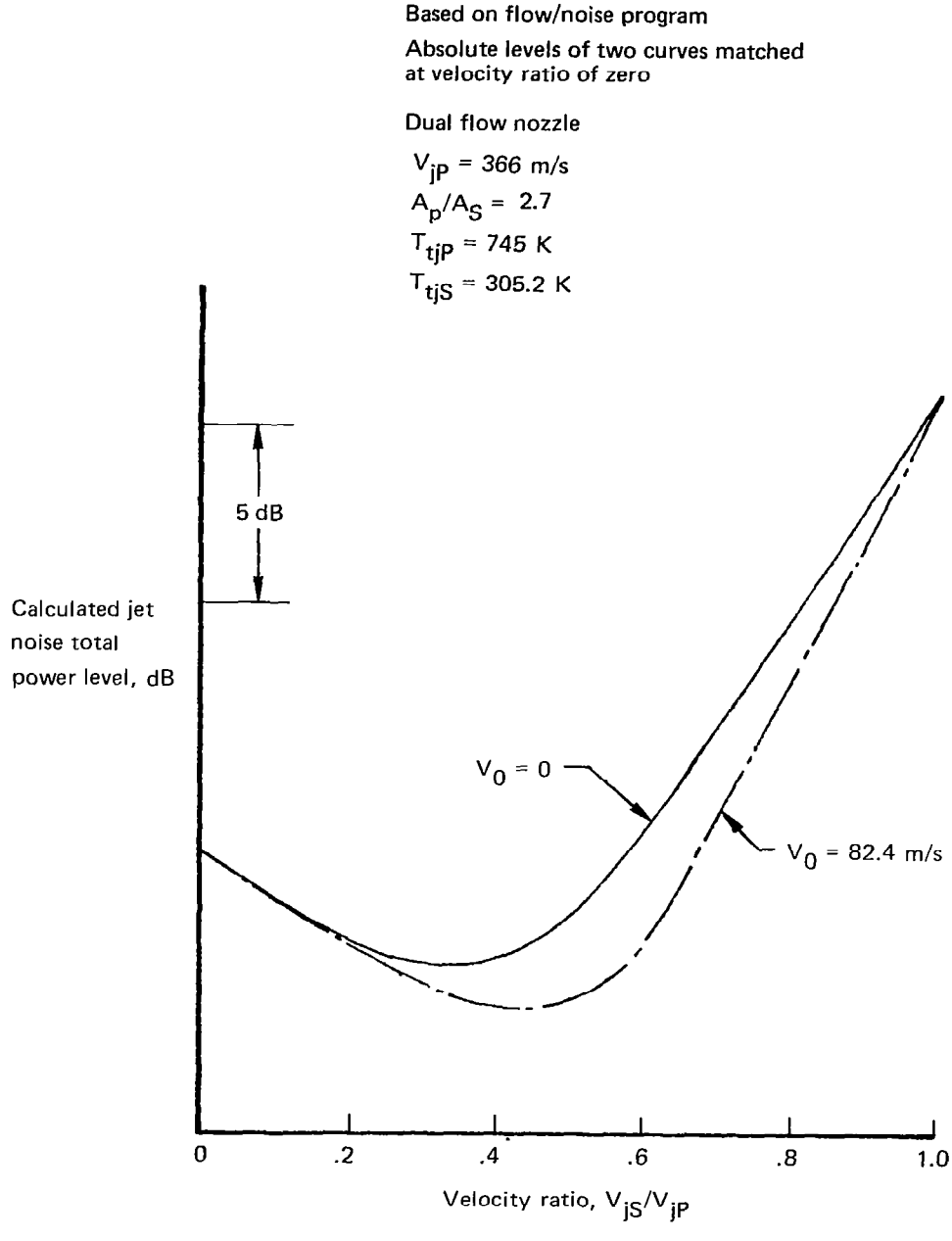

Figure 64.—Velocity Effect on Jet Noise Total Power Level, Flow/Noise Program

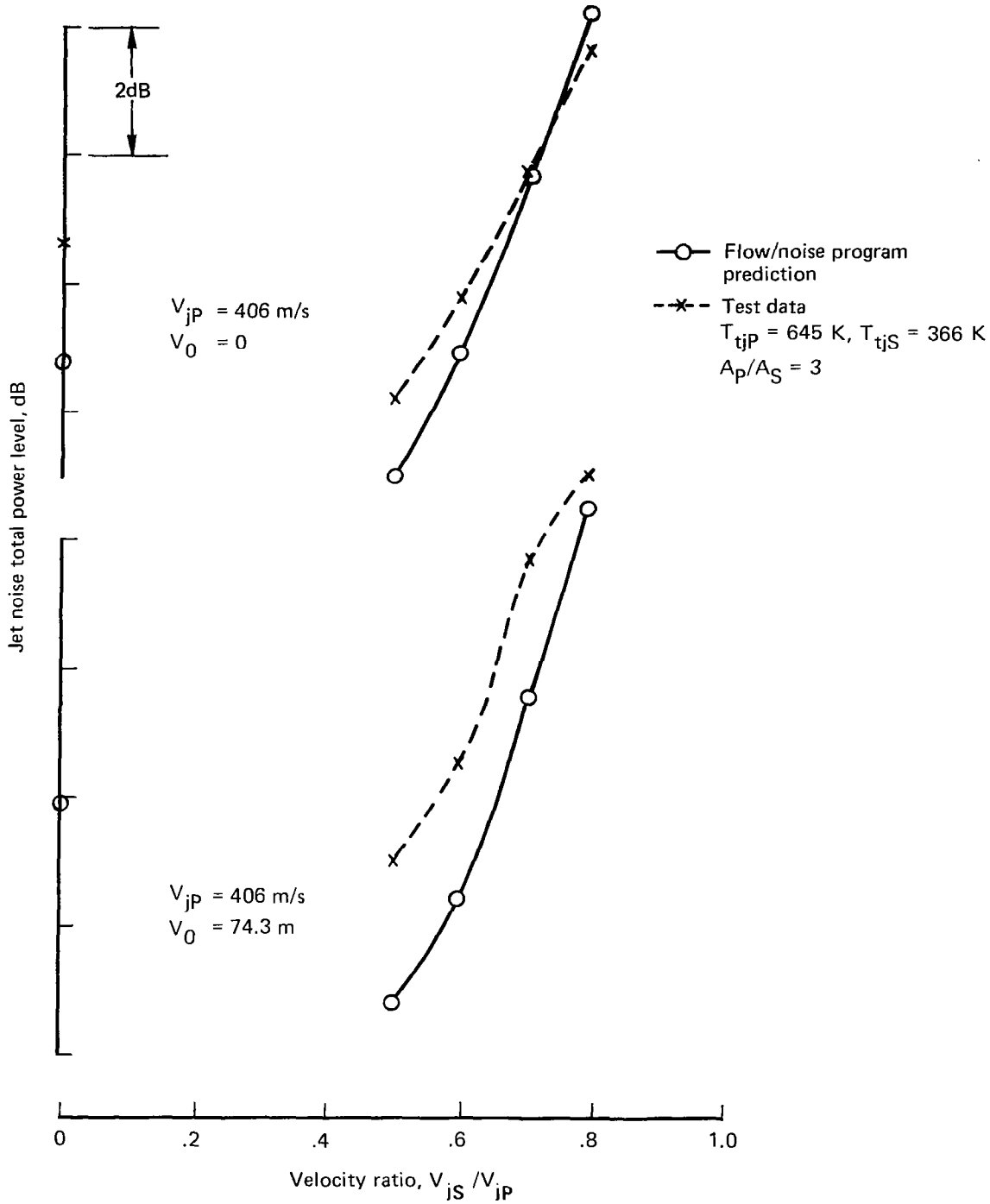

Figure 65.—Comparison Between Flow/Noise Program Prediction and Test Data

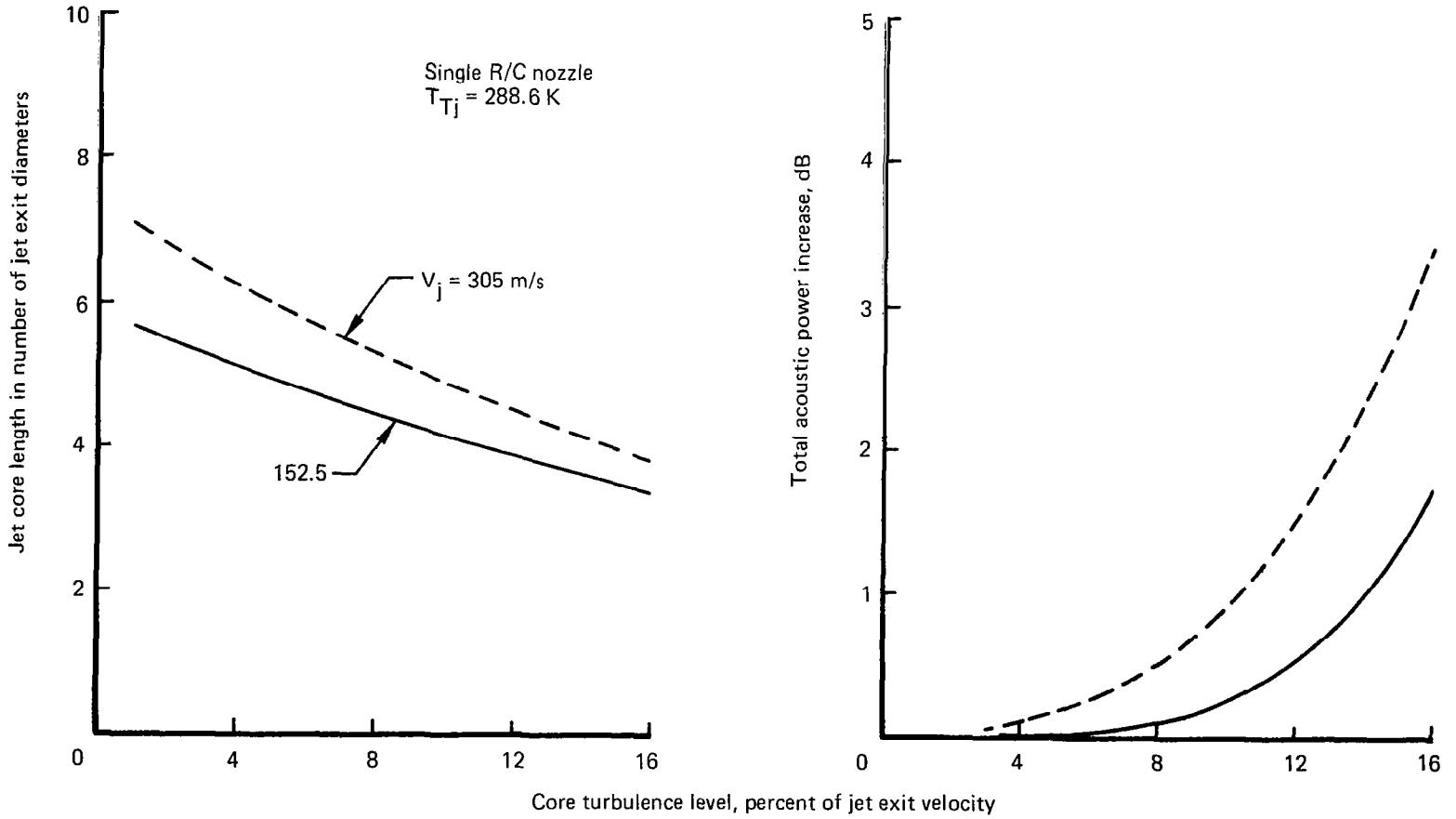

Figure 66.—Effect of Core Turbulence Level

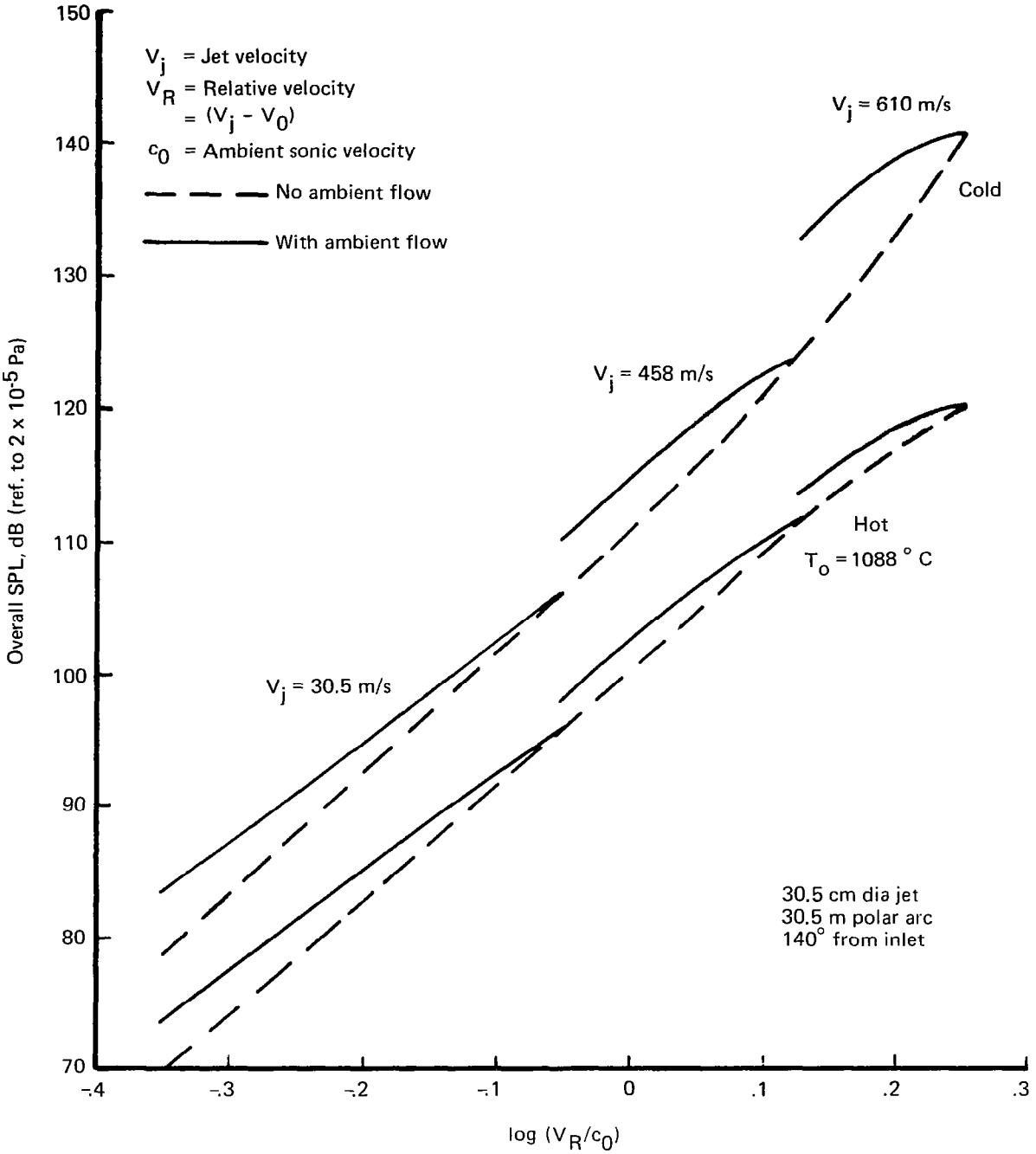

Figure 67.— Relative Velocity Effect, Single-Flow Jet

it is a function of V_j, T_j, and the ambient air velocity. The reduction of noise levels of the hot jet in comparison with the cold is a result of the density dependence of the jet noise.

These examples are ample proof that the flow/noise program is a valuable tool for studying the jet noise characteristics, including the source alteration effects. It has shortcomings, however, and work is continuing to improve the program. In the following section, comments on the shortcomings of the flow/noise program described in the previous paragraphs are briefly discussed, together with some future plans.

3.2.1.4 Improvements for the Flow/Noise Program

The prediction results of figure 61 and others indicated that the flow/noise program tends to underpredict the lower frequency jet noise and overpredict the higher frequency jet noise. This trend resulted in a mismatch of the peak SPL frequency, which occurs at too high a frequency. These discrepancies were found to be aggravated as the noise emission angle approached the jet axis.

The neglect of internal jet propagation effects occurring in the practical application of Lighthill's theory is believed to be largely responsible for these differences. As described earlier, the noise generation mathematical model includes only the self-noise term and not the shear noise term to account for the interaction between the mean flow and the turbulence. A recent analysis of Berman (ref. 60) based on Lilley's (ref. 61) approach shows that the shear noise term actually consists of a small shear noise generation term and a large sound propagation term.

The propagation effects within the jet flow can be treated using Lilley's theory as discussed in reference 60. The analysis of reference 60 indicates that the lower frequency noise found at angles greater than 90^0 to the inlet centerline receives an extra boost in level, while the high frequency noise is reduced at similar locations. This leads to the well known reduction in peak frequency at noise emission angles near the jet axis. This also results in a reasonable prediction of OASPL by the flow/noise program, even though the spectra are not necessarily predicted with good accuracy.

Therefore, work to incorporate the propagation effects within the jet should be included in the plan to improve the flow/noise program.

3.2.2 COMPARISON OF EXPERIMENTAL TECHNIQUES

A number of experimental techniques are available in the investigation of the effects of flight on jet noise. When different techniques are used, it is important to account for the particulars associated with the technique that affect the measured noise, so that it is possible to correlate noise data obtained by one technique to that by another.

Among the several currently practiced experimental techniques, the four techniques selected for discussion are:

1. Flyby tests (including taxi tests)

2. Wind tunnel tests (including airplane mounted microphone tests)

3. Free jet tunnel tests

4. Static jet operation at relative velocity

In the subsequent sections, the methods for computing in-flight jet noise of a single flow nozzle are derived for the listed techniques and the relationships of the data obtained from each technique are developed. The material included in this section is extracted from reference 62.

In the analyses presented, the problems were solved with some idealizing assumptions, neglecting, for example, the presence of the wind tunnel walls and the effect of the free jet tunnel shear layer dynamics that may affect the fluid mechanics of the tested jet, the possible noise scattering caused by the turbulence in the shear layer of the free jet tunnel, etc.

3.2.2.1 Geometric Relations

Schematic diagrams, showing the wind vector direction and sound propagation direction for the first, second, and third techniques, are presented in figure 68. In each of the figures, V_A (or M_A) represents the relative motion between the exhaust nozzle and the surrounding air, c_0 the sonic velocity of ambient air, ϕ_i the noise emission angle when V_A is zero, r's designate the distances, and ϕ_e is the noise propagation angle when the ambient air velocity is V_A (except that it is the visual angle in the flyby case in figure 68a).

From geometry, the angular and distance relations in figure 68a are given by

$$\cos \phi_i = \left[\left(1 - M_A^2 \sin^2 \phi_e\right)^{1/2}\right] \cos \phi_e - M_A \sin^2 \phi_e \tag{35}$$

$$r_i = \frac{\left(1 - M_A^2 \sin^2 \phi_e\right)^{1/2} - M_A \cos \phi_e}{1 - M_A^2} r_e \tag{36}$$

From the similarity of triangles seen in figure 68a through 68d, it can be found that the angular relationship of equation (35) also applies to figure 68b through 68d.

At the shear layer of the free jet tunnel, the sound wave emerging from the free jet undergoes a bending due to refraction as shown in figure 68c and 68d. When a parallel shear layer is assumed, the angle ϕ_0 can be expressed by the following equation,

$$\cos \phi_0 = \frac{1}{\left(1 - M_A^2\right)} \left\{ \frac{\cos \phi_e}{\left(1 - M_A^2 \sin^2 \phi_e\right)^{1/2}} - M_A \right\} \tag{37}$$

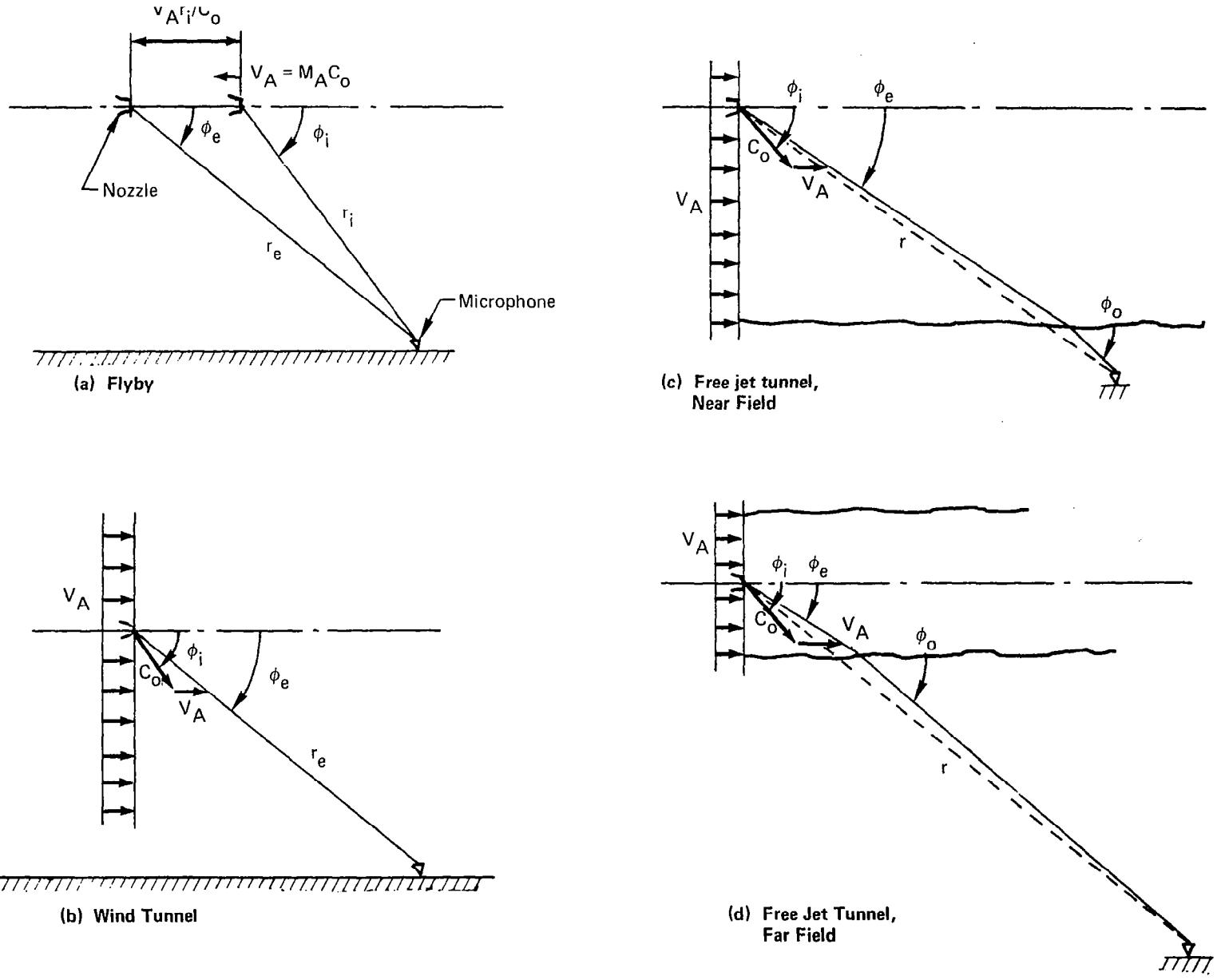

Figure 68.—Four Methods of Measuring Flight Effects

related to the known variables of the free jet tunnel. Equations (35) and (36) are sufficient to correlate the angular relationship involved in the four experimental techniques listed in this section.

In figure 69, the relationships of ϕ_i, ϕ_e, and ϕ_o as expressed by equations (35) and (37) are plotted for M_A of 0.3 and 0.5. The angular correspondences similar to those shown would be convenient for cross-comparing the noise data obtained by the various techniques mentioned. The peculiar phenomena in regard to the free jet tunnel (the zone of silence and the angle of total internal reflection) are also indicated in figure 69.

The distance relationship is important in the evaluation of atmospheric absorption and inverse-square-law losses. In the flyby case of figure 68a, r_i is the distance to be used for this evaluation. A similar distance r_i, computed by equation (36), should be used for the wind tunnel case (and the airplane-mounted microphone case). This distance is also used for the divergence loss in the wind tunnel case.

In the free jet tunnel case, the distance involved consists of two segments; the wave propagation distance r_i within the free jet and the wave propagation distance outside the free jet. The total distance, however, may be approximated by r shown in figure 68c and 68 d, for the near-field case and far-field case, respectively. In the near-field case, with a relatively small tunnel, application of this approximation should consider the jet noise source distribution downstream of the jet exit plane.

3.2.2.2 Doppler Frequency Shift

The Doppler frequency shift effects between the flyby case and the static case or the wind tunnel case have previously been discussed in section 3.1.4.

The Doppler frequency shift relationship between the flyby case and either the free jet tunnel case or the airplane-mounted microphone case is the same as that between the flyby case and the wind tunnel case. The reason for this is that the relative motion between the nozzle, microphone, and tunnel air in the free jet tunnel and airplane-mounted microphone cases is the same as that in the wind tunnel case. It is pointed out that the sound wave, emerging from the free jet into the stationary ambient air in the free jet tunnel case, does not undergo any frequency shift.

3.2.2.3 Noise Levels

The Ffowcs-Williams equation for the noise intensity of the jet of a moving aircraft, presented in section 3.1.4, can be factored in two parts; i.e., an acoustic propagation term and a noise source term as follows:

$$I_{FLT} = \frac{SD_j^2}{r_i^2} (1 + M_A \cos \phi_i)^{-1} \tag{38}$$

$$S = \frac{\rho^2}{\rho_o} \frac{(V_j - V_A)^7 V_j}{c_o^5} (1 - M_c \cos \phi_i)^{-5} \tag{39}$$

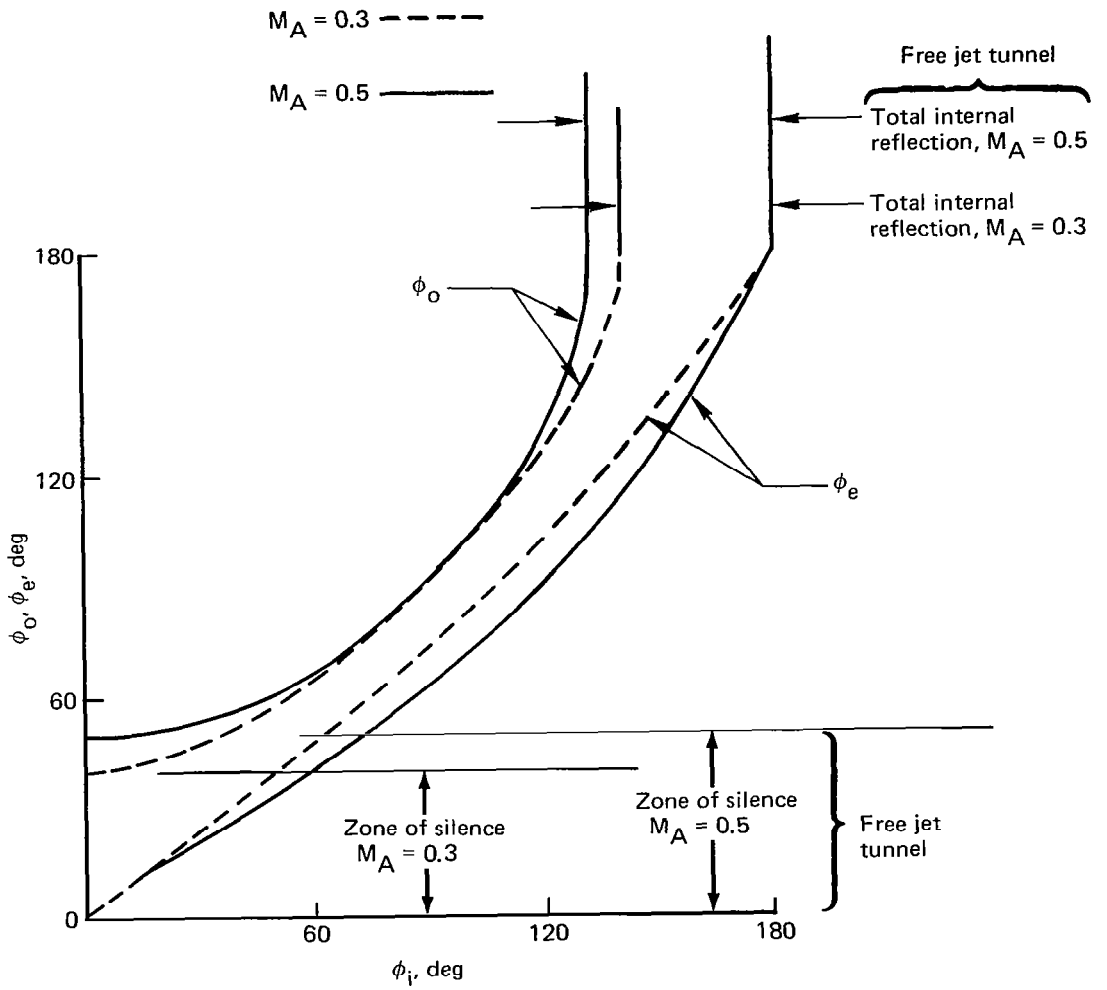

Figure 69.– Dependence of Sound Wave Propagation Angles on Flow Velocity

where D_j is the nozzle diameter, r_i is the distance between source and observer at the time of noise emission (fig. 68a), M_A is the airplane Mach number, ϕ_i is the angle between the airplane flightpath and the line r_i, ρ and ρ_0 desgnate the local and ambient air densities, V_j is the jet core velocity, V_A is the airplane velocity, c_0 the ambient air sonic velocity, and M_c is the turbulent eddy convection velocity.

It can be seen that the last term of equation (38), the Doppler factor, constitutes the factor relating the static to flyby noise levels, whereas equation (39) expresses the noise level change due to the source alteration caused by the ambient airflow.

The equation for the noise intensity for the wind tunnel case can be derived from equation (38), using equations (35) and (36), expressed as a function of the parameters relevant to the wind tunnel test as follows:

$$I_{WT} = \frac{SD_j^2}{r_e^2} \frac{1 - M_A^2}{\left(1 - M_A^2 \sin^2 \phi_e\right)^{1/2} \left\{\left(1 - M_A^2 \sin^2 \phi_e\right)^{1/2} - M_A \cos \phi_e\right\}} \tag{40}$$

This equation can be rearranged as

$$I_{WT} = \frac{SD_j^2}{r_e^2} \left(1 - M_A^2 \sin^2 \phi_e\right)^{-1} \left(1 - M_A \cos \phi_o\right)^{-1} \tag{41}$$

The sound wave received in the free jet tunnel case must go through the shear layer of the tunnel. Thus the computation of the noise level must consider the transmission of sound through the shear layer.

The ratio of acoustic intensities of a free jet tunnel and a wind tunnel is given by

$$\frac{I_{FJT}}{I_{WT}} = (1 - M_A^2 \sin^2 \phi_e)\, T^2 \tag{42}$$

This equation provides for the correction factors to be applied between the wind tunnel and free jet tunnel noise data, which have the same angle ϕ_e. Here T represents the pressure transmission coefficient (sound pressure outside the tunnel over the incident level within) across the shear layer of the free jet tunnel. The analysis of Berman (ref. 60) derives the pressure transmission coefficient for high frequencies as follows:

$$T^2 = (1 - M_A \cos \phi_o)^{-2} \left| \frac{(1 - M_A \cos \phi_o)^2 - \cos^2 \phi_o}{\sin^2 \phi_o} \right|^{1/2} \tag{43}$$

Substitution of equation (41) into equation (42) leads to the far field noise produced by a jet in a free jet tunnel to be expressed as:

$$I_{FJT} = \frac{SD_j^2}{r} \frac{T^2}{(1 - M_A \cos \phi_o)} \tag{44}$$

Note the appearance of an amplification factor which depends on the free jet tunnel Mach number and the far field observation angle in the ambient medium.

Figure 70a presents plots of the transmission coefficients as a function of ϕ_o and, in turn, as a function of ϕ_e based on the angular relation expressed by equation (37). Use of these values in equation (42) results in the plots presented in figure 70b, which relates the noise measured within the flow of the free jet tunnel (or wind tunnel) and that measured outside the tunnel. Figure 70 indicates that the shear layer of the free jet tunnel can cut off substantially the high frequency portion of jet noise near the jet axis.

In figure 71, an example is presented to show how a directivity pattern measured in one method is transformed to others that would be measured by other methods. Transformation between curves was performed utilizing the relations expressed in equations (35) and (37).

3.2.2.4 Comparison of Noise Levels

Based on the preceding analyses, comparisons of noise levels that would be measured by the four experimental techniques were performed and the results are presented below. In these analyses, two noise source models (see equation (39)) were used as presented below:

V_j^8 Static Model:

$$S = \frac{\rho^2}{\rho_o c_o^5} (V_j - V_A)^7 V_j \tag{45}$$

Modified Ffowcs-Williams Model:

$$S = \frac{\rho^2 (V_j - V_A)^7 V_j}{\rho_o c_o^5 \left\{ (1 - M_c \cos \phi_i)^2 + 0.3 M_c^2 \cos^2 \phi_i \right\}} \tag{46}$$

Further, the convection Mach number M_c was assumed to be

$$M_c = 0.5(V_j - V_A)/c_o \tag{47}$$

Two sample computation results from the use of the noise intensity equations. equations (38) and 44), and the source definitions, equations (45) and (46), are presented in figures 72 and 73. From these examples, noise level was computed as V_j

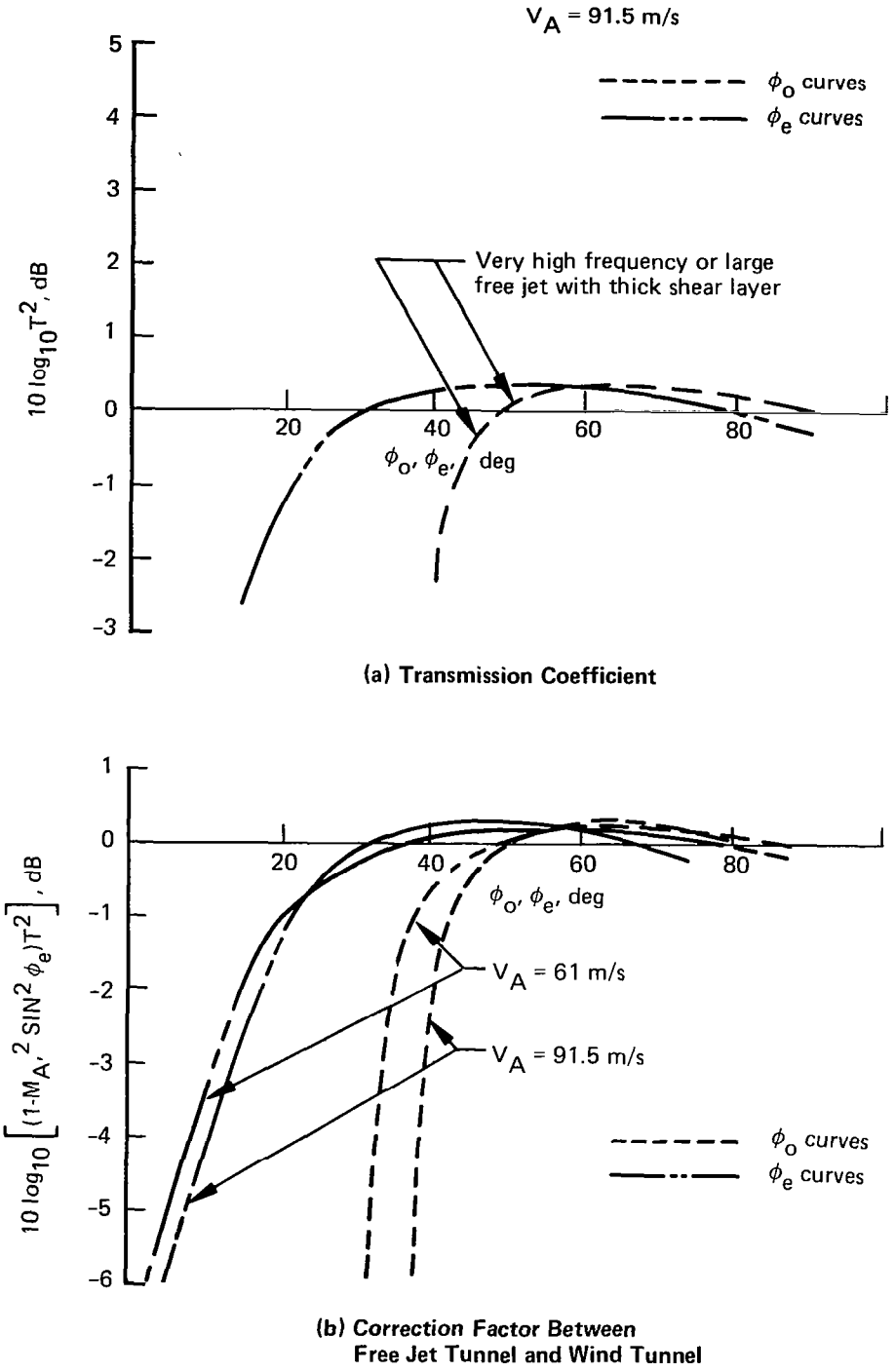

Figure 70.– Characteristics of Sound Propagation Through a Moving Fluid

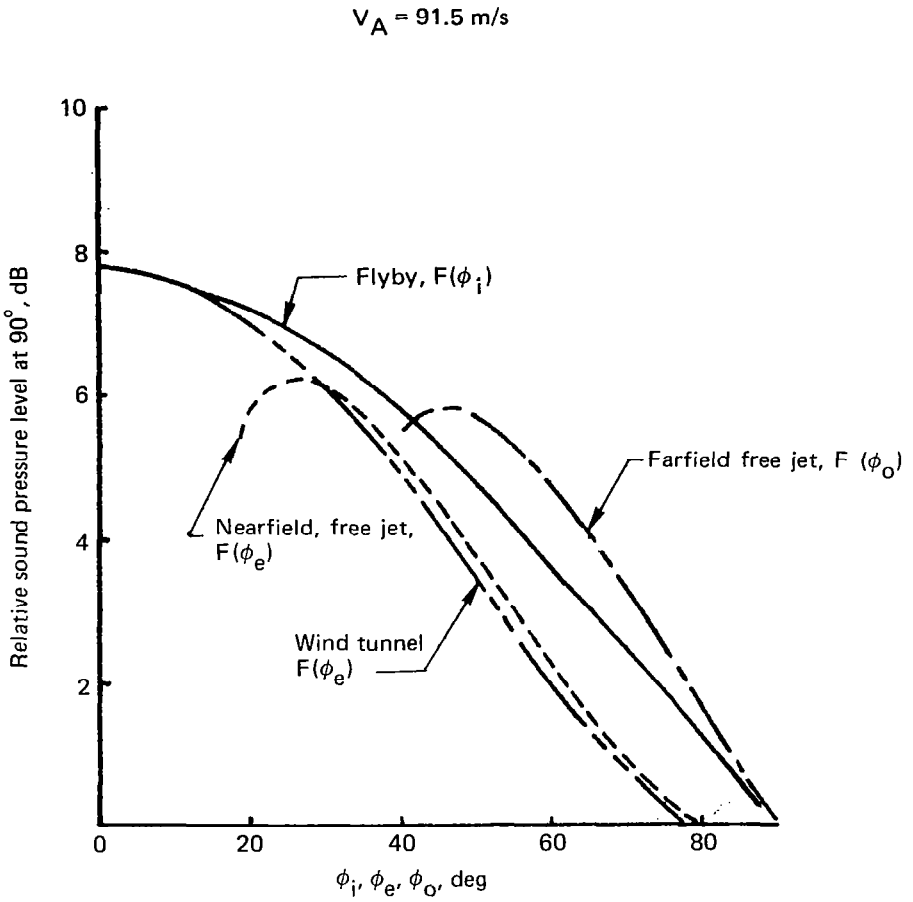

Figure 71.—Directivity Transformation

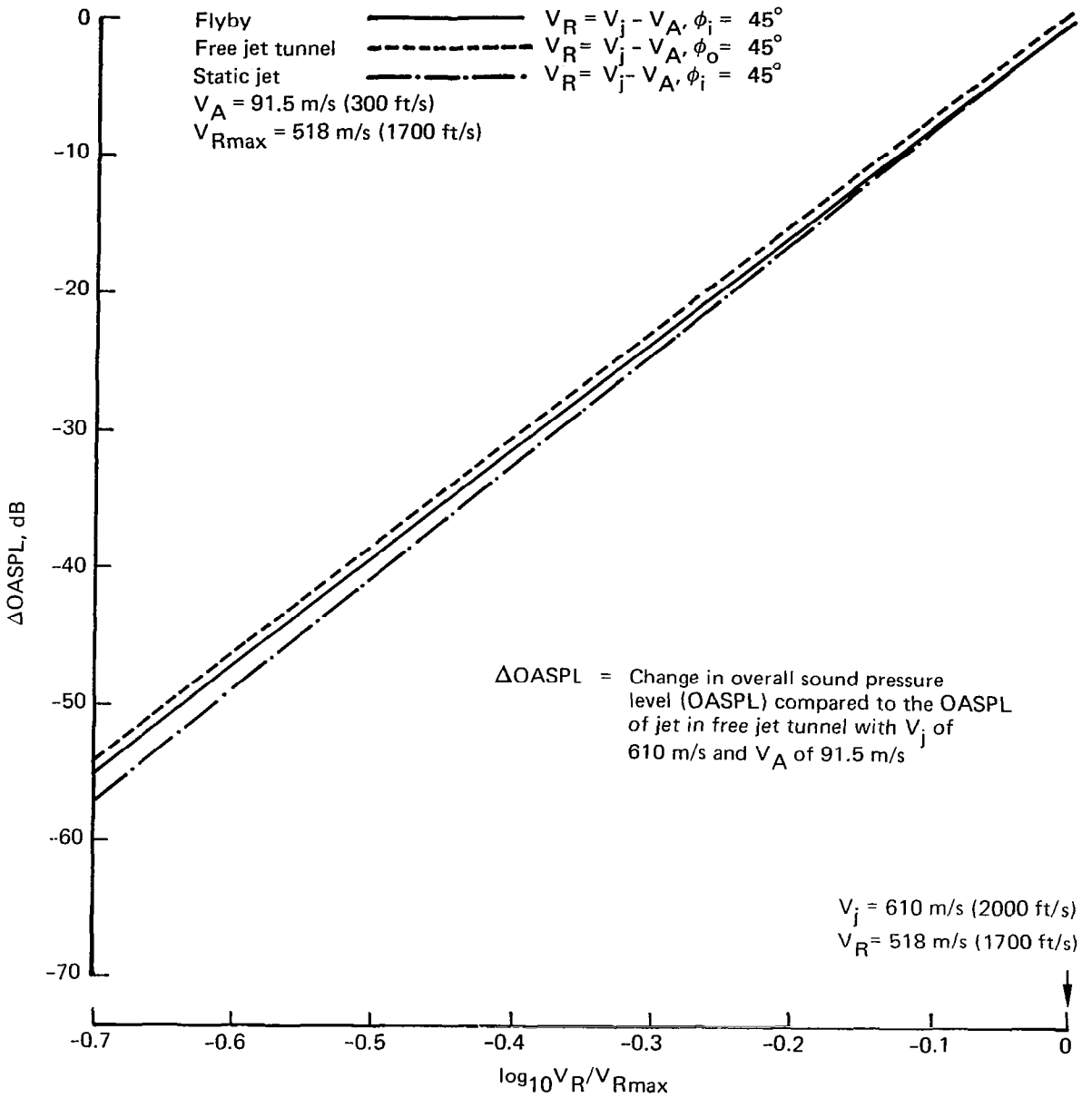

Figure 72.— V_R Effect on Jet Noise With Increasing V_j Using V_j^8 Static Model

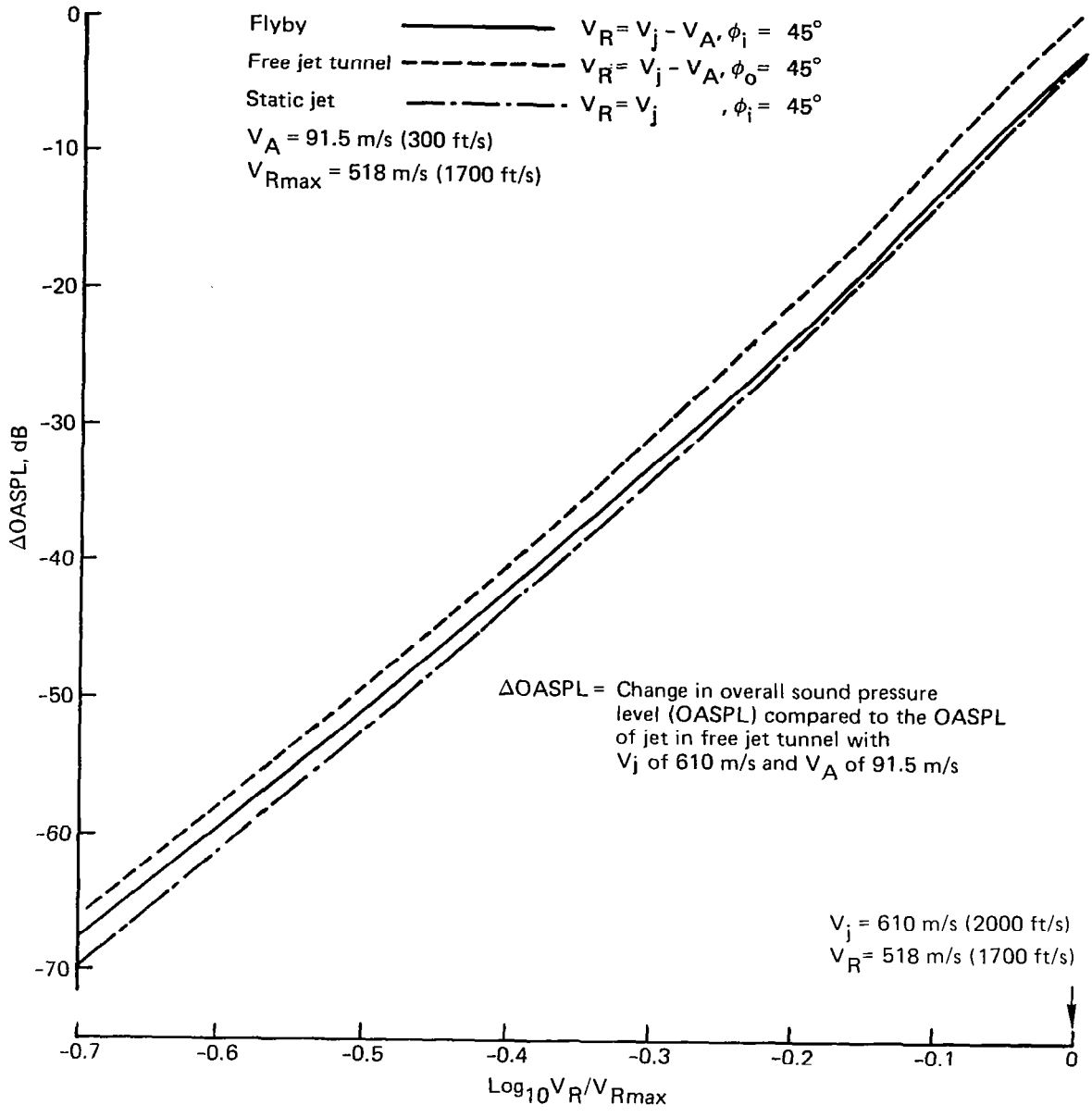

Figure 73.– V_R Effect on Jet Noise With Increasing V_i Using Modified Ffowcs-Williams Model

was reduced from 610 m/s (2000 fps) to lower values while V_A was kept constant at 91 m/s (300 fps) for the flyby and free jet cases, and it was computed as V_j equal to the relative velocity (V_j - V_A) for the static case. The zero baseline was established at the highest OASPL value of the three OASPL's at log (V_R/V_{RMAX}) = 0.

The results indicate that, regardless of the source model used, the OASPL level of the static jet and that of the flyby case are nearly equal when the static jet velocity is equal to the relative velocity of the flyby case. Because of the terms associated with the airplane motion in equations (38) and (44), the free jet tunnel has higher noise levels than others at the directivity angle shown.

Figures 74 and 75 are presented to show the variation of calculated OASPL for the static and free jet tunnel cases as compared to some test data. Included in the figures are the calculated OASPL values for the flyby case. In these figures, the trends in the variation of calculated OASPL are seen to be in agreement with that for the measured test data.

The change in the jet noise level caused by the forward velocity change is often expressed by $10n\log V_R$. Computation was made to find the variation of n, and the results are shown in figures 76 and 77. These figures show that the value varies as a function of V_j.

Variations of n as functions of the directivity angle θ_i at two jet velocities are presented in figures 78 and 79. The results indicate that the exponent decreases, in general, toward the forward quadrant as was found in some test data.

3.2.2.5 Conclusions

The analysis presented demonstrates that the noise levels and the forward velocity effects resulting from various experimental techniques can be estimated analytically. It is shown that the noise data from different techniques manifest different characteristics, but they can be interrelated. Thus, the information obtainable by the use of the analysis will be valuable in gaining the understanding of the forward velocity effects on jet noise.

This initial analysis, however, is based on several idealized conditions, as described in the preceding sections, and other simplifying assumptions. For example, the jet and ambient airflow are always parallel and at constant flow velocity, the effects of fluid mechanics extraneous to the flow system (such as the nacelle boundary layer flow, etc.) are nonexistent, the noise received consists solely of jet noise (being devoid of any other noise, such as core noise or airframe noise). The logical next step, then, is to examine the consequences of these simplifications and consider the effects of those phenomena that may have significant effects on the jet noise.

Also, the preceding analysis is limited to a single, subsonic flow jet. A similar analysis for dual-flow nozzles should therefore be conducted. The analysis should consider different types of nozzles such as suppressor nozzles, ejector/suppressor nozzles, etc.

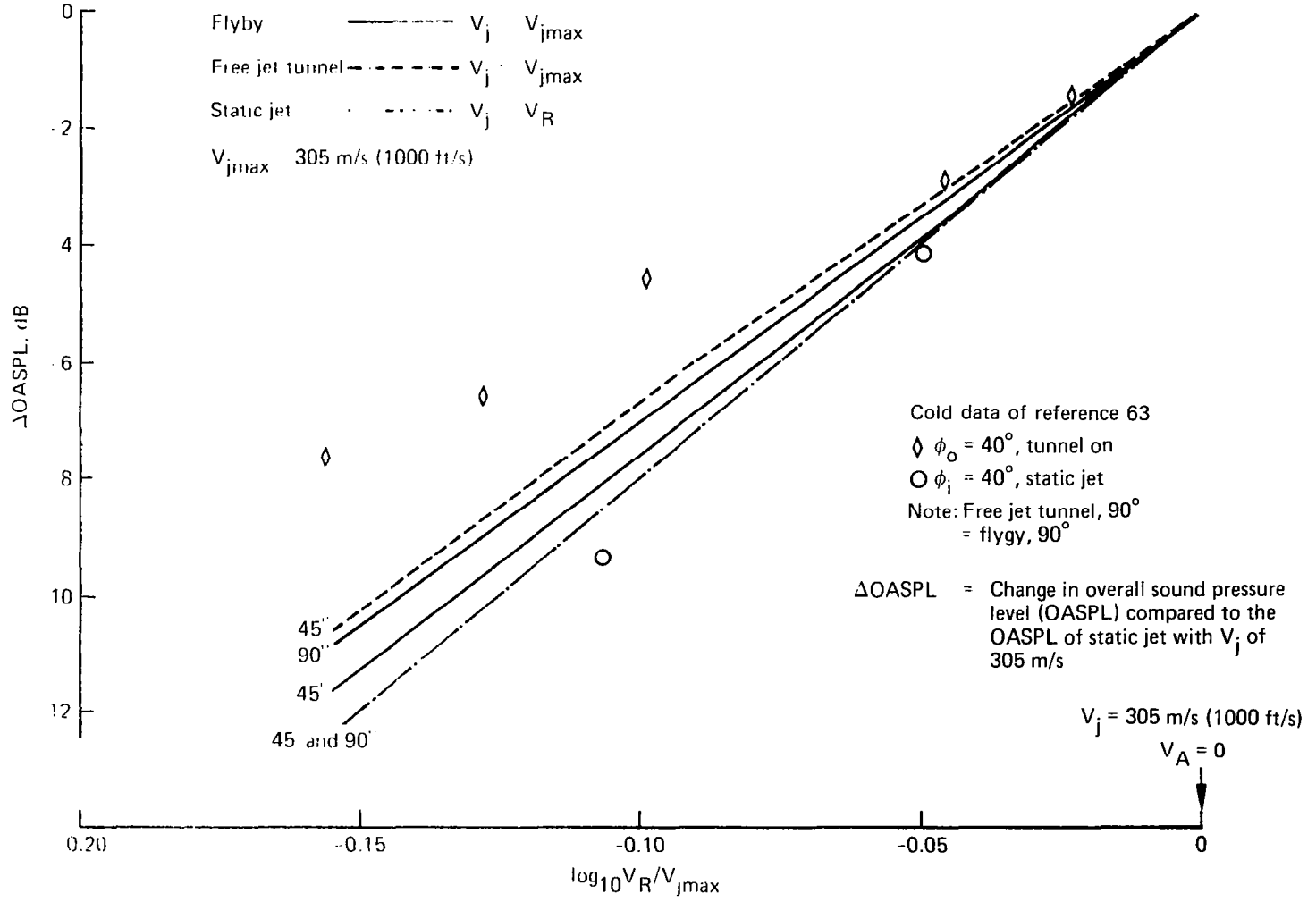

Figure 74. V_R Effect on Jet Noise With Increasing V_A Using V_j^8 Static Model

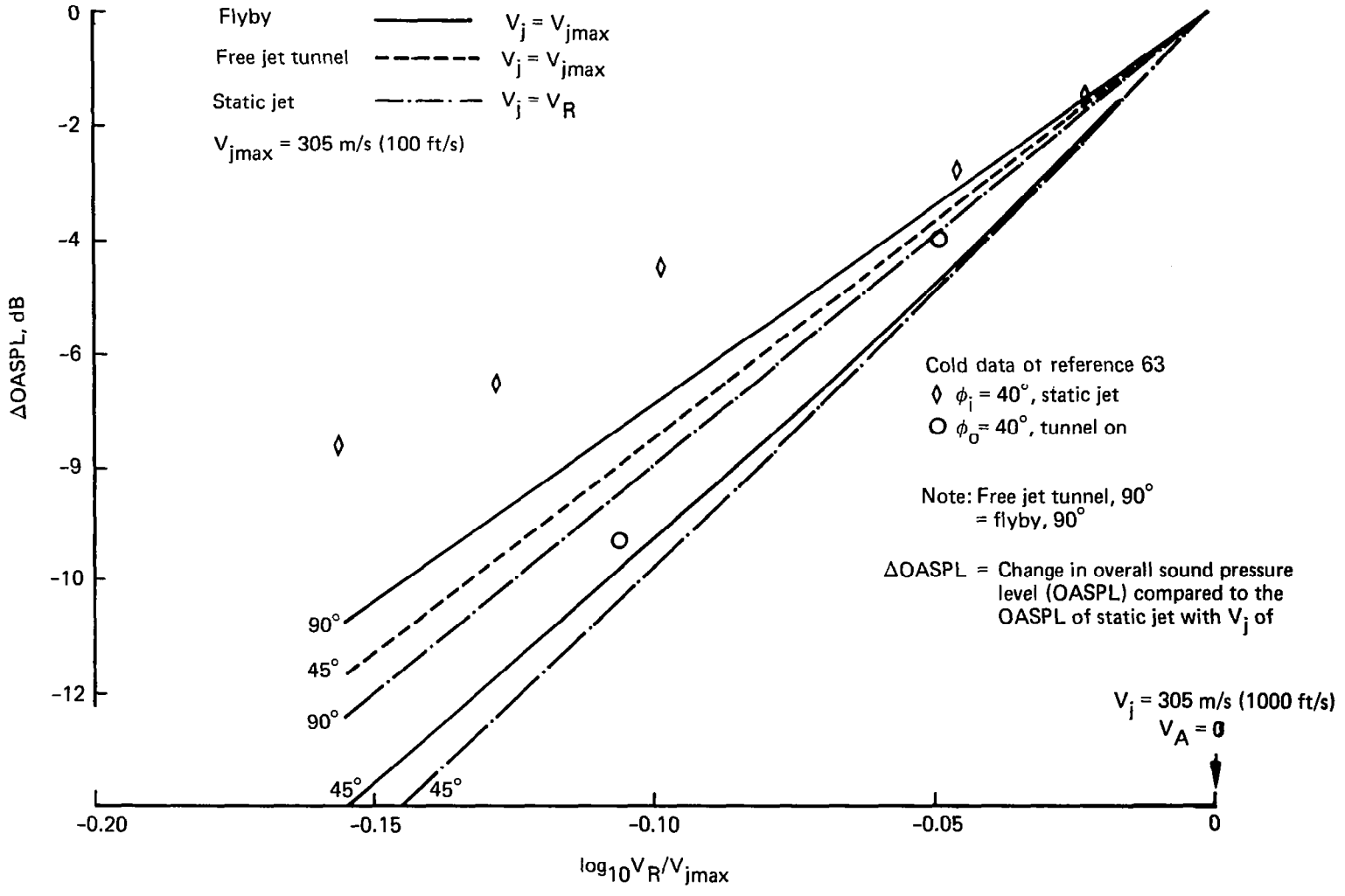

Figure 75.—V_R Effect on Jet Noise With Increasing V_A Using Modified Ffowcs-Williams Model

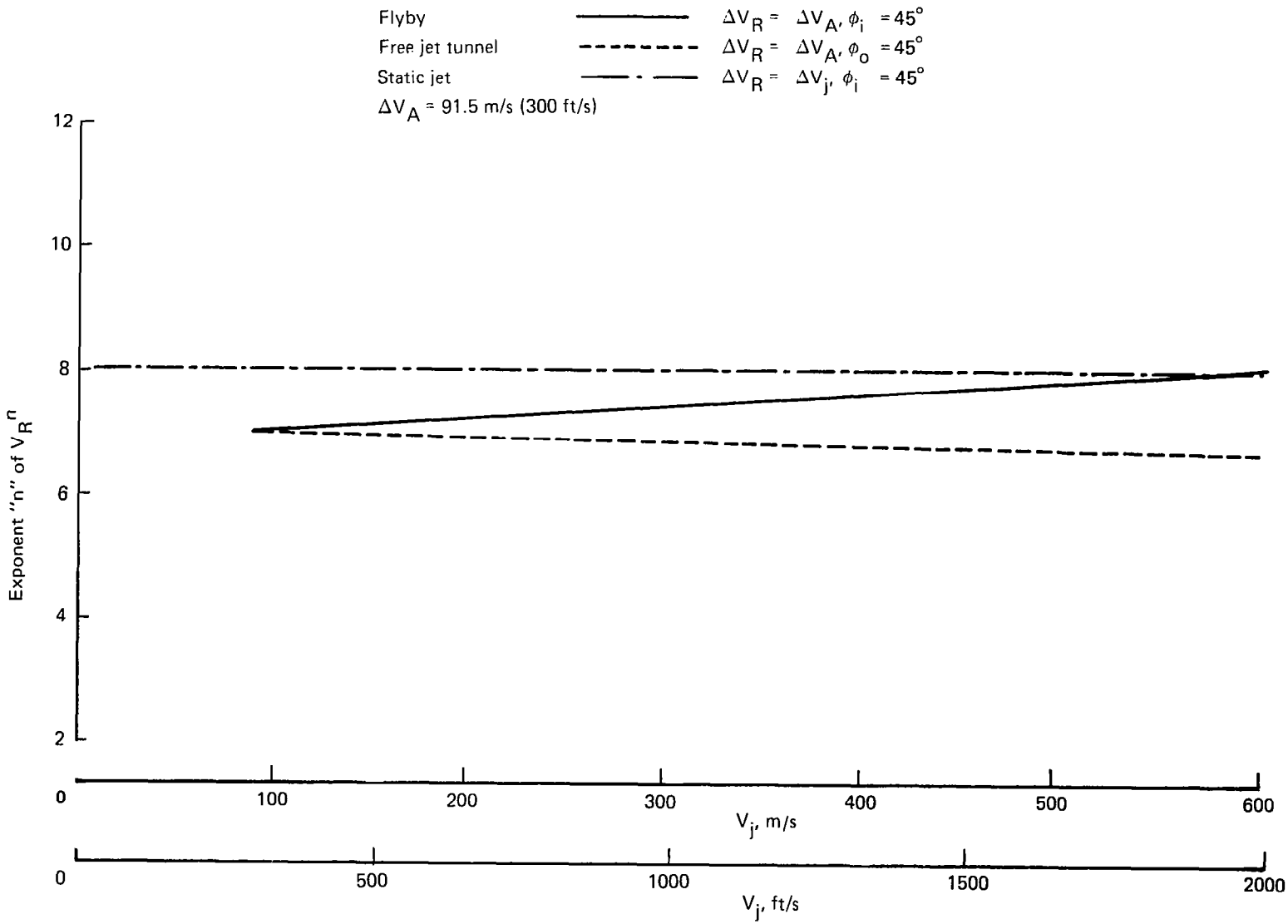

Figure 76.– Apparent V_R^n Dependence, V_j^8 Static Model

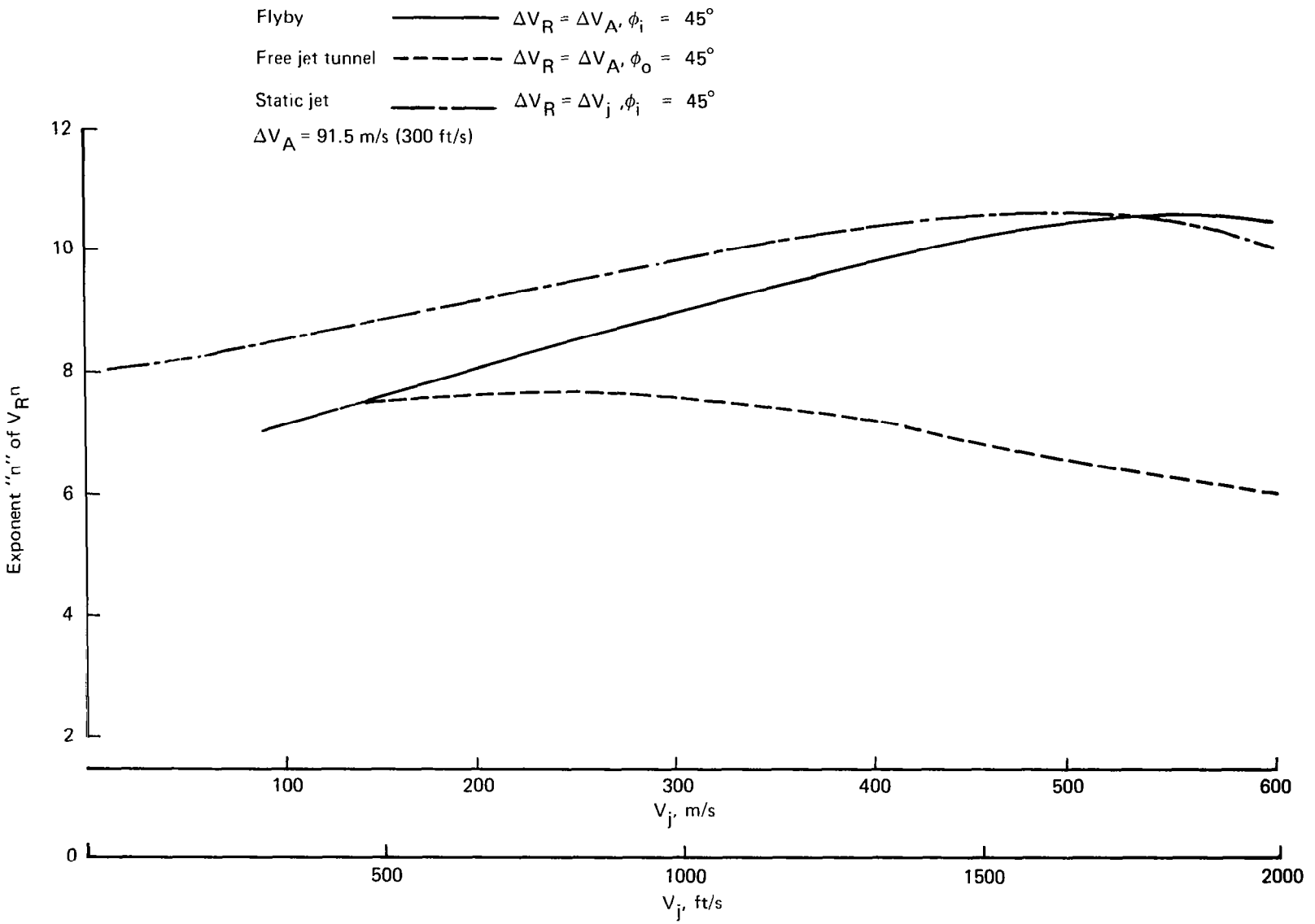

Figure 77.—Apparent V_R^n Dependence, Modified Ffowcs-Williams Model

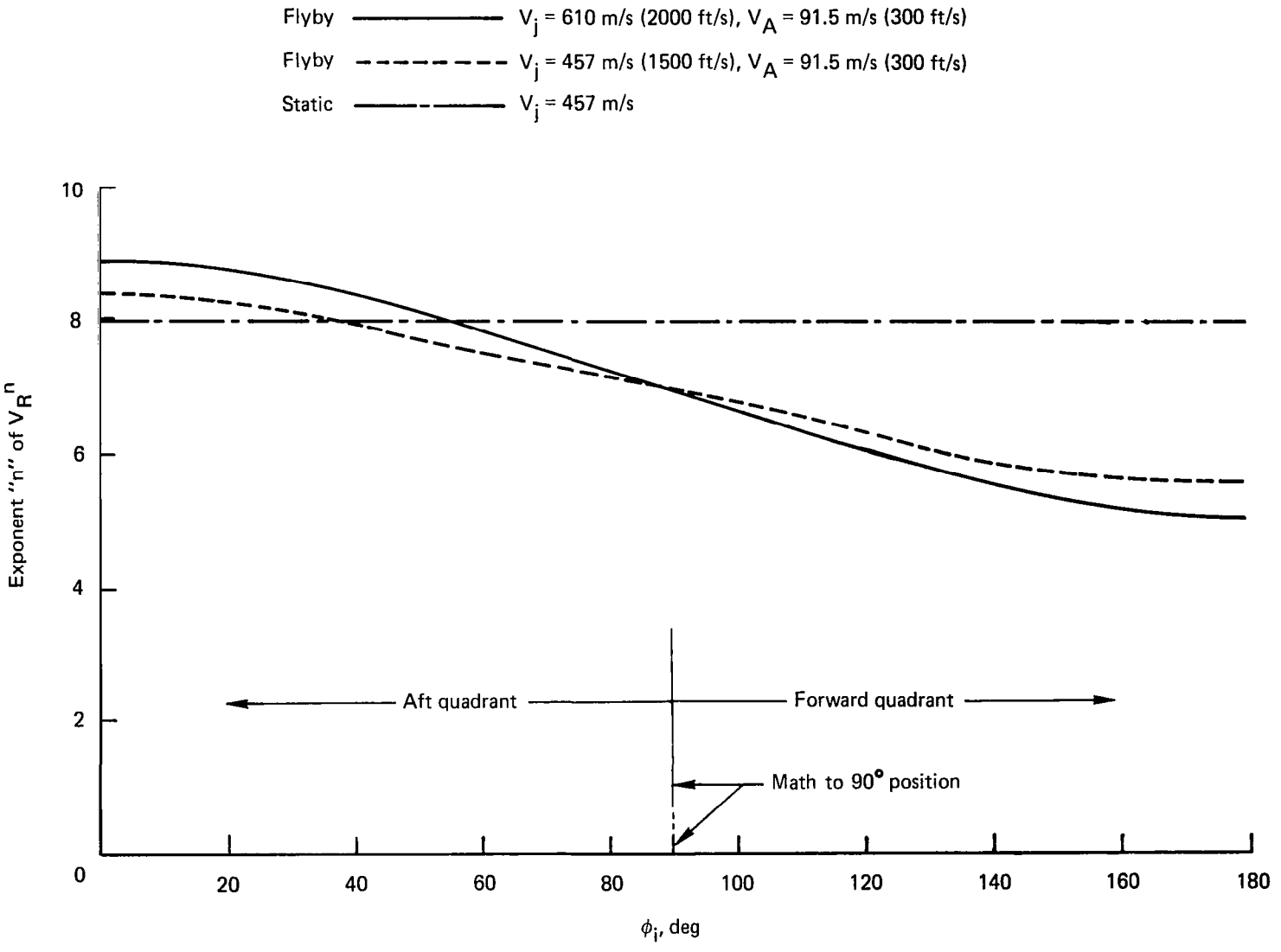

Figure 78.—Apparent Static to Flight V_R^n Law, V_j^8 Static Model

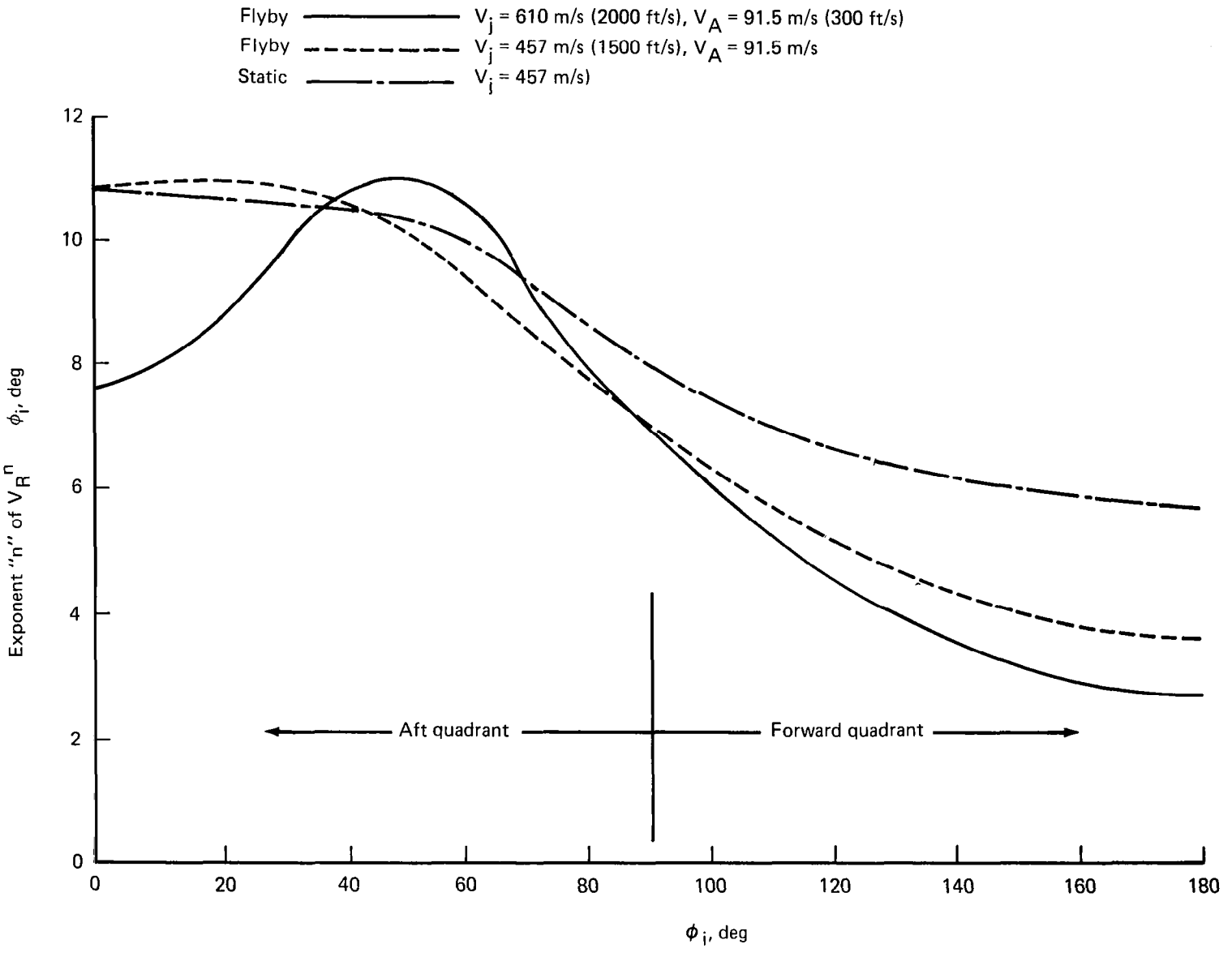

Figure 79.—Apparent Static to Flight V_R^n Law, Modified Ffowcs-Williams Model

3.2.2.6 Recommended Experimental Technique for Motion Effect Study

Selection of a specific technique depends to a large extent on many extenuating conditions; e.g., time, availability of facility, cost, etc. Thus, one technique desirable in one case may be disadvantageous in the other, and vice versa. Careful assessment of the existing situation prior to selection of a technique is therefore believed necessary. In a broad sense, however, the following observations can be given in regard to the advantages and disadvantages of each test technique.

Notwithstanding the various problems being studied in this work, a flight test would be the most desirable method among the experimental methods discussed in the previous section. A flight test gives a direct answer which qualifies for the best credibility. Flight testing, however, is normally very costly and, in some cases, it is not possible because the airplane is in the design stage.

Wind tunnel tests (e.g., those conducted in the Boeing 2.7 x 2.7 m (9 x 9 ft) tunnel and the NASA-Ames 12.2 x 24.4 m (40 x 80 ft) tunnel) have shown reliable flight effect data and are considered to be the next desirable technique. This method offers excellent freedom in controlling the test configurations and conditions. Some restrictions do exist, however, in regard to tunnel-to-nozzle size ratio (near-field noise measurement), the sound reverberation problem, wind tunnel heating, and wind tunnel self-noise. The tracked vehicle technique also has these similar advantages and disadvantages.

Free jet tunnels have been widely utilized for testing the motion effects on jet noise because of the facility availability and relatively low testing expense. However, problems associated with the free shear layer (e.g., sound wave refraction and possible scattering in the free shear layer) must be properly assessed when the noise measurement is made outside the free jet tunnel. When the noise measurement is made within the free jet, the same advantages and disadvantages discussed for a wind tunnel would apply.

3.2.3 Lilley Equation Solution

Analytical noise prediction requires a knowledge of the turbulent flow properties, the noise source strength in terms of these properties, and the transmission characteristics of the intervening jet fluid through which the acoustic energy must pass before reaching the ambient atmosphere.

The Lighthill method (ref. 54), as usually applied, considers the source strength but does not attempt to handle the propagation of the sound through the jet fluid.

Ribner (ref. 64) studies a Lighthill equation source term which is proportional to the local mean velocity shear. This leads to a low frequency shear noise source term whose magnitude must be scaled empirically with respect to the higher frequency self-noise term. However, no improvement in the high frequency directivity is attempted in this approach.

The Lilley equation analysis of Berman (ref. 60) shows that Ribner's shear noise term actually consists of a large propagation term and a small shear noise source term.

Calculations by Tester and Morfey (ref. 65) for subsonic ($V_j < c_o$) flows show that the Lilley equation approach is capable of yielding realistic noise directivities at a variety of frequencies.

Boeing work has been directed toward obtaining numerical solutions of the Lilley equation for arbitrary jet velocity and temperature profiles including $V_j > c_o$.

The Fourier transformed homogeneous Lilley equation for the case of planar parallel flow reduces to (ref. 60)

$$\frac{d^2\sigma}{dX_3^2} - \frac{2}{\Phi}\frac{d\Phi}{dX_3}\frac{d\sigma}{dX_3} + \left(\frac{\omega}{c_o}\right)^2\left[\Phi^2 - \left(\frac{c_o}{V_{12}}\right)^2\right]\sigma = 0 \tag{48}$$

where the perturbed pressure p is written in terms of its Fourier transform σ as

$$p(X_1, X_2, X_3, t) = \int \sigma(\omega, k_1, k_2, X_3) e^{ik_1X_1 + ik_2X_2 - i\omega t}\, dk_1 dk_2 d\omega \tag{49}$$

and

$$\Phi = \frac{c_o}{c(X_3)}\left(\frac{u(X_3)}{V_1} - 1\right) \tag{50}$$

where ω is the frequency of sound wave, V_1 is the component of the wave phase velocity in the flow direction and V_{12} is the component of the wave phase velocity in the X_1 - X_2 plane. The flow properties vary in the X_3 direction only. The local and ambient sound speeds are c and c_o, respectively, and u is the fluid velocity.

The problem of the transmission of a plane wave through a flow region, which is schematically shown in fig. 80, was solved. The ratio of the transmitted pressure to the incident pressure through the planar flow model with thickness L and shear layer thickness of ℓ is defined as the pressure transmission coefficient T. In figures 81 through 84, 20 $\log_{10}|T|$ is shown as a function of the wave propagation angle φ measured from a normal to the X_1 - X_2 plane. The angle defines the trace of the wave's direction in the X_1 -X_2 plane. These angles are defined in figure 80. For zero ambient flow velocity

$$V_{12} = \frac{c_o}{\sin\varphi} \tag{51}$$

$$V_1 = \frac{V_{12}}{\cos\theta} \tag{52}$$

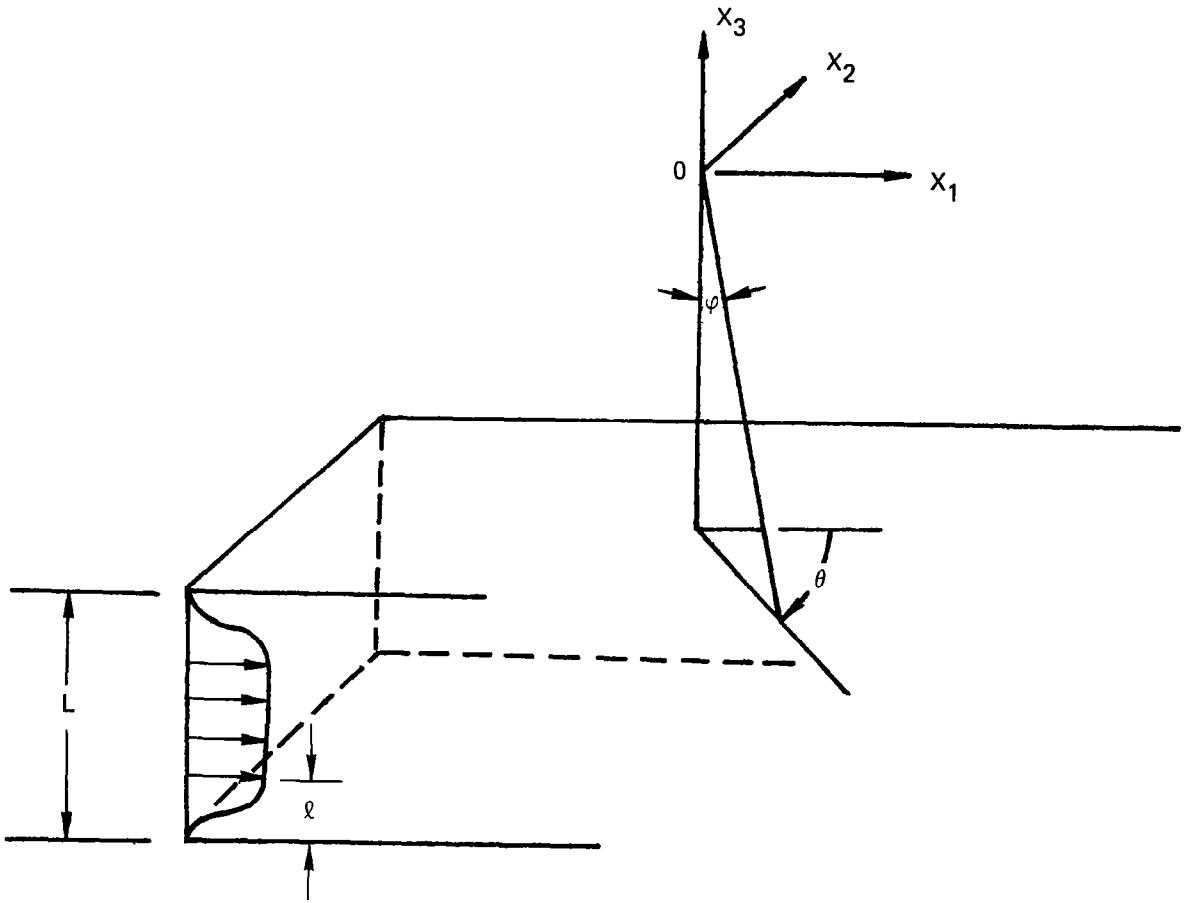

Figure 80.—Planar Flow Model

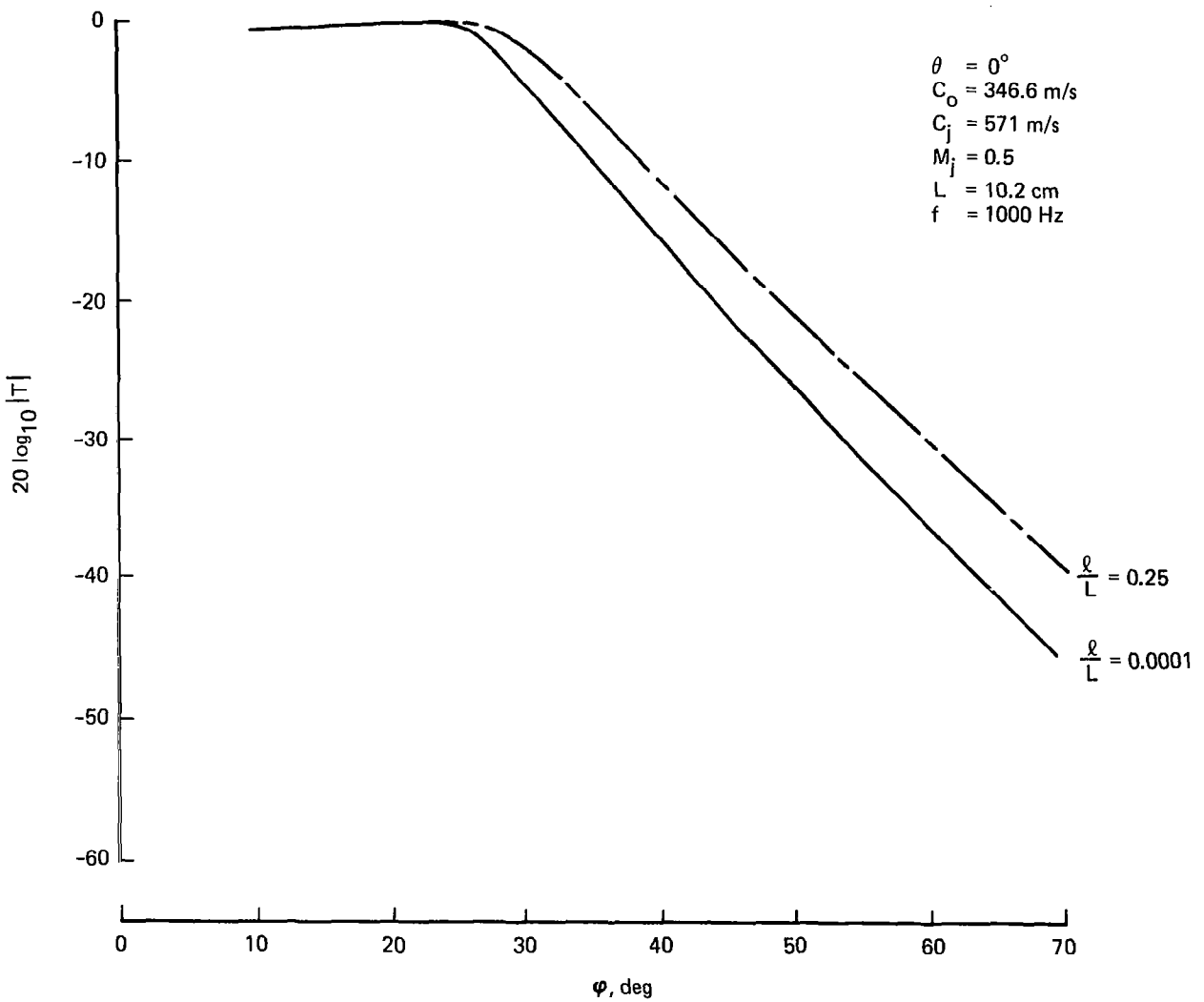

Figure 81.—Pressure Transmission Coefficient–Hot. Low Velocity Layer

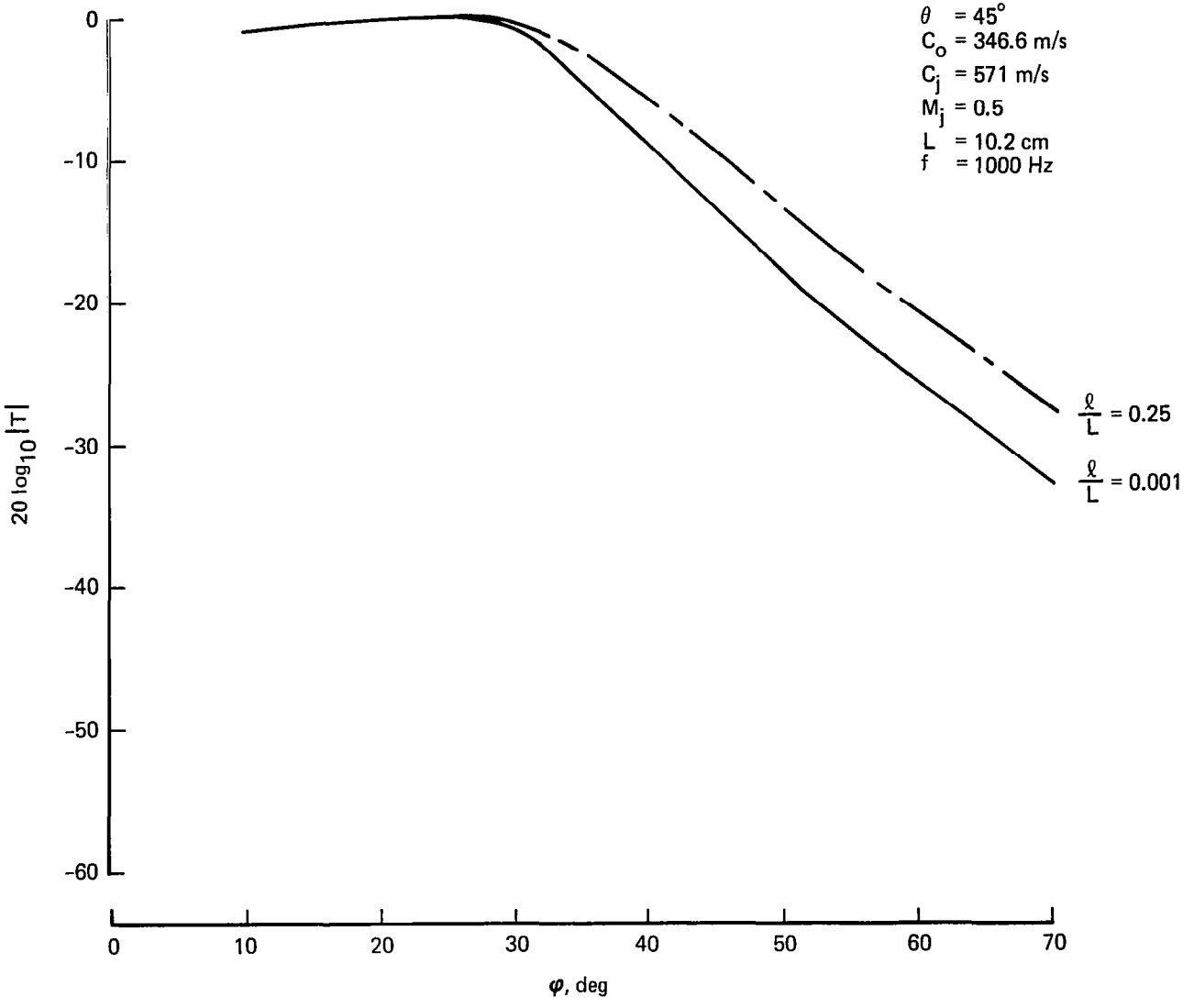

Figure 82.—Pressure Transmission Coefficient, Hot, Low Velocity Layer

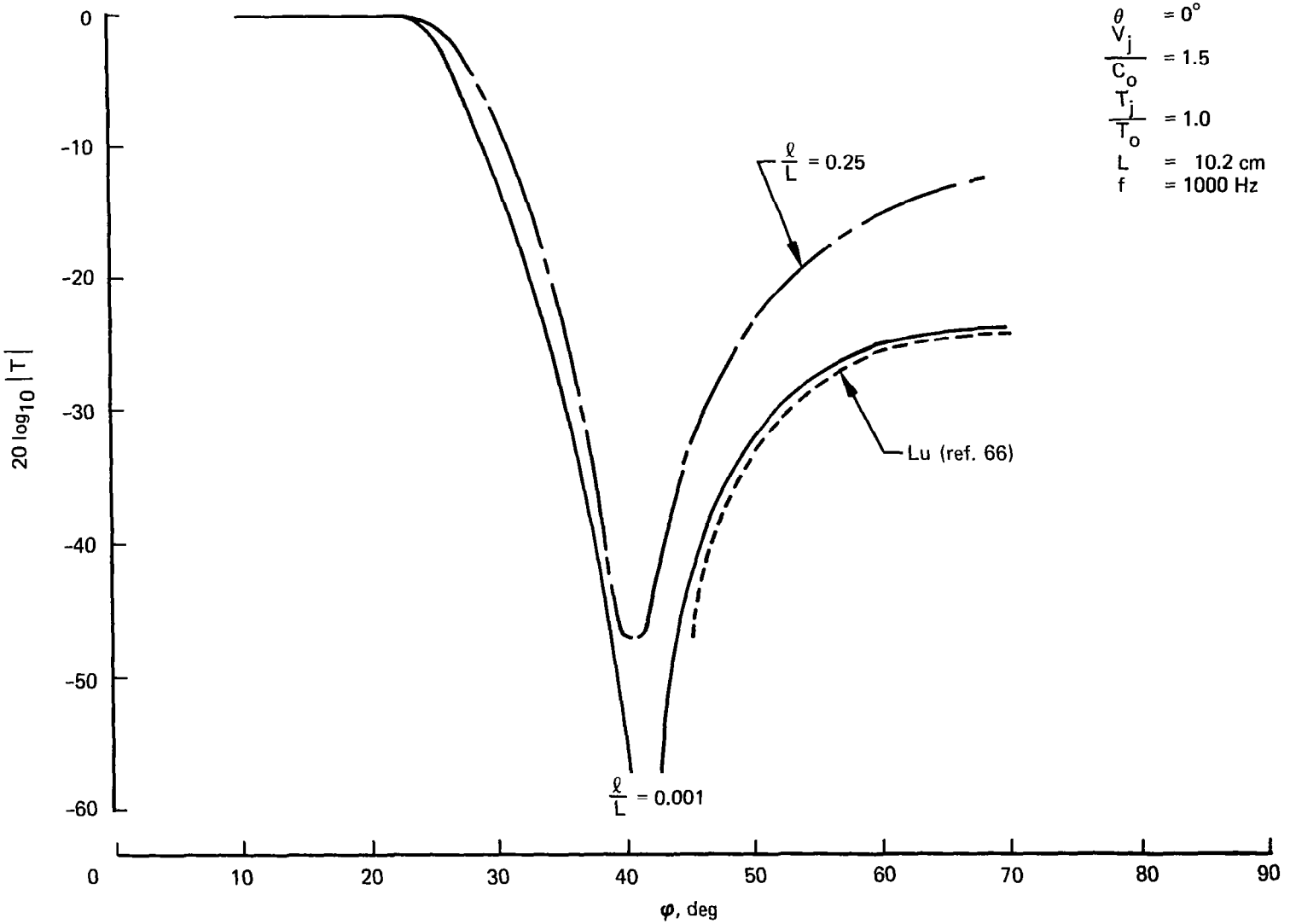

Figure 83.—Pressure Transmission Coefficient–Cold, High Velocity Layer

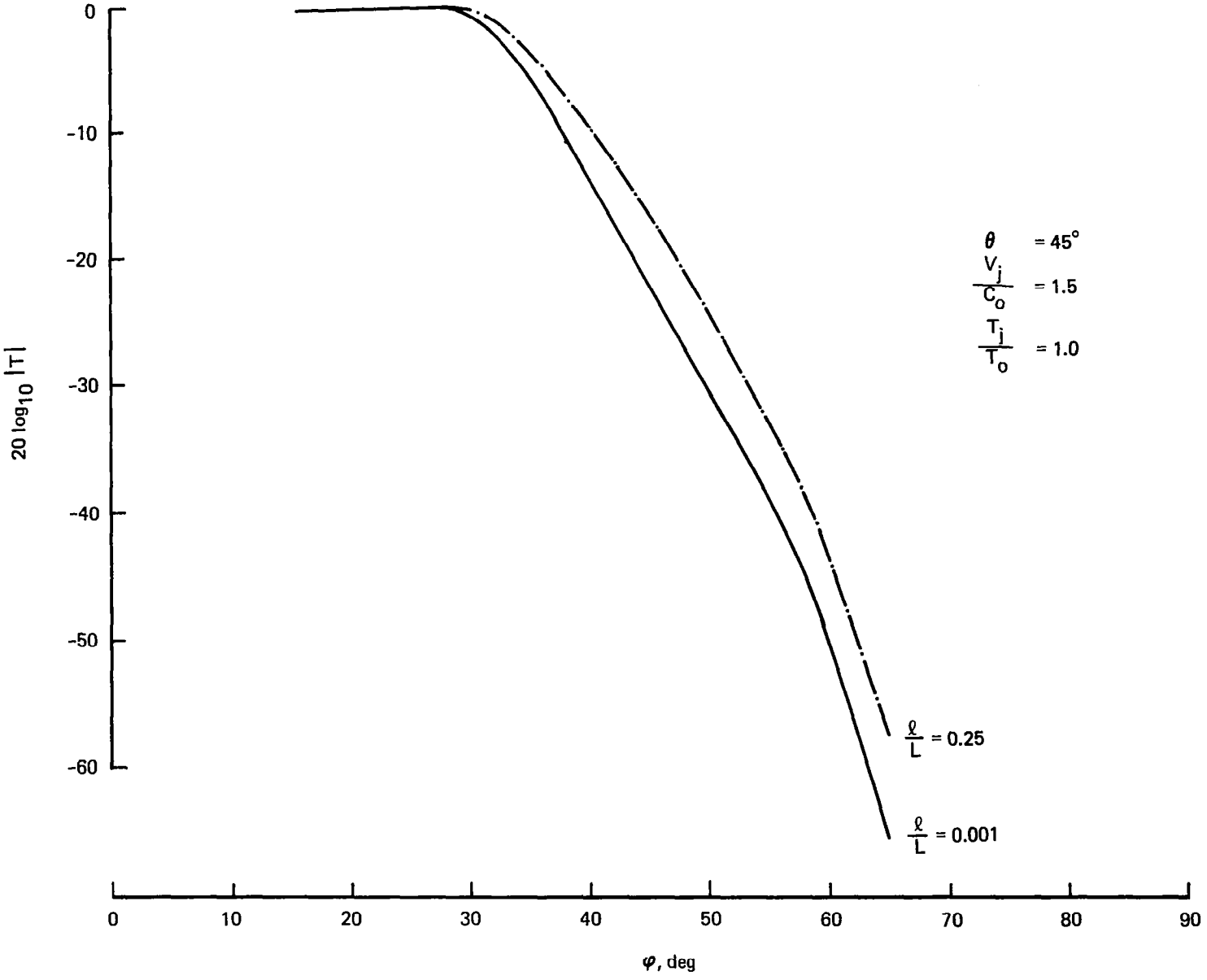

Figure 84.—Pressure Transmission Coefficient–Cold, High Velocity Layer

The resulting Lilley equation solution was plotted for a very thin mixing region, $\ell/L = 0.0001$, to approximate a square profile and $\ell/L = 0.25$ to examine a more gentle variation. An exact analytical solution for the square profile has been obtained by Lu (ref. 66). There is almost exact agreement between the analytic square profile result and the numerical Lilley equation solution whenever a critical layer does not exist; i.e., as long as $u(X_3) \neq V_1$ anywhere within the flow. When this is not the case, there is a difference as shown in figure 83 because of a viscous model used in the numerical calculation.

If $u(X_3) = V_1$ for some value of X_3, the Lilley equation experiences a resonance phenomenon for which the transmitted wave vanishes. This resonance can be controlled by including viscous terms near the critical layer, which completely changes the form and character of the Lilley equation. The governing equation is then similar to the Orr-Sommerfeld equation of stability theory (ref. 67). The importance of the inclusion of viscosity does not lie so much in the ability to accurately predict transmission properties as in the ability to calculate the noise generated at a location in or near a critical layer in a jet. The undamped resonance of the Lilley equation would lead to infinite sound wave production with a source located within a critical layer. This phenomenon is currently under study.

Work planned for the future includes solving the Lilley equation in axisymmetric coordinates for all jet velocities, decreasing computer time, and combining the Lilley equation approach with the present flow/noise program (ref. 51). All of this work is completely compatible with an ambient velocity to correspond to flight.

3.3 INVESTIGATION OF VERIFICATION TECHNIQUES

Verification of the jet noise field existing between the airplane and observer and the phenomena described in sections 3.1 and 3.2 must rest on accurate measurement of the relevant parameters and conditions. Through various experiences, several areas have been found where improvement or changes in measuring technique are required. In the following subsections these areas are discussed with a brief explanation of the current status and the recommended means for solution. Also discussed are areas relevant to data acquisition and reduction. Insofar as the takeoff and landing approach patterns are concerned, no radical difference is expected between the conventional jet aircraft and the supersonic transport. Thus, the discussion presented should apply for both kinds of airplanes.

3.3.1 MEASUREMENT OF AIRCRAFT POSITION AND ATTITUDE

A number of different instruments and techniques are applied currently in acquiring the aircraft position and attitude data during an acoustic flight test. A review of these systems is presented below together with comments on their advantages and disadvantages.

3.3.1.1 Airborne Movie Camera System

The Boeing Airplane Position and Attitude Camera System (APACS) is a well-developed system which belongs to this category. A brief description of this system is presented in the following paragraphs (ref. 68).

This system uses a 35-mm motion picture camera mounted in the belly of the airplane looking downward. The camera is synchronized with the Inter Range Instrumentation Group (IRIG) time code generator to be operated at 5 or 10 frames per second. The camera photographs the targets marked in parallel lines on the ground directly below the flightpath. The targets are 1.2 m^2 (4 ft^2) and carefully positioned on lines perpendicular to the airplane flightpath. The target squares on one perpendicular line are about 15.2 m (50 ft) apart. Figure 85 shows a typical marking in the noise range for takeoff conditions. This marking is also used for approach and level flyby conditions.

Following a flight test, the movie films are developed and read using a film reader, such as the Benson-Lehner Telereadex Type 29E film reader. The reader converts the x and y coordinates of the targets on film and film frame times into punched cards for computer entry.

To calculate the airplane position in space from the film, it is necesary to know the airplane pitch and roll angles. The airplane attitude is either obtained by a flight test gyro system or by an inertial navigation system.

The punched card information, in combination with the pitch and roll data, is used to compute the altitude and off-center distance of the airplane from the runway centerline as well as the visual overhead time with respect to a given microphone.

This system is relatively inexpensive and has been proven to provide good accuracy for acoustic flight tests. Its shortcomings are a need for elaborate target marking and the lack of on-line airplane position data.

3.3.1.2 Ground-Mounted Movie-Camera System

This system consists of one or more 35-mm movie cameras located on the ground and directed toward the airplane flying overhead. The IRIG time recorded on film is synchronized to the noise recording station. The airplane altitude and off-center distance are calculated by the use of the airplane dimensions and the camera lens focal length, knowing that the film plane is level.

This system is independent of the airplane and inexpensive but lacks on-line airplane position data. With each camera only recording one position data point per airplane flight pass, the system tends to have lower position accuracy.

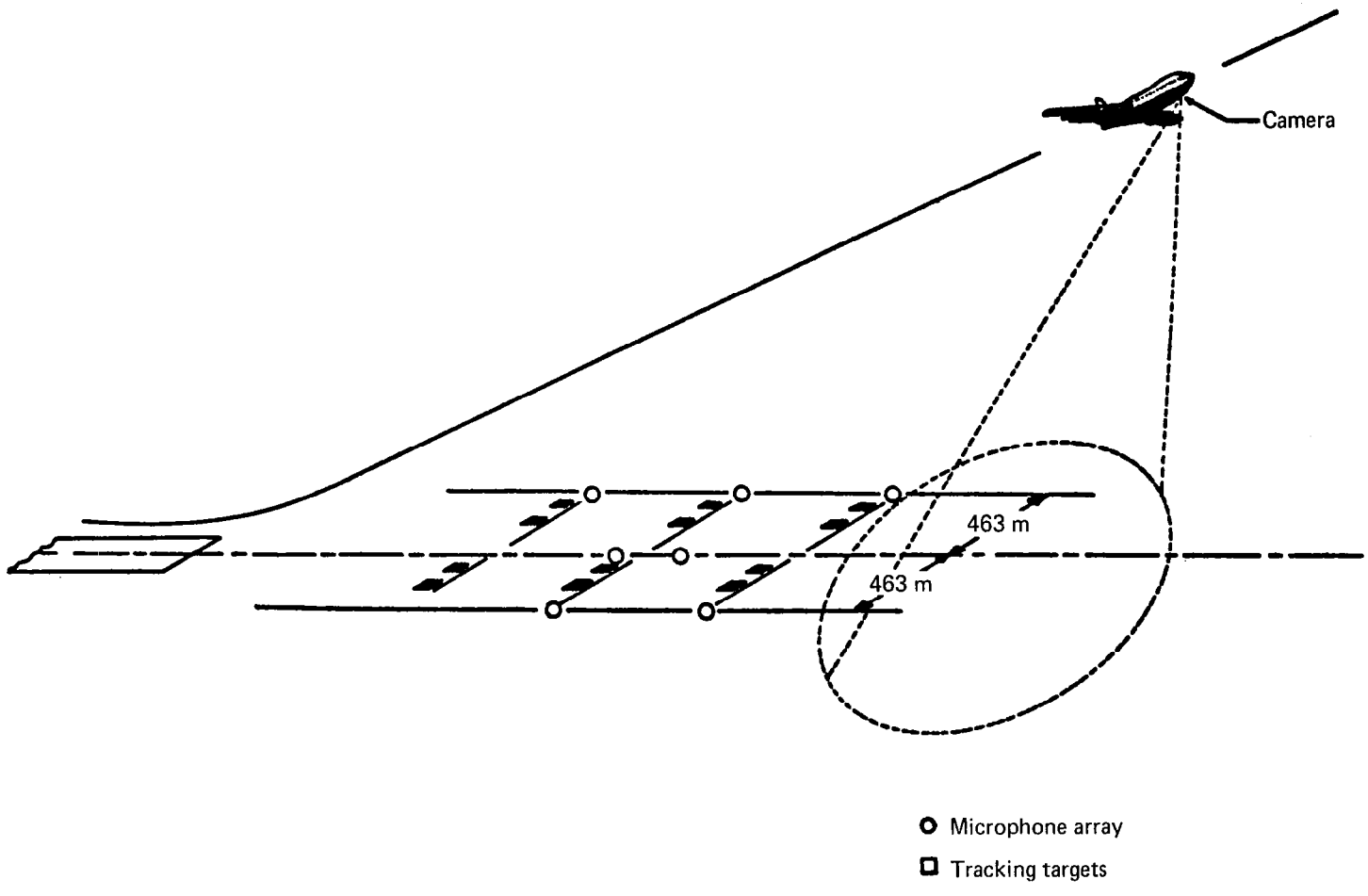

Figure 85.—A Typical Marking for Boeing Airplane Position and Attitude Camera System (APACS)

3.3.1.3 Laser System

As a representative laser system, the GTE Sylvania Precision Automated Tracking System (PATS), (refs. 69 and 70) is described in the following paragraphs. The PATS is an automatic laser tracking and ranging system and is developed for accurately determining the position of any target fitted with a retroreflector. It is a compact system that is integrated into a mobile trailer. It is provided with leveling jacks, which are used to support the van and tracking pedestal independently of one another so that the operator movements do not affect the system's accuracy.

The target retroreflector has three internal mirrors arranged so that the laser pulse is returned to the tracker with very high efficiency. The retroreflector arrays are small, lightweight, and very rugged. A variety of units have operated in all kinds of airborne environments.

An operator is required during the initial acquisition of target. For this, the operator manually slews the pedestal with a joystick while observing the TV display. When the target is positioned in the central area of the field of view, the system will lock on the target and then will automatically track the target. A video recording of the image seen by the operator is available. The system also is capable of automatic target acquisition. In this case, the pedestal must be directed by the predetermined target coordinates.

During tracking, the system accurately measures the azimuth and elevation angles and the range of the target at sample rates up to 100 measurements per second. These data may be multiplexed and recorded on magnetic tapes for later processing. In addition, pen plotters are provided to generate a real-time analog data in a variety of formats. Digital displays are also available. A computer is provided in the system; it may be used to perform data smoothing, editing, conversion, and other required computations. A block diagram of the system is presented in figure 86 (ref. 69).

The system is said to be highly accurate in determining the distance and angles (± 1.5m, $\pm 0.2^{0}$), requires a short setup time, is independent of the airplane except for the retroreflector, provides on-line data of the airplane position, and is adapted for implementing additional electronic instruments, such as a flight director guidance system. One drawback of this system, however, is the high initial cost.

3.3.1.4 Radar Systems

Radar systems, in which the principle of time required for a pulsed high frequency electromagnetic wave echoing back from an object is utilized in measuring the distance, have been in wide use in the past three decades. These systems in flight test application have many advantages of the laser systems in that they are ground located and independent of the airplane (except for a reflector or a transponder mounted on the airplane) and can provide on-line position data. The major disadvantage, however, appears to be the ranging accuracy, although some systems claim to be as accurate as the airborne movie camera systems.

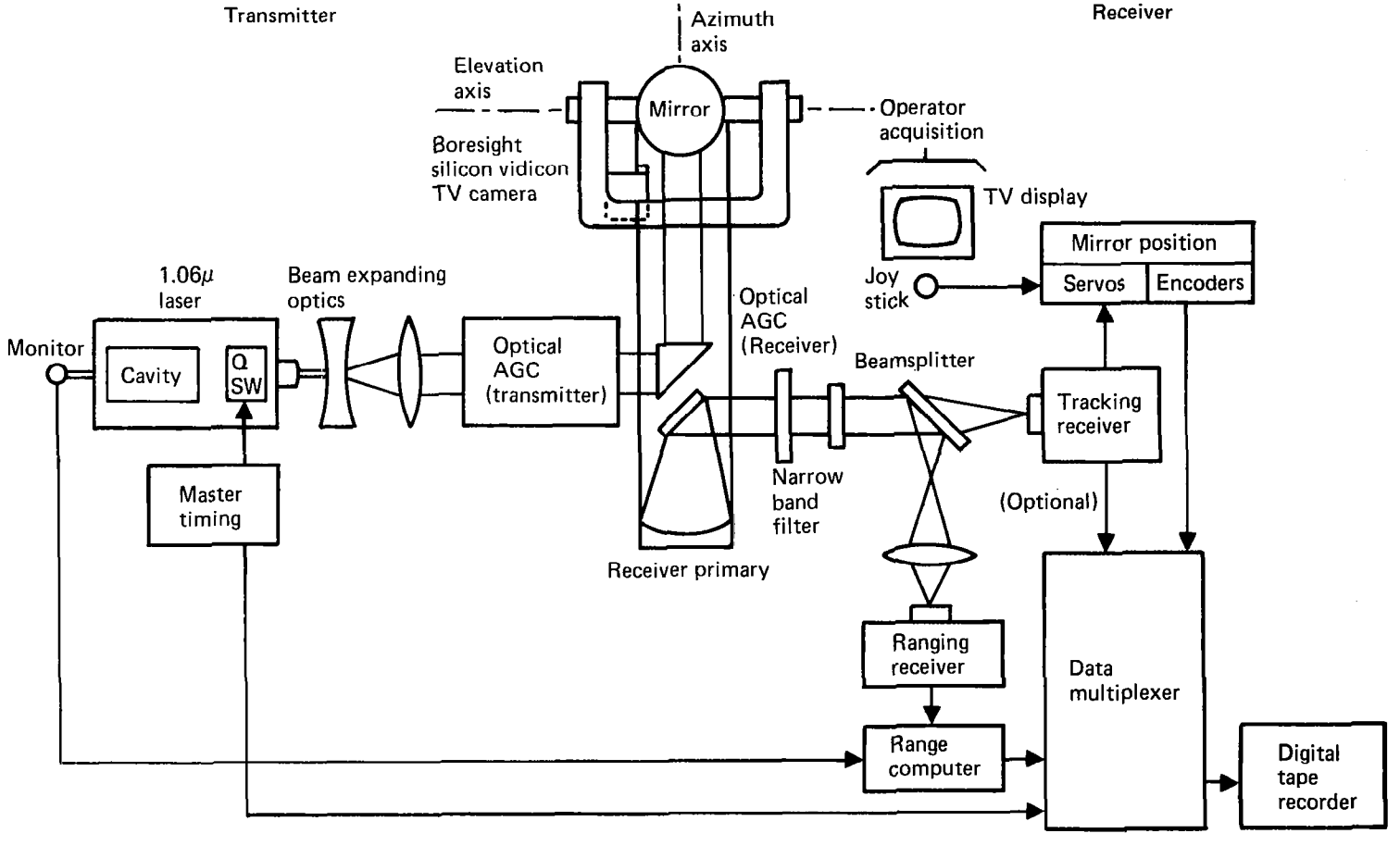

Figure 86.—Laser Tracking System Block Diagram (Ref. 69)

3.3.1.5 Airplane Attitude Measurement

In an acoustic flight test of a commercial transport, the airplane pitch and roll angles required for the acoustic analysis are either obtained by a flight test gyro system or by an inertial navigation system. When a flight test gyro system is used, it is mounted on a platform which is positioned in the airplane as close as possible to the airplane center of gravity to minimize the disturbances to the instruments.

The attitude data sensed are recorded on FM tapes by use of airborne tape recorders. Accuracies achieved by these current methods have been found satisfactory.

For smaller airplanes, a special consideration may have to be given to the size of the flight test gyro system.

3.3.1.6 Conclusions and Recommendations

In general, no space positioning system available today can provide a significant improvement in data accuracy over that currently being obtained from the photo positioning systems for testing on or near the runway. The laser system has advantages over the photo system in providing on-line position data and being able to operate into the direction of sunshine. However, the present laser system is very costly and is difficult to air transport from location to location.

The airplane attitude can be measured within the desired accuracy by either an inertial navigation system or a flight test gyro system.

In view of the on-line position data capability a laser tracking/ranging system in combination with a flight test gyro system or an inertial navigation system is most suited for measuring the airplane position and attitude during a jet noise research flight test.

3.3.2 ATMOSPHERIC PROPERTY INSTRUMENTATION

The current instrumentation for measuring atmospheric properties is divided into two categories: (1) ground-based instruments for measuring properties near the ground and (2) weather balloon instrumentation for measuring upper air properties. For an acoustic flight test in which a governmental certification is involved, methods and means for acquiring the atmospheric property information have to comply with the established regulations (ref. 71). In other nonregulatory acoustic flight tests, similar methods and means are also used, although some deviations are found as specific requirements dictate. Typical currently used atmospheric instrumentation is reviewed, and proposed improvements and new techniques suitable for the flight tests for investigation of the flight effects on jet noise are presented in following paragraphs.

3.3.2.1 Current Atmospheric Property Instrumentation

Ground-Based Instrumentation.—Air temperature, relative humidity, wind speed, and wind direction are normally measured at 1.2 m and 10 m above the ground. For

recording, 14-channel FM tape recorders or multichannel oscillographs are used.

Air temperature is commonly sensed with a thermistor, which is housed in a fan-aspirated thermal radiation shield, and an associated electrical network. One example of this type sensor is the model 44204 Thermilinear Thermistor network manufactured by Yellow Spring Instruments Company. A system using this type sensor has a system accuracy of $\pm 1.1^{\circ}$ C and a time constant of a few seconds in still air.

Relative humidity is normally sensed by a multiple lithium chloride cell humidity sensor and a transmitter integrally mounted to provide a voltage output signal as a function of relative humidity. The unit is a fan aspirated for rapid sampling of the surrounding atmosphere and is protected from thermal radiation. A sensor of this type has an accuracy of $\pm 3\%$ RH in the normal measuring range and a "response distance"of approximately 2.1 m (63% recovery).

The wind magnitude and direction are commonly measured by a propeller-vane sensor. The model 1053-III Vector Vane sensor in combination with the model 1026-III Transmitter, manufactured by Meteorology Research, Inc., is a typical sensor for wind measurements. In this unit, the vane swings horizontally as well as vertically to sense the horizontal and vertical wind directions. A light-beam chopper driven by a propeller is provided to generate a pulsed output, which is a measure of the windspeed. Response of this type vane sensor in terms of delay distance and damping ratio are 0.6 to 0.9 m (50% recovery) and 0.4 to 0.7 m, respectively. Steady-state accuracy of the sensor in terms of starting threshold is approximately 0.44 m/s. Response of the propeller speed sensor in response distance and starting threshold is about 0.6 to 0.9 m (63% recovery) and 0.44 m/s, respectively.

Upper Air Instrumentation.—The upper air properties measured are vertical profiles of air temperature, relative humidity, wind speed, and direction. Sensing of the temperature and relative humidity is commonly done with a standard 1680 MHz radiosonde (identical to that utilized by National Weather Service) manufactured by the VIZ Company.

It is carried aloft with a helium-filled balloon which is released from the ground at regular time intervals during the test. The signals telemetered from the radiosonde, sequentially activated by an aneroid-clock mechanism, are received by a ground receiver station, such as the model RD65 Receiver manufactured by Weather Measure Corporation.

The radiosonde incorporates a rod thermistor for temperature sensing and a carbon hygristor for relative humidity sensing. The wind speed and direction are computed by the information obtained by manually tracking the radiosonde with an antenna included in the ground station. A stripchart recorder is used to record the temperature and relative humidity as functions of altitude.

Accuracies and responses of the upper air temperature and relative humidity sensing are of the same order of magnitude as those for the ground-based instruments.

3.3.2.2 Proposed Instrumentation Improvements and New Techniques

For a research-type flight test, use of high accuracy instruments and acquisition of more detailed atmospheric property data may be required. The study of motion effects on jet noise demands such data acquisition systems. Proposed improvements in the current instrumentation and suggested use of new techniques, which would be desirable for a research type flight test, are presented below.

Improvements for the Balloon System.—The current balloon/radiosonde system, in which sequencing for recording of temperature and relative humidity data is controlled by the variation of atmospheric pressure as the balloon ascends to higher altitude from the ground, results in an alternate measurement of temperature and relative humidity data in altitude increments of approximately 61 m, each altitude increment being equivalent to 20 to 30 sec.

If accurate profiles of temperature and relative humidity are to be established for evaluation of sound ray bending and associated atmospheric absorption losses, the current data acquisition rate is inadequate, particularly for a low altitude flight test (e.g., 122-m level flight test). Thus, some other means of more frequent data acquisition is desired. A circuitry modification in the radiosonde may be made to increase the sampling rate to a desired value; i.e., in the order of 1-sec duration.

Because of the natural aspiration of ambient air utilized in the current balloon/radiosonde system, inaccuracies tend to be introduced in the measurement at the beginning of ascent of the balloon. This problem can be eliminated by a provision of forced aspiration by a fan system.

The temperature and relative humidity sensing elements included in any radiosonde are those screened through a normal manufacturing quality control process. A batch of premium elements with higher sensing accuracy can be obtained if the quality control process is made more stringent. Prime elements obtained by screening with such a process may be used for a higher degree of accuracy.

Tethered Balloon System.—Use of a tethered aerodynamic balloon (kytoon) equipped with necessary sensing and electric systems would provide various advantages over the free-rising balloon system. By the use of a properly designed aerodynamic surface on the balloon, it is known that the tether can be erected nearly vertical in the presence of a strong wind. With a kytoon, operations of a winch to extend and retract the tether will provide a wide range of options in controlling the rise and descent rate of the radiosonde. The altitude of the radiosonde may be determined by the length of the tether extended and the slant angle.

In addition to the temperature and relative humidity sensing elements, the tethered radiosonde should include a wind measuring device and a sample sequencing system which allows control of sampling time. An effective aspiration system is also desirable.

Accuracy/Response of Instrumentation and Atmospheric Turbulence Measurement.—A number of reports suggest that the atmospheric turbulence existing between noise source and receiver is responsible for the scatter of noise data found in flight tests.

Studies of ray acoustics (refer to sec. 3.1.6, for example) indicate that changes in ray path due to changes in mean values of atmospheric properties may result in a substantial variation of noise levels for repeat runs of a flight test. It is thus believed that precise measurement of atmospheric conditions between the noise source and receiver is important when an accurate noise level measurement is involved. In the study of the motion effects on jet noise from an aircraft, an uncertainty of measurement of noise levels could amount to a large percentage of the flight effects.

For acquisition of atmospheric inhomogeneities that are relevant to the ray acoustics as well as the sound attenuation due to atmospheric turbulences, instruments with the following characteristics are utilized in reference 72.

Parameter	Captor	Frequency response, Hz	Accuracy %
Temperature	Thermistance	*	±2
Humidity	Hygristor	0.5	±5
Wind speed	Cup anemometer	0.5	±20 for velocity larger than 1 m/s

*In ref. 72 frequency response of thermistance is given as "a few."

A review of current technical brochures (refs. 73 through 75) of commercial weather instrument manufacturers indicates that a selection of instruments with accuracy and response characteristics comparable to the above is readily available at reasonable cost. Typical accuracies and responses of commercially available high-grade sensors are: $\pm 0.25^{0}$ C and 3 Hz for temperature in still air; ±3% RH and 0.2 Hz (10 fps aspiration) for relative humidity; ±0.09 m/sec and 0.3 Hz for wind speed; and $\pm 4^{0}$ and 0.3 Hz for wind direction in horizontal plane. These accuracies and responses are believed adequate for most of the flight tests intended for jet noise study.

For an accurate and extremely fast measurement of wind and temperature (the microstructure), a sonic anemometer-thermometer (ref. 73) may be used. This instrument is said to be able to measure the wind and temperature within ±3% of true value with a frequency response of up to 100 Hz.

Remote sensing of the atmospheric conditions may also be done by "lidar," radio, acoustic echo-sounding techniques (refs. 76 through 80). The operating principle of these techniques is the same: a pulse of energy is sent into the atmosphere by a transmitter, and energy that is scattered out of the pulse by the atmosphere is detected by a receiver and measured as a function of range. Since different physical forms of transmitted energy have different interactions with the atmospheric conditions, simultaneous use of two or more devices may be needed to acquire all the information desired.

3.3.3 AVERAGING OF FLIGHT TEST DATA

Quality of jet noise data obtainable during a flight test is not in general as good as that for a static test because of several reasons; e.g., the relative motion between the airplane and microphone, variations of airplane flight conditions during the test, and others. A study to improve this situation is presented in this section.

The working hypothesis is generally made in the jet noise analysis that jet noise generation is an ergodic random process. Trends evidenced in various static tests tend to indicate that this is an acceptable hypothesis. This allows one to state that the smoothed spectrum obtained from a microphone signal during a static test correctly represents the jet noise spectrum at a given distance and a given radiation angle.

In the case of a flight test, however, the situation is different. In this case, the microphone signal is essentially nonstationary even if the noise generation remains ergodic. Not only will the spectra from this signal be different for different times, but it cannot be said of any of the spectra that it represents the jet noise spectrum at a given distance and radiation angle. This result arises because of the finite time, called the sampling or integration time, required to produce a signal spectrum, during which time the airplane has moved relative to the microphone. This motion of the airplane relative to the microphone makes the microphone signal irrevocably nonstationary.

For the case of a flight test, therefore, the relative motion has to be reduced if the nonstationarity of the signal is to be alleviated. If the sampling time is made sufficiently short, making the relative motion between airplane and microphone extremely small, then the microphone signal obtained on the ground may be considered as the static noise between a stationary airplane and a stationary microphone. It may also be reasonable to assume that theory developed for ergodic random processes is applicable to such flight test noise data. Analysis performed under this assumption on the benefit of the use of several microphones during a flight test in comparison with the use of a single microphone is presented in the following paragraphs. An example in which four microphones were used to analyze the jet noise from a taxiing airplane (F86) is also presented. In this analysis, other variables such as engine operation, airplane velocity, and altitude were assumed constant.

3.3.3.1 Estimated Errors of Flight Test Jet Noise Spectrum

An instantaneous power spectrum of the jet noise emitted from a flying airplane estimated from a finite time sample of a ground microphone signal will have two inherent sources of error resulting from the finiteness of the sample time. There will be an uncertainty because of random fluctuations of the noise and an uncertainty because of the motion of the airplane. The former varies with the inverse square root of the sample time, and the latter varies directly with the sample time. The estimate of the power in a frequency bandwidth B_S will have a normalized mean square error ϵ_S^2 due to random fluctuations associated with a sample time T given by Reference 89.

$$\epsilon_S^2 = 1/B_S T \tag{53}$$

This error is due to the randomness of the estimates: any estimate, or statistic, formed from a finite amount of information about a random variable, such as a noise signal, is itself a random variable. The estimate has a probability, or sampling, distribution associated with it which is derived from the probability distribution function of the original random variable. The sampling distribution of the sum of squared Gaussian random variables is a Chi-squared distribution with n degrees of freedom, where n is the number of independent Gaussian random variables occurring in the sum.

Since jet noise generation closely approximates a Gaussian random process, the sound power in a given frequency band is a Chi-squared random variable. Thus the Chi-squared probability distribution can be used to estimate the confidence interval of the power spectrum that is attributable to statistical fluctuations. The equivalent Chi-squared degree of freedom, n, for such an estimate is given by:

$$n = 2 B_S T \tag{54}$$

For the estimate to be meaningful n must be greater than or equal to 2. There is then a lower limit on the sampling time required to produce a meaningful estimate of the power in the bandwidth B_S:

$$T \geqslant \frac{1}{B_S} \tag{55}$$

Given the degrees of freedom and the estimate, an interval about the estimate can be computed in which there is a specified probability that the "true" mean value (even if biased) lies. For instance, when n = 20, from a table of the Chi-square distribution one finds that the ratio of the estimate to the true mean will exceed 31.41/20 = 1.57 with a 5% probability and will fall below 10.85/20 = 0.542 with a 5% probability. This means that there is a 90% probability that the ratio will lie between 0.542 and 1.57. This is equivalent to saying that the 90% confidence limits for the ratio are 0.542 and 1.57. Conversely, it can be said that the 90% confidence limits for the ratio of the true mean to the estimate are 1/1.57 and 1/0.542. In decibels, these limits about the given estimate, within which the true mean will lie, are calculated to be 10 log (1/1.57) = -1.96 dB and 10 log (1/0.542) = + 2.66 dB.

Along with this randomness in the estimate, there can be a bias. If S is the real value of the power in the bandwidth B_S of the noise at the microphone location for a particular airplane location, $\hat{S}$ is the estimate formed from a time sample of length T, and E [ ] is the true expectation operator, then the total mean square error of the estimate is

$$\Delta^2 = E\left[(\hat{S} - S)^2\right] \tag{56}$$

and the true mean value is

$$\bar{S} = E\left[\hat{S}\right] \tag{57}$$

Adding and subtracting $\bar{S}$ in equation 56 gives

$$\Delta^2 = E\left[(\hat{S} - \bar{S})^2\right] + (\bar{S} - S)^2 \tag{58}$$

The first term on the right hand side is called the variance of the estimate while the second term is the square of the bias. Normally an experiment is designed to either make the bias negligible or computable, leaving only the problem of how much data to gather to give an acceptable variance. If however, there is an inherent, not simply subtractable, bias in the estimate, then the best estimate is achieved not simply by minimizing the variance or maximizing the number of degrees of freedom, but by minimizing the total mean square error. These considerations are applied here to the design of an experiment for achieving a best estimate.

The variance of an estimate, $\hat{\bar{S}}$, of the power in a bandwidth B_S for a sampling time T is

$$E\left[(\hat{\bar{S}} - \bar{S})^2\right] = \frac{\bar{S}^2}{B_S T} \tag{59}$$

and decreases inversely with T and B_S. The airplane is continuously changing position during the sampling time so that the power estimate does not correspond to a fixed relative position but to an average over a range of relative positions. This estimate will then differ from that which would be obtained from a sample with fixed relative position. The expected difference between these two types of estimates is a bias (assuming the fixed relative position estimate is unbiased) which cannot be simply computed. It is reasonable to assume, however, that for short sampling times the difference between the fixed position estimate and that moving position estimate is proportinal to time. That is, the normalized mean square error due to the motion of the aircraft is

$$\epsilon_m^2 \propto T^2$$
$$= B_M^2 T^2$$

where B_M is the proportionality constant. Then the total normalized mean square error is expressed by the sum of the variance error, ϵ_S^2, and the bias error, ϵ_M^2:

$$\epsilon^2 = \epsilon_s^2 + \epsilon_m^2 = \frac{1}{B_S T} + B_M^2 T^2 \tag{60}$$

The bias term might be considered as follows: let $\hat{\bar{S}}_t$ be the estimate that would be made from the fixed relative position corresponding to time t so that

$$\bar{S} = E\left[\hat{\bar{S}}\right] = \frac{1}{T}\int_o^T E\left[\hat{\bar{S}}_t\right] dt \tag{61}$$

Then if $E\left[\hat{\bar{S}}_t\right]$ varies smoothly with t it can be expanded in a Taylor's series

$$E\left[\hat{\bar{S}}_t\right] \simeq \bar{S}_o + \left(\frac{d\bar{S}}{dt}\right)_o t \tag{62}$$

giving the bias term

$$\bar{S} - \bar{S}_o \simeq \frac{1}{T}\int_o^T \left(\frac{d\bar{S}}{dt}\right)_o t\, dt$$
$$= \frac{1}{2}\left(\frac{d\bar{S}}{dt}\right)_o T \tag{63}$$

Then since $\bar{S}_o$ is time dependent only through the motion of the airplane,

$$\left(\frac{d\bar{S}}{dt}\right)_o = \left(\vec{V} \cdot \vec{\nabla}\bar{S}\right)_o$$

where $\vec{V}$ is the airplane velocity vector and $\vec{\nabla}$ is the gradient operator (see Figure 87). Thus

$$B_M \simeq \frac{1}{2}\left(\vec{V} \cdot \frac{\vec{\nabla}\bar{S}}{S}\right)_o \tag{64}$$

and B_M will depend on the instantaneous distance and angle from airplane to microphone. A detailed evaluation of B_M may be made by differentiating a sound power spectrum expression such as

$$S(R,\theta) = S_S\, R^{-2}\, (1-M_A \cos\theta)^{-1}\ (1+M_c \cos\theta)^{-5}, \tag{65}$$

a form derived from Equation (38) and (39), where S_S is a constant.

The maximum value of B_M as computed via eq. (64) depends on the precise θ dependence of the radiation pattern, eq. (65) being an a priori estimate. However, the radiation pattern is one of the items which we are attempting to determine by the flight measurement. Consequently, B_M cannot be computed exactly, and therefore the bias error introduced by the motion of the aircraft represents a true uncertainty and not a quantity to be systematically subtracted from the spectral estimate.

If the assumption is made that the maximum error due to airplane motion occurs in the near overhead position (i.e., $\theta = 90°$), then using eq.'s. (64) and (65) it can be shown that

$$B_M \simeq K\left(V/H\right)$$

where V is the (level) velocity of the aircraft, H it's altitude, and K is a constant, the value of which depends on M_c and M_A of equation (65).

An optimum sampling time can now be chosen to minimize the ϵ^2 of equation (60) under the constraint imposed by equation (55). The solution to this minimization problem is (Fig. 88)

$$T_{opt} = \left(1/(2\, B_S B_M{}^2)\right)^{1/3} \tag{66}$$

for

$$B_S \geqslant \sqrt{2}\quad B_M \tag{67}$$

The minimum total mean square error for this optimum time is

$$\epsilon^2_{min} = 3\left(B_M/2B_S\right)^{2/3} \tag{68}$$

This situation can be improved by forming an ensemble averaged estimate from k separate and independent time averages which can be accomplished by sampling from k microphones placed along the flight path sufficiently spaced to achieve independence. Then if each of the k estimates derived from τ seconds of sampling are averaged, the variance of the average decreases inversely with k. If the expected bias is the same for each estimate, then it will be the same for the average. Thus, the total normalized mean square error for the averaged estimate will be

$$\epsilon_k^2 = \frac{1}{kB_S\tau} + B_M^2\tau^2 \tag{69}$$

Minimizing this with respect to τ gives the optimum sampling time per microphone:

$$\tau_{opt} = (1/(2\,k\,B_S B_M{}^2))^{1/3} \tag{70}$$

The constraint imposed by equation 55, with τ_{opt} in place of T, is

$$\tau_{opt} \geqslant \frac{1}{B_S}, \tag{71}$$

which is a constraint on each microphone spectrum estimate. Then for a given B_S and B_M, this constraint leads to the constraint on the number of microphones

$$k \leqslant \frac{1}{2}\frac{B_S{}^2}{B_M{}^2} \tag{72}$$

The balance of the total mean squared error in equation (69) is two-to-one for the variance and the bias squared, as it is for the single microphone estimate, so that both the variance and the bias have been reduced proportionately by using k microphones. Each type of error is reduced by a $(1/k)^{1/3}$ factor. By considering weighted combinations of the two squared errors, other optimum results can be obtained. In particular, any τ satisfying equation (71) and giving an acceptable bias error can be used such that the number of microphones can be determined to give the smoothness required of the spectrum.

The common procedure for displaying the error of a power spectrum estimate is the specified percent confidence band. This must be modified when a "probable bias" is a part of the total error of the estimate. When the bias is small then a delta SPL computed from $10\ \log_{10}\ (1 + B_M\tau)$ can be used to extend both sides of the 90% confidence band established by the number of degrees of freedom of the estimate. When $B_M\tau$ approaches or exceeds unity then other ways of displaying this probable bias will have to be found.

For a typical 122-m (400-ft) altitude level flyby test with an airplane velocity of 76 m/s (250 fps), the airplane sweep rate near overhead is approximately 36°/sec. Use of a four microphone system could give an airplane position resolution of approximately ±4°. Several factors should be considered in the selection of the number of microphones: the airplane position resolution desired, the minimum sample integration time that is compatible with the spectrum analyzer (some are limited to 1/8 sec), and the cost of instrumentation and data reduction, etc.

The optimum sampling time analysis presented in the preceeding paragraphs is appropriate for a constant bandwidth spectrum. For constant percentage bandwidth spectra, however, this solution indicates an optimum sampling time dependent on the frequency: the higher the frequency, the smaller the optimum sampling time. Since generally, the same sampling time is used for all bands in generating a constant percentage bandwidth spectrum, another constraint must be imposed in order to determine a single "best" time interval. A balance must be made between increasing the statistical error in the lower frequency bands and reducing the motion error that becomes dominant at higher frequency bands when the sampling time is chosen to optimize a lower frequency band error.

One way of achieving this is to establish an acceptable upper limit to the statistical error for the lowest band for deriving the best sampling time. If the sampling time thus derived gives a reasonable bias error because of the airplane motion (which remains the same for all bands on account of equation (60) or (69)), then the sampling time would be satisfactory for all other 1/3 octave bands because of increasing n as the band moves toward high frequencies. On the other hand, if the sampling time is optimized for the highest band, then use of this sampling time will give poor statistical errors for lower frequency bands because of decreasing n at these bands, possibly resulting in unacceptable statistical error limits at some lower band. This point must be examined before using the selected sample time. Assuming the use of four microphones and B_M = 0.25, the results of an example to illustrate this aspect are presented in the following table:

Sampling time	90% statistical error confidence limits		Bias error for all bands
	50 Hz band	10,000 Hz band	
0.55 sec, optimized for 50 Hz band (Eq. 70)	+1.5 dB −1.3 dB	±0.1 dB	±0.6 dB
0.094 sec, optimized for 10,000 Hz band (Eq. 70)	+4.4 dB −2.7 dB	±0.3 dB	±0.1 dB

The table indicates that the sampling time of 0.55 sec is preferable to 0.094 sec. The sampling time thus selected must now be examined against the desired resolution of airplane position and noise emission angle.

3.3.3.2 Example of Use of Multiple Microphones

During an F86 taxi/flight jet noise test at Boeing, 12 microphones were installed parallel to the taxi and flightpath of the airplane. Noise data recorded by four of these microphones during a taxi test were analyzed to obtain the SPL spectra, OASPL, PNL, and PNLT at every 0.125 sec as the airplane rolled by the microphones. Selecting four airplane position times at which the airplane assumed the same relative angle toward each of the four microphones, the noise data analyzed were ensemble-averaged to improve the quality of the noise spectra representing that airplane position. A sketch of the taxi-testing arrangement and the spectra analyzed for the emission angle of 110° is

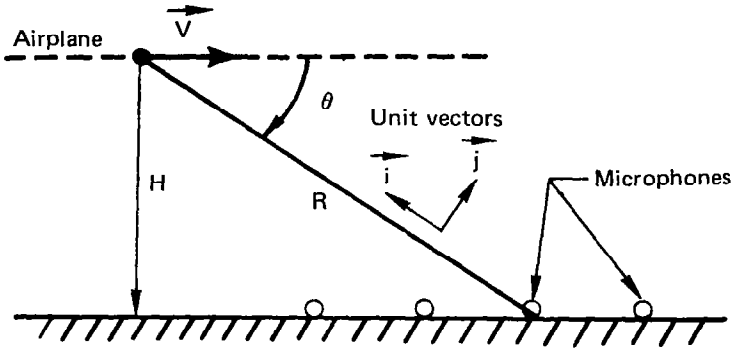

$\vec{V}$ = Airplane velocity vector

$= \vec{i}\frac{dR}{dt} + \vec{j}\,R\frac{d\theta}{dt}$

$\vec{\nabla}$ = Gradient operator

$= \vec{i}\frac{\partial}{\partial R} + \vec{j}\frac{1}{R}\frac{\partial}{\partial \theta}$

$\vec{V} \cdot \vec{\nabla}$ = Time derivative

$= \frac{dR}{dt}\frac{\partial}{\partial R} + \frac{d\theta}{dt}\frac{\partial}{\partial \theta}$

Figure 87.—Geometry of Motion Error Analysis

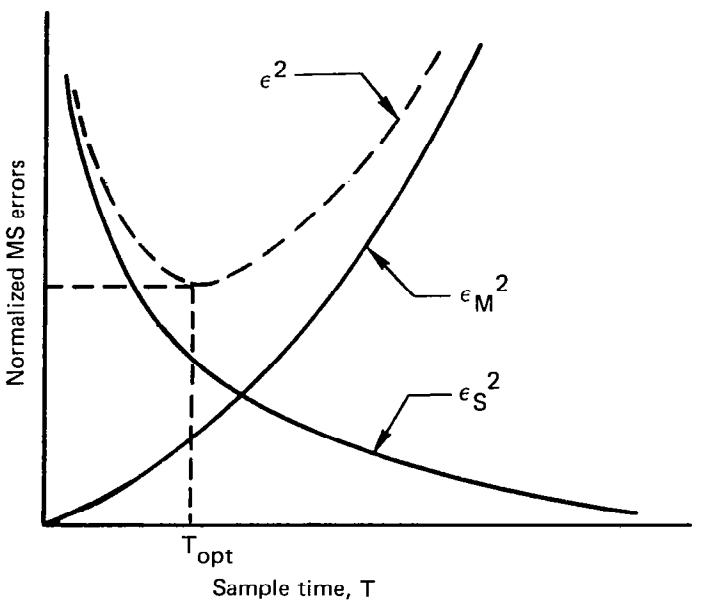

Figure 88.—Normalized Mean Square (MS) Error Variations Versus Sample Time

presented in Figure 89. It shows two single microphone spectra obtained by using a 0.5 sec integration time and one obtained by ensemble-averaging four spectra, each of which was obtained by using a 0.125 sec integration time.

Equations (60) and (69) show that the statistical and motion errors for the ensemble-averaged spectra and the single-microphone spectra are the same because $T = k\tau = 0.5$ sec. However, the airplane position (and the noise emission angle) resolution for the ensemble spectra has now improved about four times over the other. For example, near overhead, data recorded during an 18^0 sweep were analyzed for the ensemble-averaged spectra, while noise data recorded during a 66^0 sweep were analyzed for the single-microphone spectra, which is a considerable quality improvement.

3.3.4 DUPLICATION OF STATIC JET CONDITION IN FLIGHT

There are two problems present in establishing the in-flight jet condition during a flight test for the study of jet forward motion effects. They are: (1) the criteria for selection of jet parameter(s) which must be set equal for the ground static and in-flight conditions, and (2) the instrumentation and techniques for ensuring that the desired jet operating conditions are achieved during flight test. Discussion of and comments for answering these problems follow.

3.3.4.1 Criteria for Comparison of Static and In-Flight Jet Noise

Ideally, for an evaluation of the forward velocity effects, the jet flow conditions (primary, secondary, etc.) at the nozzle exit plane should be identical between the static and the in-flight operations. With these conditions identical, all changes that occur in and around the jet flow due to flight and all consequent jet noise changes can be viewed as the flight effects. Such a criterion can be satisfied in a motion effect simulation with model nozzles, but it is not generally possible with an engine. Thus with an engine, matching of the absolute primary jet velocity only has been normally substituted as the criterion.

This criterion for an engine leaves other jet flow conditions (secondary, entrained ejector air, etc.) unmatched and results in a jet noise level change which may not be considered as a motion effect on jet noise. Therefore, one feels that there should be an additional qualification specified to the flight effect under the criterion of equal primary jet velocities.

An exploratory study was performed to evaluate the extent of this level change with a current high-bypass engine. By way of an engine cycle analysis computer program, two sets of engine performance data, which had the same primary jet velocity, were obtained: one for the ground static takeoff power condition and the other for the takeoff power condition with $M = 0.2$ and altitude 610 m (2000 ft). The following relative values of the parameters required for jet noise prediction by the JEN2 program (sec. 3.1.5) show some appreciable differences:

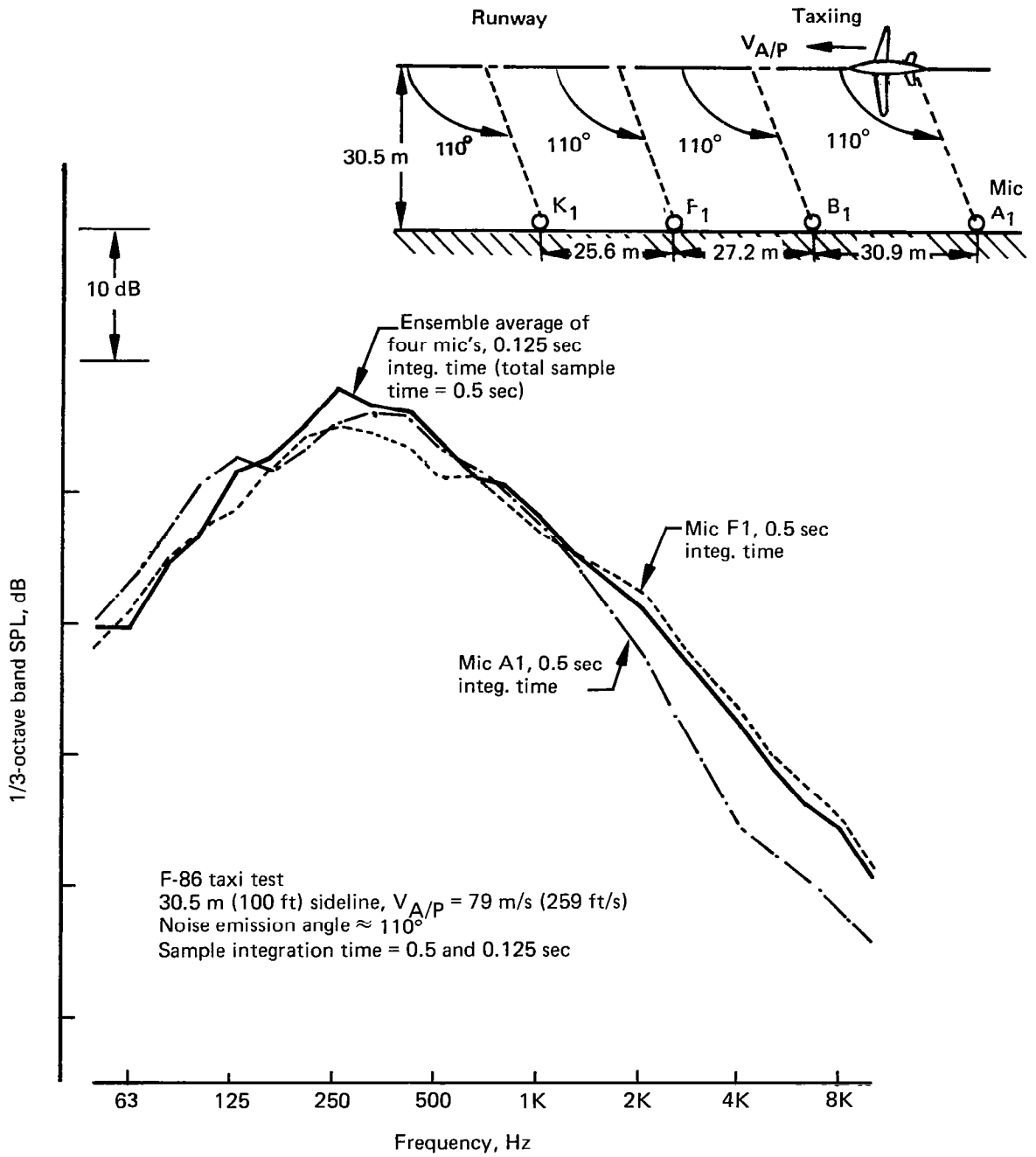

Figure 89.—Comparison Between Ensemble Averaged and Single Microphone Spectra

		Mass flow	Jet velocity	Total temperature
Condition 1, ground static	Pri	W_{jp}	V_{jp}	T_{Tjp}
	Sec	W_{js}	V_{js}	T_{Tjs}
Condition 2, M = 0.2 Alt = 610 m (2000 ft)	Pri	0.996 W_{jp}	1.0 V_{jp}	0.979 T_{Tjp}
	Sec	0.965 W_{js}	1.021 V_{js}	0.991 T_{Tjs}

To obtain the source noise level changes that result only from the performance parameter changes, static jet noise levels using the two sets of parameters were computed. The results are summarized in figure 90. Figure 90a shows the subcomponent jet noise levels at the ground static condition and the noise level differences between condition 1 and condition 2 or (condition 1 minus condition 2). Views b and c of figure 90 show the similar comparisons for the total jet noise level and OASPL. The comparisons indicate that by the performance mismatch alone the jet noise of the engine at the flight condition would be lower by about 0.4 dB at the source.

The exploratory study shows that this difference could mean a substantial portion, if the total flight effect itself is small. Thus, in the case of a high-bypass engine, where a larger effect of secondary flow mismatch would be found, it is recommended that the noise level change be examined for assuring the appropriateness of neglect of this noise level change.

3.3.4.2 Flight Test Engine Performance Instrumentation

The current Boeing flight test engine performance (including the nozzle performance) instrumentation consists of various pressure, temperature, and rpm sensors, and FM and pulse code modulation (PCM) airborne tape recording systems (figure 91). The recorders may be provided with cathode ray tube (CRT) monitors as seen in the figure.

The present magnetic tape data system consists of PCM and FM recorded on a number of 14-track tape recorders, which provide for 2 hr of record time per reel. The PCM and FM data can be selectively distributed on 13 tracks of each recorder, while an Inter Range Instrumentation Group (IRIG) time code is recorded on one track of each magnetic tape. The time code, which provides a resolution of 0.001 sec, is later utilized for time-correlating the engine performance data with the acoustical data recorded on the ground.

The PCM system is a 14-bit recording system formatted in 45-channel frames sampled every 0.4 sec. For digital data, two channels are used for framing and 53 channels are used for data recording. For analog data, two additional channels are required for accurate scaling of analog channels and 41 channels are used for data recording. Recording/reduction accuracies of 0.1% are obtained for digital signals and 0.5% for analog signals.

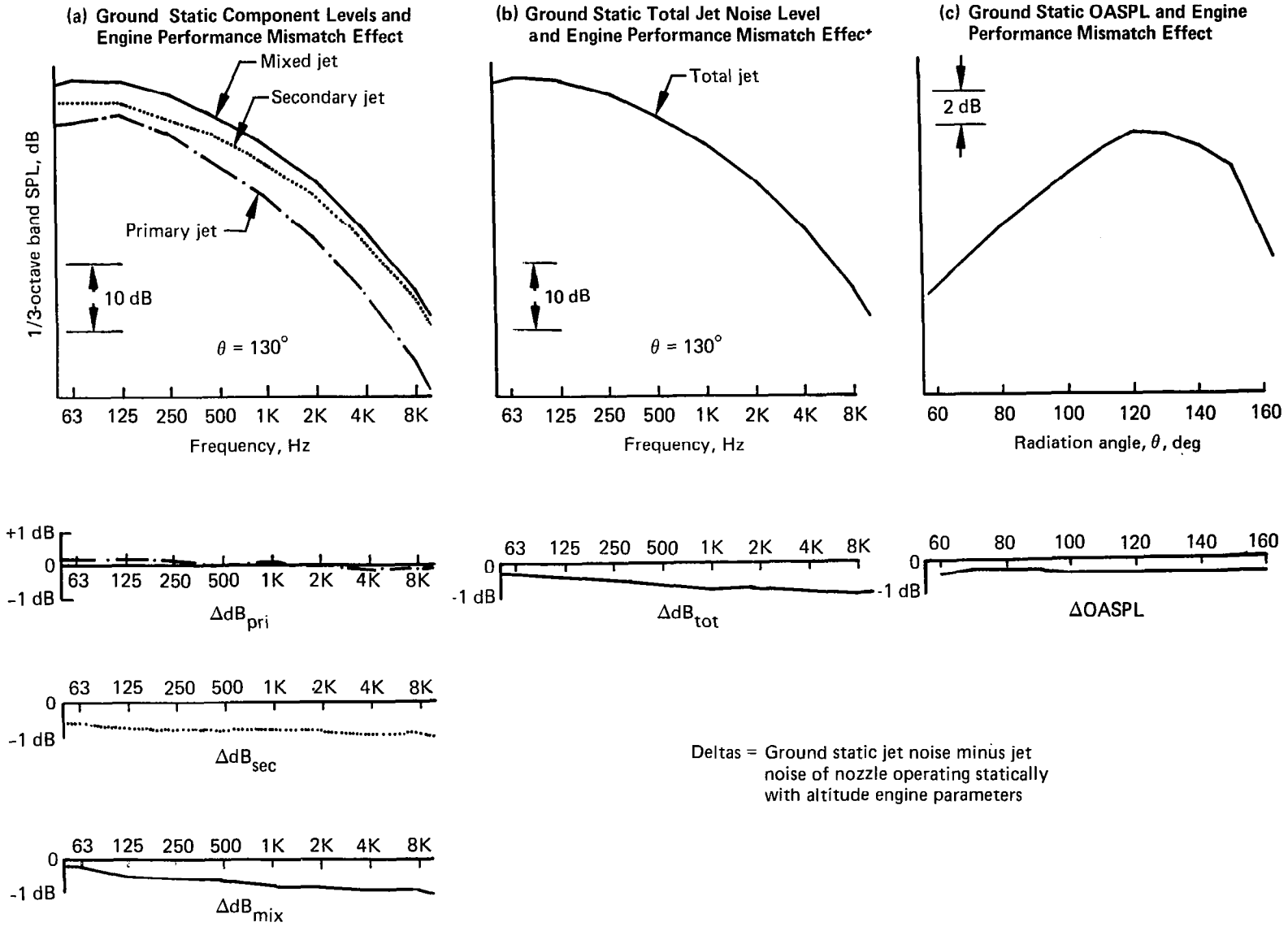

Figure 90.– Comparisons of Jet Noise at Ground Static Operation and at Static Operation With Altitude Engine Performance Parameters (0.2 Mach/610 m), High-Bypass Engine

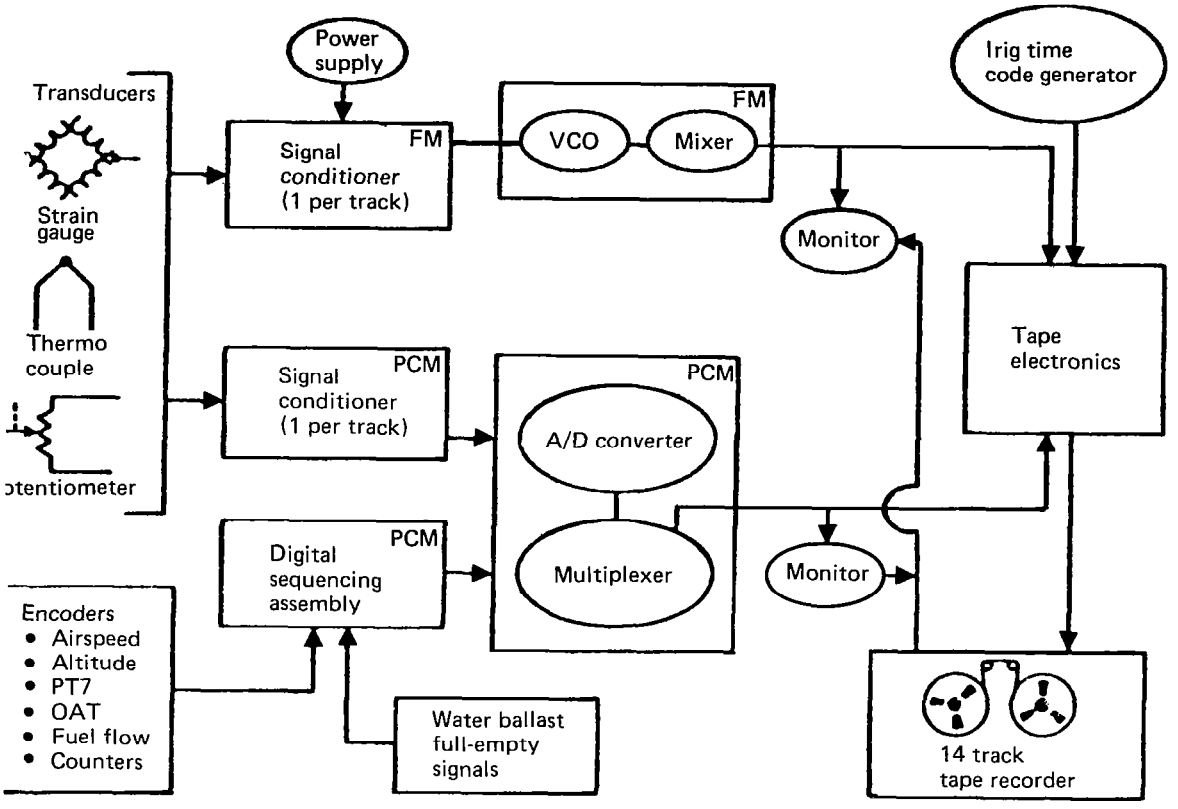

Figure 91.— Airborne Tape Recording System

The 10-channel FM system is used to record dynamic data in frequency ranges up to 110 Hz. Signal conditioning networks of the system allow for biasing, attenuation, or amplification of analog signals to obtain the desired range for each measurement. By periodic calibration, the system can achieve a recording/reduction accuracy of 2%. Up to 128 channels of FM data plus IRIG time can be recorded on one tape recorder with this FM system.

The PCM and FM data may be monitored by CRT on-board monitor systems. The CRT raster can present all channels of one track as 45 (PCM) or 10 (FM) vertical bars, the height of each representing the value in a data channel in percent of full scale. All 10 FM channels on a track can also be displayed on analog meters. Monitors can be selectively switched to display the data before it is recorded or to read from the tape after it has been recorded.

The parameters normally measured for the nozzle performance are the nozzle exit total pressures, total temperatures, and the ambient pressure and temperature. The jet velocities and weight flows are functions of these variables. For a flight test in which a steady nozzle operation is important, it is desired that the nozzle performance parameters be monitored by the use of a CRT monitor or other equivalent means.

The accuracies of the engine-related pressure, temperature, and rpm measurement, attainable by the flight test engine instrumentation, which depend largely on calibration and other precautionary steps taken to the electric/electronic instrument involved, are estimated to be 0.2% of full scale, $\pm 0.6^{0}$ C to 2.8^{0} C ± 10 rpm in the normal range, respectively. These accuracies are considered to be adequate for a jet noise research flight test. Confidence levels are further improved by averaging the data from several repeat tests.

3.3.4.3 Future Flight Test Instrumentation

The data system being implemented for test programs in 1975 and beyond includes a high-speed party line PCM system; a monitor system with on-board computing, multiple CRT displays, and a high-speed printer; and auxiliary special recording systems.

The compact, lightweight, remotely located airborne components,coupled with the communication features of the party line PCM system, would make a recording system suitable for small as well as large aircraft. The programmable recording format and the use of submultiplexers will allow a wide range of sampling rates to record data frequencies from 1 to 1000 cps.

The major characteristics of this system are as follows:

System type	Stored program random access, party line
Party line	2-wire, Manchester biphase
	4 lines per system
System speed	Up to 512 000 bits/sec

System capacity	Up to 2000 measurements normal Up to 9000 measurements special case
System accuracy	0.1 to 1% depending on gain setting for analog signals
PCM word length	8 or 10 bits
Programmable formats	Multiple formats—computer controlled
Programmable sampling	1 to 1000 samples per second in normal usage–above 10 000 samples per second possible

The flight test instrumentation planned will greatly enhance the quality and efficiency of future acoustic tests.

3.3.5 EXTRACTION OF JET NOISE COMPONENT FROM TOTAL NOISE

In many cases, noise data given for studying the jet noise characteristics are a composite of various component noise, such as, fan, turbine, core noise, etc., in addition to jet noise. This requires an isolation of the jet noise from the composite noise. A method for identifying the jet component noise is presented in this section.

The problem to be solved is defined as follows: noise data of an engine in a ground static test stand are given, and the jet noise component is to be extracted from the total engine noise measured. Solution of this problem will be discussed first, then discussion of the same type of problem with flight test data will be presented. The latter case can be handled similarly to the first, but examination of some additional criteria is required.

No direct method for solving the problem of extraction of jet noise from a total noise appears available to date. For some cases in which jet noise is the dominant noise, the problem is more amenable. In cases where other component noise (e.g., core noise) is dominant, credibility of the extracted jet noise is diminished. The example discussed below is a case that could be categorized in the first group.

In general, the static engine noise data given will be in the form of tabular arrays of 1/3-octave-band SPL's as functions of frequency (f) and directivity angle (θ) for a number of power settings. Associated nozzle performance data (e.g., primary and secondary jet velocities, nozzle total pressures, total temperatures, mass flow rates, etc.) and information on the nozzle geometry will also be given. The SPL arrays may be plotted to obtain the SPL frequency spectra for various radiation angles such as those shown in figures 13 and 14.

The method of solution for this problem assumes the availability of an engine noise prediction computer program similar to one described in reference 82, which includes subprograms for calculating all engine noise components; i.e., jet noise, fan noise, and core noise. The initial problem then reduces to a task of performing a series of computer runs with the prediction program, simulating the test conditions, and examining the computed jet noise levels to determine if the levels are compatible with the measured total engine noise.

An engine noise prediction computer program, being usually developed for general application, may not predict the jet noise of the given engine with the accuracy desired. If this is found to be the case, the jet noise subprogram must be modified to compute the jet noise component for the given engine. Prediction of other noise components may also be questionable. Problems arising from this uncertainty can be alleviated by concentrating the extraction of jet noise on the cases with high power settings, for which the jet noise is usually predominant.

Various criteria for examining the compatibility of jet noise components have been tried with varying degrees of success. In any approach, however, a good knowledge of jet noise acoustics will be found to be an important requirement. The method described in the following paragraphs is one that has given an excellent result in one of the Boeing programs. Part of this method is based on the material presented in reference 83.

This method consists of identifying the jet noise, substantiating the prediction program at high power-setting conditions, and then using the jet noise at lower power settings as calculated by the extrapolation of the prediction procedures. Three sets of plots are used in this method; a sample of each is presented in figure 92.

The first are plots of jet noise spectra at various radiation angles. Figure 92a, which is for θ of 130^0, shows that the normalized jet noise spectra are independent of engine power settings; i.e., a function only of θ. In the figure, two sets of points are shown: the test data points for high power condition (filled symbols) and the predicted points (open symbols) for two power settings as calculated by the Boeing JEN2 jet noise computer program. (Because of the expected predominance of jet noise in the test data, the prediction points shown are results of calculation of the jet noise component only.) Plots similar to figure 92a can be made for all radiation angles, and agreement between the test values and the predicted values can be checked.

The second set of plots is for checking the "power law" of the peak SPL's. For jet noise at the jet velocities of greatest interest the peak frequency 1/3-octave SPL plotted against log V_j at a given radiation angle is nearly linear, and the larger the radiation angle, the steeper the slope. Figure 92b shows an example of these plots at θ of 130^0. Not only is the linear relationship apparent, but a good agreement between test and prediction in the higher V_j range (V_j greater than 305 m/s (1000 fps)) is seen. Thus, it can be concluded that the test data plotted are jet dominant and the prediction is accurate. Similar plots at other radiation angles would be required for a complete examination.

The third is a check for the constancy of Strouhal number at the peak SPL frequency at a given radiation angle for various power settings. The constancy of Strouhal number will result in a straight line when the peak SPL frequencies are plotted against the jet primary velocity at one θ. A sample plot of this relation is present in figure 92c. The figure shows the linear relationship and an acceptable agreement between the test and predicted data. The relationship should be checked at all radiation angles.

When these checks provide sufficient evidence that the jet noise component is the dominant component in several of the high power-setting cases, final checks to be made

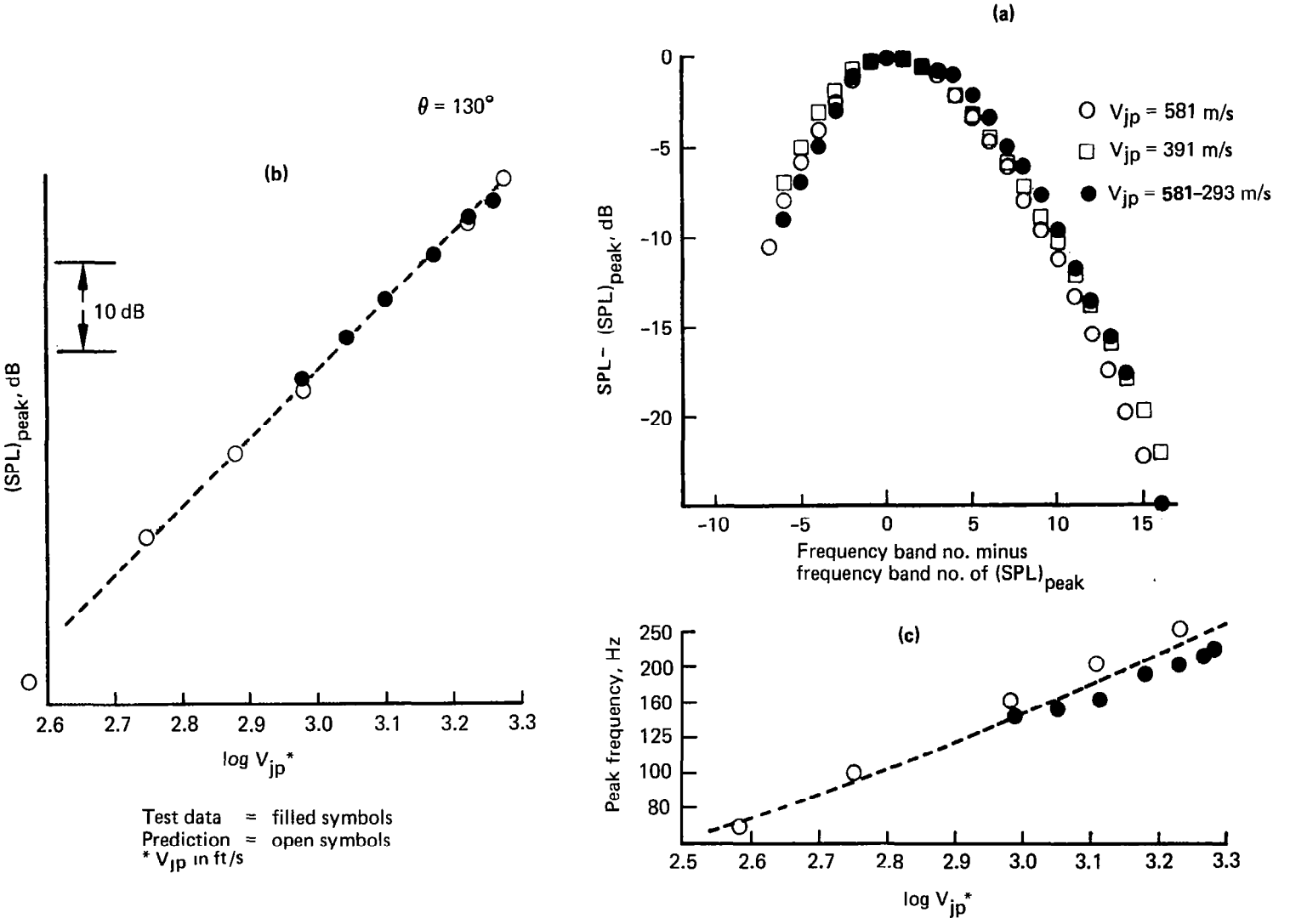

Figure 92.– Three Comparison Plots Recommended for Identifying Jet Component Noise

will be the comparisons of total noise spectra at all radiation angles and at all power settings (including the low power range). Examples of these comparisons are presented in figure 93. In the figure, the predicted total noise includes jet component and other component noise. The agreement shown in the figure suggests that the predicted jet component as well as other predicted component noise levels are reasonable, although some improvement in the jet noise could be attempted.

Another final check recommended is the comparison of OASPL, tone corrected perceived noise level, (PNLT), and tone correction as shown in figure 94. At higher power settings where the compatibility of jet noise has been checked, the agreement between test and prediction in the aft radiation angles should show a good agreement as is seen in this figure. The desired agreement between the test and prediction values in the two final checks should be used as a criterion for deciding whether the computed jet noise is the desired extraction of jet noise from the given total noise.

In a case where the flight test noise data are given, the jet noise can be extracted, following the same procedure presented in figure 92, but now using an airplane noise prediction computer program. Important final checks in this case are comparisons of total PNLT and PNL time histories between the test and predicted values.

A sample of PNLT comparison is presented in figure 95. Modification of jet noise prediction procedure (as well as other component procedures) may be required in some cases to achieve better matching between the predicted and test PNLT time histories.

Agreement of the predicted PNLT variations to the test data and matching of the underlying jet and other noise component variations to the total PNLT curves seen in figure 95 are excellent, indicating that the predicted jet noise component must represent reasonably well the jet noise included in the total measured noise.

Two final suggested checks are comparisons of maximum component PNLT's and EPNL's at various thrust, as shown in figure 96. A good agreement in the predicted and test values and absence of sharp variation in these plots can be considered as criteria for successful separation of jet noise.

3.3.6 VERIFICATION AIRCRAFT

Use of an airplane with a single jet noise source provides several important advantages in the investigation of the motion effects on jet noise. Among the advantages are elimination of the complication arising from receiving noise from discrete, separately located sources, elimination of need for evaluating more than one nozzle installation effect, exclusion of errors that may be introduced by assuming that multiple sources are identical sources, reduction in the quantity of propulsion data acquisition, and others. One of the reasons that the motion effects on jet noise of a flying aircraft have not been clearly understood may be due to the complexities introduced by these factors.

For the investigation of forward motion effects on the single-flow, round convergent (RC) nozzle, the F86-type simple airplane has been proven to be ideal. A sample of spectra plots manifesting the forward velocity effects of the RC nozzle, obtained by comparing the ground static and taxiing conditions, is presented in figure 97.

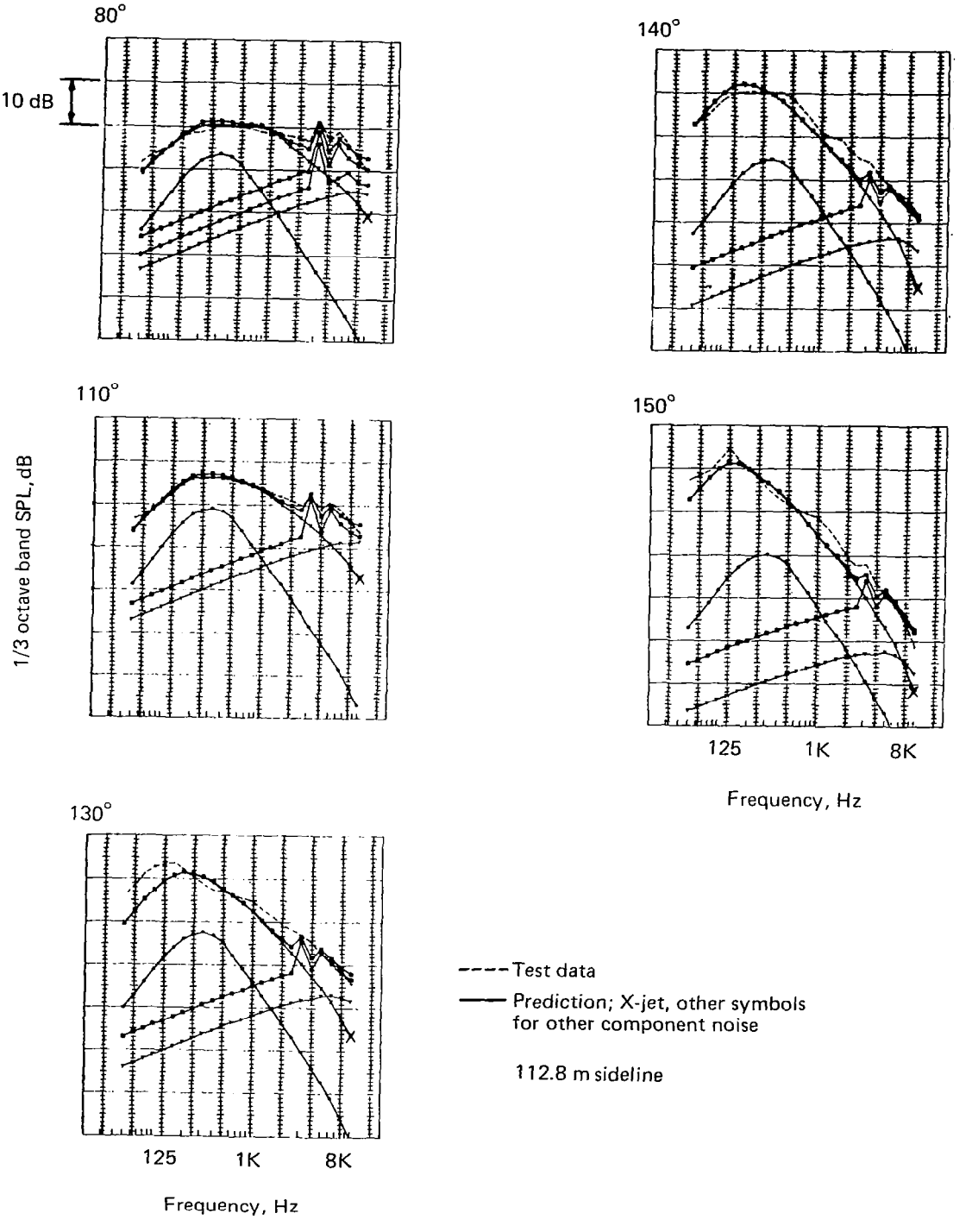

Figure 93.– Comparisons of Predicted Noise and Test Data, Total Noise and Noise Components

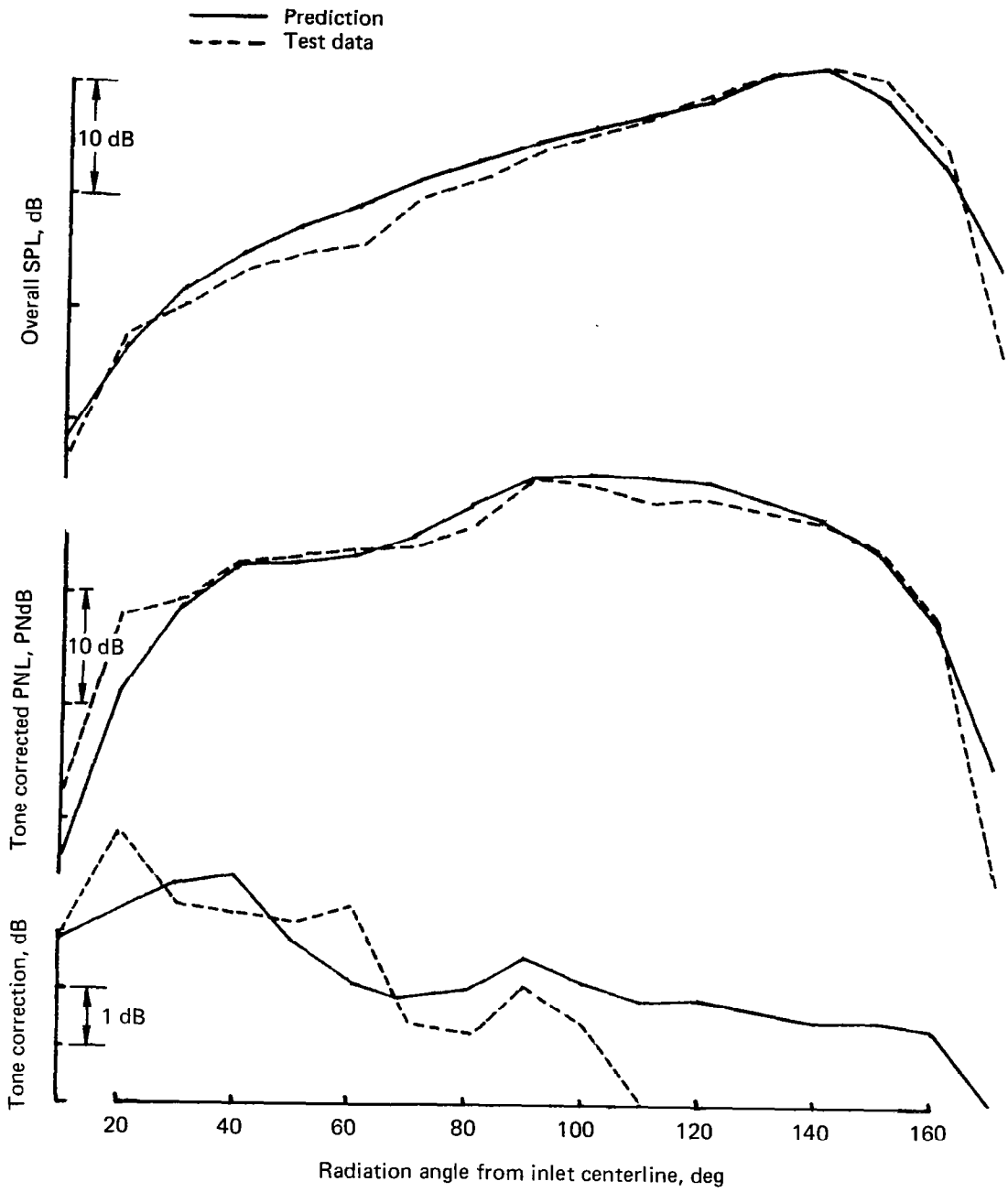

Figure 94.— Comparison Between Prediction and Test Data; Overall Sound Pressure and Tone Corrected Perceived Noise Levels and Tone Correction, Ground Static

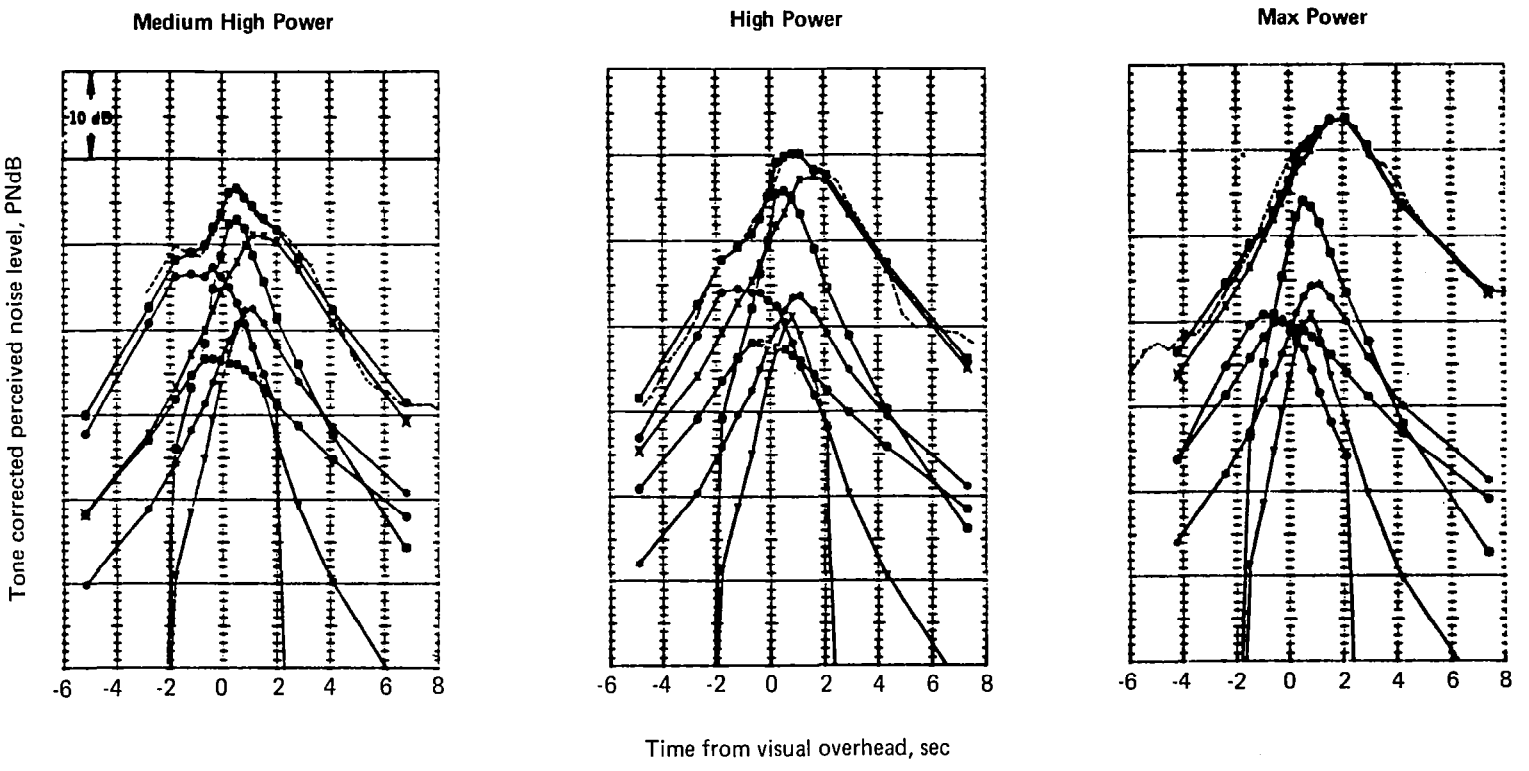

Figure 95.—Comparisons Between Predicted Tone Corrected Perceived Noise Level and Test Data (Level Flight)

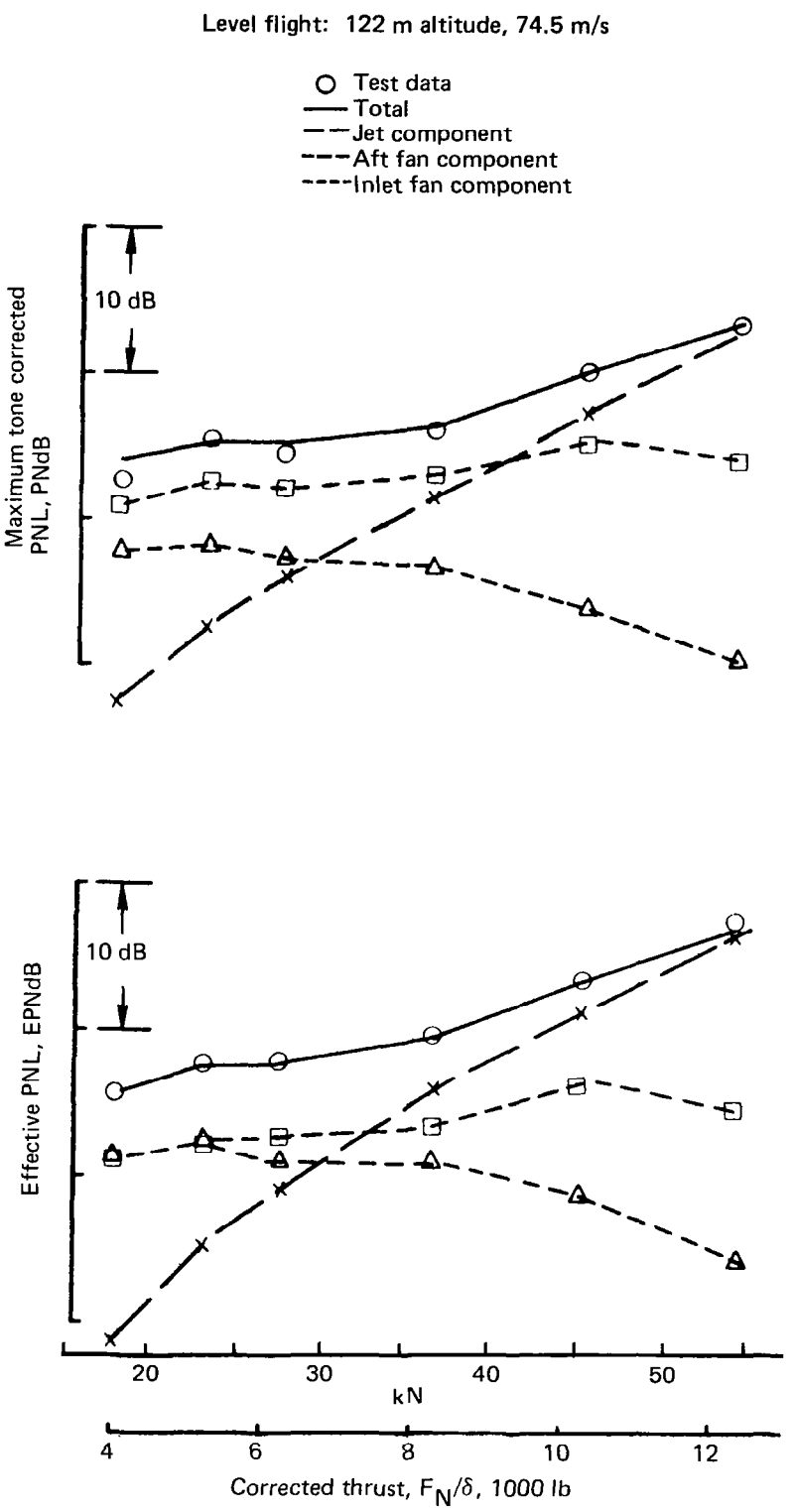

Figure 96.– Comparisons of Predicted Maximum Tone Corrected and Effective Perceived Noise Levels With Test Data

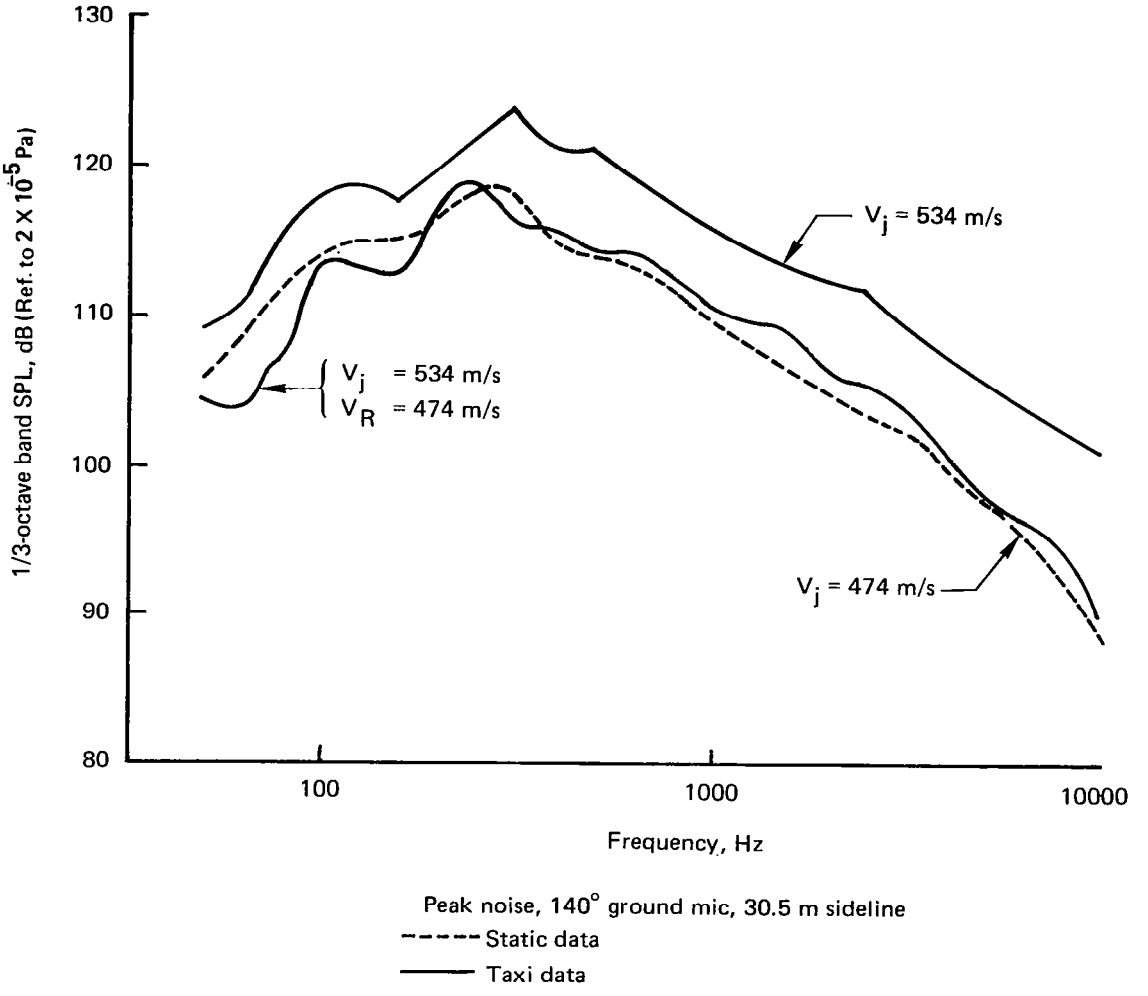

Figure 97.— F-86 Taxi Test, Static, and Flight Spectra

For the dual-flow, low-bypass nozzle, the use of a Boeing 727 airplane with the center engine at powered operation while the two side engines are at low idle will be an equally ideal forward motion effect test method. Although exploratory, Boeing has conducted a flight test, in which such flight operations were tried. During the test, two different nacelle configurations were utilized to generate noise data that were useful in isolation of a certain engine component noise from a specific engine. Duct linings or other devices to suppress the fan-generated noise may be effectively used to extend the engine operation range in which jet noise is the dominating noise component.

The same 727 airplane will also be suited to test other types of bypass nozzles; e.g., multitube or multilobe suppressor nozzles with or without ejectors. Testing of high-bypass dual-flow nozzles would be effectively conducted by the use of one engine of a 747, DC-10 or L1011 airplane.

4.0 RECOMMENDATIONS

The recommended further work, different approaches, and new techniques considered necessary in relation to the topics included in section 3.0 have been discussed in the appropriate places of this document. In this section, outlines of six recommended follow-on programs, which include most of the more important ones of those described in section 3.0, are presented. A program plan to pursue these programs in an effective order is shown in figure 98. Programs 4.1.1 through 4.1.3 are for solving problems identified in the study, and programs 4.2.1 through 4.2.3 are for verification of results. Time flow and information flow are, in general, from left to right, and the final results are shown in the right margin. A coordinated program in accordance with the suggested program plan would result in a comprehensive knowledge in the field of the effects of motion on jet noise from an aircraft.

4.1 RECOMMENDED FOLLOW-ON PROGRAMS FOR PROBLEMS IDENTIFIED

4.1.1 GROUND MICROPHONE WITH LIMITED REFLECTING SURFACE

4.1.1.1 Problem

Limitations of the ground microphone technique and recommended solutions to the problems have been discussed in some length in section 3.1.3.1. It is believed that the most serious problem of this technique is that the acoustic characteristics of the ground surface between the source and receiver can have a substantial effect on the measured noise. Ground static test data have substantiated that the theoretically predicted pressure-doubling can be obtained when the surface is composed of a completely acoustically hard reflecting material from the source to receiver. However, in practice, it is desired that a limited reflecting surface around a ground microphone be used. The test data in an anechoic room and at the Tulalip test site with a partial hard surface have suggested that the advantages of the ground microphone technique could be exploited at a lower frequency range.

4.1.1.2 Objective of Program

The objective of the program is to experimentally establish the best method of applying the ground microphone technique when nonideal ground conditions exist between the noise source and microphone at the test site. The problems should be studied for the case of ground static testing as well as flight testing.

4.1.1.3 Approach

A standard model jet of well defined acoustic properties would be utilized in geometric configurations simulating static and flyover test conditions. For the best control of surrounding atmosphere, it is recommended that the test be conducted in a large anechoic room. With each of the simulated conditions, the extensions of hard and soft

surfaces between the noise source and the microphone would be systematically varied in measuring the noise field characteristics. The soft surfaces to be used should have a range of resistance and reactance characteristics to simulate all possible ground surfaces encountered in practice.

The test data would first be analyzed to determine the relationship between the extent of hard surface around the microphone and the frequency range for the pressure-doubling. Then the relationship between the mode of acoustic reflection and impedance as well as extent variations of soft surface would be determined. Finally, the best method of applying the ground microphone technique when nonideal ground conditions exist between the noise source and the microphones, such as combined use of high and ground microphones, would be determined.

4.1.2 ANALYTICAL STUDY OF MOTION EFFECT SIMULATION TECHNIQUES

4.1.2.1 Problem

A number of experimental methods are practiced in the investigation of the effects of motion on jet noise;i.e., closed wind tunnels, free jet tunnels, and flyby testing. When different techniques are available, it is important to account for the particular phenomena associated with each technique, so that correlation of the noise data obtained by different techniques can be made. This capability of cross correlation of data is important in the identification of the real motion effects.

4.1.2.2 Objective of Program

A theoretical solution for acoustic propagation through nonuniform moving media would be applied to the conditions existing in the motion simulation arrangements. The calculated differences for each simulation should be compared with the test data obtained from a series of tests conducted with a constant or a pseudoconstant noise source.

4.1.2.3 Approach

The currently existing numerical solution of the planar Lilley acoustic equation should be extended to axisymmetric form. The jet noise field from source to receiver would then be determined by combination of the solution of jet noise generation by the use of the Boeing Flow/Noise Program with the solution of acoustic propagation. Using these theoretical solutions, the jet noise field for the various motion simulation arrangements would be calculated.

The program should include a series of tests from which data will be acquired for substantiating the analytical work described above. The tests should be conducted with a well-defined jet noise source or a noise source that would not be affected in the different facility arrangements, so that only the simulation effects are determined. Noise should be measured as principal test parameters are varied. The test data should be compared with the theoretically calculated results.

4.1.3 MEASUREMENT OF ATMOSPHERIC FLUCTUATION AND ANALYSIS OF ITS EFFECTS

4.1.3.1 Problem

There are a considerable number of cases which suggest that atmospheric conditions (the mean value profiles and fluctuations from mean) not properly accounted for are responsible for the large discrepancies in repeat test data. Problems involved are twofold: accurate measurement of the atmospheric conditions and the determination of the effects of the atmospheric conditions on the noise attenuation.

4.1.3.2 Objective of Program

The currently used weather data instrumentation should be replaced by new, accurate, and fast-responding instruments. These instruments would be positioned in such a manner that necessary atmospheric information can be obtained in sufficient quantity and superior quality for noise energy attenuation evaluation. The parameters required in the calculation of excess attenuation discussed in section 3.1.2.2 should be evaluated. Validity of the theoretical equation of the excess attenuation should be checked by the test data.

4.1.3.3 Approach

To acquire the atmospheric information for an altitude range relevant to acoustic tests for an aircraft in takeoff and landing approach patterns, a kytoon system (as mentioned in sec. 3.3.2) and/or a tower system would be required. In addition, a laser or acoustic-sounding radar system may be utilized. A collimated noise source, which will be capable of issuing trains of pure tone pulses, microphones to measure the noise intensity, and a telemetering system would constitute the principal elements for the acoustic tests. The theory of acoustic ray paths (sec. 3.1.2.1) and the excess attenuation would be applied to predict the test data. The comparison between the prediction and the test data would be used for substantiation or modification of the analytical approaches.

4.2 RECOMMENDED FOLLOW-ON PROGRAMS FOR VERIFICATION OF RESULTS

4.2.1 TAXI/FLIGHT TEST UTILIZING NEW TECHNOLOGY

4.2.1.1 Problem

A substantial number of improved approaches and techniques have been recommended in enhancing the quality of the acoustic test data from a flight test as a result of the contract work presented in section 3.0. Application of the new approaches and techniques is expected to reduce the scatter and inconsistency of the flight test data substantially. It is considered essential that these items be demonstrated in an actual flight test.

4.2.1.2 Objectives of Program

A taxi/flight test would be conducted utilizing all improved methods and techniques recommended. Specifically, use of (1) the ground microphone technique to obtain ground-reflection-free jet noise, (2) a simpler airplane for easier assessment of the engine installation effects, (3) more accurate and fast instruments and new methods to measure precise atmospheric mean profiles as well as turbulence, (4) several microphones for applying ensemble-averaging technique for higher quality noise data, (5) improved airplane position and attitude-measuring instruments, and (6) improved airborne engine parameter monitoring/recording systems. Superior repeatability of test data and, therefore, more accurate motion effects assessment would be demonstrated from this test.

4.2.1.3 Approach

The test should use a simple, single-engine airplane (e.g., Boeing-owned F86 chase airplane). A simple, single-engine airplane is ideal for conducting the verification test with a reduced cost. Not only will the single-engine airplane simplify the airplane operation and engine data acquisition, but it will eliminate the complication arising from having multinoise sources. There should be noise data measured with the current conventional data acquisition methods for the selected airplane, so that the new data can be compared with the old data.

A generous number of repeat taxiing and level flights (e.g., four or five repeats for each engine power setting) are recommended for studying the data scatter in detail.

4.2.2 COMPARISON OF PREDICTION/EXTRAPOLATION TECHNIQUE TO EXISTING DATA

4.2.2.1 Problem

Accuracy and applicability of empirical prediction/extrapolation procedures depend to a great degree on the size and extent of the data base utilized. Thus, the prediction procedures require constant improvement and modification as more data become available. New procedures must be compared to data for a wide variety of conditions to establish confidence and to discover discrepancies that will direct improvement efforts.

4.2.2.2 Objectives of Program

Existing static and flight test data should be analyzed and compared with the predicted values by the use of the prediction procedure such as that discussed in section 3.0. Based on the results of the comparisons, the prediction procedures would be improved.

4.2.2.3 Approach

A considerable number of tests have been conducted, the objective of which was to determine the effects of motion on jet noise. These include static tests. Existing data and additional analysis of these data should be reviewed and presented on a common

basis so that the results can be utilized in the substantiation or improvement of the existing jet noise prediction procedure.

The following list includes the tests from which the data are recommended for use in this program:

- Boeing F86 taxi/flyby tests
- 727/JT8D FAA quiet nacelle tests
- Effects of forward velocity on dual-flow nozzle (ref. 63)
- NASA-Lewis model nozzle test (ref. 84)
- Boeing 2.7 x 2.7 m (9 x 9 ft) wind tunnel test
- Boeing/NASA-Ames 12 x 24 m (40 x 80 ft) wind tunnel tests (full and model scale) (ref. 85)
- Boeing/P&WA free jet tunnel tests
- Rolls-Royce spin rig test (ref. 86)

4.2.3 HIGH-BYPASS TURBOFAN ENGINE TEST IN WIND TUNNEL

4.2.3.1 Problem

The current wind tunnel tests at NASA-Ames (ref. 85) with a full-scale JT8D-1 engine will provide an excellent data base for low-bypass engine wind tunnel test data for evaluation of the effects of motion on jet noise. A similar data base with a high bypass ratio (BPR) engine would be highly desirable from a number of points of view; i.e., it would provide test data to determine the motion effects as measured in a wind tunnel that is devoid of atmospheric turbulence effects, the motion effects can be compared with those for the lower bypass ratio to establish the BPR effect on the motion effects, and the test data can be used for analysis of jet noise source alteration due to ambient airflow, etc.

4.2.3.2 Objective of Program

A high BPR turbofan engine would be mounted in a flight nacelle with coplanar exit ducts. Noise data should be acquired and analyzed utilizing the techniques developed in the current low-bypass engine 12 x 24 m (40 x 80 ft) wind tunnel test contract (ref. 85). The engine would be run in a baseline and suppressed configuration, and jet noise data will be acquired for tunnel wind-off and wind-on conditions.

4.2.3.3 Approach

The engine to be used in the program should be a low-thrust, high BPR engine, such as TF34 (BPR = 6.0) or ALF 502 (BPR = 6.1) for ease of operation in the wind tunnel and

to have tunnel-to-engine size advantage. It would be advantageous if the selected engine has a good quantity of static test data obtained elsewhere for comparison and for proper planning. The engine in the wind tunnel should be operated at a range of power settings while the tunnel is operated in wind-off and wind-on conditions.

Jet noise data would be acquired by fixed and traversing microphones at an appropriate sideline distance. Analyses of wind-off and wind-on data would provide the effects of motion on the high-bypass dual-flow nozzle. The 12 x 24 m (40 x 80 ft) tunnel results should be compared with that obtained with small model nozzles in the Boeing 2.7 x 2.7 m (9 x 9 ft) induction wind tunnel. Sufficient nozzle flow conditions should be measured to obtain data for use in the analysis of dual-flow jet noise source alteration due to ambient airflow.

5.0 CONCLUSION

The study conducted under this contract has culminated in a comprehensive and critical review of all important problems involved in the evaluation of the jet noise field existing between an aircraft and an observer on the ground. It is believed that the major objective of this contract effort is satisfactorily achieved through this review; i.e., determination and recommendation of theoretical and experimental approaches and techniques required to characterize and verify the jet noise field have been adequately accomplished. Specific areas of importance determined in this regard, for which immediate further work is recommended, are:

- More accurate definition of atmospheric absorption coefficients in the lower ultrasonic frequency range for use in model nozzle tests.
- Additional theoretical and experimental study on the effects of atmospheric turbulence on jet noise propagation.
- Improved method of eliminating ground reflection effects on the measured jet noise.
- Additional analytical and experimental work on the in-flight engine installation effects on jet noise of dual-flow nozzles.
- Continued effort for improved empirical jet noise prediction procedure and flight effect computation procedures.
- Continued work on the flow/noise mathematical models, including the advanced Lilley equation solution.
- More rigorous analysis of noise propagation in the nonhomogeneous airflow surrounding the jet in various motion simulation techniques (wind tunnel, free jet tunnel, etc.).
- More accurate measurements of atmospheric conditions.
- Use of multimicrophone system and application of ensemble-averaging technique to improve the quality of the flight noise data.

Proposed plans for accomplishing these work items have been presented in the recommended follow-on programs included in this report. Carrying out of the programs would greatly enhance the understanding of the effects of motion on jet noise from aircraft.

It is concluded that the study was valuable in recapitulating the important areas of the problem and in forming a methodical approach to the solution of the problem. It is hoped that the study results may also serve as a useful guide for grasping the scope of the problem in the motion effects on jet noise.

6.0 LITERATURE SURVEYS

Results of surveys of literature relevant to the effects of motion on jet noise from an aircraft are presented in the bibliography of this report. The surveys have been conducted as part of Task 1 of this contract work.

The literature survey was made in the following categories:

- Jet Noise Fundamentals, Reviews, and Bibliographies
- Propagation
- Source Alteration (General)
- Source Alteration (Coaxial Jets)
- Verification Techniques (Measurement Methods)
- Verification Techniques (Acoustic Sounding)

Boeing Commercial Airplane Company
P.O. Box 3707
Seattle, Washington 98124
March 1976

LIST OF SYMBOLS

A	area
B_S	frequency bandwidth
c	speed of sound
c_o	speed of sound in ambient air
c_p	specific heat of air under constant pressure
C_T	structure constant for thermally induced turbulence
C_V	structure constant for wind shear
deg mag	direction in degrees referenced to magnetic North
$d\sigma/d\Omega$	differential scattering cross section
$d\Omega$	differential solid-angle element
D_j	jet diameter at nozzle exit
E	energy spectral density function describing velocity turbulence; energy contained in local fluid of jet flow
EPNL	effective perceived noise level
EPR	engine pressure ratio: nozzle total pressure over ambient pressure
f	sound wave frequency
f_c	1/3-octave-band center frequency
F( )	function
F_N/δ	corrected net engine thrust; δ is ambient pressure divided by the standard atmospheric pressure
h_a	absolute humidity
$h_{MOL\ MAX}$	absolute humidity at which molecular absorption is maximum
I	noise intensity
k	acoustic wave number

K	turbulence wave number
K_L	a threshold turbulence wave number
L	a scale of turbulence; planar flow model thickness
L_t	characteristic length of turbulent mixing
M	Mach number
M_c	turbulent eddy convection Mach number
M_A	Mach number corresponding to V_A
M_{AP}	airplane Mach number
M_o	Mach number corresponding to ambient air velocity
n	exponent for flight effect correction; number of degrees of freedom for Chi-squared-probability distribution
N_1	fan rpm
OASPL	overall sound pressure level
P	static pressure
PNL	perceived noise level
PNLT	tone corrected perceived noise level
q	local turbulence velocity
r	distance between noise source and observer
R	microphone array polar arc radius; jet radial coordinate; distance between airplane (noise source) and observer
S	noise spectrum level; noise source model; sound power spectrum
SPL	sound pressure level
S_t	Strouhal number
t	time
T	static temperature; pressure transmission coefficient
T_T	total temperature

u, v	wind velocities
V	wind velocity; local jet velocity
V_A	relative velocity between nozzle and ambient air
V_{AP}	airplane velocity
V_c	turbulence convection velocity
V_j	jet core velocity
V_o	ambient air velocity
V_R	relative velocity: primary jet velocity minus ambient air velocity
$V_{\mathring{L}}$	jet velocity at nozzle centerline
W	volume of turbulence; jet mass flow rate
x, X	jet axial coordinate
x_1, x_2, x_3	rectangular coordinates
y	rectangular coordinate; jet radial coordinate
z	rectangular coordinate
Z_o, Z_1	acoustic wave impedance
α	atmospheric absorption
α_{CLASS}	classical atmospheric absorption
α_{MOL}	molecular absorption
Γ	gamma function
ΔE	uncertainty band in atmospheric absorption
ϵ	normalized rms error
θ	noise propagation angle measured from a reference line
θ_c	difference between the actual scattering and Bragg diffraction directions
ν	kinematic viscosity
ν_e	nondimensionalized kinematic viscosity

ν_j	a reference kinematic viscosity
ρ	density
ρ_{IAS}	international standard air density
τ, T	sample times
ϕ	sound emission angle measured from jet axis
Φ	angle defined in figure 11; energy spectral density function describing thermally induced turbulence
φ	angle defined in figure 80
ω	angular frequency of sound wave
Ⓗ	angle defined in figure 11
ℓ_{cr}	turbulence correlation function

Subscript frequency used:

j	refers to jet core or to nozzle exit plane
jP and P	refer to primary jet core or to primary nozzle exit plane
jS and S	refer to secondary (fan) jet core or to secondary nozzle exit plane
o, O	refer to ambient air
M	refers to mixed jet region of dual-flow nozzle

REFERENCES

1. "Aerospace Recommended Practice ARP 866: Standard Values of Atmospheric Absorption as a Function of Temperature and Humidity for Use in Evaluating Aircraft Flyover Noise." SAE, August 31, 1964.

2. Kneser, H. O.: "The Interpretation of the Anomalous Sound-Absorption in Air and Oxygen in Terms of Molecular Collisions." *J. Acoust Soc of America,* October 1933.

3. Mintzer, D.; and Nyborg, W. L.: *Review of Sound Propagation in the Low Atmosphere.* Technical report 54-602, Wright Air Development Center (WADC), May 1955.

4. Evans, E. J.; and Bazley, E. N.: "The Absorption of Sound in Air at Audio Frequencies." *Acustica,* vol. 6, 1959.

5. Harris, Cyril M.: "Absorption of Sound in Air in the Audio Frequency Range." *J. Acoust Soc of America,* vol. 35, no. 1, January 1963.

6. Harris, Cyril M.: *Absorption of Sound in Air Versus Humidity and Temperature.* NASA CR-647, January 1967.

7. Miller, R. L.; and Oncley, P. E.: *The Experimental Determination of Atmospheric Absorption From Aircraft Acoustic Flight Tests.* NASA CR-1891, November 1971.

8. "Standard Values of Atmospheric Absorption As a Function of Temperature and Humidity." Society of Automotive Engineers Committee A-21, SAE ARP, ARP-866A, June 1975.

9. Evans, L. B.; Bass, H. E.; and Sutherland, L. C.; "Atmospheric Absorption of Sound: Theoretical Predictions." *J. Acoust Soc of America,* vol. 51, no. 5, part 2, 1972.

10. "Calculation of the Absorption of Sound by the Atmosphere." (Draft) American National Standard Institute (ANSI), March 1, 1974.

11. Sivian, L. J.: "High Frequency Absorption in Air and Other Gases." *J. Acoust Soc of America,* September 1947.

12. McKaig, M. B.; and Ossenkop, D. G.: *Long Range Noise Data–727 Noise Retrofit Feasibility Program.* Boeing document D6-41229, August 15, 1973.

13. Walker, D. Q.: *Some Effects of the Local Atmosphere Upon Acoustic Data From Full Scale Static Engine Tests.* Boeing document D6-40607TN, August 31, 1972.

14. *Aerospace Information Report (AIR) 923.* SAE, August 15, 1966.

15. Malone, T. F., ed.: *Compendium of Meteorology.* American Meteorology Society, Waverly Press, August 1951.

16. Thompson, R. J.: "Ray Theory of an Inhomogeneous Moving Medium." *J. Acoust Soc of America,* vol. 51,no. 5 (part 2) May 1972, pp. 1675-1682.

17. Sawhill, R. H.: *Proposed Standard Values of Air-Ground Excess Attenuation for Calibration of Aircraft Noise.* The Boeing Company, document no. D6-4084TN.

18. Tatarski, V. I.: *Wave Propagation in a Turbulent Medium.* Translated into English from Russian by R. A. Silverman, McGraw-Hill, 1961.

19. Kallistratova, M. A.; and Tatarski, V. I.: "Accounting for Wind Turbulence in the Calculation of Sound Scattering in the Atmosphere." Translated from *Russian Acoust Journal,* vol. 6, no. 4, pp. 503-505.

20. Pekeris, C. L.: "Note on the Scattering of Radiation in an Inhomogeneous Medium." *Physics Review,* vol. 71, no. 4, February 1947.

21. Lighthill, M. J.: "On the Energy Scattered From the Interaction of Turbulence With Sound or Shock Waves." Proceedings of Cambridge Philosophical Society, vol. 49, part 3, Cambridge University Press, July 1953.

22. Monin, A. S.: "Characteristics of the Scattering of Sound in a Turbulent Atmosphere." *Soviet Physics–Acoustics,* vol. 7, no. 4, April to June 1962, pp. 370-373.

23. Batchelor, G. K.: *Wave Scattering Due to Turbulence; Symposium on Naval Hydrodynamics.* Publication 515, National Academy of Sciences, National Research Council, 1957, pp. 409-430.

24. Baerg, W.; and Schwarz, W. H.: "Measurement of the Scattering of Sound From Turbulence." *J. Acoust Soc of America,* vol. 39, April 1965.

25. DeLoach, R.: *On the Excess Attenuation of Sound in the Atmosphere.* NASA TN-D-7823, March 1975.

26. Richardson, E. G.: "The Fine Structure of Atmospheric Turbulence in Relation to the Propagation of Sound Over the Ground." Proceedings of the Royal Society of Acoustics, vol. 23, September 1950.

27. Schilling, H. K.; Givens, M. P.; Nyborg, W. L.; Pielmeier, W. A.; and Thorp, H. A.: "Ultrasonic Propagation in Open Air." *J. Acoust Soc of America,* vol. 19, January 1947.

28. Ingard, Uno: "A Review of the Influence of Meteorological Conditions on Sound Propagation." *J. Acoust Soc of America,* vol. 25, May 1953.

29. Ingard, Uno; and Oleson, S. K.: "Measurements of Sound Attenuation in the Atmosphere." part I; Mintz, M. D.: "Pulse Distribution Analysis of Scattered Sound," part II, Final Report, AFCRL-TR60-431, Geophysics Research Directorate, Air Force Cambridge Research Center, Air Research and Development Command, November 1960.

30. Hunter, G. H.: *Sound Turbulence Interaction.* Final report, TT 7404, Department of Transport Technology, April 1974.

31. Aubry, M.; and Baudin, F.: "Measurement of the Total Attenuation of Acoustic Waves in the Turbulent Atmosphere." *J. Geophys Res,* vol. 79, December 20, 1974.

32. Hilton, D. A.; and Kasper, Peter: *Studies of Noise Propagation and Âtmospheric Attenuation Using Instrumental Towers.* An Abstract published in the program of the 88th Meeting, Acoust Soc of America, vol. 56, Supplement, Fall 1974.

33. McKaig, M. B.: "Use of Flush-Mounted Microphones to Acquire Free-Field Data." AIAA paper no. 74-92, January 30 to February 1, 1974.

34. Mariano, S.: *Ground Effect of a Plane Uniform Sound Source Distribution.* Boeing document D6-22600TN, January 20, 1969.

35. Toth, W. J.: *Proposed AIR, Acoustic Effects Produced by a Reflecting Plane–AIR 1327.* SAE reference no. 74-167, March 19, 1974.

36. Conticelli, V. M.; DiBlasi, A.; and O'Keefe, J. O.: "Noise Shielding Effects for Engine-Over-Wing Installations." AIAA paper 75-474, March 1975.

37. Morse, P. M.; and Ingard, K. Uno: *Theoretical Acoustics.* McGraw-Hill, chapter 11, 1968.

38. Ffowcs-Williams, J. E.: *The Noise From Turbulence Convected at High Speed.* Philosophical Transactions of the Royal Society of London, vol. 255, no. 1061, April 1963.

39. Dunn, D. G.; and Peart, N. A.: *Aircraft Noise Source and Contour Estimation.* NASA CR-114649, July 1973.

40. Bushell, K.: "Jet Exhaust Noise Prediction (Second Draft)." Presented to the SAE A-21 committee, October 30, 1973.

41. Jaeck, C. L.: *Empirical Jet Noise Prediction Procedures, Vol. I: Single-Flow Clean Jet* Boeing document D6-42367TN, January 1975.

42. Jaeck, C. L.: *Empirical Jet Noise Prediction Procedures, Vol. II: Dual-Flow Jet.* Boeing document D6-42367TN-2, January 1975.

43. Mangiarotty, R. A.; and Turner, B. A.: "Wave Radiation Doppler Effect Correction for Motion of a Source, Observer, and the Surrounding Medium." *J. Sound and Vibration,* vol. 6 (I), 1967, pp. 110-116.

44. Toth, W. J.: "Proposed AIR, Acoustic Effects Produced by a Reflecting Plane–AIR 1327." SAE Committee A-21, Aircraft Noise Measurements, March 19, 1974.

45. *Vortex Wake Turbulence, Flight Tests Conducted During 1970.* FAA-FS-71-1, February 1971.

46. McGowan, W. A.: *Avoidance of Aircraft Trailing Vortex Hazards.* NASA, Washington, D.C., October 1970.

47. McGowan, W. A.: "Trailing Vortex Hazard." SAE paper no. 680220, April 1968.

48. Spreiter, J. R.; and Sacks, A. H.: "The Rolling Up of the Trailing Vortex Sheet and Its Effect on the Downwash Behind Winds." *J. Aeronaut Sciences,* January 1951.

49. Bisgood, P. L.; Moltby, R. L.; and Dee, F. W.: "Some Work on the Behavior of Vortex Wakes at the Royal Aircraft Establishment." Royal Aircraft Establishment Tech Memo Aero 1244, August 1970.

50. McCormick, B. W.: "Structure of Trailing Vortices." *J. Aircraft,* May to June 1968.

51. Berman, C. H.; Jaeck, C. L.; and Lu, H. Y.: *Analytical Prediction of the Jet Noise Generation.* Boeing document D6-40614TN, June 1974.

52. Lu, H. Y.: *Calculation of Axisymmetric Compressible Turbulent Jet Flows.* Boeing document D6-40611, November 1972.

53. Heck, P. H.; and Ferguson, D. R.: "Analytical Solution for Turbulent Mixing in Compressible Flows." AIAA paper no. 71.4, 1971.

54. Lighthill, M. J.: "On Sound Generated Aerodynamically; I. General Theory." Proceedings of the Royal Society, 211A, 1952, pp. 564-587.

55. Jones, I. S. F.: "Fluctuating Turbulent Stresses in the Noise-Producing Region of a Jet." *J. Fluid Mech,* vol. 36, 1969, pp. 529-543.

56. Jones, I. S. F.: "Influence of Retarded Time on Jet Noise." *Physics of Fluids,* vol. 13, 1970, pp. 2629-2633.

57. Laurence, J. C.: *Intensity, Scale, and Spectra of Turbulence in Mixing Region of Free Subsonic Jet.* NASA report 1292, 1956.

58. Grosche, F. R.; Jones, J. H.; and Wilhold, G. A.: "Measurements of the Distribution of Sound Source Intensities in Turbulent Jets." AIAA paper no. 73-989, October 1973.

59. MacGregor, G. R.; and Simcox, C. D.: "The Location of Acoustic Sources in Jet Flows by Means of the Wall Isolation Technique." AIAA paper no. 73-1041, October 1973.

60. Berman, C. H.: "Noise From Nonuniform Turbulent Flows." AIAA paper no. 74-2, January 1974.

61. Lilley, G. M.: *The Generation and Radiation of Supersonic Jet Noise.* Lockheed-Georgia Company, AFAPL-TR-72-53, vol. 4, July 1972.

62. Berman, C. H.: *An Analytical Study of Flight Effects on Jet Noise and the Simulation of These Effects.* Boeing document D6-42504, April 1975.

63. Reed, D. H.: "Effect of Forward Velocity on the Noise Characteristics of Dual-Flow Jet Nozzles." ASME 74-WA/AERO-4, September 1974.

64. Ribner, H. S.: "Quadrupole Correlation Governing the Pattern of Jet Noise." *J. Fluid Mech*, vol. 38, August 14, 1969, pp. 1-24.

65. Tester, B. J.; and Morfey, C. L.: "Developments in Jet Noise Modeling–Theoretical Predictions and Comparisons With Measured Data." AIAA paper no. 75-477, AIAA Second Aero-Acoustics Conference, March 1975.

66. Lu, H. Y.: "Acoustic Far Field of a Point Source in Cylindrical and Parallel Flowing Fluid Layers." AIAA paper no. 75-500, AIAA Second Aero-Acoustics Conference, March 1975.

67. Lin, C. C.: *The Theory of Hydrodynamic Stability.* Cambridge University Press, Cambridge, Massachusetts, 1967.

68. *Boeing Flight Test Data System.* The Boeing Company, 1973.

69. Cooke, C. R.: "Automatic Laser Tracking and Ranging System." Paper presented at IEEE/OSA Conference on Laser Engineering Applications, GTE Sylvania Company, June 1971.

70. "Tracking Systems for Flight Development of Today's Commercial Aircraft." Douglas paper 6148 presented at Society of Flight Test Engineers, August 1973.

71. *Federal Aviation Regulations; Vol. III, Part 36, Noise Standards: Aircraft Type Certification.* Department of Transportation, FAA, December 1, 1969.

72. Aubry, M.; Baudin, F.; Weill, A.; and Rainteau, P.: "Measurement of the Total Attenuation of Acoustic Waves in Turbulent Atmosphere." *J. Geophys Res,* vol 79, December 20, 1974.

73. "Weather Measure Instruments, Scientific Products." *Catalog 772,* Weather Measure Corporation.

74. "Instruments and Systems for the Atmosphere and Environment." *Catalog 8,* Science Associates, Inc.

75. *Temperature and Relative Humidity Sensors, Wind Sensors.* Meteorology Research, Inc.

76. Hall, F. F., Jr.: *Temperature and Wind Structure Studies byAcoustic Echo-Sounding.* Edited by V. E. Derr, U. S. Government Printing Office, Washington, D.C., 1972, pp. 18-1 to 18-26.

77. Derr, V. E.; and Little, C. G.: "A Comparison of Remote Sensing of the Clear Atmosphere by Optical, Radio, and Acoustic Radar Techniques." *Applied Optics,* vol. 9, no. 9, September 1970.

78. Russell, P. B.; Uthe, E. E.; Ludwig, F. L.; Shaw, N. A.: "A Comparison of Atmospheric Structure as Observed With Monostatic Acoustic Sounder and Lidar Techniques." *J. Geophys Res,* December 1974.

79. McAllister, L. G.: "Acoustic Sounding of the Lower Troposphere." *J. Atmosphere and Terrestrial Physics,* vol. 30, 1968, pp. 1439-1440.

80. Brown, E. H.: "Some Recent NOAA Theoretical Work on Echo Sounding in the Atmosphere." *J. Geophys Res,* vol. 79, no. 30, December 1974.

81. Bendat, J. S.; and Piersol, A. G.: "Random Data: Analysis and Measurement Procedures." *Wiley-Interscience,* 1971.

82. Crowley, K.C.; Jaeger, M. A.; Meldrum, D. F.: *Aircraft Noise Source and Contour Programs, User's Guide.* NASA CR-114650, July 1973.

83. Mathews, D. C.; and Peraecchio, A. A.: "Progress in Core Engine and Turbine Noise." AIAA Paper no. 74-948, August 1974.

84. VonGlahn, U.; and Goodykoontz, J.: "Velocity Decay and Acoustic Characteristics of Various Nozzle Geometries in Forward Flight." AIAA paper no. 73-629.

85. Strout, F. G.: *Flight Effects on Noise Generated by the JT8D-17 Engine in a Quiet Nacelle and a Conventional Nacelle as Measured in the NASA-Ames 40 x 80 Foot Wind Tunnel.* NASA CR-2576.

86. Smith, W.: The Use of a Rotating Arm Facility to Study Flight Effects on Jet Noise." 2nd International Symposium on Air Breathing Engines, Sheffield, England, March 1974.

BIBLIOGRAPHY

JET NOISE FUNDAMENTALS, REVIEWS AND BIBLIOGRAPHIES

Ahuja, K. K.: "Correlation and Prediction of Jet Noise." *J. Sound and Vibration,* vols. 29, 2, July 1973, pp. 155-168.

Ahuja, K. K.; and Bushell, K.W.: "An Experimental Study of Subsonic Jet Noise and Comparison With Theory." *J. Sound and Vibration,* vols. 30, 3, October 1973, pp. 317-341.

Atvars, J.; Schubert, L. K.; Grande, E.; and Ribner, H. S.: "Refraction of Sound by Jet Flow or Jet Temperature." AIAA paper 65-82 or NASA CR-494, May 1966.

Barra, V.; Slutsky, S.; and Panunzio, S.: "Ambient and Induced Pressure Fluctuations in Supersonic Jet Flows." AIAA paper 75-482, March 1975.

Benzakein, M. J.; Chen, C. Y.; Knott, P. R.: "A Computational Technique for Jet Aerodynamic Noise." AIAA paper 71-583, June 1971.

Brinkmann, K.; Rademacher, H. J.; and Schroeder, H. J.: "Measurement of Acoustic Quantities and Properties of Matter." Arch. Tech. Messen, Germany, no. 397, February 1969, pp. 47 and 48.

Bschorr, Oskar: "Turbulent Noise Studies (Untersuchunger Ueber den Turbulenzlaerm)." Ph.D. thesis, Technische Hochschule, Munchen, West Germany, 1968.

Burrin, Robert H.; Lush, Peter A.; and Wynne, George A.: *The Generation and Radiation of Supersonic Jet Noise. Volume 5, Appendix 1: Turbulence Mixing Region Noise Data–Final Technical Report, May 1, 1971 through May 31, 1972.* AFAPL-TR-72-53-Vol-5-APP-1, July 1972.

Chen, C. Y.: "Calculations of Far-Field and Near-Field Jet Noise." AIAA paper 75-93, January 1975.

Chen, C. Y.: "Investigation of Far-Field and Near-Field Jet Noise." Ph.D. thesis, Cincinnati University, Ohio, 1973.

Cowan, S. J.; and Crouch, R. W.: "Transmission of Sound Through a Two-Dimensional Shielding Jet." AIAA paper 73-1002, October 1973.

Csanady, G. T.: "The Effect of Mean Velocity Variations on Jet Noise." *J. Fluid Mech,* vols. 26, 1, September 1966, pp. 183-197.

Damkevala, R. J.; and Norman, R. S.: *Determination of the Distribution of Sound Source Intensities in Subsonic and Supersonic Jets–Final Technical Report, June 1971 to February 1973.* NASA CR-124563, February 1973.

Davies, P.O.A.L.; Hardin, J. C.; Mason, J. P.: "A Potential Flow Model for Calculation of Jet Noise." AIAA paper 75-441, March 1975.

Delany, M. E.: "Index of Current Noise Research in the United Kingdom." National Physical Lab, Teddington, England, NPL-Aero-Ac-48, December 1970.

de Ruig, C. J.: *Bibliography on Aircraft Noise, Supplement II, September 1958 to September 1966.* Technisch Documentatie en Informatie Centrum Voor de Krijgsmacht, The Hague, Netherlands, TDCIK-5350-SII, May 1967.

Doak, Philip E.: *The Generation and Radiation of Supersonic Jet Noise; Volume 3: Progress Toward a Unified Theory of Jet Engine Noise–Final Technical Report, May 1, 1971 through May 31, 1972.* AFAPL-TR-72-53-Vol-3, July 1972.

Doak, P. E.: "Analysis of Internally Generated Sound in Continuous Materials II–A Critical Review of the Conceptual Adequacy and Physical Scope of Existing Theories of Aerodynamic Noise, With Special Reference to Supersonic Jet Noise." *J. Sound and Vibration,* vol. 25, November 22, 1972, pp. 263-335.

Doak, P. E.: "Fundamentals of Aerodynamic Sound Theory and Flow Duct Acoustics." *J. Sound and Vibration,* vol. 28, June 8, 1973, pp. 527-561.

Doak, P. E.: "On the Interdependence Between Acoustic and Turbulent Fluctuating Motions in a Moving Fluid." *J. Sound and Vibration,* vol. 2, November 19, 1971, pp. 211-225.

Duggins, K.: "The Mixing of a Jet With a Parallel Stream." Proceedings of the Joint Meeting, Society of Mechanical Engineers, Atlanta, Georgia, June 20-22, 1973 (A73-35501 17-12) New York, 1973, pp. 181-188.

Ffowcs-Williams, J. E.: "Generation of Jet Noise; The Noise of Highly Turbulent Jets at Low Exhaust Speeds." Aviation Acoustics Seminar, 3, 1967, pp. 32-37.

Ffowcs-Williams, J. E.: "Sound Production at the Edge of a Steady Flow." *J. Fluid Mech,* vol. 66, December 11, 1974, pp. 791-816.

Ffowcs-Williams, J. E.: *Technical Evaluation Report on Fluid Dynamics Panel Specialists Meeting on Noise Mechanisms.* AGARD-AR-66, AGARD-CP-131, September 1973.

Fisher, Michael J.; Mayo, William T.; Meadows, Donald M.; Burrin, Robert H.; and Beisel, George E.: *The Generation and Radiation of Supersonic Jet Noise. Volume 6: Jet Flow Meausrement and Analysis With Special Emphasis on Remote Sensing Devices: Crossed Beam Schlieren, Laser Doppler, Velocimeter, Pulsed Laser Interferometer–Final Technical Report, May 1, 1971 to May 31, 1972.* AFAPL-TR-72-53-Vol-6, July 1972.

Fisher, M. J.; Lush, P. A.; and Bourne, M. H.: "Jet Noise." *J. Sound and Vibration*, vol. 3, June 28, 1973, pp. 563-585.

Fuchs, V.; and Michalke, A.: "Introduction to Aerodynamic Noise Theory." *Progress in Aerospace Sciences*, vol. 14, Pergamon Press, 1973, pp. 227-297.

Goldburg, Arnold: "Aerodynamic Noise." AIAA selected reprint series, vol. II, 1970.

Goldstein, Marvin E.: *Aeroacoustics*. NASA-SP-346, 1974.

Goldstein, Marvin E.; and Howes, Walton L.: *New Aspects of Subsonic Aerodynamic Noise Theory*. NASA TN-D-7158, February 1973.

Goldstein, M. E.; and Rosenbaum, B. M.: *Emission of Sound From Axisymmetric Turbulence Convected by a Mean Flow With Application of Jet Noise*. NASA TN-D-6939, September 1972.

Graham, E. W.; and Graham, B. B.: *Theoretical Study of the Effects of Refraction on the Noise Produced by Turbulence in Jets*. NASA CR-2390, 1974.

Graham, R. C.: "Aircraft Noise: An Annotated Bibliography." *British Research and Development Reports*, December 15, 1968.

Gray, V. H.; Gutierrez, O. A.; and Walker, D. Q.: "Assessment of Jets as Acoustic Shields by Comparison of Single- and Multitube Suppressor Nozzle Data." AIAA paper 73-1001, October 1973.

Groesbeck, D.; Huff, R.; and vonGlahn, U.: *Peak Axial-Velocity Decay With Mixer-Type Exhaust Nozzles*. NASA TM-X-67934, Sepember 1971.

Grosche, F. R.: "Distributions of Sound Source Intensities in Subsonic and Supersonic Jets." *AGARD Noise Mechanics*, March 1974.

Hammersley, R. J.; and Jones, B. G.: "Turbulent Pressure Field in a Co-Annular Jet." AIAA paper 75-95, 1975.

Hardin, Jay C.: *Effects of Temperature-Profile Variation on Refraction of Sound by Jet Flow*. NASA TN-D-5779, April 1970.

Hardin, Jay C.: *Analysis of Noise Produced by an Orderly Structure of Turbulent Jets*. NASA TN-D-7242, April 1973.

Hardin, J. C.: "Noise Produced by the Large-Scale Transition Region Structure of Turbulent Jets." AIAA paper no. 74-550, June 1974.

Hay, J. A.; and Rose, E. G.: "In-Flight Shock Cell Noise." *J. Sound and Vibration*, vol. 11, April 1970, pp. 411-420.

Hoch, R. G.; Duponchel, J. P.; Cocking, B. J.; and Bryce, W. D.: "Studies of the Influence of Density of Jet Noise." *J. Sound and Vibration,* vol. 4, June 28, 1973, pp. 649-668.

Hoch, R. G.; Duponchel, J. P.; Cocking, B. J.; and Bryce, W. D.: "Studies of the Influence of Density on Jet Noise." Presented at the First International Symposium on Air-Breathing Engines, Marseille, France, June 19-23, 1972.

Horonjeff, Robert; and Soroka, Walter W.: *Transportation System Noise Generation, Propagation and Alleviation. Phase 1: part 2. Bibliography.* DOT-OST-ONA-71-2-Pt-2, September 1970.

Hurdle, P. M.: "Pressure Cross-Correlations in the Investigation of Aerodynamic Noise From Jets." Ph.D. thesis, 1973, U.C.L.A., California. (Available from university microfilms, No. 73-28714.)

Ingram, J. D.: *A Survey of Aerodynamic Noise.* FDL-TDR-64-132, December 1964.

Jones, I. S. F.: "The Effect of Vortex Generators on the Noise-Producing Region of a Jet." *J. Sound and Vibration,* vol. 11, January 1, 1970, pp. 65-81.

Kobrynski, M.: "Experimental Verification and Application of a Method of Calculation for the Sound Spectrum of Jets on the Ground and in the Air." Paper for Colloque d'Acoustique Aeronautique, 2nd, Paris, France, May 4 and 5, 1971.

Krause, Fritz; Lennox, R.; Wilson, N.: *Optical Crossed-Beam Investigation of Local Sound Generation in Jets.* N69-11542 02-02, 1968.

Krishnappa, G.: *Estimation of the Intensity of Noise Radiated From a Subsonic Circular Jet.* A70-16776 05-02, May 1968.

Krishnappa, G.; and Csanady, G. T.: "An Experimental Investigation of the Composition of Jet Noise." *J. Fluid Mech,* vol. 37, June 1, 1969, pp. 149-159 plus figure.

Laufer, J.; Kaplan, R. E.; and Chu, W. T.: "On the Generation of Jet Noise." *AGARD Noise Mechanics,* March 1974.

Lee, H. K.; and Ribner, H. S.: "Direct Correlation of Noise and Flow of a Jet." *J. Acoust Soc of America,* vol. 52, November 5, 1972, pp. 1280-1290, and AIAA paper 640, 1972, p. 8.

Lilley, G. M.: "On the Noise From Jets." *AGARD Noise Mechanics,* March 1974.

Lilley, G. M.; Morris, P.; and Tester, B. J.: "On the Theory of Jet Noise and Its Applications." AIAA paper 73-937, October 1973.

Liu, C. H.; and Maestrello, L.: "Propagation of Sound Through a Real Jet Flow-Field." AIAA paper 74-5, 1974.

Liu, C. H.; and Maestrello, L.: "Simulation by Vortex Rings of the Unsteady Pressure Field Near a Jet." AIAA paper 75-438, March 1975.

Liu, J. T. C.: "Developing Large-Scale Wavelike Eddies and the Near Jet Noise Field." *J. Fluid Mech,* vol. 62, February 11, 1974, pp. 437-464.

Louis, J. F.; et al.: "A Systematic Study of Supersonic Jet Noise." AIAA paper 641, June 1972, p. 12.

Lowson, M. V.: *The Sound Field for Singularities in Motion.* NASA CR-62226, December 1964.

Lush, P. A.; and Fisher, M. J.: "Noise From Hot Jets." *AGARD Noise Mechanics,* March 1974.

Lush, Peter A.; and Burrin, Robert H.: *The Generation and Radiation of Supersonic Jet Noise. Volume 5, Appendix 2: Shock Associated Noise Data–Final Technical Report, May 1, 1971 to May 31, 1972.* AFAPL-TR-72-53-Vol-5-App-2, July 1972.

Lush, Peter A.; and Burrin, Robert H.: *The Generation and Radiation of Supersonic Jet Noise. Volume 5: An Experimental Investigation of Jet Noise Variation With Velocity and Temperature–Final Technical Report, May 1, 1971 to May 31, 1972.* AFAPL-TR-72-53-Vol-5, July 1972.

Lush, P. A.: "Measurements of Subsonic Jet Noise and Comparison With Theory." *J. Fluid Mech*, vol. 46, 3, April 1971, pp. 477-500.

Maestrello, L.: "On the Relationship Between Acoustic Energy Density Flux Near the Jet and Far Field Acoustic Intensity." AIAA paper 73-988, October 1973 and NASA TN D-7269.

Mani, R.: "A Moving Source Problem Relevant to Jet Noise." *J. Sound and Vibration,* vol. 25, 2, November 1972, pp. 337-347.

Mani, R.: "Further Studies on Moving Source Solutions Relevant to Jet Noise." *J. Sound and Vibration,* vol. 35, July 8, 1974, pp. 101-117.

Mani, R.: "Refraction of Acoustic Duct Waveguide Modes by Exhaust Jets." Quarterly of *Applied Mathematics,* vol. 30, January 1973, pp. 501-520.

Mani, R.: "The Issue of Convective Amplification in Jet Noise." *AGARD Noise Mechanics,* March 1974.

Massier, P. F.; Parthasarathy, S. P.; and Cuffel, R. F.: *Experimental Evaluation of Fluctuating Density and Radiated Noise From a High Temperature Jet.* NASA CR-133789, September 1973.

Meecham, W. C.; and Hurdle, P. M.: "Use of Cross-Correlation Measurements to Investigate Noise Generating Regions of a Real Jet Engine and Model Jet." *AGARD Noise Mechanics,* March 1974.

Montealegre, A. P.; and Weinstein, H.: "The Mixing of Homogeneous Co-Axial Streams." *Israel Journal of Technology,* vol. 9, no. 1-2, 1971, pp. 141-150.

Moon, L. F.; and Zelazny, S. W.: "Jet Noise Modeling–Experimental Study and Models for the Noise and Turbulence Fields." AIAA paper 74-3, 1974.

Morfey, C. L.: "Amplification of Aerodynamic Noise by Convected Flow Inhomogeneities." *J. Sound and Vibration,* vol. 31, December 22, 1973, pp. 391-397.

Mungur, P.: "Analysis of Acoustic Radiation in a Jet Flow Environment." *J. Sound and Vibration,* vol. 36, September 8, 1974, pp. 21-52.

Nagamatsu, H. T.; Sheer, R. E., Jr.; Gill, M. S.: *Flow and Acoustic Characteristics of Subsonic and Supersonic Jets From Convergent Nozzle.* NASA CR-1693, December 1970.

Nosseir, N. S. M.: *Correlation of Jet Noise Data in Terms of a Self Noise-Shear Noise Model.* University of Toronto report UTIAS-TN-193, January 1975.

Pao, S. P.: *Analytical Properties of Noise Generating Mechanisms in a Supersonic Jet Exhaust Flow.* NASA CR-1848, May 1971.

Pao, S. P.: "Development of a Generalized Theory of Jet Noise." *AIAA Journal,* May 1972, pp. 596-602.

Pao, S. P.: "A Generalized Theory on the Noise Generation From Supersonic Shear Layers." *J. Sound and Vibration,* vol. 4, December 19, 1971, pp. 401-410.

Pao, S. P.; and Maestrello, L.: "New Evidence of Subsonic Jet Noise Mechanisms." AIAA paper 75-437, March 1975.

Parthasarathy, S. P.: "Evaluation of the Noise Autocorrelation Function of Stationary and Moving Noise Sources by a Cross-Correlation Method." AIAA paper 73-186, 1973.

Petersen, R. A.; Kaplan, R. E.; and Laufer, J.: *Ordered Structures and Jet Noise,* NASA CR-134733, October 1974.

Pinkel, B.: "Jet Noise Analysis Utilizing the Rate of Decay of Kinetic Power." AIAA paper 75-94, January 1975.

Plumblee, Harry E.; and Doak, Philip E.: *The Generation and Radiation of Supersonic Jet Noise. Volume 1: Summary of Supersonic Jet Noise Studies–Final Technical Report, May 1, 1971 to May 31, 1972.* AFAPL-TR-72-53-Vol-1, July 1972.

Plumblee, Harry E.; and Burrin, Robert H.: *The Generation and Radiation of Supersonic Jet Noise. Volume 2: Future Studies for Definition of Sueprsonic Jet Noise Generation and Reduction Mechanisms–Final Technical Report, May 1, 1971 to May 31, 1972.* AFAPL-TR-72-53-Vol 2, July 1972.

Potter, R. C.: *An Investigation to Locate the Acoustic Sources in a High Speed Jet Exhaust Stream.* NASA CR-101105, February 1968.

Ribner, H. S.: "Jets and Noise." *Canadian Aeronautics and Space Journal,* vol. 14, 8, October 1968, pp. 282-298.

Robinson, D. W.: *Index of NPL Acoustics Publications, 1960-1970.* National Physical Lab., Teddington, England, NPL-Aero-Ac-47, March 1971.

Rott, N.; and Thomann, H.: "Finite-Amplitude and Diffusive Effects in Acoustics–A Report on Euromech 23." *J. Fluid Mech,* vol. 49, September 29, 1971, pp. 391-397.

Schetz, J. A.; and Favin, S.: "Analysis of Free Turbulent Mixing Flows Without a Net Momentum Defect." *AIAA Journal,* vol. 10, November 1971, pp. 1524-1526.

Schubert, L. K.: "Numerical Study of Sound Refraction by a Jet Flow. Ray (Wave) Acoustics." *J. Acoust Soc of America,* vol. 51, February 1972.

Schubert, L.: *Refraction of Sound by a Jet: A Numerical Study.* U.S. Government Research and Development Reports, April 1970, (8) 205.

Taillet, J.: *Description and Implementation of a Method for Characterizing Noise Sources in Jets.* NASA TT-F-14851, April 1973.

Tam, C. K. W.: "Supersonic Jet Noise Generated by Large Scale Disturbances." *J. Sound and Vibration,* vol. 38, January 8, 1975, pp. 51-79.

Tester, B. J.; and Burrin, R. H.: "On Sound Radiation From Sources in Parallel Sheared Jet Flows." AIAA paper 74-57, 1974.

Tirumalesa, D.: "Theoretical Analysis of the Noise Characteristics of an Ejector Jet." *J. Sound and Vibration,* vol. 30, October 22, 1973, pp. 465-481.

Viviand, Henri: "The Fundamental Equation of Aerodynamic Noise Theory for the Case of Surfaces in Uniform Translation Motion." *J. Mecanique,* vol. 9, June 1970, pp. 335-350.

VonGlahn, Uwe H.; Gray, Vernon H.; Krejsa, Eugene A.; Lee, Robert E., Jr.; and Minner, Gene L.: "Jet Noise." *Aircraft Engine Noise Reduction,* 1972, pp. 103-137.

Wang, R. L.; and de Plessis, M. P.: "An Explicit Numerical Method for the Solution of Jet Flows." Paper 72-WA/FE-20, American Society of Mechanical Engineers, Winter Annual Meeting, New York, New York, November 26-30, 1972.

Wilson, L. N.; Krause, F. R.; and Kadrmas, K. A.: "Infrared Measurements of Sound Source Intensities in Jets." *Research on Electromagnetic Correlation Technology,* March 17, 1970.

Wilson, L. N.: *Application of Crossed Beam Technology to Direct Measurements of Sound Sources in Turbulent Jets, Part 1–Final Report.* NASA CR-129018, February 1970.

Witze, P. O.: "A Generalized Theory for the Turbulent Mixing of Axially Symmetric Compressible Free Jets." *Fluid Mechanics of Mixing,* proceedings of the Joint Meeting, Atlanta, Georgia, June 20-22, 1973, American Society of Mechanical Engineers, 1973, pp. 63-77.

Yates, J. E.; and Sandri, G.: "Bernoulli Enthalpy–A Fundamental Concept in the Theory of Sound." AIAA paper no. 75-439, March 1975.

Zimmerman, G.: "The Consideration of Convection Effects in Aerodynamic Sound Generation Theory." Max-Planck-Institut Fuer Stroemungsforschung, Ber-4/1974, February 1974.

Aircraft Engine Noise and Sonic Boom. AGARD-CP-42, May 1969.

Aircraft Engine Noise Reduction. NASA SP-311, May 1972.

Fluid Dynamic Aspects of Jet Noise Generation. Final Technical Report, September 1, 1972 to September 30, 1973. New York University, New York, NASA CR-138623.

Fluid Dynamic Aspects of Jet Noise Generation. Final Report, October 1, 1973 to September 30, 1974. New York University, New York, NASA CR-140673.

Investigation of the Jet Noise Prediction Theory and Application Utilizing the Pao Formulation. Final Technical Report. Alabama University, Huntsville, Alabama, November 1973. (Available through NTIS (N74-22638).)

Noise Bibliography. Great Britain Ministry of Aviation, Nottingham Technical Information and Library Services, TIL/BIB/73-vol. 3, June 1964.

Bibliography on Noise Control. Noise and Vibration Control Engineering Proceedings of the Purdue Noise Control Conference, Lafayette, Indiana, July 14-16, 1971.

PROPAGATION

Abrahamson, A. L.: "Propagation of Aircraft Noise Over Long Distances Through the Lower Atmosphere." AIAA paper no. 75-542, March 1975.

Austin, Michael E.: "Ray Tracing in a Sectioned and Layered Atmosphere Using a Shifting Coordinate System." *IEEE Transactions on Geoscience Electronics,* vol. GE-7, July 1969.

Bart, G. C. J.: "Spatial Crosscorrelation in Anisotropic Sound Fields." *Acustica,* vol. 28, January 1973.

Bass, H. E.; Evans, B.; and Bauer, H. J.: "Atmospheric Absorption of Sound–Analytical Expressions." *J. Acoust Soc of America,* vol. 52, September 1972.

Beckemeyer, R. J.: "On the Effect of Thin Shear Layers With Flow and Density Gradients on Small Disturbances in Inviscid, Compressible Flows." *J. Sound and Vibration,* vol. 31, November 22, 1973, pp.251-256.

Beran, D. W.; and Gething, J. T.: "Use of a Sailplane in Measuring Acoustic Attenuation in the Atmosphere." *Aero-Revue,* February 1972, pp. 93-95.

Bishop, Dwight E.; Simpson, Myles A.; and Chang, David: *Experimental Atmospheric Absorption Values From Aircraft Flyover Noise Signals.* NASA CR-1751, June 1971; also Acoust Soc of America, 80th Meeting, Houston, Texas, November 3-6, 1970, Paper.

Buell, C. Eugene: *Variability of Sound Propagation Prediction Due to Atmospheric Variability.* NASA CR-1338, April 1969.

Buell, C. Eugene: *Variability of Sound Propagation Prediction Due to Atmospheric Variability--Final Report.* NASA CR-61160, June 1966; also NASA CR-76464, June 1966.

Buell, C. Eugene: "Effects of Atmospheric Variability on Sound Intensity Estimates." Proceedings, National Conference on Aerospace Meteorology, 3rd, New Orleans, Louisiana, May 6-9, 1968.

Bundgaard, R. C.: *The Effects of Atmospheric Fluctuations and Representation Upon Propagated Sound.* NASA CR-1337, April 1969.

Candel, S. M.: "Diffraction of a Plane Wave by a Half Plane in a Subsonic and Supersonic Medium." *J. Acoust Soc of America,* vol. 54, October 1973, pp. 1008-1016.

Censor, D.: "Propagation and Scattering of Sound Waves in Moving Media." *Israel J. of Technology,* vol. 9, no. 1-2, 1971.

Chandiramani, K. L.: "Diffraction of Evanescent Waves, With Applications to Aerodynamically Scattered Sound and Radiation From Unbaffled Plates." *J. Acoust Soc of America,* vol. 55, January 1974.

Chang, David T.: *Some Analyses of the Variability of Atmospheric Parameters at Low Altitudes Significant for Aircraft Propagation.* NASA CR-1945, January 1972; also International Conference on Aerospace and Aeronautical Meteorology, First, Washington, D. C., May 22-26, 1972.

Chessell, C. I.: "Three-Dimensional Acoustic-Ray Tracing in an Inhomogeneous Anisotropic Atmosphere Using Hamilton's Equations." *J. Acoust Soc of America,* vol. 53, January 1973, pp. 83-87.

Chien, F.: *A Resonance Tube Apparatus for Absorption Measurements.* Wyle Labs., Inc., Huntsville, Alabama, AD-764286; AROD-8725-8-F, June 1973.

Chow, P. L.; Liu, C. H.; and Maestrello, L.: "Scattering of Coherent Sound Waves by Atmospheric Turbulence." AIAA paper no. 75-545, March 1975.

Clifford, Steven Francis: "Wave Propagation in a Turbulent Medium." Dartmouth College, Hanover, New Hampshire, Ph.D. thesis, 1969.

Clifford, S. F.; and Brown, E. H.: "Propagation of Sound in a Turbulent Atmosphere." *J. Acoust Soc of America,* vol. 48, 5, part 2, November 1970, pp. 1123-1127.

Coffman, John W.: "The Focusing of Sound Propagating Vertically in a Horizontally Stratified Medium." Army Electronics Research and Development Activity, White Sands Missile Range, New Mexico, ERDA-285, April 1965.

Cole, John E., III; and Dobbins, Richard A.: "Propagation of Sound Through Atmospheric Fog." *J. Atmospheric Sciences,* vol 27, May 1970, pp. 426-434; and Brown University, Providence, Rhode Island, Division of Engineering, AD-699188.

Coles, G. M.: "Atmospheric Absorption of Noise." *Aerodynamic Noise,* proceedings of the Symposium, University of Toronto, Ontario, Canada, May 20 and 21, 1968.

Cooke, J. C.: "Notes on the Diffraction of Sound." London Aeronautical Research Council, ARC-CP-1192, 1971.

Cooper, D. C.; and Blogh, J.: "An Investigation Into the Practicability of Using an Electromagnetic-Acoustic Probe to Detect Air Turbulence." *Radio and Electronic Engineer,* vol. 38, December 1969, pp. 315-325.

Davis, R. S., Jr.; and Austin, M. E.: "Acoustic Ray Tracing in a Layered Atmosphere: An Analog Approach." *J. Acoust Soc of America,* vol. 45, no. 1, January 1969, pp. 242-243.

Delany, M. E.; and Bazley, E. N.: "Monopole Radiation in the Presence of an Absorbing Plane." *J. Sound and Vibration,* vol. 13, November 1, 1970, pp. 269-279.

Delany, M. E.: "A Review of Sound Propagation in the Lower Atmosphere." British Acoustical Society, Acoustic, Atmospheric, Propagation and Applications Meeting, University College, London, England, June 30, 1971.

de Vahl Davis, G.; and Richardson, P. D.: "Natural Convection in a Sound Field Giving Large Streaming Reynolds Numbers." *International Journal of Heat and Mass Transfer,* vol. 16, June 1973.

Dickinson, M. D.; Hower, G. L.; Rigas, H. B.; Rockway, J. W.: "Ray Tracing for Atmospheric Acoustic Waves Using a Hybrid Computer." *IEEE Transactions on Geoscience Electronics,* USA, vol. GE-10, no. 4, October 1972, pp. 166-172.

Duran, Phillip H.: *Sound Intensity in Atmospheric Shadow Zones Assuming a Constant Velocity Gradient–Final Technical Report, July 1 to September 30, 1970.* Texas University, El Paso,Texas, AD-728836; ECOM-0359-F2, December 1970.

Engelke, R.: "Ray Trace Acoustics in Unsteady Inhomogeneous Flow." *J. Acoust Soc of America,* vol. 56, October 1974.

Essenwanger, O. M.: "Wind Influence Upon Acoustic Focusing." Army Missile Command, Huntsville, Alabama, *AERDA Atmospheric Acoustical Propagation,* 1964, pp. 151-171.

Essenwanger, Oskar M.: *On the Frequency of Returning Acoustic Rays and Focusing for Huntsville and Mississippi Test Facility.* NASA CR-76125, January 1966.

Evans, L. B.; and Sutherland, L. C.: *Absorption of Sound in Air–Final Report, June 23, 1969 to June 22, 1970.* Wyle Labs., Inc., Huntsville, Alabama, AD-710291, WR-70-14, AROD-8725-2-E, July 1970.

Evans, Landon B.: *Continued Investigation Into the Anomalous Behavior of Sound Absorption by Molecular Relaxation–Research Report, June 23, 1969 to September 15, 1972.* Wyle Labs., Inc., Huntsville, Alabama, AD-750220, WR-72-11, AROD-8725-7-F, September 1972.

Evans, L. G.; and Bass, H. E.: *Tables of Absorption and Velocity of Sound in Still Air at 68° F, 20° C.* Wyle Labs., Inc., Huntsville, Alabama, AD-738576, WR-72-2, AROD-8725 6-E, January 1972.

Frick, R. H.: *Propagation of Sound as Affected by Wind and Temperature Gradients.* Rand Corporation, Santa Monica, California, AD-693090, RM-5830-ARPA, July 1969.

Grande, E.: *Refraction of Sound by Jet Flow and Jet Temperature. Extension of Temperature Range Parameters and Development of Theory.* NASA CR-840, August 1967.

Grant, L.; Murphy, John N.; and Bowser, Merle L.: *Effect of Weather on Sound Transmission From Explosive Shots.* Bureau of Mines, Pittsburgh, Pennsylvania, Explosives Research Center, BM-RI-6921, 1967.

Guest, S. H.; Adams, B. B.: *Methods of Determining the Excess Attenuation for Ground-to-Ground Noise Propagation.* NASA SP-189 conference at Hampton, Virginia, October 8-10, 1968.

Guiraud, Jean-Pierre: *Theoretical Study of the Propagation of Sound, Applications to the Anticipation of Explosive Noise Caused by Supersonic Flight.* Office National d'Etude et de Recherches Aerospatiales, Chatillon-sous-Bagneaux, France, TP-104(1964), February 1964.

Hardin, Jay C.; and Brown, Thomas J.: "Statistics of the Sound Field of a Source Above a Rough, Imperfectly Reflecting Surface." Paper, Acoust Soc of America, Annual Meeting, 80th, Houston, Texas, November 3-6, 1970.

Harris, Cyril M.: "Effects of Humidity on the Velocity of Sound in Air." *J. Acoust Soc of America,* vol. 49, March 1971.

Harris, Cyril M.; and Tempest, W.: *Absorption of Sound in Air Below 1000 cps.* NASA CR-237, June 1965.

Harris, Cyril M.: "On the Absorption of Sound in Humid Air at Reduced Pressures." *J. Acoust Soc of America,* March 1968.

Harris, W. L., Sr.: "Farfield Viscous Effects in Nonlinear Noise Propagation."*J. Acoust Soc of America,* vol. 56, August 1974.

Hayes, W. D.; Haefeli, R. C.; Kulsrud, H. E.: *Sonic Boom Propagation in a Stratified Atmosphere With Computer Program.* NASA CR-1299, April 1969.

Henley, David C.; and Hoidale, Glenn B.: *Attenuation and Dispersion of Acoustic Energy by Atmospheric Dust.* Atmospheric Sciences Laboratory, White Sands Missile Range, New Mexico, AD-728103-ECOM-5370, March 1971.

Hoch, R.; and Thomas, P.: *The Influence of Reflections on the Sound-Pressure Spectra of Jets.* NASA TT-F-12246, April 1969.

Howe, M. S.: "Multiple Scattering of Sound by Turbulence and Other Inhomogeneities." *J. Sound and Vibration,* vol. 27, April 22, 1973.

Huang, M. N.: "Sound Scattering From Atmospheric Turbulence." AIAA paper no. 75-544, March 1975.

Ingard, U.; and Singhal, V. K.: "Upstream and Downstream Sound Radiation Into a Moving Fluid." *J. Acoust Soc of America,* vol. 54, November 1973, pp. 1343-1346.

Ingard, U.: "On Sound Transmission Anomalies in the Atmosphere." *J. Acoust Soc of America,* vol. 45, April 1969.

Jones, D. S.: "Diffraction Theory–A Brief Introductory Review." *J. Sound and Vibration,* vol. 20, January 8, 1972.

Kallistratova, M. A.: "Experimental Investigation of Sound Wave Scattering in the Atmosphere." Translated into English from a Russian book, *Atmosfernaya Turbulentnost,* Air Force Systems Command, Wright-Patterson AFB, Ohio, Foreign Technology Division, FTD-TT-63-441/1+2+4, June 1963.

Krasil'shchikova, A.: "Diffraction of an Acoustic Wave by a Stationary Plate." *Revue Roumaine des Sciences Techniques, Serie de Mechanique Appliquee,* vol. 17, no. 3, 1972, pp. 521-530.

Lee, Robert P.: *Acoustical Ray Tracing.* Army Electronics Research and Development Activity, White Sands Missile Range, New Mexicao, ERDA-137, June 1964.

Levine, H.: "Diffraction Radiation." Imperial College of Science and Technology, London, England, Department of Mathematics, May 1972.

Lighthill, H.: "The Fourth Annual Fairey Lecture–The Propagation of Sound Through Moving Fluids." *J. Sound and Vibration,* vol. 24, October 22, 1972, pp. 471-492.

Little, John W.; Miller, Robert L.; Oncley, Paul B.; and Panko, Raymond E.: "Studies of Atmospheric Attenuation of Noise." NASA, Washingotn, D. C., Acoustically Treated Nacelle Program, 1969, pp. 125-135.

Liu, C. H.: "Ducting of Acoustic-Gravity Waves in the Atmosphere With Spatially Periodic Wind Shears." *J. Geophys Res,* vol. 75, March 1, 1970, pp. 1339-1341.

Liu, C. H.: "Propagation of Acoustic-Gravity Waves in a Turbulent Atmosphere." *Annales de Geophysique,* vol. 26, January to March 1970.

Liu, C. H.; and Maestrello, L.: "Propagation of Sound Through a Real Jet Flowfield." AIAA paper no. 74-5, January 1974.

Lyon, R. H.: *Lectures in Transportation Noise.* Harvard, Massachusetts, Grozier Publishing, Inc., 1973.

Maestrello, L.; Liu, C. H.; Ting, L.; and Gunzburger, M.: "Sound Propagation Through a Real Jet Flow Field With Scattering Due to Interaction With Turbulence." AIAA paper no. 74-551, June 1974.

Mahoney, A. R.; Gage, K.; Ottersten, H.; and Tennekes, H.: "The Interaction Between Atmospheric Micro-Structure and Acoustic and Electromagnetic Waves." Inter-Union Commission on Radio Meteorology, Symposium on Waves and Turbulence in Stable Layers and Their Effects on EMP Propagation, 3rd, La Jolla, California, June 5-15, 1972.

Mani, R.: "Diffusion of Radiation Patterns Due to Scattering by Random Inhomogeneities." *J. Sound and Vibration,* vol. 17, July 8, 1971.

Martin, J. J.: "Multipath Reflections From a Random Surface." *J. Acoust Soc of America,* vol. 47, May 1970.

McKenzie, James F.: "The Reflection and Amplification of Acoustic-Gravity Waves at a Density and Velocity Discontinuity." European Space Research Institute, Frascati, Italy, 1971.

Miller, Robert L.; and Large, John B.: "The Propagation of Aircraft Noise." Paper 68-46, Sixth Congress International Council of the Aeronautical Sciences, Munich, Germany, September 9-13, 1968.

Morris, P. J.; Richarz, W.; and Ribner, H. S.: "Reduction of Peak Jet Noise Using Jet Refraction." *J. Sound and Vibration,* vol. 29, August 22, 1973.

Mungur, P.; and Tree, D.: "Sound Propagation in Sheared Flow in a Duct With Transverse Temperature Gradients." Seventh International Congress on Acoustics, Proceedings, Budapest, Hungary, August 18-26, 1971.

Oncley, P. B.: "Correction Procedure for Outdoor Noise Measurements." International Conference on Noise Control Engineering, Proceedings, Washington, D. C., October 4-6, 1972.

Oncley, P. B.: "Low Frequency Sound Propagation Anomaly." *J Acoust Soc of America,* 1970.

Oncley, P. B.: "Propagation of Jet Engine Noise Near a Porous Surface." *J. Sound and Vibration,* vol. 13, 1, September 1970, pp. 27-35.

Oncley, P. B.: "Review of Theory and Methods for the Prediction of Ground Effects on Aircraft Noise Propagation." AIAA paper 75-538, March 1975.

Oswatitsch, Kl.: "Dispersion and Absorption of Sound in Clouds." Translated into English from *Physik, Z.,* West Germany, vol. 42, no. 21/22, 1941, pp. 365-378, (NASA TT-F-10939).

Padula, S. L.; and Liu, C.: *A Computing Method for Sound Propagation Through a Nonuniform Jet Stream.* NASA TM-X-71941, December 1974.

Pao, S. Paul: *Sound Propagation and Attenuation Characteristics Over a Heavily Vegetated Terrain.* Wyle Laboratories, Inc., Huntsville, Alabama, AD-706845, AROD-8871-1-E, June 1970.

Pena, Ricardo; and Diamond, Marvin: *Atmospheric Sound Propagation Near the Earth's Surface.* Army Electronics Research and Development Activity, White Sands Missile Range, New Mexico, ECOM-5018, AD-473746, October 1965.

Pierce, Allan D.: *Geometrical Acoustics' Theory of Waves from a Point Source in a Temperature-Stratified and Wind-Stratified Atmosphere–Scientific Report No. 5.* Research and Technology Labs., Avco Corporation, Wilmington, Massachusetts, Research and Technology Labs., AVSSD-0135-66-CR, August 1966.

Pierce, A. D.: "Propagation of Acoustic-Gravity Waves in a Temperature- and Wind-Stratified Atmosphere." *J. Acoust Soc of America,* vol 37, no. 2, February 1965.

Rachele, Henry; and Mathews, Doyle: "Sound Propagation Through a Windy Atmosphere." Environmental Sciences Directorate, Army Electronics Research and Development Activity, White Sands Missile Range, New Mexico, April 1965.

Ramsey, Vernon Wayne: "Acoustic Scattering From an Aircraft Trailing Vortex." Ph.D. thesis, Stanford University, California, 1973.

Rudd, M. J.: "A Note on the Scattering of Sound in Jets and the Wind." *J. Sound and Vibration,* vol. 26, February 22, 1973.

Schmidt, D.: "Experimental Investigations on the Scattering of Sound in a Turbulent Stream." Max-Planck-Institute fur Stromungsforschung, Gottingen, West Germany, 1962.

Scholes, W. E.; and Parkin, P. H.: "The Effect of Small Changes in Source Height on the Propagation of Sound Over Grassland." *J. Sound and Vibration,* vol. 6, November 1967.

Shapiro, N.: "Atmospheric Absorption Considerations in Airplane Flyover Noise at Altitudes Above Sea Level." Acoust Soc of America, 85th Meeting, Boston, Massachusetts, April 10-13, 1973.

Sherr, Paul E.; and Chang, David T.: *Meteorological Aspects of the Aircraft Noise Problem.* Fourth National Conference on Aerospace Meteorology, Las Vegas, Nevada, preprints, A70-30551 14-20, May 4-7, 1970.

Smith, C. M.: *Atmospheric Attenuation of Aircraft Noise. Experimental Values Measured in a Range of Climatic Conditions, Volume 1.* Final report, Hawker Siddeley, HSA-HAD-R-GEN-214, September 1973.

Smith, C. M.: *Atmospheric Attenuation of Aircraft Noise. Experimental Values Measured in a Range of Climatic Conditions, Volume 2.* Final report, Hawker Siddeley, HSA-HAD-R-GEN-214, September 1973.

Smith, C. M.: "Atmospheric Attenuation of Noise Measured in a Range of Climatic Conditions." American Institute of Aeronautics and Astronautics, Paper 73-242, Aerospace Sciences Meeting, Washington, D. C., January 10-12, 1973.

Solomon, Louis: *The Propagation Path of a Wave in a Variable Speed of Sound Medium Obtained by Employing Fermat's Principle.* Report 65-48, California University, Department of Engineering, Los Angeles, California, November 1965.

Sperry, William C.: "Governing Equations for Wave Propagation in a Homogeneous, Isotropic, Continuous Fluid." Presented at Noise Generation and Suppression in Aircraft Symposium, Space Institute, Tennessee University, Tullahoma, Tennessee, January 29 to February 2, 1968.

Steinmetz, George G.; and Singh, Jag J.: *Reflection and Transmission of Acoustic Waves From a Moving Layer.* NASA TN-D-6673, March 1972; and *J. Acoust Soc of America,* vol. 51, part 2, January 1972.

Stuff, R.: "Vertical Propagation of a Plane Sound Pulse in a Gravitational Atmosphere With a Temperature Gradient." *Zeitschrift fur Flugwissenschaften 18,* 2/3, February/ March 1970, pp. 80-83.

Sutherland, L. C.; Piercy, J. E.; and Bass, H. E.: "A Method for Calculating the Absorption of Sound by the Atmosphere." Invited paper, Acoust Soc of America, St. Louis, Missouri, November 1974.

Tamez, Jesus Roberto Armijo; and Ramirez, Jose Javier: *The Theoretical Investigation of Wind Gradient Effects on Atmospheric Shadow Zones–Technical Report, August 2, to September 30, 1972.* Texas University, El Paso, Texas, AD-754634, September 1972.

Tanner, C. S.: *Experimental Atmospheric Absorption Coefficients.* Department of Transportation, FAA-RD-71-99, November 1971.

Tatarkski, V. I.: "The Effects of the Turbulent Atmosphere on Wave Propagation." Translated into English from the book *Rasprostranenie Voln v Turbulentnoi Atmosfere,* Nauka Press, Moscow, U.S.S.R., Department of Commerce and NSF, 1967.

Tedrick, Richard N.; and Polly, Robert C.: *A Preliminary Investigation of the Meausred Atmospheric Effects Upon Sound Propagation.* NASA TM-X-50142, March 24, 1963.

Thomas, P.: *Acoustic Interference by Reflection Application of the Sound Pressure Spectrum of Jets.* NASA TT-F-14185, May 1969; also in *AGARD Aircraft Engine Noise and Sonic Boom,* May 1969, in French.

Thompson, R. J.: "Computing Meteorological Effects on Aircraft Noise." *AIAA Journal,* vol 11, January 1973; also First International Conference on Aerospace and Aeronautical Meteorology, Washington, D. C., May 22-26, 1972, preprints.

Thompson, R. J.: *Computing Sound Ray Paths in the Presence of Wind.* Sandia Corporation, Albuquerque, New Mexico, SC-RR-67-53, February 1967.

Thompson, R. J.: *Sound Rays in the Atmosphere.* Sandia Corporation, Albuquerque, New Mexico, SC-RR-64-1756, January 1965.

Ugincius, Peter; and Zondek, Bernd: *Acoustic Rays in an Arbitrary Moving Inhomogeneous Medium,* Naval Weapons Lab., Warfare Analysis Department, Dahlgren, Viriginia, NWL-TR-2446, August 1970.

Varley, E.; and Cumberbatch, E.: "Large Amplitude Waves in Stratified Media–Acoustic Pulses." *J. Fluid Mechanics,* vol. 43, September 16, 1970, pp. 513-537.

Weedfall, Robert O.; and Linsky, Benjamin: "Air Pollution Potential and Noise Related to Stagnation Indices at SST Airports." Fourth National Conference on Aerospace Meteorology, Las Vegas, Nevada, May 4-7, 1970, preprints (A70-30551 14-20).

Wenzel, Alan R.; and Keller, Joseph B.: "Propagation of Acoustic Waves in a Turbulent Medium." *J. Acoust Soc of America,* vol. 50, September 1971.

Wooten, D. C.; and Eidemiller, R. L.: *Effects of Local Meteorological Factors Upon Aircraft Noise Measurements–Final Report, August to November 1972.* Ultrasystems, Inc., Newport Beach, California, FAA-RD-72-145, November 1972.

SOURCE ALTERATION

General

Atencio, A., Jr.; and Soderman, P. T.: "Comparison of Aircraft Noise Meanred in Flight Test and in the NASA-Ames 40- by 80-ft Wind Tunnel." AIAA paper 73-1047, October 1973.

Atencio, Adolph, Jr.; Kirk, Jerry V.; Soderman, Paul T.; and Hall, Leo P.: *Comparison of Flight and Wind Tunnel Measurements of Jet Noise for the XV-5B Aircraft.* NASA TM-X-62182, October 1972.

Atvars, Janis; Mangiarotty, R. A.; and Walker, David Q.: "Acoustic Results of 707-320B Airplanes With Acosutically Treated Nacelles." NASA Acoustically Treated Nacelles Program, Washington, D. C., 1969, pp. 95-108.

Banerian, G.: "Jet Noise–The State of the Art." *Sound and Vibration,* vol. 8, February 1974, pp.;30-34.

Beulke, M. R.; Clapper, W. S.; McCann, E. O.; and Morozumi, H. M.: *A Forward Speed Effects Study on Jet Noise From Several Suppressor Nozzles in the NASA/Ames 40- By 80-Foot Wind Tunnel.* Final report, NASA CR-114741, May 3, 1974.

Brausch, J. F.: *Flight Velocity Influence on Jet Noise of Conical Ejector, Annular Plug, and Segmented Suppressor Nozzles.* NASA CR-120961, August 1972.

Brooks, J. R.; and Woodrow, R. J.: "The Effects of Forward Speed on a Number of Turbojet Exhaust Silencers." AIAA paper 75-506, March 1975.

Burley, Richard R.; Karabinus, Raymond J.; and Freedman, Robert J.: *Flight Investigation of Acoustic and Thrust Characteristics of Several Exhaust Nozzles Installed on Underwing Nacelles on an F106 Airplane.* NASA TM-X-2854, August 1973.

Burley, Richard R.; and Kaabinus, Raymond J.: *Flyover and Static Tests to Investigate External Flow Effect on Jet Noise From Nonsuppressor and Suppressor Exhaust Nozzles.* NASA TM-X-6816, January 1973, and AIAA paper 73-109, 1973.

Burley, Richard R.; and Johns, Albert L.: *Flight Velocity Effects on Jet Noise of Several Variations of a Twelve-Chute Suppressor Installed on a Plug Nozzle.* NASA TM-X-2918, February 1974.

Burley, Richard R.; and Head, Verlon L.: *Flight Velocity Effects on Jet Noise of Several Variations of a 48-Tube Suppressor Installed on a Plug Nozzle.* NASA TM-X-2919, February 1974.

Burley, R. R.: *Flight Velocity Effects on the Jet Noise of Several Variations of a 104-Tube Suppressor Nozzle.* NASA TM-X-3049, Washington, D. C., July 1974.

Burley, R. R.: "Suppressor Nozzle and Airframe Noise Measurements During Flyover of a Modified F106B Aircraft With Underwing Nacelles." Paper 74-WA/Aero-1 American Soc of Mech Eng, November 1974.

Bushell, K. W.: "Measurement and Prediction of Jet Noise in Flight." AIAA paper no. 75-461, March 1975.

Chamberlin, Roger: *Flyover and Static Tests to Study Flight Velocity Effects on Jet Noise of Suppressed and Unsuppressed Plug Nozzle Configurations.* NASA TM-X-2856, August 1973.

Chu, W. T.: "Moving-Frame Analysis of Jet Noise." *J. Acoust Soc of America,* vol. 53, May 1973, pp. 1439 and 1440.

Cocking, B. J.; and Bryce, W. D.: "Subsonic Jet Noise in Flight Based on Some Recent Wind-Tunnel Results." AIAA paper no. 75-462, March 1975.

Crow, S. C.; and Champagne, F. H.: "Orderly Structure in Jet Turbulence." *J. Fluid Mechanics,* vol. 48, part 3, 1971, pp. 547-591.

Ffowcs-Williams, John E.: "Jet Noise From Moving Aircraft." *AGARD Aircraft Engine Noise and Sonic Boom,* May 1969.

Gubkina, G. I.; and Melnikov, B. N.: "Effects of Air Speed on the Flight Noise of Airliners and of Noise Duration on Its Subjective Intensity Rating." *Soviet Physics–Acoustics,* vol. 13, 4, April/June 1968, pp. 478-481.

Kobrynski, Michel: "On the Calculation of the Maximum Sound Pressure Spectrum From Fixed and Mobile Jets." Presented at the International Congress on Aeronautics, Paris, France, May 29-31, 1967, Association Francaise des Ingenieurs et de l'Espace; also ONERA-TN-108, 1967; also *J. Sound and Vibration,* vol. 7, 2, March 1968, pp. 263-286.

Kobrynski, Michel: "General Method for Calculating the Sound Pressure Field Emitted by Stationary or Moving Jets." *Aerodynamic Noise;* proceedings of the Symposium, University of Toronto, Toronto, Ontario, Canada, May 20 and 21, 1968; and ONERA, TP 578, 1968.

Kobrynski, Michel: *Generalization of the Representation of the Spectral Density of the Acoustic Energy Emitted by Rotating Jets.* Academie des Sciences, Paris, France, Comptes Rendus, Serie B.–Sciences Physiques, vol. 266, no. 7., February 12, 1968, pp. 370-373.

Kobrynski, Michel: "Determination of the Acoustic Field Generated by a Jet Aircraft in Motion." ONERA, TP 687, 1969.

Kobrynski, Michel: "Determination of Sound Field Produced by Changing Airplane Processes." *AGARD Aircraft Engine Noise and Sonic Boom,* May 1969; and NASA TT-F-14489, 1969.

Kobrynski, Michel: "General Method for Computation of the Acoustic Field Generated by Aircraft Jets." ONERA-NT-187, 1971; also Office National d'Etudes et de Recherches Aerospatials Note Technique no. 187, 1971, 29 pages.

Morfey, C. L.: "The Sound Field of Sources in Motion." *J. Sound and Vibration,* vol. 23, August 8, 1972, pp. 291-295.

Packman, A. B.; Ng, K. W.; and Paterson, R. W.: "Effect of Simulated Forward Flight on Subsonic Jet Exhaust Noise." AIAA paper no. 75-869, June 1975.

Parthasarathy, S. P.: "Evaluation of the Noise Autocorrelation Function of Stationary and Moving Noise Sources by a Cross Correlation Method." AIAA paper 73-186, January 1973.

Pinkel, B.: "An Analysis of Pulsating Pressure Fields in Jets in Respect to Noise Generation." AIAA paper 76-6, 1974.

Richter, G.; and Schmidt, C.: "Contribution to the Study of Noise From Jet Aircraft During Flight." Royal Aeronautical Society, London, England; Proceedings, Second International Symposium on Air Breathing Engines, Sheffield, England, March 1974.

Smith, W.: "The Use of a Rotating Arm Facility to Study Flight Effects on Jet Noise." Royal Aeronautical Society, London, England; Proceedings, Second International Symposium on Air Breathing Engines, Sheffield, England, March 1974.

Viaz'menskaia, L. M.: *Theory of Turbulent Jet Noise.* Leningradskii Universitet, Vestnik, Matematika, Mekhanika, Astronomiia, January 1973, pp. 88-93.

VonGlahn, U.; Sekas, N.; Groesbeck, D.; and Huff, R. G.: *Forward Flight Effects on Mixer Nozzle Design and Noise Considerations for STOL Externally Blown Flap Systems.* NASA TM-X-68102, August 1972; also AIAA paper 72-792.

VonGlahn, U.; and Goodykoontz, J.: *Forward Velocity Effects on Jet Noise With Dominant internal Noise Source.* NASA TM-X-71438, November 1973.

VonGlahn, U.; Goodykoontz, J.; and Wagner, J.: *Nozzle Geometry and Forward Velocity Effects on Noise for CTOL Engine-Over-The-Wing Concept.* NASA TM-X-71453, October 1973.

Wilcox, F. A.: "Comparison of Ground and Flight Test Results Using a Modified F106B Aircraft." Ninth AIAA and SAE Propulsion Conference, Las Vegas, Nevada, AIAA paper 73-1305, November 5-7, 1973.

Comparison of Ground-Runup and Flyover Noise Levels. SAE Aerospace Information Report, AIR 1216, April 1972.

Coaxial Jets

Ancell, J. E.; and Shapiro, N.: "Model Study of High Bypass Jet Noise." Acoustical Society of America, Paper, Spring Meeting, 79th, Atlantic City, New Jersey, April 21-24, 1970.

Bhutiani, P. K.; Dosanjh, D. S.; and Abdelhamid, A.: "Role of Lip Thickness in Noise Suppression by Interacting Coaxial Supersonic Jets." AIAA paper no. 75-96, January 1975.

Bushell, K. W.: "A Survey of Low Velocity and Coaxial Jet Noise With Application to Prediction." *J. Sound and Vibration,* vol. 2, July 17, 1971, pp. 271-282; also in Loughborough University of Technology, Symposium on Aerodynamic Noise, Loughborough, Leics, England, September 14-17, 1970.

Champagne, F. H.; and Wygnanski, I. J.: "An Experimental Investigation of Coaxial Turbulent Jets." *International J. Heat and Mass Transfer,* vol. 14, September 1971.

Dahlen, H. W.: "Some Experiments on the Noise Emission of Coaxial Jets." First International Symposium on Air Breathing Engines, Marseille, France, June 19-23, 1972.

Dosanjh, D. S.; Abdelhamid, A. N.; and Yu, J. C.: "Reduction of Noise From Supersonic Jet Flows." AIAA paper 70-236, January 1970.

Dosanjh, Darshan S.; Abdelhamid, A. N.; and Yu, James C.: *Noise Generation From Interacting High Speed Axisymmetric Jet Flows–Semiannual Status Report, June 1, 1968 to December 31, 1969,* NASA CR-107012, January 1969.

Dosanjh, D. S.; and Yu, J. C.: "Supersonic Jet Noise Suppression Using Coaxial Flow Interaction," Seventh International Congress on Acoustics, Budapest, Hungary, August 18-26, 1971, proceedings, vol. 2.

Durao, D.; and Whitelaw, J. H.: "Turbulent Mixing in the Developing Region of Coaxial Jets." American Soc of Mech Eng, Applied Mechanics and Fluids Engineering Conference, Atlanta Georgia, paper 73-FE-19, June 20-22, 1973.

Eldred, Kenneth M.: *Far Field Noise Generation by Coaxial Flow Jet Exhausts. Volume 1: Detailed Discussion–Final Report, March 1968 to November 1971.* FAA-RD-71-101-Vol-1, November 1971.

Gal, George: "Self-Preservation in Fully Expanded Turbulent Coflowing Jets." AIAA Journal, vol. 8, April 1970, pp. 814 and 815.

Kono, N.: *Aerodynamic Noise of a Circular Double Jet.* National Aerospace Laboratory, TR-212, 1970.

Olsen, W.; and Friedman, R.: "Jet Noise From Coaxial Nozzles Over a Wide Range of Geometric and Flow Parameters." AIAA paper 74-43, 1974.

Ribeiro, M. M.; and Whitelaw, J. H.: *Turbulent Mixing of Coaxial Jets With Particular Reference to the Near Exit Region.* Imperial College of Science and Technology, Department of Mechanical Engineering, London, England, August 1973.

Viets, H.: "Prandtl Eddy Viscosity Model for Coaxial Jets." *AIAA Journal,* vol. 10, December 1972.

Williams, T. J.; Ali, M. R. M. H.; and Anderson, J. S.: "Noise and Flow Characteristics of Coaxial Jets." *J. Mech Eng Science,* vol. 11, 2, April 1969, pp. 133-142.

Yu, J. C.; and Dosanjh, D. S.: "Noise Field of Coaxial Interacting Supersonic Jet Flows." AIAA paper 71-152, January 1971.

Zelazny, Stephen W.: "Eddy Viscosity in Quiescent and Coflowing Axisymmetric Jets." *AIAA Journal,* Vol. 9, November 1971.

Zelazny, S. W.; Morgenthaler, J. H.; and Herendeen, D. L.: "Reynolds Momentum and Mass Transport in Axisymmetric Coflowing Streams." Heat Transfer and Fluid Mechanics Institute, proceedings, 22nd Meeting, U.S. Naval Postgraduate School, Monterey, California, June 10-12, 1970.

Measurement Methods

Auzolle, S.; and Hay, J: *Method of Measurement and Analysis of Noise of an Aircraft in Flight.* NASA, Washington, December 1971, 39 pages; translated into English from *Methodes de Mesure et d' Analyse du Bruit des Auions en Vol,* Paris, Societe National d'Etude et du Construction de Moteurs d'Aviation, 1971, 27 pages.

Beauchamp, K. G.; Thomasson, P. G.; Williamson, M. E.: "A Hybrid Computer Analysis of a Nonstationary Process." Proceedings of the Symposium on Computer-Aided Engineering, Waterloo, Ontario, Canada, May 11-13, 1971.

Besson, J.; and Boillot, J.: "A Time-Frequency Localization System Applied to Acoustic Certification of Aircraft." AIAA Guidance and Control Conference, Stanford, California, August 14-16, 1972.

Bies, D. A.; and Scharton, T. D.: *Relation Between Near Field and Far Field Acoustic Measurements.* Bolt, Beranek and Newman, Inc., Contract NAS 2-6726, NASA CR-114756, March 29, 1974.

Bishop, Dwight E.: "Variability of Flyover Noise Measures for Repeated Flights of Turbojet and Piston Engine Transport Aircraft." NASA Washington, NASA CR-1752, March 1971.

Blässer, Heinz: *The Present State of the Art Regarding the Measurement of Sound. I.* Hewlett-Packard GmbH, Böblingen, West Germany, VDI-Z, vol. 112, no. 13, 1970.

Borgioli, R. C.: "A High-Speed Third-Octave Filtering Algorithm for Real-Time Noise Analysis." 85th meeting of the Acoust Soc of America, Boston, Massachusetts, U.S.A., April 10-13, 1973.

Brown, D. L.; and Halvorsen, W. G.: "Application of the Coherence Function to Acoustic Noise Measurements." Proceedings, International Conference on Noise Control Engineering, Washington, D. C., October 4-6, 1972.

Bruel, V.: "Electroacoustical Performance Requirements for Aircraft Noise Certification Measurements." Proceedings of the International Conference on Noise Control Engineering, Copenhagen, Denmark, August 22-24, 1974.

Cambell, Jon: "Measuring Noise." *Machine Design,* vol. 39, September 14, 1967.

Chernyshev, V. O.; and Smorodinskii, S. S.: "Accuracy of a Complex Determination of the Location of a Moving Object." Akademiia Nauk BSSR, Doklady, vol. 17, February 1973, in Russian.

Delaney, M. E.; and Bazley, E. N.: "A Note on the Effect of Ground Absorption in the Measurement of Aircraft Noise." *J. Sound and Vibration,* vol. 16, 3, June 1971, pp. 315-322.

El-sum, H. M. A.; Mawardi, O. K.: *Diagnostic Techniques for Measurement of Aerodynamic Noise in Free Field and Reverberant Environment of Wind Tunnels.* NASA CR-114636, May 1973.

Fredricksen, R.; and Soeberg, J.: "Real-Time Analysis." Proceedings of the 78th meeting of the Acoust Soc of America, San Diego, California, U.S.A., November 4-7, 1969.

Gaudron, Jean: "Determination of Sound Fields of Aircraft in Flight by Treatment of Noise Measurements." Colloque d'Acoustique Aeronautique, 2nd, Paris, France, May 4 and 5, 1971, in French.

Gonter, R. H.; "Aircraft Flyover Noise–Spectral Analysis of Sounds and Sound Intensity Fluctuations." 85th Meeting of Acoust Soc of America, Boston, Massachusetts, April 10-13, 1973.

Hay, Jacques: "Acoustical Data Processing Methods in the Study of Aircraft Noise." Presented at AGARD meeting on Aircraft and Sonic Boom Noise, St. Louis, Missouri, May 27-30, 1969, in French.

Herz, F.; Stawinski, H.; and Elasser, W.: "Acoustic Data Collection and Evaluation With the Aid of a Small Computer." *Bruel & Kjaer Technical Review,* Denmark, no. 1, 1970, pp. 3-18.

Hilton, David A.; and Henderson, Herbert R.: "Variability in Airplane Noise Measurements." Program of NASA Research Relating to Noise Alleviation of Large Subsonic Jet Aircraft, 1968, pp. 359-367.

Hoch, R.; and Thomas, P.: "The Influence of Reflections on the Sound-Pressure Spectra of Jets." *Scientific and Technical Aerospace Reports.* Clearinghouse for Federal Scientific and Technical Information, Springfield, Virginia, July 8, 1969.

Hosman, R. J. A. W.: *A Method to Derive Angle of Pitch, Flight-Path Angle, and Angle of Attack From Measurements in Nonsteady Flight.* Technische Hogeschool, Delft, Netherlands.

Jacobsen, F. D.: "Real Time Analyzer and Its Connection to External Instruments." *Messen Steuern Regeln,* Germany, vol. 14, no. 1, January 1971, pp. 28-31.

Kao, Kai: *Subsonic Jet Noise Measurements by Means of a Directional Microphone System.* University of Southern California, Los Angeles, California, Ph.D. thesis, 1973, University microfilms.

Kapuskar, W.; and Balmforth, C.: "Real-Time Measurement and On-Line Processing of Acoustical and Other Audio Frequency Spectra." *Hewlett-Packard Journal,* July 1969.

Kobatake, H.; Ishii, Y.; and Igarashi, J.: *Location of Aircraft by an Acoustic Method.* Tokyo University, Institute of Space and Aeronautical Science, Bulletin, vol. 9, October 1973, pp. 854-869, in Japanese.

Lapointe, J. A.; Kundert, W. R.; and Partridge, G. R.: "Real-Time Hybrid Sound and Vibration Analyzer." Proceedings of the 78th Meeting of the Acoustical Society of America, San Diego, California, U.S.A., November 4-7, 1969.

Lowder, E. M.: "Effective Data Monitoring During Airplane Flyover Noise Tests." *Advancements in Flight Test Engineering,* Proceedings of the Fifth Annual Symposium Society of Flight Test Engineers, 1974, pp. 4-1 to 4-8.

McCann, John C.: "Critical Review of Methods for Evaluating Aircraft Noise." Proceedings of 16th International Aerospace Instrumentation Symposium, Seattle, Washington, May 11-13, 1970.

Melchoir, H.: "Computer Programming Requirements for Acoustic Measurements." Proceedings of the Seventh International Congress on Acoustics, Budapest, Hungary, August 18-26, 1971.

Moller, P. K.; and Pedersen, S. B.: "Digital Noise Measurements." Proceedings of the International Conference on Noise Control Engineering, Copenhagen, Denmark, August 22-24, 1973.

Moore, C. J.: "A Solution to the Problem of Measuring the Sound Field of a Source in the Presence of a Ground Surface." *J. Sound and Vibration,* vol. 16, May 22, 1971.

Morgan, William R.; and Sucin, Spiridon N.: "Aircraft Engine Noise Measurement Techniques, Facilities, and Test Results." *AGARD Aircraft Engine Noise and Sonic Boom,* May 1969.

Mukai, R. S.: "Digital Instrumentation for Acoustic Testing." Proceedings, Instrument Society of America, 24th Annual Conference, Houston, Texas, October 27-30, 1969.

Nitsche, J. R.: "A Survey of Spectral Analysis Techniques Pertinent to the Study of Moving Sound Sources." Proceedings of the Purdue Noise Control Conference, Lafayette, Indiana, July 14-16, 1971.

Skode, F.: "Computer Interface and Software for the On-Line Evaluation of Noise Data." *Bruel & Kjaer Technical Review,* Denmark, no. 1, 1972, p. 21-6.

Soeberg, Jan: "The Use of Digital Systems in Acoustic Measurements." *Bruel & Kjaer Technical Review,* no. 1, 1969, pp. 3-6.

Soeberg, J.: "Optimizing Computerized Acoustic Measuring Systems." Proceedings of the Seventh International Congress on Acoustics, Budapest, Hungary, August 18-26, 1971 (Budapest, Hungary: Akademiai Kiado 1971), pp. 513-516.

Stearns, John; Turner, Donald: "Acoustic Data Acquisition and Control System." Proceedings, 17th International Aerospace Instrumentation Symposium, Las Vegas, Nevada, May 10-12, 1971.

Thorpe, Howard, A.: "Repeatability of Ground-Test Noise Measurements on an Aircraft Engine." *J. Acoust Soc of America,* vol. 47, part 1, June 1970, p. 1485.

van Niekerk, C. G.; and Muller, J. W.: "Assessment of Aircraft Noise Disturbance." *Aeronautical Journal,* vol. 73, May 1969.

Waters, John F.; McFadden, John V.; and Glass, Ray E.: *Aircraft Noise Type, Certification Orientation Session: Lecture Notes, Supplement 2, Final Report.* Contract DOT-FA70WA-2446, October 1970.

Winkler, J. H.; and Blaesser, H.: "New Hybrid Real-Time Spectrum Analysis System." Proceedings of the 78th Meeting of Acoust Soc of America, San Diego, California, November 4-7, 1969.

Wooten, E. J.; and Cary, H.: "Instrumentation for Space-Averaged Acoustic Measurements." *Noise and Vibration Control Engineering;* proceedings of the Purdue Noise Control Conference, Lafayette, Indiana, July 14-16, 1971; Purdue University 1972.

Zuckerwar, Allan J.: *A Solid-State Converter For Measurement of Aircraft Noise and Sonic Boom, Final Report, September 1, 1971 to August 31, 1972.* NASA CR-112260, November 1972.

Zuckerwar, A. J.: "A Solid-State Converter for Measurement of Aircraft Noise and Sonic Boom." *IEEE Transactions on Instrumentation and Measurement,* vol. IM-23, March 1974, pp. 23-27.

Zuckerwar, Allan J.: *Instrumentation for Measurement of Aircraft Noise and Sonic Boom Patent Application.* NASA Case-LAR-11173-1, April 25, 1973.

Zwieback E. L.: "Aircraft Flyover Noise Measurements." AIAA paper 75-537, Mach 1975.

Zwieback, Edgar L.: "Recording Aircraft Flyover Noise." *Sound and Vibration,* vol. 1, September 1967.

Zwieback, E. L.: "Flyover Noise Testing of Commercial Jet Airplanes." Fourth AIAA Aircraft Design, Flight Test, and Operations Meeting, Los Angeles, California, August 7-9, 1972, paper 72-786.

Acoustic Sounding

Balster, Martin; Nagy, Arthur E.; and Proudian, Andrew P.: *Vortex* observations by the Xonics Acoustic Radar at NAFEC, Final Report. Xonics, Inc., Van Nuys, California, December 1971.

Beaubien, David J.; Bisberg, Arthur; and Pappas, Arthur: *Design, Development, and Testing of an Acoustic Anemometer, Final Report, June 1, 1963 to May 31, 1966.* Cambridge Systems, Inc., Newton, Massachusetts June 1966.

Beran, D. W.: "Acoustics–A New Approach for Monitoring the Environment Near Airports." *J. Aircraft,* vol. 8, November 1971.

Beran, D. W.; and Clifford, S. F.: "Acoustic Doppler Measurement of the Total Wind Vector." Second Symposium on Meteorological Observations and Instrumentation, San Diego, California, March 27-30, 1972, preprints, (A72-25076 10-20).

Beran, D. W.; Little, C. G.; and Willmarth, B. C.: "Acoustic Doppler Measurements of Vertical Velocities in the Atmosphere." *Nature,* vol. 230, March 19, 1971.

Beran, D. W.; Willmarth, B. C.; Carsey, F. C.; and Hall, F. F., Jr.: "An Acoustic Doppler Wind Measuring System." *J. Acoust Soc of America,* vol. 55, February 1974.

Beran, D. W.: "Wind Measurement With Acoustic Doppler." *Atmospheric Technology,* Winter 1974-1975, pp. 94-99.

Bourne, I. A.; and Keenan, T. D.: "High Power Acoustic Radar." *Nature,* vol.'251, September 20, 1974, pp. 206-208.

Brown, E. H.: "Some Recent NOAA Theoretical Work on Echo Sounding in the Atmosphere." *J. Geophys Res,* vol. 79, December 20, 1974, pp. 5567-5571.

Burnham, D.; Kodis, R.; and Sullivan, T.: "Observations of Acoustic Ray Deflection by Aircraft Wake Vortices." *J. Acoust Soc of America,* vol. 52, July 1972.

Casti, J.; Detchmendy, D.; Kagiwada, H.; and Kasaba, R.: *Estimating the Parameters of an Inhomogeneous Medium by Probing With Rays.* U.S. Government Research and Development Reports, AD 684 151, Rand Corporation, Santa Monica, California, May 1969.

Clifford, S. F.; and Brown, E. H.: "Acoustic Scattering From a Moving Turbulent Medium." *J. Acoust Soc of America,* vol. 55, May 1974, pp. 929-933.

Closs, R. L.; and Surridge, A. D.: "The Temperature Profile in the Lower Atmosphere Obtained by Acoustic Sounding." *J. Physics,* part E, Scientific Instruments, vol. 7, May 1974, pp. 369-371.

Coffman, John W.; and Price, Robert G.: *Some Errors Associated With Acoustical Wind Measurements Through a Layer.* Army Electronics Research and Development Activity, White Sands Missile Range, New Mexico, October 1962.

Fox, Herbert L.: *Continuous-Wave Three-Component Sonic Anemometer, Final Report, April 15, 1964 to June 30, 1967.* Bolt, Beranek and Newman, Inc., Cambridge, Massachusetts, March 1968.

Fox, Herbert L.: *Vertical Profiles of Wind and Temperature by Remote Acoustical Sounding.* Bolt, Beranek and Newman, Inc., Cambridge, Massachusetts, January 1969.

Fox, H. L.; Abilock, R.; Lyon, R. H.; and Ingard, U.: *On the Feasibility of Remote Acoustic Sensing of Low-Level Winds and Temperatures, Final Report.* Bolt, Beranek and Newman, Inc., Cambridge, Massachusetts, November 1968.

Galbraith, L. K.: *Atmospheric Speed-of-Sound Measurement Device.* Sandia Labs., Albuquerque, New Mexico, August 1973.

Georges, T. M.; and Clifford, S. F.: "Acoustic Sounding in a Refracting Atmosphere." *J. Acoust Soc of America,* vol. 52, November 1972.

Gjaerdman: *Investigation Into the Effects of Wind and Temperature Gradients on a Sound Measuring System.* Research Institute of National Defence, Stockholm, Sweden, February 1972, in Swedish.

Greenfield, R. J.; Teufel, M.; Thomson, D. W.; and Coulter, R. L.: "A Method for Measurement of Temperature Profiles in Inversions From Refractive Transmission of Sound." *J. Geophys Res,* vol. 79, December 20, 1974, pp. 5551-5554.

Hagelin, G.: "Wind Velocity Measurements by Acoustics." *Forsvarets Forskningsanstalt,* Stockholm, Sweden, October 1967, in Swedish.

Hall, F. F., Jr.; and Wescott, J. W.: "Acoustic Antennas for Atmospheric Echo Sounding." *J. Acoust Soc of America,* vol. 56, November 1974, pp. 1376-1382.

Hall, F. F., Jr.; Westcott, J. W.; Simmons, W. R.: "Acoustic Echo Sounding of Atmospheric Thermal and Wind Structure." Proceedings of the Seventh International Symposium on Remote Sensing of Environment, Ann Arbor, Michigan, May 17-21, 1971.

Jones, D. L.; Kakli, G. M.; and Carignan, G. R.: *The Acoustic Wind Measurement, Final Report.* NASA CR-102791, June 1969.

Kelly, Edward H.: *Acoustic Sounding in the Planetary Boundary Layer.* NASA, Washington, D. C., NASA CR/2431 (Contract NAS8-28659), May 1974.

Lee, Robert P.: *A Dimensional Analysis of the Errors of Atmospheric Sound Ranging.* Atmospheric Sciences Lab., White Sands Missile Range, New Mexico, March 1969.

Little, C. G.: *Acoustic Methods of Remote Probing of the Lower Atmosphere.* Environmental Science Services Adminstration, Boulder, Colorado, Research Labs, January 1969.

Little, Gordon: "Acoustic Sounding of the Lower Atmosphere." Meteorological Observations and Instrumentation, American Meteorological Society, Symposium, Washington, D. C., February 10-14, 1969, proceedings.

Little, C. G.: "On the Detectability of Fog, Cloud, Rain, and Snow by Acoustic Echo-Sounding Methods." *J. Atmos Sciences,* vol. 29, May 1972.

Marshall, James M.: *A Radio Acoustic Sounding System for the Remote Measurement of Atmospheric Parameters.* Stanford University, Electronics Labs, California, August 1970.

McAllister, Linday, G.; Pollard, John R.; and Mahoney, Allan R.: "Acoustic Sounding–A New Approach to the Study of Atmospheric Structure." IEEE, Proceedings, vol. 57, April 1969.

McAllister, G.; and Pollard, J. R.: "Acoustic Sounding of the Lower Atmosphere." Sixth International Symposium on Remote Sensing of Environment, Ann Arbor, Michigan, proceedings, vol. 1, October 13-16, 1969.

McAllister, L. G.: *Acoustic Radar Sounding of the Lower Atmosphere.* NASA-Ames Research Center, August 1962.

Mahoney, A. R.; McAllister, L. G.; and Pollard, J. R.: "The Remote Sensing of Wind Velocity in the Lower Troposphere Using an Acoustic Sounder." Third Symposium on Waves and Turbulence in Stable Layers and Their Effects on EM Propagation, La Jolla, California, June 5-15, 1972.

Morris, A. L.: "Remote Sensing of the Atmosphere by Sound." *Atmospheric Technology,* Winter 1974-1975, pp. 84-93.

Smith, Paul L., Jr.: *Limitations on the Accuracy of Sonic Thermometers, Final Report, May 1, 1962 to April 30, 1963.* Midwest Research Institute, Kansas City, Missouri, June 1, 1963.

"Report of Project Michigan Section on 6A; An Investigation of Factors Affecting Sound Ranging Literature Search and Analysis, Quarterly Progress Report, January 1, to March 31, 1969." University of Michigan, Institute of Science and Technology, Ann Arbor, Michigan, 1969.